AD NUMBER

ADB212361

NEW LIMITATION CHANGE

TO

Approved for public release, distribution unlimited

FROM

Distribution authorized to U.S. Gov't. agencies and their contractors; Critical Technology; Jan 96. Other requests shall be referred to WLFIGC, Eigth St., Wright-Patterson AFB, OJ r454433.

AUTHORITY

AFRL Ltr., 14 Sep 99

WL-TR-96-3074

INNOVATIVE CONTROL EFFECTORS (ICE)

E. L. Roetman
S. A. Northcraft
J. R. Dawdy

Boeing Defense and Space Group
P.O. Box 3999, M/S 4C-61
Seattle WA 98124-2499

MARCH 1996

FINAL REPORT FOR OCTOBER 1994 - JANUARY 1996

Distribution authorized to U.S. Government agencies and their contractors, Critical Technology; Jan 1996. Other requests for this document shall be referred to: WL/FIGC, 2210 Eighth St, Suite 11, WPAFB OH 45433-7521

WARNING - This document contains technical data whose export is restricted by the Arms Export Control Act (Title 22, U.S.C., Sec 2751, et seq.) or the Export Administration Act of 1979, as amended, Title 50, U.S.C., App. 2401, et seq. Violations of these export laws are subject to severe criminal penalties. Disseminate in accordance with the provisions of DOD Dir. 5230.25. (Include this statement with any reproduced portions.)

DESTRUCTION NOTICE: Destroy by any method that will prevent disclosure of contents or reconstruction of the document.

FLIGHT DYNAMICS DIRECTORATE
WRIGHT LABORATORY
AIR FORCE MATERIEL COMMAND
WRIGHT-PATTERSON AIR FORCE BASE, OHIO 45433-7562

NOTICE

This technical report has been reviewed and is accepted for publication.

William J. Gillard

WILLIAM J. GILLARD
Project Engineer
Control Dynamics Branch

Siva S. Banda

SIVA S. BANDA, Chief
Control Dynamics Branch
Flight Control Division

David P. LeMaster

DAVID P. LEMASTER, Chief
Flight Control Division
Flight Dynamics Directorate

If your address has changed, if you wish to be removed from our mailing list, or if the addressee is no longer employed by your organization, please notify WL/FIGC, 2210 Eighth St. Suite 11, WPAFB OH 45433-7521 to help maintain a current mailing list.

Copies of this report should not be returned unless return is required by security considerations, contractual obligations, or notice on a specific document.

The following notice applies to any unclassified (including originally classified and now declassified) technical reports released to "qualified U.S. contractors" under the provisions of DoD Directive 5230.25, Withholding of Unclassified Technical Data From Public Disclosure.

NOTICE TO ACCOMPANY THE DISSEMINATION OF EXPORT-CONTROLLED TECHNICAL DATA

1. Export of information contained herein, which includes, in some circumstances, release to foreign nationals within the United States, without first obtaining approval or license from the Department of State for items controlled by the International Traffic in Arms Regulations (ITAR), or the Department of Commerce for items controlled by the Export Administration Regulations (EAR), may constitute a violation of law.

2. Under 22 U.S.C. 2778 the penalty for unlawful export of items or information controlled under the ITAR is up to two years imprisonment, or a fine of $100,000, or both. Under 50 U.S.C., Appendix 2410, the penalty for unlawful export of items or information controlled under the EAR is a fine of up to $1,000,000, or five times the value of the exports, whichever is greater; or for an individual, imprisonment of up to 10 years, or a fine of up to $250,000, or both.

3. In accordance with your certification that establishes you as a "qualified U.S. Contractor", unauthorized dissemination of this information is prohibited and may result in disqualification as a qualified U.S. contractor, and may be considered in determining your eligibility for future contracts with the Department of Defense.

4. The U.S. Government assumes no liability for direct patent infringement, or contributory patent infringement or misuse of technical data.

5. The U.S. Government does not warrant the adequacy, accuracy, currency, or completeness of the technical data.

6. The U.S. Government assumes no liability for loss, damage, or injury resulting from manufacture or use for any purpose of any product, article, system, or material involving reliance upon any or all technical data furnished in response to the request for technical data.

7. If the technical data furnished by the Government will be used for commercial manufacturing or other profit potential, a license for such use may be necessary. Any payments made in support of the request for data do not include or involve any license rights.

8. A copy of this notice shall be provided with any partial or complete reproduction of these data that are provided to qualified U.S. contractors.

DESTRUCTION NOTICE

For classified documents, follow the procedures in DoD 5200.22-M, Industrial Security Manual, Section II-19 or DoD 5200.1-R, Information Security Program Regulation, Chapter IX. For unclassified, limited documents, destroy by any method that will prevent disclosure of contents or reconstruction of the document.

REPORT DOCUMENTATION PAGE

Form Approved
OMB No. 0704-0188

1. AGENCY USE ONLY *(Leave blank)*

2. REPORT DATE
March 1996

3. REPORT TYPE AND DATES COVERED
FINAL 10/22/94 - 01/31/96

4. TITLE AND SUBTITLE

INNOVATIVE CONTROL EFFECTORS (ICE)

5. FUNDING NUMBERS

C F33615-94-C-3609
PE 62201F
PR 2403
TA 05
WU 9D

6. AUTHOR(S)

E. L. Roetman, S. A. Northcraft, and J. R. Dawdy

7. PERFORMING ORGANIZATION NAME(S) AND ADDRESS(ES)

Boeing Defense and Space Group
P.O. Box 3999, M/S 4C-61
Seattle WA 98124-2499

8. PERFORMING ORGANIZATION REPORT NUMBER

9. SPONSORING/MONITORING AGENCY NAME(S) AND ADDRESS(ES)

Flight Dynamics Directorate
Wright Laboratory
Air Force Materiel Command
Wright-Patterson AFB OH 45433-7562

10. SPONSORING/MONITORING AGENCY REPORT NUMBER

WL-TR-96-3074

11. SUPPLEMENTARY NOTES

Export Restrictions Apply

12a. DISTRIBUTION/AVAILABILITY STATEMENT

Distribution authorized to U.S. Government agencies and their contractors; Critical Technology; Jan 1996. Other requests for this document shall be referred to WL/FIGC, 2210 Eighth St, Suite 11, Wright-Patterson OH 45433-7521

12b. DISTRIBUTION CODE

C

13. ABSTRACT *(Maximum 200 words)*

This report describes a joint U.S. Air Force - U.S. Navy sponsored investigation of innovative aerodynamic control concepts for fighter aircraft without vertical tails. Land-based and carrier-based configurations were analyzed to determine the flying qualities, performance, and aircraft-level integration impacts of the innovative controls. Six control concepts were evaluated for their potential to provide sufficient lateral-directional control power to a highly maneuverable tailless fighter. They were: (1) split ailerons; (2) movable chine strakes; (3) seamless leading and trailing edge flaps; (4) pneumatic forebody devices; (5) wing leading edge blowing; (6) wing mounted yaw vanes. After a preliminary screening, only the first two and a new concept, variable dihedral horizontal tails were chosen for further investigation. Detailed evaluations of the three selected controllers against baseline fighter configurations with vertical tails included low-speed, high-speed, and high AOA flying qualities performance, structural weight and subsystem integration impacts, signature performance, and carrier suitability impacts. The variable dihedral horizontal tail was evaluated as the best all-round control effector of those investigated. The split aileron and movable chine strake were ranked 2nd and 3rd, respectively.

14. SUBJECT TERMS
Tailless Aircraft, Lateral-Directional Control Power, Variable Dihedral Horizontal Tail, Split Ailerons, Movable Chine Strakes, Flight Control Effectors, Effector Integration

15. NUMBER OF PAGES
223

16. PRICE CODE

17. SECURITY CLASSIFICATION OF REPORT	18. SECURITY CLASSIFICATION OF THIS PAGE	19. SECURITY CLASSIFICATION OF ABSTRACT	20. LIMITATION OF ABSTRACT
UNCLASSIFIED	UNCLASSIFIED	UNCLASSIFIED	SAR

FOREWORD

This technical report summarizes research performed by The Boeing Defense & Space Group, Seattle, Washington 98124 on the Innovative Control Effectors (ICE) Study between October 1994 and January 1996 under Air Force Contract F33615-94-C-3609. The ICE study was co-sponsored by Wright Laboratory, Wright Patterson Air Force Base, Ohio and Naval Air Warfare Center of Warminster, Pennsylvania. Mr. William J. Gillard, WL/FIGC and Mr. Steve Hynes, NAWCADWAR were the technical monitors for this contract with Mr. Gillard serving as the USAF Program Manager.

The Boeing Defense & Space Group (BD&SG) Program Manager was Dr. Ernest L. Roetman, Chief Aerodynamicist of the Flight Organization. The overall Principal Investigator was Mr. Stephen A. Northcraft. Mr. John R. Dawdy was Principal Investigator for the Aerodynamic Stability and Control Study, Task 2.

Other key personnel included:

H. Beaufrere	Aerodynamic Stability and Control
D. Gilmore	Aerodynamic Stability and Control
J. Kuta	Aerodynamic Stability and Control
A. Meeker	Aerodynamic Stability and Control
J. O'Callaghan	Aerodynamic Stability and Control
R. Dailey	Flight Control System Development
J. Montgomery	Flight Control System Development
W. Herling	Computational Fluid Dynamics
T. Lowe	Signature Analysis
W. Price	Mechanical/Electrical Systems
J. Ott	Cost Analysis
W. Dean	Mass Properties
W. Mannick	Mass Properties
W. Moore	Configuration Integration
W. Bigbee-Hanson	Propulsion
S. Bockmeyer	Graphics

TABLE OF CONTENTS

		Page
FOREWORD		*iii*
TABLE OF CONTENTS		*iv*
LIST OF FIGURES		*vi*
LIST OF ACRONYMS		*ix*
LIST OF SYMBOLS		*xi*
SUMMARY		1
1.0	INTRODUCTION	5
2.0	TASK 1 - VEHICLE AND EFFECTOR SELECTION	7
	2.1 Selection of Baseline Vehicle	7
	2.2 Selection of Study Effectors	9
	2.3 Flight Condition Selection	11
3.0	TASK 2 - EFFECTOR PERFORMANCE STUDY	12
	3.1 Flight Condition Selection and Study Guidelines	13
	3.2 Database Descriptions and Limitations	15
	3.3 Flight Control System Description	19
	3.4 Effector Study Results (including Thrust Vectoring)	30
	3.5 Carrier Suitability Performance	58
	3.6 Summary of Performance Study	80
4.0	TASK 3 - EFFECTOR INTEGRATION STUDY	82
	4.1 Effector Integration Overview	82
	4.2 Actuation Study	87
	4.3 Carrier Suitability Requirements	91
	4.4 Thrust Vectoring Integration	94
	4.5 Radar Cross Section Analysis	99
	4.6 Summary of Integration Results	101
5.0	TASK 4 - RISK ASSESSMENT AND REDUCTION PLAN	102
	5.1 Aerodynamic Performance Risk Assessment	103
	5.2 Integration Risk Assessment	105
	5.3 Risk Assessment and Reduction Summary	106

TABLE OF CONTENTS (cont.)

		Page
6.0	CONCLUDING REMARKS	108
7.0	REFERENCES	110

APPENDICES

A	Summary of Candidate Control Effectors	112
B	Summary of Performance Results	128
C	Summary of Signature Data	175
D	Summary of Analysis of Variable Dihedral Horizontal Tail Concepts	193
E	Boeing Model-24F and Wind Tunnel Model 1798 Geometry Characteristics	208

LIST OF FIGURES

	Title	page
Figure 1	Innovative Control Effectors (ICE) Program Overview	4
Figure 2.1-1	Baseline Test Database	7
Figure 2.1-2	Baseline Aircraft	8
Figure 2.2-1	Innovative Control Effector Options	10
Figure 2.3-1	Analysis Flight Conditions	11
Figure 3.1-1	Performance Study Flight Conditions	13
Figure 3.1-2	Longitudinal and Directional Stability Level for Model-24F	15
Figure 3.2-1	Lift and Pitching Moments with Alpha Limits	17
Figure 3.3-1	Flight Control Law Block Diagrams	20
Figure 3.3-2	Use of Control Effectors by the Flight Control System	21
Figure 3.3-3	Control Effector Limits	22
Figure 3.4.1-1	Takeoff and Approach	32
Figure 3.4.1-2	Roll Control Effectiveness Landing Approach	33
Figure 3.4.1-3	Roll Control Effectiveness Approach-Thrust Vectoring	34
Figure 3.4.2-1	Power On Departure Stall	36
Figure 3.4.2-2	Departure Stall - Roll Rate Time Constant	37
Figure 3.4.2-3	Departure Stall - Roll Performance	38
Figure 3.4.2-4	Departure Stall - Lateral-Directional Dynamics	39
Figure 3.4.3-1	Air Combat Maneuver Corner Speed	41
Figure 3.4.3-2	Longitudinal Control in Maneuvering Flight - Baseline/Rotating Tail	43
Figure 3.4.3-3	Maximum Sustained Load Factor at Mid Altitude	44
Figure 3.4.3-4	Air Combat Maneuver Corner Speed	45
Figure 3.4.4-1	Penetration Speed	46
Figures 3.4.4-2	Maximum Sustained Local Factor - Penetration	48
Figures 3.4.4-3	Longitudinal Control in Maneuvering Flight - Penetration Speed	49
Figure 3.4.5-1	Maximum Sustained Load Factor	51
Figure 3.4.5-2	Maximum Sustained Load Factor at High Altitude - Subsonic	52

LIST OF FIGURES (Continued)

	Title	page
Figure 3.4.5-3	Longitudinal Control in Maneuvering Flight - Maximum Sustained	53
Figure 3.4.6-1	Supersonic Condition	55
Figure 3.4.6-2	Sustained Load Factor at High Altitude - Supersonic Penetration	56
Figure 3.4.6-3	Longitudinal Control in Maneuvering Flight - Supersonic Condition	57
Figure 3.5-1	Pop-up Maneuver-RPAS Simulation Results	61
Figure 3.5-2	Pop-up Maneuver - Comparison between RPAS and MEATBALL	62
Figure 3.5-3	Wave-off Maneuver-RPAS Simulation Data	63
Figure 3.5-4	Wave-off Maneuver - Comparison between RPAS and MEATBALL	64
Figure 3.5-5	Level Flight Longitudinal Acceleration	65
Figure 3.5-6	Flight Path Stability-Comparison between RPAS and MEATBALL	67
Figure 3.5-7	Flight Path Stability-RPAS Comparison to Baseline	68
Figure 3.5-8	Landing Approach Nose Down Pitch Acceleration - 22° Angle-of-Attack	61
Figure 3.5-9	30 Knot at 90°Crosswind	70
Figure 3.5-10	30 Knot at 90° Crosswind - Rotating Tails,Spit Aileron with Thrust Vectoring	71
Figure 3.5-11	Carrier Suitability Roll Rate Summary	73
Figure 3.5-12	Dutch Roll Characteristics	74
Figure 3.5-13	V_{mc} with Right Engine Out	75
Figure 3.5-14	Catapault Launch	77
Figure 3.5-15	Critical Requirements for Carrier Takeoff and Approach	78
Figure 3.6-1	Flight Condition and Flying Qualities Items	81
Figure 4.1-1	Benefits from Removing Vertical Tail	83
Figure 4.1.1-1	Chine Strake Installation	83
Figure 4.1.2-1	Split Aileron Installation	84

LIST OF FIGURES (Continued)

	Title	page
Figure 4.1.3-1	Rotating Horizontal Tail Installation	85
Figure 4.1.3-2	Cycles vs. Hinge Moment	86
Figure 4.2-1	Electrical and Hydraulic Actuator Candidates	89
Figure 4.3-1	Approach Speed	92
Figure 4.3-2	Mark 7 Mod 3 Arresting Engine	92
Figure 4.3-3	USN Baseline Weight Buildup	93
Figure 4.4-1	Thrust Vectoring Nozzle Mounting Concepts	95
Figure 4.4-2	Thrust Vectoring Nozzle Concepts	96
Figure 4.4-3	Thrust Vectoring Figures-of-Merit	97
Figure 4.4-4	Determinant-Attribute Model	98
Figure 4.5-1	Signature Comparison 50%	99
Figure 4.5-2	Signature Comparison 96%	99
Figure 5.0-1	Risk Rating Guide	102
Figure 5.1-1	Future Testing	103
Figure 5.1-2	Performance Risk Assessment	104
Figure 5.2-1	Integration Risk Assessment	105
Figure 5.3-1	BMA-S-1768-6A Model	107

LIST OF ACRONYMS

6DOF	Six Degrees of Freedom
A/A	Air-to-Air
A/G	Air-to-Ground
ACM	Air Combat Maneuver
ADAPT	Data Plotting Program
AGPS	Aerodynamic Grid & Panel System
AEOLAS	Aeroelastic Prediction Code
AOA	Angle-of-Attack
ARBSCAT	Signature Prediction Code
BD&SG	Boeing Defense & Space Group
BMA	Boeing Military Airplanes
BSWT	Boeing Supersonic Wind Tunnel
CFD	Computational Fluid Dynamics
EHA	Electro Hydraulic Actuator
EMA	Electro Mechanical Actuator
FCS	Flight Control System
FDWT	Flight Design Weight
IA	Integrated Actuator
ICE	Innovative Control Effectors
IR	Infrared Radiation
IRAD	Internal Research and Development
JAST	Joint Advanced Strike Technology
JAF	Joint Strike Fighter
KEHS	Equivalent air speed in knots
LaRC	Langley Research Center
LE	Leading Edge
LO	Low Observable
LQR	Linear Quadratic Regulator

LIST OF ACRONYMS (Continued)

LRU	Line Replaceable Unit
MAC	Mean Aerodynamic Center
MRF	Multi-Role Fighter
NASA	National Aeronautics and Space Administration
NAWCADWAR	Naval Air Warfare Center, Aircraft Division, Warminster, PA
PANAIR	Panel method potential flow code
PIO	Pilot Induced Oscillation
PLTSUM	Total Vehicle Signature Budgeting Code
RCAH	Pitch Rate Command Altitude Hold
RCS	Radar Cross Section
RM&S	Reliability, Maintainability, and Supportability
RPAS	Rapid Prototype Analysis System
SCFN	Spherical Convergent Flap Nozzle
SI	Structurally Integrated
SISO	Single-Input Single-Output
TE	Trailing Edge
TV	Thrust Vectoring
TOGW	Takeoff Gross Weight
USAF	United States Air Force
USN	United States Navy
WL	Wright Laboratory
XPATCH	Ray Trace, Physical Optics Signature Prediction Code

List of Symbols

CL	Lift Coefficient
CL_o	Lift Coefficient at Zero Angle of Attack
CL_α	Rate of Change of Lift Coefficient with Respect to Angle of Attack (/degree)
V_{mc}	Minimum Control Speed (knots)
V_{STALL}	Stall Speed (knots)
V_s	Stall Speed (knots)
V_{pa}	Velocity of Approach (knots)
U	Forward Velocity in Body Axis x-direction (knots)
V	Velocity in Body Axis y-direction (knots)
W	Velocity in Body Axis z-direction (knots)
P	Roll Rate (radian/sec)
R	Yaw Rate (radian/sec)
Q	Pitch Rate (radian/sec)
Qbar	Dynamic Pressure (lbs/Ft^2)
n_z	Load factor for pitch control inputs
Nz	Load factor for pitch control inputs
$\dot{q}$	Pitch Acceleration ($radians/sec^2$)
k	Break Point Frequency
s	Transform Frequency Variable
α	Angle of Attack (degrees)
α_{app}	Angle of Attack for Carrier Approach (degrees)
β	Side Slip Angle (degrees)
$\frac{\delta \gamma}{\delta \nu}$	Flight Path Stability (degrees/knot)
$\Delta \frac{\delta \gamma}{\delta \nu}$	Difference in Flight Path Stability Slopes (degrees/knot)
ω_{nd}	Undamped Natural Frequency of the Dutch Roll Oscillation (radians/sec)

List of Symbols Contd.

ζ_d	Damping Ratio of the Dutch Roll Oscillation
ϕ	Bank Angle (degrees)
Γ_H	Dihedral Angle of the Rotating Tail (degrees)

SUMMARY

This report reviews work performed by the Boeing Company under USAF contract F33615-94-C-3609 Innovative Control Effectors (ICE). This is a joint Air Force and Navy program whose purpose is to develop and analyze aerodynamic control devices applicable to modern tactical aircraft where it is desired to eliminate or at least severely reduce the size of the vertical tail surfaces for reduced vehicle signature. The program addresses the development of a control device, or set of devices, effective across the broad flight envelope of tactical aircraft with minimal size, weight, cost and aerodynamic hinge moments. All this to be achieved while maintaining acceptable vehicle signature properties. Careful attention is to be given to the performance, signature and integration issues associated with the devices.

This document reports on the activity of the first phase of the two phase ICE program. Phase I covers initial selection and development of devices along with preliminary screening analysis for effectiveness. A proposed Phase II will concentrate on the testing and validation of selected effectors deemed to have the most promise. This contract was divided into four distinct tasks :

(1) Selection of a baseline vehicle concept and the identification of a set of control devices to study.

(2) The effector performance study selected three devices for detailed study and assessed their performance alone and in combination.

(3) The effector integration study task looked at the system impact of the chosen effectors.

(4) The risk reduction study addressed the technical risks associated with the selected effectors/and proposed future work to reduce the risks of implementation.

A baseline vehicle concept with which to evaluate control device effectiveness was required for realistic evaluation. The selected vehicle for this work was a Boeing advanced tactical aircraft concept, designated the Model-24F, a single engine, diamond wing, chined forebody configuration with conventional empennage designed for both air-to-air and air-to-ground missions as part of the multirole fighter design study. The vehicle and the corresponding data base was described in detail in the body of the report. As this is a joint services program, two baselines were carried, the

second being a vehicle with proposed adjustments (such as increased wing area, ...) to accommodate Navy specific performance and operational objectives.

The effectors initially chosen for study as offering the best potential for satisfying the operational requirements were a pneumatic forebody device, a movable chine/strake, wing leading edge blowing, wing mounted yaw vanes, split ailerons and seamless leading edge and trailing edge which was later replaced with a unique variable dihedral horizontal tail. A representative set of six flight conditions was chosen for assessing the effectiveness of the concepts.

The performance study was a dominant part of this effort. After initial performance screening, the number of effectors for detailed analysis was reduced to two concepts, chine stakes and split ailerons, as having the most promise of satisfying the requirements. In the search for a more promising device the concept of a variable dihedral (rotating) horizontal tail was proposed. These three concepts were then analyzed in greater detail. The performance of chine strakes was after further study deemed below that desired, and their integration into the vehicle posed such difficulty that this concept was not fully studied. The split aileron concept was found to be adequate for marginal control at low angles of attack, but its effectiveness dropped off dramatically at angles of attack above ten degrees. For the more stringent carrier suitability requirements it was not adequate.

The rotating horizontal tail was found to be effective throughout the flight envelope of interest including carrier operations. It therefore received the most attention.

Performance studies for the combined effectiveness of the rotating tail and split ailerons were conducted to determine the gains that might be achieved with integrated multiple aerodynamic effectors. For completeness, a limited comparison with the inclusion of thrust vectoring was done.

The performance analysis of the control effectiveness was done by defining an appropriate, integrated, modern set of control laws for the baseline configuration and the control device configurations. The control laws were then combined with the available aerodynamic data and subsequently included in full six degree of freedom vehicle simulations to investigate the control device characteristics and the vehicle flying qualities.

The feasibility of using any control effector is dependent on how it is to be incorporated into the vehicle. Successful incorporation requires the efforts of several technical disciplines investigating issues of structure, actuation, weight, signature, cost and the operational demands.

The integration of chine strakes has many difficulties. The forebody area near the cockpit is critical real estate for radar systems and a sensitive area for signature control. Since the performance of this device was of limited effectiveness, a complete integration was not performed.

The integration of the split aileron exposed concerns for the thickness of the outboard wing, the actuation concept and the effects on the radar cross section. These issues were investigated in some detail.

The rotating horizontal tail shows great promise if it can be reasonably incorporated into a vehicle design. Since this is a unique concept without a design history, it required additional effort at integration. The developed actuation concept did not have an excessive weight penalty. Within an appropriate design philosophy it seems that this is a viable concept worthy of further investigation.

Risk is apparent in incorporating any of the actuator concepts, both in performance and integration. The risks associated with each selected effector are outlined in the report. Additional data are needed in each case, but especially for the rotating tail which has no significant data base due to its novelty. Additional wind tunnel testing focused on the data sparsity for application of these concepts will significantly reduce the risk in transitioning the concepts to application.

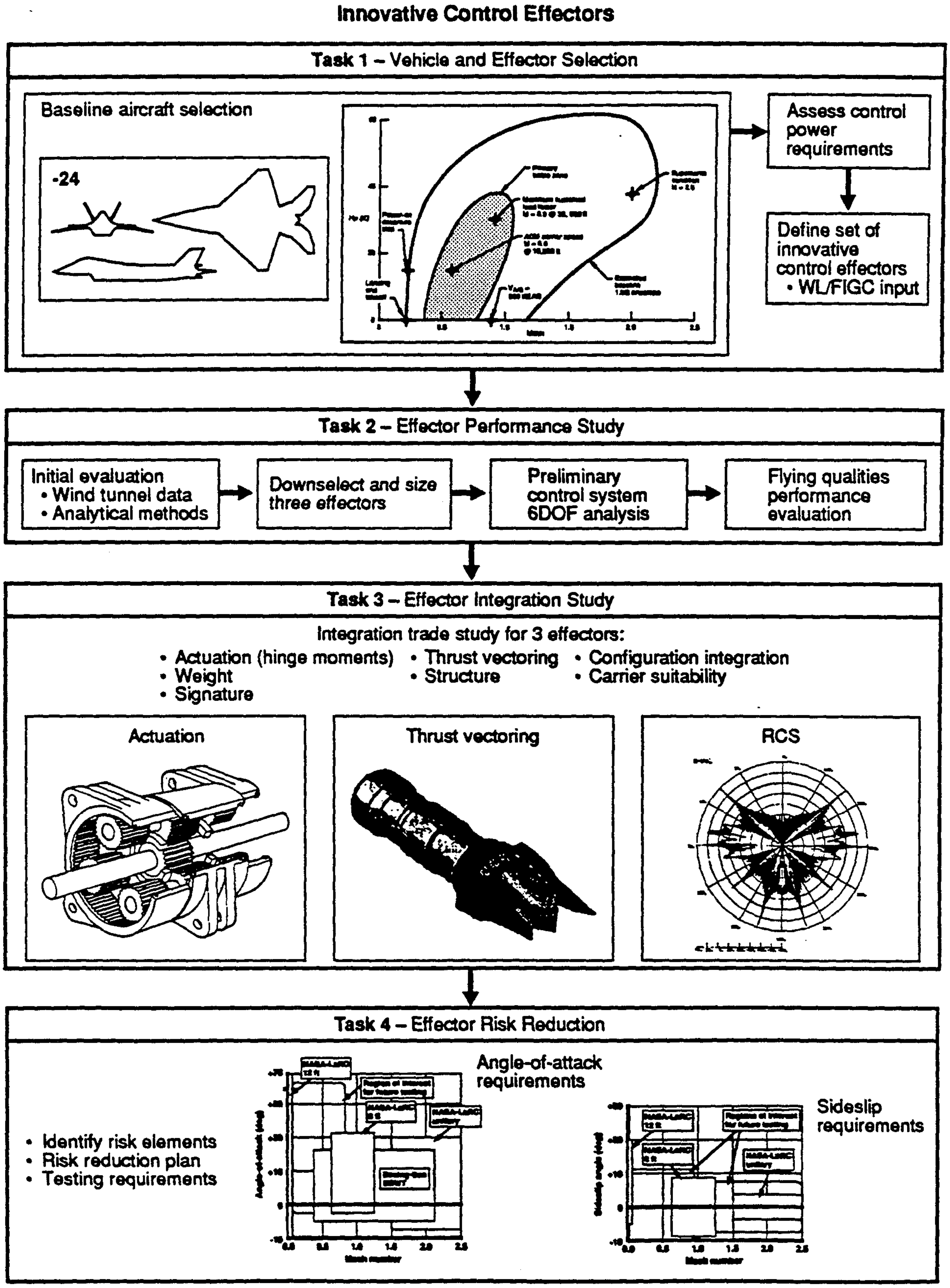

Figure 1. Innovative Control Effectors (ICE) Program Overview

-Ad11

1.0 Introduction

The purpose of the Innovative Control Effectors (ICE) program is to develop and analyze innovative aerodynamic control devices that might be applied to joint advanced strike aircraft with either nonexistent or reduced size vertical tail surfaces. This contract addresses the continuing need to develop new aerodynamic control effectors which are effective across a broad flight envelope with minimal integration impact while maintaining acceptable vehicle signature properties.

The objective of this contract is to develop a control effector or set of effectors which will achieve the goal of reducing or eliminating the vertical tail surfaces while maintaining vehicle lethality and improving survivability. The focus of this contract is to study the performance and integration issues associated with innovative control effectors, and develop an effector, or set of effectors, which can be integrated into future aircraft and achieve the goals stated above.

The overall ICE effort is divided into two phases. Phase I covers the initial development and preliminary analysis of the candidate effectors, while Phase II will concentrate on the testing and validation of the chosen effector concepts.

This contract is focused on the Phase I efforts and is divided into four distinct tasks. The first task is the selection of the baseline vehicle concept and the identification of a set of control effectors for inclusion in this study. The second task, the effector performance study, consists of the final selection of a set of three effectors for detailed analysis and conducting an assessment of the performance characteristics of these effectors separately and in combination. This assessment includes detailed 6 degree of freedom (6DOF) analysis using the Boeing Rapid Prototype Analysis Program (RPAS) to build a preliminary flight control system for the baseline aircraft with these effectors. The third task, the effector integration study, addresses a broad range of integration issues involving multiple technologies and the impact on the overall system of each selected effector. The final task addresses the technical risks and requirements for further development associated with the selected effector concept(s). The purpose of this task is to develop an overall risk reduction scheme and propose testing and other validation exercises which will reduce the risks associated with introducing new control effector schemes onto advanced aircraft.

As a joint Air Force and Navy contract, certain aspects of the contract were unique to each of the services. The selection of the baseline vehicle required carrying two baseline aircraft to separately assess the aircraft carrier unique operational requirements of USN aircraft and reconfiguring the vehicle layout to meet the specific performance and operational objectives.

2.0 Task 1

2.1 - Selection of Baseline Aircraft

The baseline aircraft chosen for this effort was the Boeing developed advanced tactical aircraft designated the Model-24F, which is a single engine, diamond wing configuration with a conventional empennage designed for both the air-to-air and air-to-ground missions. The wing design is similar to the F-22, with standard control surfaces including ailerons, flaperons, horizontal tail, and rudders. Thrust vectoring (TV) is available on the baseline vehicle, resulting in reduced empennage size to take advantage of this capability. The reduced vertical fin size results in directionally unstable aircraft at supersonic speeds, but stability is augmented by sideslip feedback to the rudders. Extensive wind tunnel data are available for this configuration and are summarized in Figure 2.1-1. For these tests, two complete wind tunnel models, 12.5% and 5% scale, were constructed and tested at NASA's Langley Research Center and at Boeing-Seattle. These tests resulted in a database ranging in velocity from 0.05 to 2.50 Mach. The vehicle characteristics are summarized in Figure 2.1-2, the geometry is described in Appendix E. Flight characteristics of the baseline vehicle are included in the performance data assembled in Appendix B.

Note that a second baseline aircraft was defined (see Section 4.3) to meet the USN carrier suitability requirements.

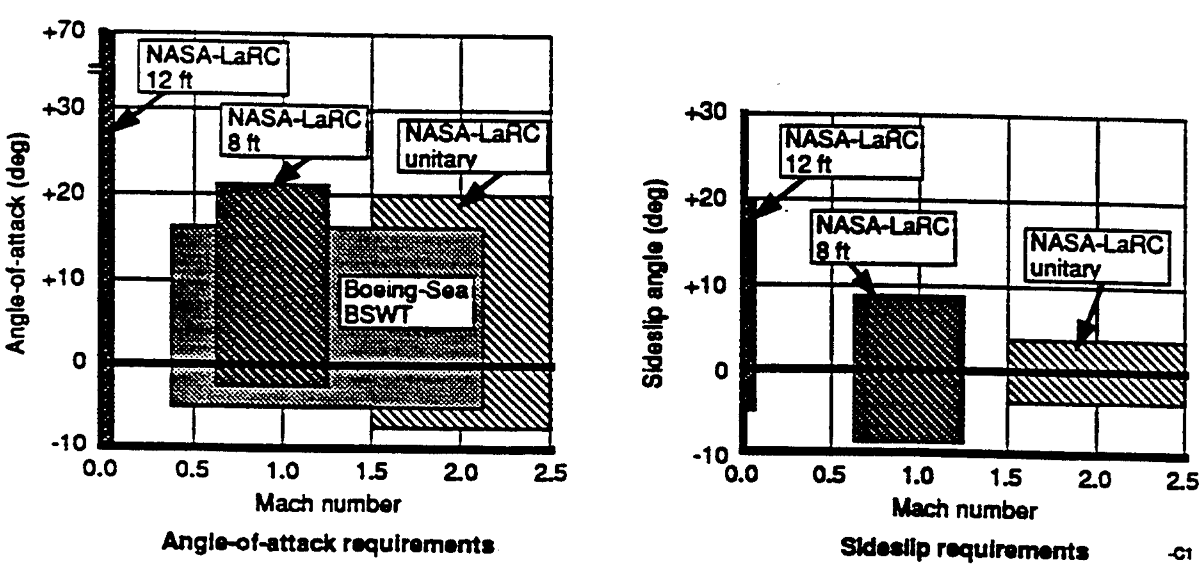

Figure 2.1-1. Baseline Test Database

• **Model -24**

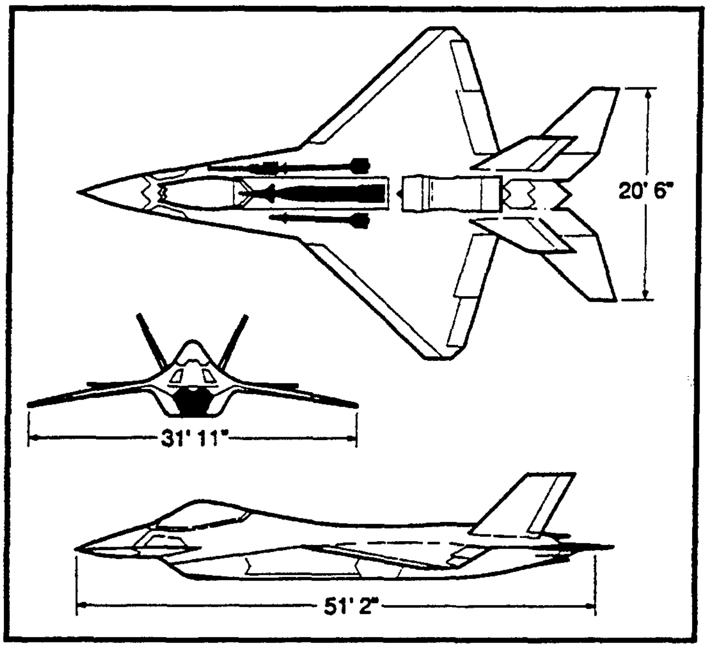

General

• 1998 technology, 2005 IOC	
• Single crew	
• FDWT: mission TOGW – 0.5 internal fuel	
• Design LF: 9g @ FDWT, GR/TP structure	
• Q-placard: 2,130 psf, M1.2 @ S.L.	
• Maximum internal fuel capacity (lb)	8,690
• Installed avionics (lb)	1,598

Weights

• Takeoff gross weight	34,720
• FDWT	25,460
• Operating weight empty	19,980
• Mach, combat/max	0.9 / 2.2

Propulsion (lb)

• Sea level static A/B, installed (lb)	
• T/W @ takeoff gross weight	
• Nozzle	2-D/C-D, TV
• Inlet	Fixed

Geometry

• Wing area, ref (sq ft)	465
• W/S @ takeoff gross weight (psf)	74.7
• Wing aspect ratio/taper	2.20 / 0.13
• Wing sweep, LE/TE (deg)	47.5 / 17.0
• Wing t/c @ (SOB/tip) (%)	4.5 / 3.0

-Ad1

Figure 2.1-2. Baseline Aircraft

2.2 - Selection of the Study Effectors

The initial list of possible candidates for study during this effort is shown in Figure 2.2-1. From this original list of candidate devices, the following were chosen for further study:

- Pneumatic Forebody Vortex Control
- Moveable Chine/Strake
- Wing Leading Edge Blowing
- Wing Mounted Yaw Vanes
- Split Aileron Devices
- Seamless Moveable Leading Edges and Trailing Edges

The criterion for selecting these devices was that they exhibit the greatest potential for meeting the objectives of the study. A secondary criterion was to study devices which differed in the primary axis of operation, the location on the vehicle, and the flow physics involved in the effector operation. The above concepts were chosen because they offered the best potential for meeting the performance enhancement goals of this contract with minimal impact on integration. A summary of each of the control options shown in Figure 2.2-1 is included in Appendix A.

Reduction from six to three effectors resulted from further analysis of the six effectors to more effectively screen them for those that looked to be the most promising effectors. The baseline vehicle database was reviewed and its flying qualities simulated. The simulation was adjusted to assess the relative effectiveness of the individual control element. The down selection was guided by the criteria that the primary focus of the study was lateral-directional control capacity, that there be possibility for realistic integration of the control element and that the effectors be distributed around the vehicle.

We readily agreed to select the moveable chine/strake and split aileron devices. The choice of the third effector was more difficult, and it was finally resolved by introducing the concept of variable dihedral all moving tail elements "rotating tail" concept that became the third effector.

Control effector	Primary control function	Benefits	Risk
Porous forebody	Yaw and pitch control	Improves yaw control at moderate and high alphas. This yaw control is used to roll around the velocity vector.	Operating phenomena not well understood. Supersonic characteristics unknown. Limited database. Stealth may be poor. Hard to integrate with radar.
Pneumatic forebody vortex control	Yaw and pitch control	Improves yaw control at moderate and high alphas. This yaw control is used to roll around the velocity vector.	Limited success on chined forebodies. Unknown supersonic characteristics. Signature impact unknown and hard to integrate with radar.
Nose yaw vanes	Yaw control	Improves yaw control at moderate and high alphas. This yaw control is used to roll around the velocity vector.	Stealth may be poor. Integration with radar is difficult.
Vortex flaps, outboard fraction of wing span	Yaw and pitch control	Exploits special features of the leading edge vortex on highly swept wings.	May not be effective at 1 g or at supersonic speeds.
Differential H tail for moderate and high alpha yaw control	Yaw and roll control	Enhance roll capability. Roll around the velocity vector.	Larger actuator range. Complex software. Simultaneous control issues.
Differential canard deflections for moderate and high alpha yaw control	Yaw and roll control	Enhance roll capability. Roll around the velocity vector.	High signature levels.
Pivoting wing tip fins for side force	Low alpha side force	Exploit flat turns for heading agility. Stealth during air-to-ground maneuvering.	Heavy. Defeats the concept.
Fuselage mounted vanes side force	Low alpha side force	Skid turns for stealth air-to-ground weapon delivery.	May not be a net stealth improvement.
Differential leading edge flaps for roll control	Roll control	Improves roll control.	Roll reversal occurs, consequently need special software combined with a thorough database to define the reversal alpha with Mach and flexibility effects.
Seamless LEF and TEF hinges	L/D and stealth improvement	Extrapolation of MAW technology. Eliminates the seams associated with conventionally hinged flaps.	4 bar linkages are heavy and complex.
Wing tip split panel flaps	Yaw control	Can be used to replace the rudders. Good alt low alpha. Effective at all alphas. Effective for full flight envelope.	Supersonic characteristics not well known. Defeats stealth if used at 1 g.
Wing mounted yaw vanes mounted like spoilers or pop up vanes	Yaw control	Can be used to replace the rudders. Good alt low alpha. Effective at all alphas. Effective for full flight envelope.	Supersonic characteristics not well known. Defeats stealth if used at 1 g.
Speed brake using crossed controls	Speed brake functions	Eliminates a dedicated speed brake panel. Saves empty weight. Improves stealth by deleting seams.	May not meet deceleration goals.
Wing leading edge blowing	Lift enhancement, roll control	Maintain attached vortex wing flow to higher angles-of-attack.	Weight penalty, interference with standard high lift system.
Circulation control (wing trailing edge blowing)	Lift enhancement, roll control	Increased wing circulation and lift at given flight condition.	Weight penalty, integration with trailing edge flaps.
Variable dihedral horizontal tail	Yaw and pitch control	Remove vertical tails lower RCS	Could be heavy, complex interference with wing – could reduce effectiveness
Thrust vectoring with inflight thrust reversing	Speed brake functions	Eliminates a dedicated speed brake panel. Saves empty weight. Improves stealth by deleting seams.	Expensive and heavy, and non-stealthy. Poor IR and RCS.
Thrust vectoring pitch	Pitch control	Allows size of the horizontal tail to be reduced. Excellent low speed control for takeoff rotation. Significantly improves airplane pitch agility.	Difficult to compensate for operations at or near flight idle. Expensive, heavy, and non-stealthy. Poor IR.
Thrust vectoring yaw	Yaw control	Maybe the answer to making a finless airplane. Full flight envelope yaw control.	Difficult to compensate for operations at or near flight idle. Expensive, heavy, and non-stealthy. Poor IR. -W1

Figure 2.2-1. Innovative Control Effector Options

2.3 Flight Condition Selection

In evaluating the chosen effectors, a representative set of flight conditions was chosen for assessing the vehicle performance. These conditions were selected to offer a wide range of operational capability to adequately determine the control characteristics of each of these effectors. The conditions chosen are summarized in Figure 2.3-1.

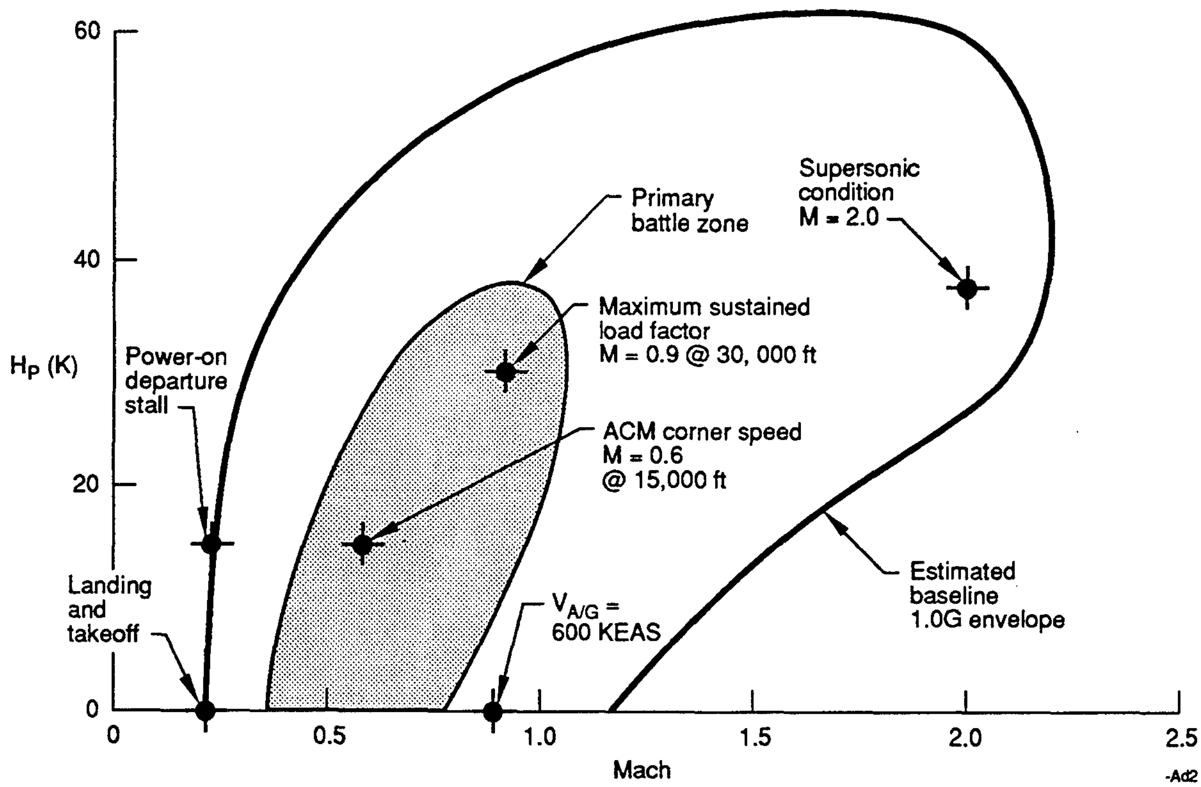

Figure 2.3-1. Analysis Flight Conditions

3.0 TASK 2 - EFFECTOR PERFORMANCE STUDY

The primary focus of the effector performance study was to evaluate the selected effectors and determine if Level 1 flying qualities could be achieved for a fighter size aircraft without a vertical tail or one of reduced size. No matter how effective a control surface is at high angle of attack, if it cannot be used to achieve adequate flying qualities in the normal flight regime, it may not be a viable option. Consequently this performance study will be valuable in the selection of realistic innovative control effectors. Of course, combinations of effectors may meet specific requirements in some flight regimes if the significance of the requirement will support the weight and cost penalties. The high angle of attack evaluation was beyond the scope of the current aerodynamic data base.

Three effectors were used in the performance study:

- Split Ailerons
- Chine Strakes
- Rotating Tail

The effectors were evaluated individually with the vertical tails removed. Additionally the baseline Model-24F (with vertical tails and rudders) was evaluated to provide a reference performance baseline. Limited evaluation of a combination of Rotating Tail and Split Ailerons with and without 2 axis thrust vectoring was also conducted. The performance study was conducted with an operating flight control system due to the instability of the configuration about the longitudinal axis, for subsonic speeds, and directionally with the vertical tails off.

3.1 Flight Condition Selection and Study Guidelines

The performance study was conducted at six flight conditions which were selected with WL/FIGC and NAWC concurrence. These conditions are summarized in Figure 3.1-1.

Flight Condition	Gross Weight (lbs)	Altitude (ft)	V_e/Mach	Leading Edge Flaps	Trailing Edge Flaps
Takeoff and Approach	25,000	1,000	132 kts	TO/LDG	30°
Power-On Departure Stall	27,000	15,000	Maximum Database Angle of Attack	Transonic Maneuver	0°
Air Combat Maneuver Corner Speed	27,000	15,000	0.6	Transonic Maneuver	0°
Penetration Speed	27,000	1,000	600 kts	Transonic Cruise	0°
Maximum Sustained Load Factor	27,000	30,000	0.9	Transonic Maneuver	0°
Supersonic Condition	27,000	35,000	2.0	Supersonic Cruise	0°

Figure 3.1-1 Performance Study Flight Conditions

These flight conditions are also plotted on the flight envelope shown in Figure 2.3-1.

The Boeing Rapid Prototype Aircraft Simulation (RPAS) software tool was used to compute trims and maneuver time histories at the flight conditions. The performance of the airplane, with the various effectors, was evaluated against MIL-F-8785C and MIL-STD-1797A. The criteria selected did not include control force requirements because it was assumed that an artificial "feel" system would be used and could be tailored to meet the specifications.

The evaluation was conducted at the aft center of gravity (38% MAC) which was assumed to be the critical condition. An active flight control system was included for all of the performance studies due to the instability of the Model-24F. The configurations were longitudinally unstable at aft center of gravity for subsonic speeds and with the vertical tails removed the vehicle was directionally unstable at all Mach numbers. The longitudinal and directional stability levels are shown in Figure 3.1-2.

The evaluation of the rotating tail effector was limited to a single fixed dihedral configuration in this study in order to reduce the impact on the flight control system. Inclusion of horizontal tail dihedral variation in the control system results in multiple solutions for trim and control inputs. The weighting functions required for the automatic selection of dihedral angle must be developed with additional testing and evaluation of other criteria than aerodynamic forces and moments. For this performance study the rotating tail effector was fixed at 20° of dihedral on each side.

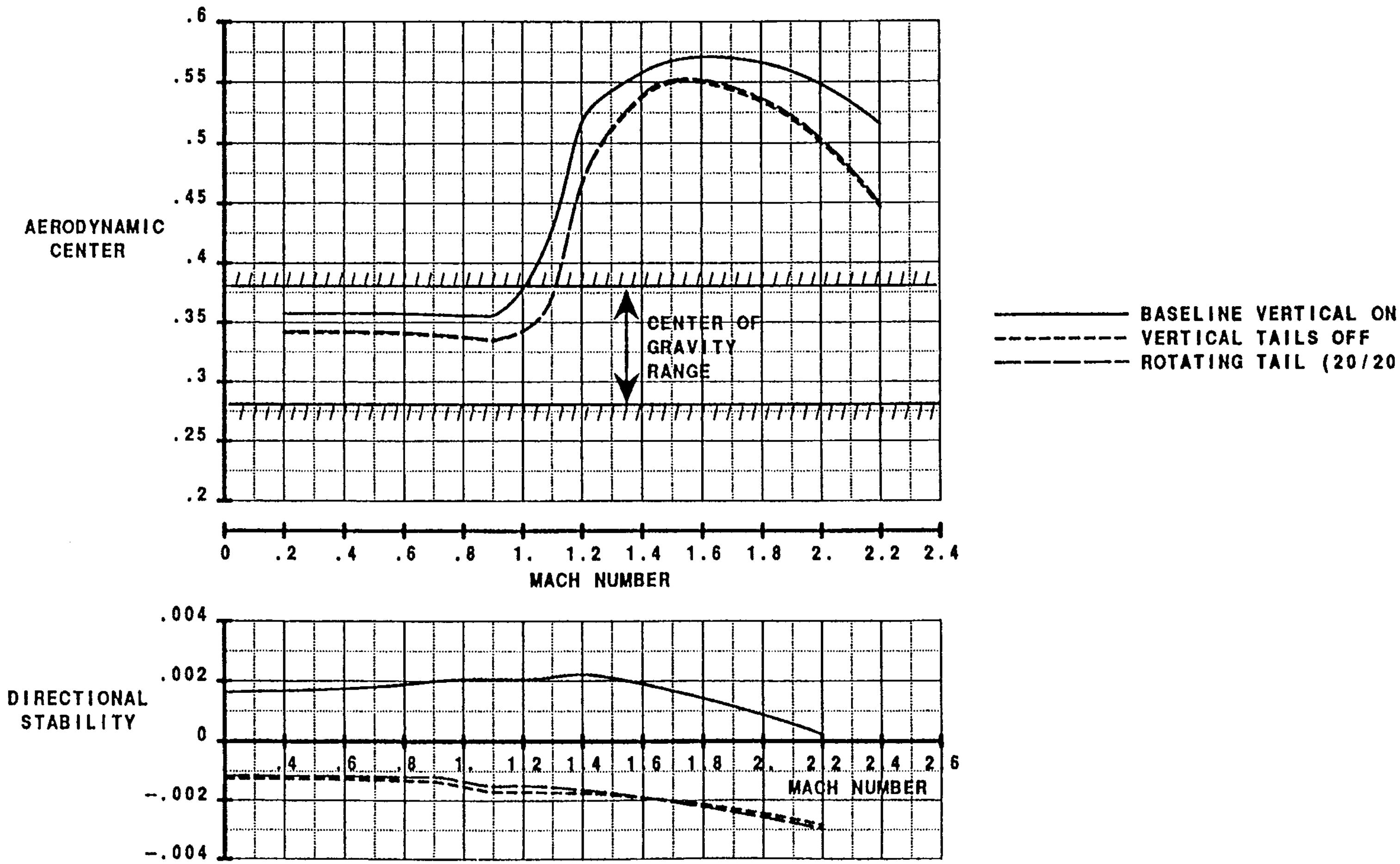

Figure 3.1-2 Longitudinal and Directional stability Level for Model-24F

3.2 Database Description and Limitations

The Model-24F aerodynamic data base used in the RPAS simulation is based on wind tunnel test data along with analytical results described below. The wind tunnel test data included a test in the Langley Unitary Tunnel, conducted in May of 1991, a Langley 8 ft Transonic test, LaRC 1039 conducted in September 1992, and a transonic/supersonic test in the Boeing Supersonic Wind Tunnel, BSWT 633 conducted in August 1995. The BSWT 633 test included the use of the transonic insert to allow test at Mach numbers down to 0.4. Analytical studies were conducted using the Boeing AEOLAS program which is a code based on a linear potential flow code called PANAIR. The AEOLAS program was used to estimate rate derivatives and to assess the impact of configuration changes for which no wind tunnel test data are available.

The aerodynamic data base covers the Mach range from 0.2 to 2.2 and is structured to allow the user to select tails on or off and which effectors are operational. The aerodynamic data are referenced to body station 475 (35% MAC) and the moments transferred to the user selected center of gravity.

The range of Mach number, angle of attack, and sideslip for each of the tests is shown in Figure 3.1-2. The simulation database limits are $-4° \leq \alpha \leq 22°$ and $-10° \leq \beta \leq +10°$. Figure 3.2-1 shows an example of the lift and pitching moment curves with the simulation database limits. These data are from a test in the Langley 12 ft tunnel conducted in October of 1991. These data show that the simulation data base is valid down to approximately 1.2 VSTALL. The test data at higher angles of attack from the 12 ft test was at very low speed and was not extensive enough to allow for its inclusion in the aerodynamic database.

The sideslip limits were eliminated for the carrier suitability study and the simulation was allowed to extrapolate on the database. This was done to allow the carrier landing crosswind studies to be completed.

The mass model used in the performance study was simplified since the majority of the study was conducted at one gross weight and center of gravity. No change in inertia's with weight and center of gravity were programmed. The inertia's in the mass model were changed for the carrier suitability portion of the study.

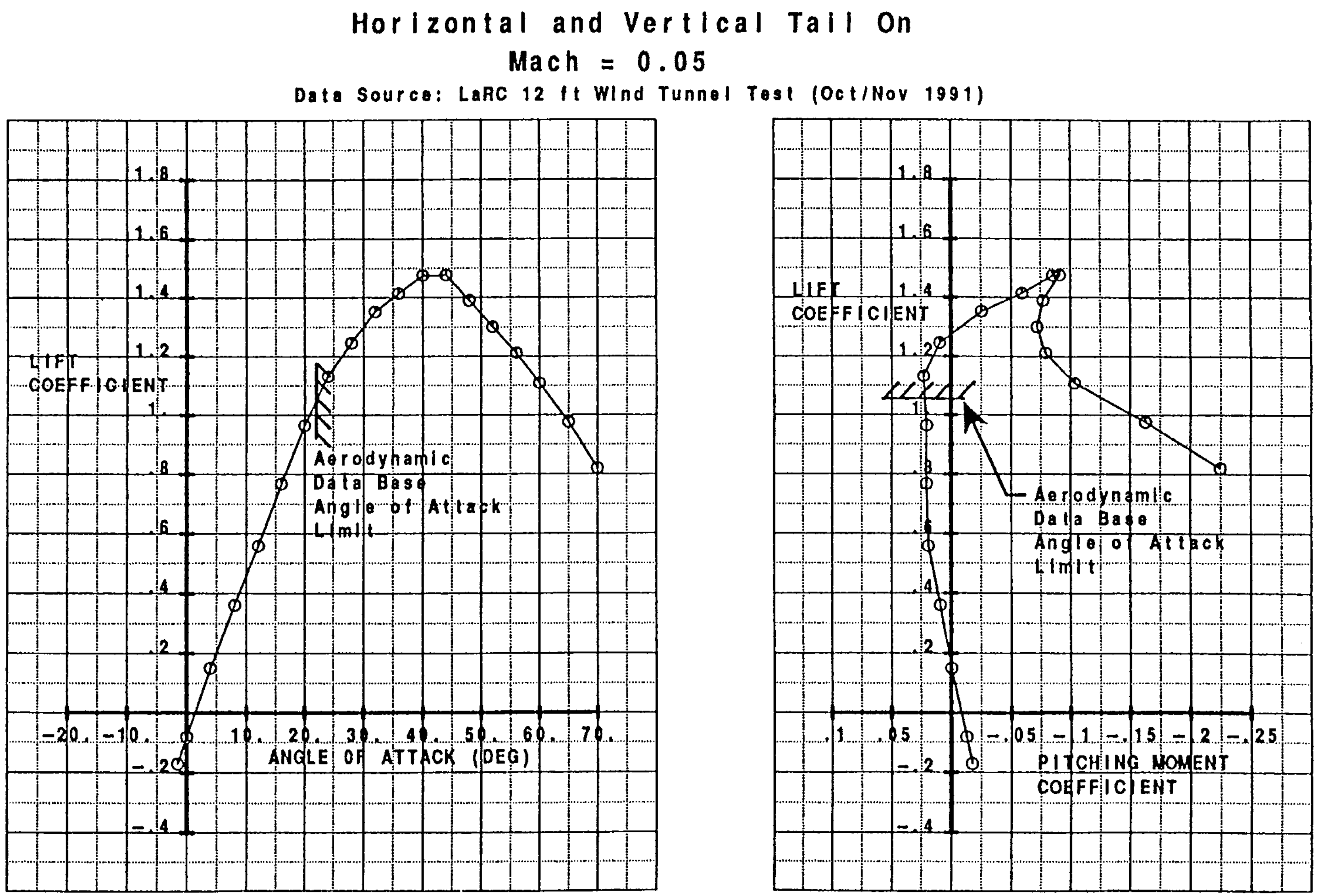

Figure 3.2-1 Lift and Pitching Moments with Alpha Limits

A simplified engine model of the F119 thrust class was also used. Engine dynamics were approximated using first order lags. The gross thrust and ram drag were implemented as a function of Mach number and altitude. This engine model was not developed as part of the ICE contract but was one used for a number of Boeing IRAD studies over the years.

No landing gear dynamic model was included in the MEATBALL model for the carrier performance study. A drag increment due to landing gear deployment was included as part of the aerodynamic model.

3.3 Flight Control System Description

The evaluation of effectiveness of control elements requires a baseline operational capability. The as drawn, as tested vehicle, the Model-24F, that we are using in this study is longitudinally unstable at aft CG in subsonic flight, thereby, requiring a flight control system definition in enough detail to have a meaningful simulation for operational flying qualities. A flight control system has been developed for the Model-24F based on the aerodynamic data base for modeling in the simulation program RPAS. Figure 3.3-1 illustrates a summary diagram of the flight control law.

The flight control system was optimized, subject to some constraints such as rate and position limits, for the baseline and the effector configurations to provide the most realistic simulation. The control laws developed are very integrated, blending all the available effectors to optimize the total control effectiveness of the overall vehicle. Figure 3.3-2 presents a summary of the use by the flight controls system of the various effectors and combinations of effectors.

There are limiting values to effector operations in both the extremes and rates. For reference, Figure 3.3-3 contains a list of the effector limits assumed for this study.

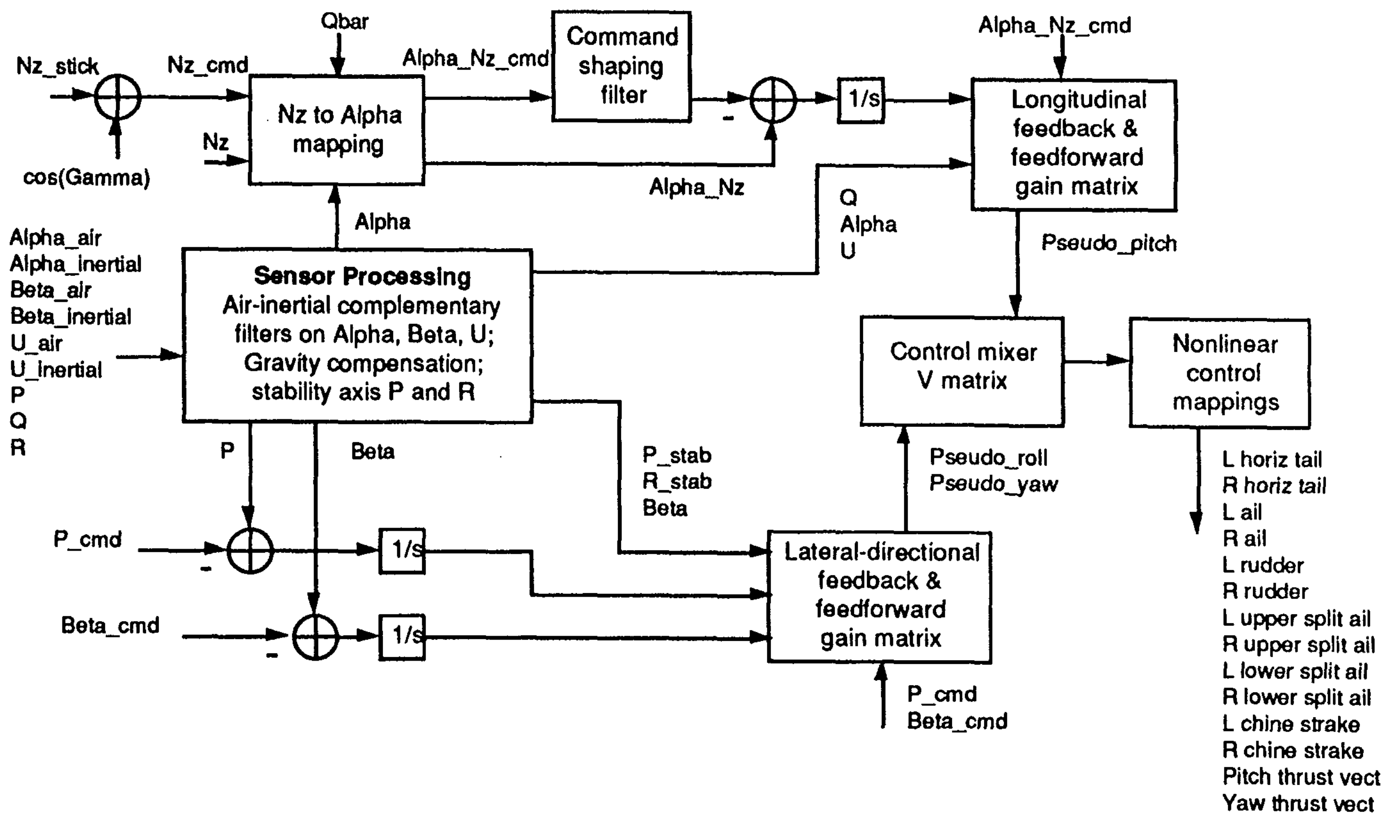

Figure 3.3-1 Flight Control Law Block Diagram

With Vertical Tails	Without Vertical Tails				
Baseline no TV	**Split Ailerons no TV**	**Chine Strakes no TV**	**Rotating Tail (Γ_H = 20°/20°) no TV**	**Rotating Tail+ Split Ailerons no TV**	**Rotating Tail+ Split Ailerons with TV**
6 Effectors • Left Horizontal Tail • Right Horizontal Tail • Left Rudder • Right Rudder • Left Aileron • Right Aileron	6 Effectors • Left Horizontal Tail • Right Horizontal Tail • Left Upper Aileron • Left Lower Aileron • Right Upper Aileron • Right Lower Aileron	6 Effectors • Left Horizontal Tail • Right Horizontal Tail • Left Aileron • Right Aileron • Left Chine Strake • Right Chine Strake	4 Effectors • Left Horizontal Tail • Right Horizontal Tail • Left Aileron • Right Aileron Tail dihedral angle not controlled by FCS	6 Effectors • Left Horizontal Tail • Right Horizontal Tail • Left Upper Aileron • Left Lower Aileron • Right Upper Aileron • Right Lower Aileron Tail dihedral angle not controlled by FCS	8 Effectors • Left Horizontal Tail • Right Horizontal Tail • Left Upper Aileron • Left Lower Aileron • Right Upper Aileron • Right Lower Aileron • Pitch Thrust Angle • Yaw Thrust Angle Tail dihedral angle not controlled by FCS

Additional effectors not controlled by the FCS:

- **Left Flap**
- **Right Flap**
- **Left Leading Edge**
- **Right Leading Edge**
- **Throttle**

- **Each effector controlled individually**
- **Each effector contributes to:**
  - **Pitch (Commanded n_Z)**
  - **Roll (Commanded Roll Rate)**
  - **Yaw (Commanded Sideslip)**
- **FCS mixes control input for optimal results**

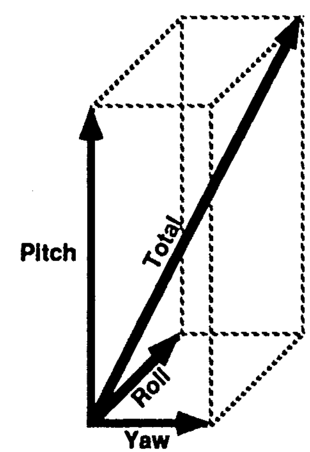

Individual Effector

Figure 3.3-2 Use of Control Effectors by the Flight Control System

Effector	Deflection limits	Rate limits
Horizontal Stabilizers Incidence	±30°	100 deg/sec
Horizontal Stabilizers Dihedral	±20°	20 deg/sec
Rudder	±30°	100 deg/sec
Ailerons	±30°	100 deg/sec
Split Ailerons •Upper •Lower	 45° TEU 45° TEU	 100 deg/sec 100 deg/sec
Chine Strakes	118° from Side of Body	100 deg/sec
Thrust Vectoring •Pitch •Yaw	 ±30° ±30°	 100 deg/sec 100 deg/sec

Figure 3.3-3 Control Effectors Limits

3.3.1 Nonlinear Control Mappings

Chine Strakes. Because the aero model data showed the chine strakes having very low incremental control effectiveness at deflection angles below 28 deg, the nonlinear control mapping was set up to bias both chine strakes at this nominal value. A single strake input signal is mapped into both strakes by commanding differential motion around this nominal bias value. For example, a strake command of +10 deg is mapped into 18 deg for the left strake and 38 deg for the right. For commands greater than the bias value, one strake simply goes to its 0 deg limit. An upper limit of 73 deg was also imposed, even though the model permits strake angles up to 118 deg, because the aero data show a reversal of control effectiveness beyond 73 deg. By biasing at the "knee" of the effectiveness curve in this way, the combined control moment generated by both strakes becomes an approximately linear function of the command. Without this approach, the strake command effectiveness would show a near-deadband effect at low commanded angles, which would be likely to cause limit cycle behavior in the control system.

Split Ailerons These four surfaces are biased at a nominal 5 deg value, in a manner similar to the chine strakes. The 5 deg bias value was chosen by examining two-dimensional maps of the effectiveness of upper and lower split ailerons on both roll and yaw. They display a "knee" of control effectiveness near this value. Both roll and yaw commands are mapped into the four surfaces through a simple mapping matrix, and summed with the nominal 5 deg bias settings. Hard limits are applied to the results at the 0 deg and 45 deg deflection limits.

Rotating Tail The control law does not directly command tail dihedral angles, because realistic servo response time and inertial coupling effects might permit only a slow loop bandwidth through this feedback path. Instead, only the left and right tail incidence angles are commanded over a ±30 deg range, with the tail dihedral angles fixed at the RPAS simulation user's settings, ranging over ±20 deg. Independent pitch and yaw commands from the longitudinal and lateral control laws are mapped into these two incidence angles. The yaw command is scaled by the reciprocal of the dihedral angle over a 5 to 20 deg dihedral range, to provide approximately constant yaw control sensitivity allowing for the tail dihedral angles to vary.

3.3.2 Linear Multivariable Control Law Design

Control Mixer Matrix As the overview diagram of Figure 3.3-1 shows, the control law gain matrices directly produce only three output commands, which are "pseudo-control" signals commanding certain blends of pitch, roll, and yaw moment. These blended signals are mapped into commands to each actuator by an additional control mixer gain matrix called V, see Figure 3.3-1. For the "linear" control surfaces (conventional ailerons, rudders, nonrotating horizontal tails, and pitch and yaw thrust vectoring) these outputs of the matrix V are sent directly to the control surface servos. For the "nonlinear" control surfaces (split ailerons, chine strakes, rotating tail incidence angles) the outputs of V are passed through the nonlinear control mappings described above to produce control surface commands.

Using the control mixer matrix V allows the control law to use the least-squares optimal blend of all available control surfaces to produce roll, pitch, and yaw using minimal total control surface activity. The matrix V is calculated for each flight condition and for each configuration set of control surfaces, using linear least squares matrix theory. This allows each surface to be used simultaneously for roll, pitch, and yaw in proportion to its control effectiveness in each axis. For this reason, it increases the maximum vehicle performance when compared against the traditional technique of assigning ailerons for roll only, rudders for yaw only, etc., in a single-input single-output (SISO) control system.

This technique also differs from a better-known pseudo-control method in which the columns of the V matrix attempt to provide pure, decoupled roll, pitch, and yaw moments. That technique, called the pseudo-inverse method, tends to degrade the loop stability margins in vehicles with strong roll-yaw coupling. In contrast, Boeing's method preserves the loop stability margins. One side-effect is that the signals labeled "pseudo-roll" and "pseudo-yaw" in the diagram do not actually command pure roll and yaw moments: they command certain optimal blends of moments and forces that depend on the vehicle's natural cross-axis coupling.

H-infinity state feedback design. Boeing has developed a set of very efficient techniques for designing the multivariable feedback and feed forward gain matrices using H-infinity optimal control theory. These allow the designer to specify the desired closed-loop dynamic responses (pole locations and cross-axis decoupling behavior) and to produce a corresponding gain matrix with little or no design iteration. The design process was repeated for each of six control surface configurations: baseline, split ailerons, chine strakes, rotating tail, split ailerons with rotating tail, and baseline with split ailerons, rotating tail, and thrust vectoring. For each configuration, a "point design" was produced for each of four flight conditions: takeoff/approach, corner speed, penetration speed, and supersonic. The remaining flight conditions were covered by interpolating these gain matrices versus the reciprocal of dynamic pressure. Each point design consisted of a longitudinal and a lateral gain matrix design, for a total of 48 gain matrices. The baseline design was performed under IR&D funding, the others under contract.

The efficient H-infinity method allowed all eight gain matrices for each configuration to be designed in, typically, a single afternoon. Much less trial and error was required than would have been needed for either LQR (linear quadratic regulator) multivariable control or for conventional SISO control law designs.

Implicit integration for anti windup. The control law uses integrating feedback on the three commanded variables: stability-axis roll rate, sideslip angle, and normal acceleration Nz. (The Nz regulator actually uses a blend of Nz with speed acceleration Udot, as explained below.) Integrating feedback is desirable because it drives steady-state tracking error to zero. Conventional integrating control laws require special care to properly initialize the integrator states and to prevent them from "winding up" or ramping during control surface saturation. Boeing has developed a technique called implicit integration that prevents these problems and simplifies the implementation of integrating control laws. This technique was applied to the ICE control law, eliminating the need for special integrator logic to reinitialize the integrator states or to freeze them during saturation. The benefit is significant, since integrator logic can occupy more lines of code than the linear control law gains in conventional controllers.

3.3.3 Longitudinal axis control law

Nz-Alpha mapping. The stick command is interpreted as a commanded increment to normal acceleration Nz in units of g, above what is required to maintain a straight-line flight path at the current flight path angle μ. In this way, zero stick force will always command a straight-line flight path when the wings are level. To do this, the commanded increment Nz_stick is summed with cos (γ), which is 1 g in level flight.

Without this cos(γ) compensation, Nz regulators tend to cause mild flight path instability when attempting to hold a steady climb or descent.

Both the commanded and measured total Nz values are converted into nominally equivalent values of angle of attack α. This is done using the standard formulas relating lift coefficient CL, dynamic pressure Qbar, wing area, and weight to Nz. CL is assumed to be a linear function of angle of attack α: $CL = CL_0 + CL_\alpha \, \alpha$. Nominal values of CL_0, CL_α, wing area, and weight are used by the control law.

The equivalent commanded and measured values of Alpha, based on the Nz values, are labeled Alpha_Nz_cmd and Alpha_Nz in the diagram. The regulator uses these instead of using Nz values directly. The reason is to accommodate high-α flight regimes, when CL_α changes sign and an Nz regulator could become unstable. At high-α conditions, the Nz to Alpha mapping can blend the Nz-equivalent Alpha values with true Alpha values, so that the control law becomes an Alpha regulator. Doing this with a smooth blending function as Alpha approaches stall allows the vehicle to be flown into post-stall conditions with no mode switching by the pilot.

Meanwhile, basing the regulator on Nz in normal flight allows the control law to be self-trimming. While flying post-stall was not required for ICE, this structure was retained in the controller to permit such use in the future.

<u>Nz-Udot regulator.</u> At landing and approach speeds, it is desirable to slightly modify the response of a pure Nz regulator. If, for instance, the airplane held Nz firmly at 1.1 g at low airspeeds, Alpha would have to increase rapidly to compensate for the rapidly dropping airspeed as the flight path curved upward. This can cause unexpected stalls with only small values of steady stick force. To prevent this, the landing/approach control law gain matrices were designed to provide a low-frequency "washout" behavior in Nz command tracking. In effect, the quantity being tracked by the regulator is a blend of Nz with speed acceleration Udot = dU/dt, so that the stick step response is an initial jump in Nz followed by a steady airspeed deceleration while Nz returns to its straight-line value of cos(γ). The controller structure remains the same as shown in the diagram: the Udot regulation behavior is provided implicitly by the appropriate proportional feedback gain terms on U.

Command shaping filter. While regulation of Nz is desirable for auto-trim behavior over a time scale of many seconds, the stick response of a "tight" Nz regulator can cause undesirable flying qualities on a shorter, transient time scale. Specifically, pilots expect the "nose to follow the stick" on a short time scale, meaning that pitch rate, not Nz, should be proportional to stick force. A tight Nz regulator would ordinarily cause high levels of pitch rate overshoot and "bobble tendency." But since a pitch rate regulator is not auto-trimming and causes flight path instability at low airspeeds, we need to combine the best of both schemes.

We have resolved this problem by inserting a unity-gain lag-lead command shaping filter in the feed forward path. Airplanes have a natural transmission zero in their response from pitch moment to pitch rate, caused by the effect of CL_{α} on lift and flight path as an airplane pitches. The transmission zero frequency is typically near 1 rad/s for the Model-24F. The shaping filter places a pole at this zero frequency and a zero at a higher frequency near 4 rad/s. The effect is to make the stick response mimic that of a pitch rate command attitude hold (RCAH) system on a short time scale, restoring good flying qualities for pitch acquisition tasks. At the same time, the high-gain Nz regulator provides tight control over Nz and Alpha during aggressive roll maneuvers, as well as providing auto-trim. Also, the filter still provides a direct (no-lag) gain term from stick to control surfaces to help prevent pilot-induced oscillation (PIO) from excessive lag.

3.3.4 Lateral-Directional Axis Control Law.

The multivariable control law regulates two variables in the lateral-directional axis: roll rate p and sideslip angle β. The commands are normally generated by processing lateral stick force and pedal force through appropriate deadbands and shaping functions. For unpiloted simulation studies, the control law can accept p and β commands directly. There is no artificial separation of control surfaces into "roll-only" and "yaw-only" sets as in classical single-input single-output (SISO) design. The control law gain matrix is free to command all available control surfaces to track both commands. Generally the lateral-directional gain matrix maps roll rate, sideslip angle, and yaw rate into two commands to the "pseudo-roll" and "pseudo-yaw" inputs of the control mixer matrix V, see Figure 3.3-1. The V matrix, designed by the Singular Value Decomposition technique, then maps these commands into the full set of control effectors. The control law uses integrating feedback to drive steady-state command tracking error to zero for both p and β.

3.3.5 Standard Sensor Processing

Air-referenced and inertial-referenced measurements of angle of attack α, sideslip angle β, and body-axis velocities U, V, and W (in the x, y, and z body axes respectively) are passed through a standard set of first-order complementary filters. The purpose is for the feedback law to use air-referenced measurements at low frequencies and inertial-referenced measurements at high frequencies. Each complementary filter applies a transfer function of $k/(s+k)$ to the air-referenced input and $s/(s+k)$ to the inertial input, where k is a breakpoint frequency in radians per second. A typical value of k is 0.3 rad/s. This reduces the system sensitivity to air data noise. Most control laws use only the α and β signals, but U, V, and W are provided for use in hover-mode control laws for STOVL vehicles.

The estimated angle of attack α from the complementary filter is used to derive stability-axis rotation rates, velocities, and accelerations from the body-axis values reported by the sensors. Standard transformations involving $\sin(\alpha)$ and $\cos(\alpha)$ are applied. Also, a stability-axis direction cosine matrix is derived from the body-axis matrix. This can be used when stability-axis Euler angles such as bank angle ϕ are used by the feedback law.

Gravity-compensated values of roll rate p, pitch rate q, and yaw rate r are made available to the control law by calculating the contributions to the rotation rates of the vehicle caused by the acceleration of gravity for the vehicle's current flight path and inertial speed. These gravity increments are subtracted from the measured rotation rates, and the results can be used by the control law when desired. The benefit of this is to prevent the control law from "fighting against gravity" during rapid maneuvers such as rolls. Without gravity compensation, for example, a control law using yaw rate feedback may produce strong attitude-dependent rudder commands in a sustained roll as it fights gravity's tendency to yaw the vehicle back and forth. This effect is most pronounced at low speeds.

3.3.6 Automatic Command Limiting.

Boeing has developed a powerful real-time optimization method for preventing cross-axis coupling between pitch, roll, and yaw commands during aggressive maneuvers or large sudden disturbances that produce control saturation. This technique is distinct from the implicit integration method used to prevent integrator windup during control saturation. The Boeing automatic command limiting method allows penalty weights to be assigned to each controlled variable (e.g., roll rate, sideslip angle, and Nz) so that the controller will allow tracking errors in the lower-priority controlled variables first, rather than incurring tracking errors in all variables at once. For example, without command limiting, applying a very large roll rate command can cause excessive sideslip angle to develop when the ailerons or rudders are saturated. With command limiting, the control system will automatically "back off" from the commanded roll rate just enough so that tight regulation of sideslip can be maintained. These command limits are implicit in the position and rate limits of the control surfaces themselves, and are not arbitrarily imposed. This allows the full maneuver performance envelope of the vehicle to be realized safely.

3.4 Effector Study Results (including Thrust Vectoring)

Overview

The individual effectors and effector combinations were evaluated at the six flight conditions previously summarized in Figure 3.1-1. Note that the "best" effector combination (rotating horizontal tail + split ailerons) was also evaluated with 2-axis thrust vectoring (TV).

The evaluation criteria are summarized below (Reference: MIL-F-8785C):

Level 1:

Flying qualities clearly adequate for the mission Flight Phase.

Level 2:

Flying qualities adequate to accomplish the mission Flight Phase, but with some increase in pilot work load or degradation in mission effectiveness, or both, exists.

Level 3:

Flying qualities such that the airplane can be controlled safely, but pilot work load is excessive or mission effectiveness is inadequate, or both. Category A Flight Phases can be terminated safely, and Category B and C Flight Phases can be completed.

Pass:

Meets specification (for sections without Level 1, 2 or 3 requirements)

Fail:

Does not meet specification (for sections without Level 1, 2 or 3 requirements)

Note that where results are inferred for this Phase I study they are indicated in the Summary Charts with an asterisk.

3.4.1 Takeoff and Approach

Analysis for takeoff and approach stability and control was conducted under the following conditions:

Vehicle gross weight	=	25,000 lb.
Equivalent velocity v_e	=	132kts
Altitude	=	1,000 ft

In total, 10 flying qualities items were addressed with the results summarized in the performance summary sheet of Figure 3.4.1-1, based on data such as contained in Figures 3.4.1-2 and 3.4.1-3.

In a number of cases the flying qualities evaluation was done by inspection (without detailed evaluation) where a specific effector would have no impact on the result. For example, if the Baseline configuration passed the trim requirements (Longitudinal control in unaccelerated flight) the Split Ailerons and Chine Strake configurations were assumed to pass since the horizontal tail configuration was unchanged. Additionally, without the vertical tails and with limited directional control power these configurations were assumed to fail for some of the lateral-directional items.

The crosswind evaluation was conducted to the limit of the simulation data base ($\beta=\pm10^{o}$). At 132kts, the $\beta=10^{o}$ condition equates to approximately 23kts of 90^{o} crosswind.

The baseline Model-24F configuration includes vertical tails but without thrust vectoring. The baseline vehicle, as tested, meets the Level 1 or pass criteria of the Military Specification, MIL-F-8785C, revised above, for 6 of the 10 conditions. It meets Level 2 criteria in 2 flying quality items for two longitudinal control in maneuvering flight and turn coordination which failed due to angle of attack limit of the simulation data base with only a limited load factor capability.

For the split ailerons configuration (without thrust vectoring) the "Level 1" or "pass" criteria are met only for longitudinal control in unaccelerated flight, the "Level 2" criteria are estimated to be met for Flight Path Stability while for all other qualities the configuration fails.

The reader can summarize the remaining elements of the summary sheet, Figure 3.4.1-1, in a similar fashion. The rotating tail shows the overall best performance among the effectors. The reader is to keep in mind that only the baseline configuration had a vertical tail. For more details, see the data collected in Appendix B.

GW = 25,000 lbs **V_e =132 kts** **Altitude = Sea Level**

		CONFIGURATIONS					
DESCRIPTION	REQUIRMENTS SOURCE	Baseline no TV	Split Ailerons no TV	Chine Strakes no TV	Rotating Tail (Γ_H = 20°/20°) no TV	Rotating Tail+ Split Ailerons no TV	Rotating Tail+ Split Ailerons with TV
Flight-path Stability	MIL-F-8785C §3.2.1.3 MIL-STD-1797A §4.3.1.2	**Level 2**	**Level 2***	**Level 2***	**Level 2**	**Level 2***	**Level 2***
Longitudinal control in unaccelerated flight	MIL-F-8785C §3.2.3.1 MIL-STD-1797A §4.2.7.1	**Pass**	**Pass**	**Pass**	**Pass**	**Pass***	**Pass***
Longitudinal control in maneuvering flight	MIL-F-8785C §3.2.3.2 MIL-STD-1797A §4.2.7.2	**Fail**	**Fail***	**Fail***	**Fail**	**Fail***	**Fail***
Lateral-directional oscillations Dutch roll	MIL-F-8785C §3.3.1.1 MIL-STD-1797A §4.1.11.7 §4.6.1.1	**Level 1**	**Fail***	**Fail***	**Level 1**	**Level 1***	**Level 1***
Roll mode	MIL-F-8785C §3.3.1.2 MIL-STD-1797A §4.5.1.1	**Level 1**	**Fail***	**Fail***	**Level 1**	**Level 1***	**Level 1***
Spiral mode	MIL-F-8785C §3.3.1.3 MIL-STD-1797A §4.5.1.2	**Level 1**	**Fail***	**Fail***	**Level 1**	**Level 1***	**Level 1***
Turn coordination	MIL-F-8785C §3.3.2.6 MIL-STD-1797A §4.5.9.5.1 §4.6.7.2	**Fail (data base α limit)**	**Fail (data base α limit)**	**Fail (data base α limit)**	**Fail (data base α limit)**	**Fail (data base α limit)**	**Fail (data base α limit)**
Roll control effectiveness	MIL-F-8785C §3.3.4 MIL-STD-1797A §4.5.8.1	**Level 2**	**Fail**	**Fail**	**Level 3**	**Level 3**	**Level 1**
Lateral-directional control in cross winds	MIL-F-8785C §3.3.7 MIL-STD-1797A §4.5.6 §4.5.8.3 §4.5.9.5.3 §4.6.4 §4.6.7.4	**Pass (data base β limit)**	**Fail**	**Fail**	**Fail**	**Fail**	**Pass (data base β limit)**
Final approach in cross winds	MIL-F-8785C §3.3.7.1 MIL-STD-1797A §4.5.8.3 §4.5.9.5.4 §4.6.6.1	**Pass (data base β limit)**	**Fail**	**Fail**	**Fail**	**Fail**	**Pass (data base β limit)**

*** Evaluated by Inspection**

Figure 3.4.1-1 Takeoff and Approach

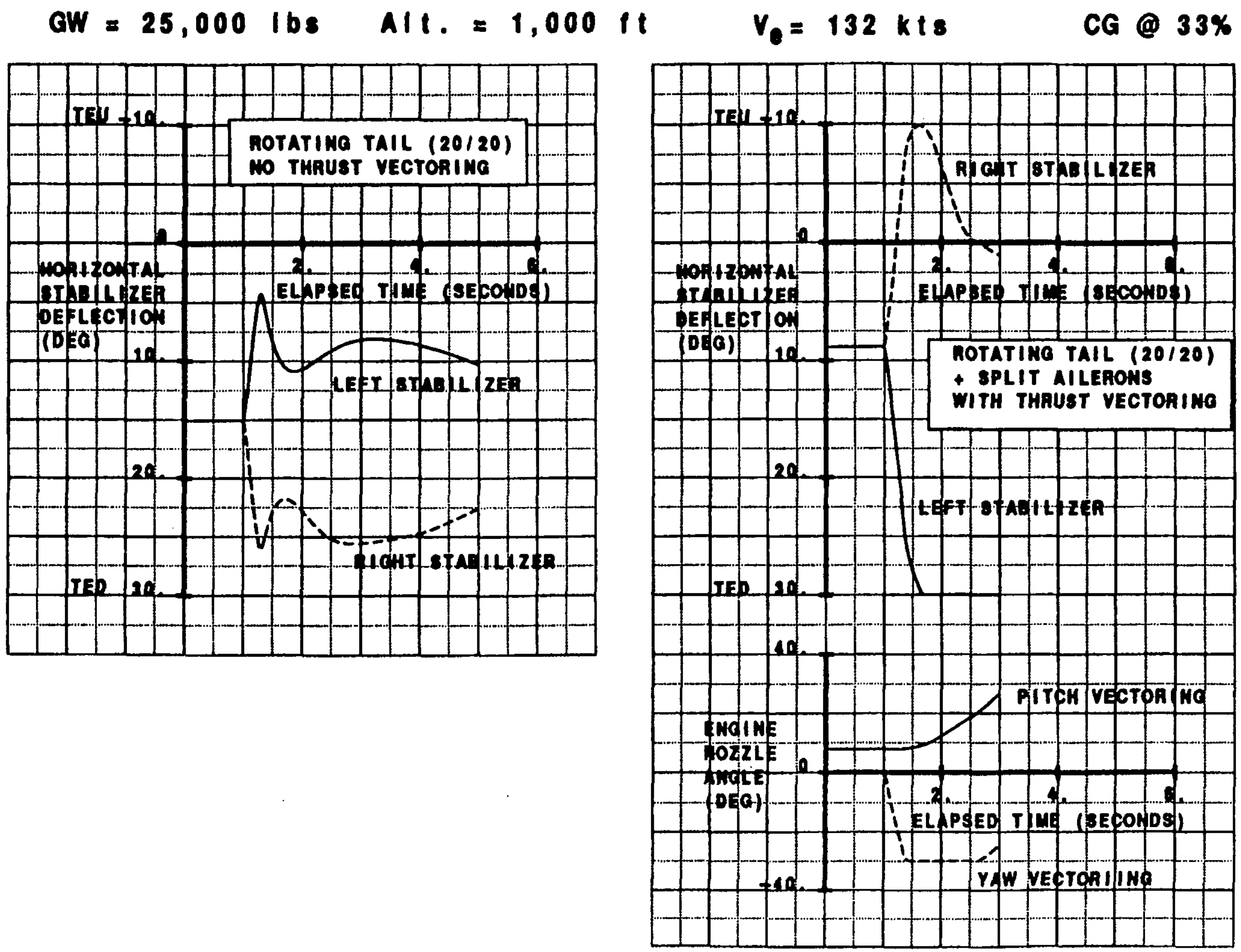

Figure 3.4.1-2 Roll Control Effectiveness Landing Approach

GW = 25,000 lbs   Alt. = 1,000 ft V_e = 132 kts   CG @ 33% mac

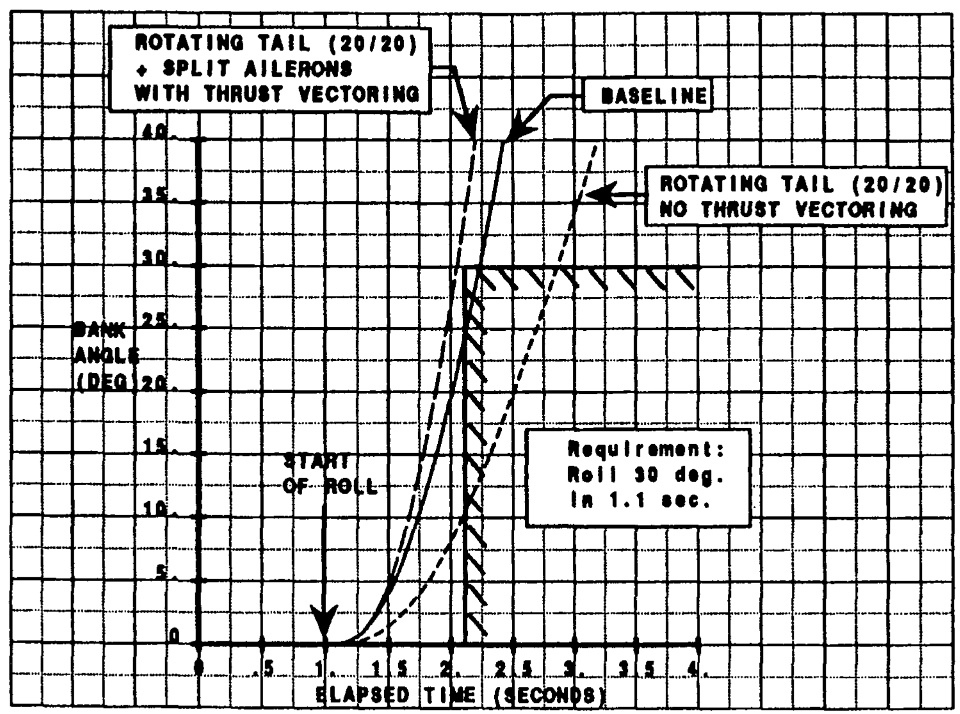

Figure 3.4.1-3 Roll Control Effectiveness Landing Approach-Thrust Vectoring

3.4.2 Power on Departure Stall

Analysis for power on departure stall flying qualities was conducted under the following conditions:

Vehicle gross weight	=	27,000 lb.
Altitude	=	15,000 ft
Maximum database AOA (22°) low speed		

In total seven (7) flying qualities items were addressed with the results summarized in the performance summary sheet of Figure 3.4.2-1 with sample data in Figures 3.4.2-2, 3.4.2-3 and 3.4.2-4.

Again in this assessment as in others, a number of cases the flying qualities evaluation was done by inspection (without detailed evaluation) where a specific effector would have no impact on the result. Additionally, without the vertical tails and with limited directional control power some configurations were assumed to fail for some of the lateral-directional items. The moments that could be generated are just not large enough.

The baseline Model-24F configuration is with vertical tails but without thrust vectoring. The baseline vehicle, as tested, meets the Level 1 or pass criteria of the Military Specification, MIL-F-8785C, reviewed above, for five of the seven conditions.

The Level 3 performance in roll control of the baseline is due to the fact that small amounts of sideslip degrades the available roll control power through the flow interaction with the canted tail and swept wings.

The baseline fails in longitudinal control in maneuver because of this simulation software, it can hold the speed or altitude only with severe degradation of flight path angle.

The reader can summarize the remaining elements of the summary sheet, Figure 3.4.2-1, in a similar fashion. Again the rotating tail shows the overall best performance among the effectors. The reader is to keep in mind that only the baseline configuration had a vertical tail. See the Appendix B for more detailed information.

GW = 27,000 lbs V_e = low Altitude = 15,000 ft

DESCRIPTION	REQUIRMENTS SOURCE	CONFIGURATIONS: Baseline no TV	Split Ailerons no TV	Chine Strakes no TV	Rotating Tail (Γ_H = 20°/20°) no TV	Rotating Tail+ Split Ailerons no TV	Rotating Tail+ Split Ailerons with TV
Longitudinal control in unaccelerated flight	MIL-F-8785C §3.2.3.1 MIL-STD-1797A §4.2.7.1	Pass	Pass	Pass	Pass	Pass*	Pass*
Longitudinal control in maneuvering flight	MIL-F-8785C §3.2.3.2 MIL-STD-1797A §4.2.7.2	Fail	Fail*	Fail*	Fail	Fail*	Fail*
Lateral-directional oscillations Dutch roll	MIL-F-8785C §3.3.1.1 MIL-STD-1797A §4.1.11.7 §4.6.1.1	Level 1	Fail*	Fail*	Level 1	Level 1*	Level 1*
Roll mode	MIL-F-8785C §3.3.1.2 MIL-STD-1797A §4.5.1.1	Level 1	Fail*	Fail*	Level 2	Level 2	Level 1
Spiral mode	MIL-F-8785C §3.3.1.3 MIL-STD-1797A §4.5.1.2	Level 1	Fail*	Fail*	Level 1	Level 1*	Level 1*
Turn coordination	MIL-F-8785C §3.3.2.6 MIL-STD-1797A §4.5.9.5.1 §4.6.7.2	Pass	Pass	Pass	Pass	Pass*	Pass*
Roll control effectiveness	MIL-F-8785C §3.3.4 MIL-STD-1797A §4.5.8.1	Level 3	Fail	Fail	Fail	Fail	Level 1

* Evaluated by Inspection

Figure 3.4.2-1 Power-On Departure Stall

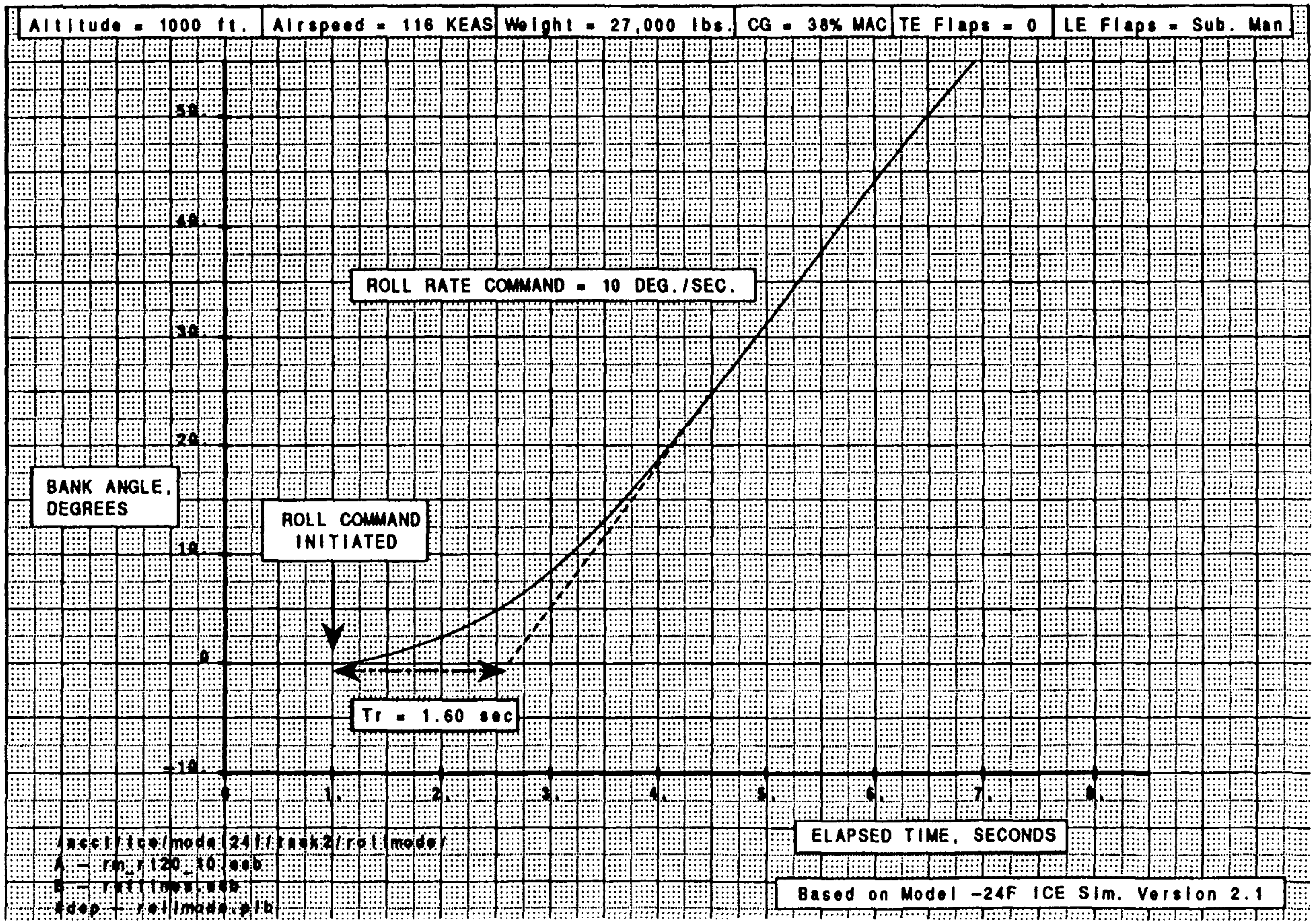

Figure 3.4.2-2 Departure Stall-Roll Rate Time Constant

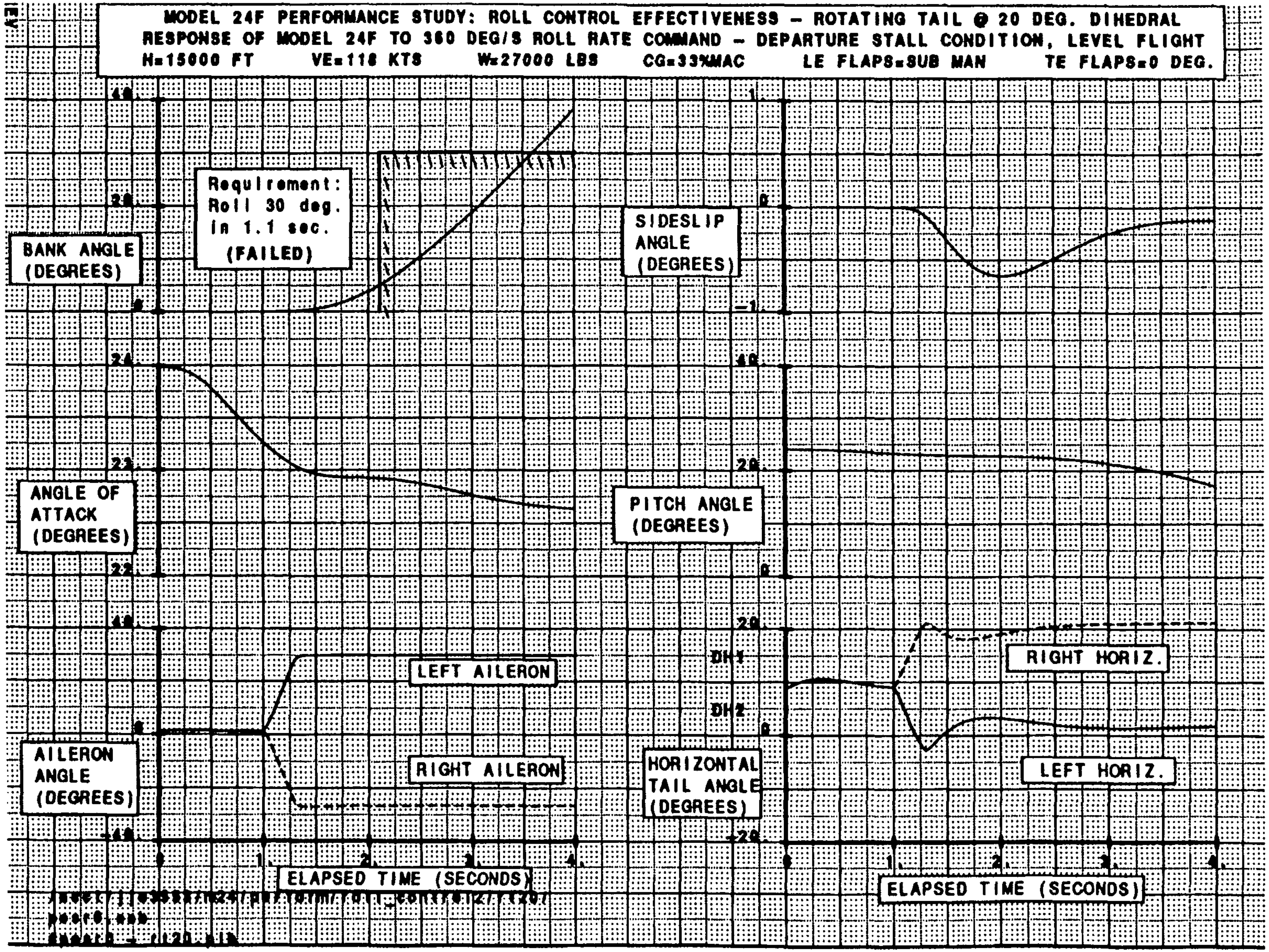

Figure 3.4.2-3 Departure Stall-Roll Performance

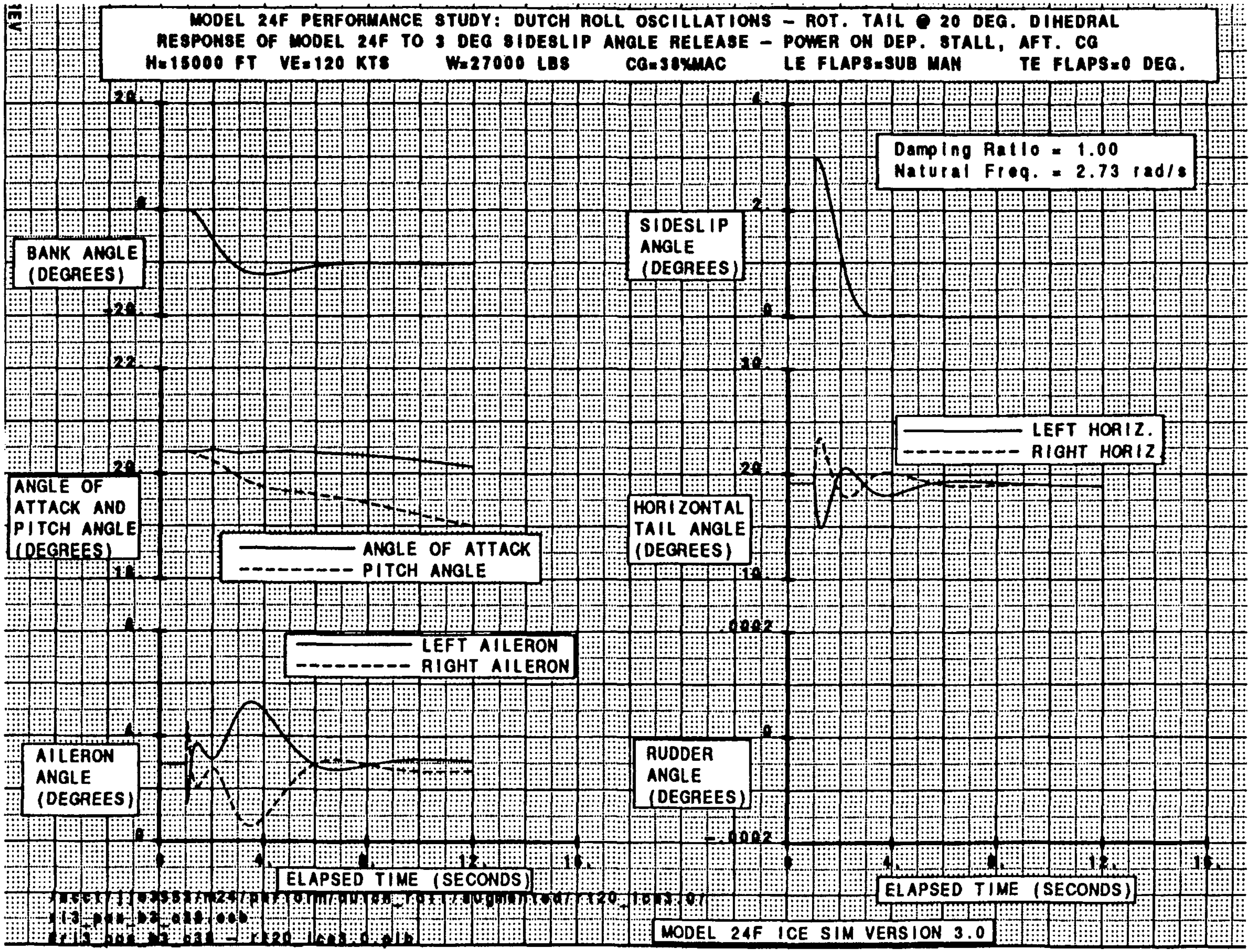

Figure 3.4.2-4 Departure Stall-Lateral-Directional Dynamics

3.4.3 Air Combat Maneuver Condition

Analysis for air combat maneuver stability and control was the most extensive flying qualities analysis of this project and was conducted for the following conditions:

Vehicle gross weight	=	27,000 lb.
Altitude	=	15,000 ft
Mach number	=	0.6

In total, 18 flying qualities items were addressed for 5 configurations in addition to the baseline configuration with the results summarized in the performance summary sheet of Figure 3.4.3-1, with illustrative data in Figures 3.4.3-2 through 3.4.3-4.

In a number of cases the flying qualities evaluation was again done by inspection (without detailed evaluation) where a specific effector would have no impact on the result. (See the remarks for earlier sections.)

The majority of the analysis concentrated on the baseline vehicle or the rotating tail configuration since the other effectors did not generate the desired control power.

The baseline Model-24F configurations with vertical tails but without thrust vectoring, as tested, meets the Level 1 or pass criteria of the Military Specification, MIL-F-8785C, reviewed above, for 16 of the 18 conditions. It meets Level 2 criteria for one flight quality, short period frequency and acceleration sensitivity, and fails for one quality, longitudinal control in maneuvering flight. Failure to meet this requirement is mainly due to the way the simulation analysis is performed in the simulation code RPAS. The simulation tries to hold the speed and the altitude while trimming at load factor. This results in a solution where the flight path angle is varied. For a high load factor (Nz) very large negative flight path angles result, approaching -90^{o} in limit. See Figure B-1 in the Appendix B to the report. This result and its explanation holds true for all configurations.

The rotating tail meets or exceeds Level 1 for all items except longitudinal control in maneuvering flight. This failure is again mainly a result of the simulation as discussed in the previous paragraph.

The simulation tries to hold a constant velocity. The dynamic maneuver where the speed bleeds off is not a problem. There is plenty of control power.

The split ailerons and chine strakes (without vertical tails) fail (by inspection) to meet the lateral-directional dynamics requirements. They do not generate required control power for important flying qualities conditions.

The reader can review the remaining elements of the summary sheet, Figure 3.4.3-1, in a similar fashion. The rotating tail shows the overall best performance among the effectors. The reader is to keep in mind that only the baseline configuration had a vertical tail. For more details, see the data collected in Appendix B.

GW=27,000 lbs M = 0.6 Altitude = 15,000 ft

DESCRIPTION	REQUIRMENTS SOURCE	CONFIGURATIONS Baseline no TV	Split Ailerons no TV	Chine Strakes no TV	Rotating Tail (Γ_H = 20°/20°) no TV	Rotating Tail+ Split Ailerons no TV	Rotating Tail+ Split Ailerons with TV
Phugoid stability	MIL-F-8785C § 3.2.1.2 MIL-STD-1797A § 4.2.1.1	Level 1	Level 1*	Level 1*	Level 1	Level 1*	Level 1*
Flight-path Stability	MIL-F-8785C § 3.2.1.3 MIL-STD-1797A § 4.3.1.2	Pass	Pass*	Pass*	Pass	Pass*	Pass*
Short-period frequency and acceleration sensitivity	MIL-F-8785C § 3.2.2.1.1 MIL-STD-1797A § 4.2.1.2	Level 2	Level2*	Level2*	Level 1	Level 1*	Level 1*
Short-period damping	MIL-F-8785C § 3.2.2.1.2 MIL-STD-1797A § 4.2.1.2	Level 1	Level 1*	Level 1*	Level 1	Level 1*	Level 1*
Longitudinal control in unaccelerated flight	MIL-F-8785C § 3.2.3.1 MIL-STD-1797A § 4.2.7.1	Pass	Pass	Pass	Pass	Pass*	Pass*
Longitudinal control in maneuvering flight	MIL-F-8785C § 3.2.3.2 MIL-STD-1797A § 4.2.7.2	Fail	Fail*	Fail*	Fail	Fail*	Fail*
Lateral-directional oscillations Dutch roll	MIL-F-8785C § 3.3.1.1 MIL-STD-1797A § 4.1.11.7 § 4.6.1.1	Level 1	Fail*	Fail*	Level 1	Level 1*	Level 1*
Roll mode	MIL-F-8785C § 3.3.1.2 MIL-STD-1797A § 4.5.1.1	Level 1	Fail*	Fail*	Level 1	Level 1*	Level 1*
Spiral mode	MIL-F-8785C § 3.3.1.3 MIL-STD-1797A § 4.5.1.2	Level 1	Fail*	Fail*	Level 1	Level 1*	Level 1*

* **Evaluated by inspection**

Figure 3.4.3-1a Air Combat Maneuver Corner Speed

Coupled roll-spiral oscillation	MIL-F-8785C § 3.3.1.4 MIL-STD-1797A § 4.5.1.3	Pass	Fail*	Fail*	Pass	Pass*	Pass*
Roll rate oscillations	MIL-F-8785C § 3.3.2.2 MIL-STD-1797A § 4.5.1.4	Level 1	Fail*	Fail*	Level 1	Level 1*	Level 1*
Additional roll rate requirements for small inputs	MIL-F-8785C § 3.3.2.2.1 MIL-STD-1797A § 4.5.1.4	Level 1	Fail*	Fail*	Level 1	Level 1*	Level 1*
Bank angle oscillation	MIL-F-8785C § 3.3.2.3 MIL-STD-1797A § 4.5.1.4	Level 1	Fail*	Fail*	Level 1	Level 1*	Level 1*
Sideslip excursions	MIL-F-8785C § 3.3.2.4 MIL-STD-1797A § 4.6.2	Level 1	Fail*	Fail*	Level 1	Level 1*	Level 1*
Additional sideslip requirements for small inputs	MIL-F-8785C § 3.3.2.4.1 MIL-STD-1797A § 4.6.2	Pass	Fail*	Fail*	Pass	Pass*	Pass*
Turn coordination	MIL-F-8785C § 3.3.2.6 MIL-STD-1797A § 4.5.9.5.1 § 4.6.7.2	Pass	Pass	Pass	Pass	Pass*	Pass*
Roll control effectiveness	MIL-F-8785C § 3.3.4 MIL-STD-1797A § 4.5.8.1	Level 1	Level 2	Level 2	Level 1	Level 1*	Level 1*
Lateral-directional characteristics in steady sideslip	MIL-F-8785C § 3.3.6 MIL-STD-1797A § 4.5.5 § 4.6.1.2	Pass	Fail	Fail	Pass	Pass*	Pass*

* **Evaluated by inspection**

Figure 3.4.3-1b Air Combat Maneuver Corner Speed

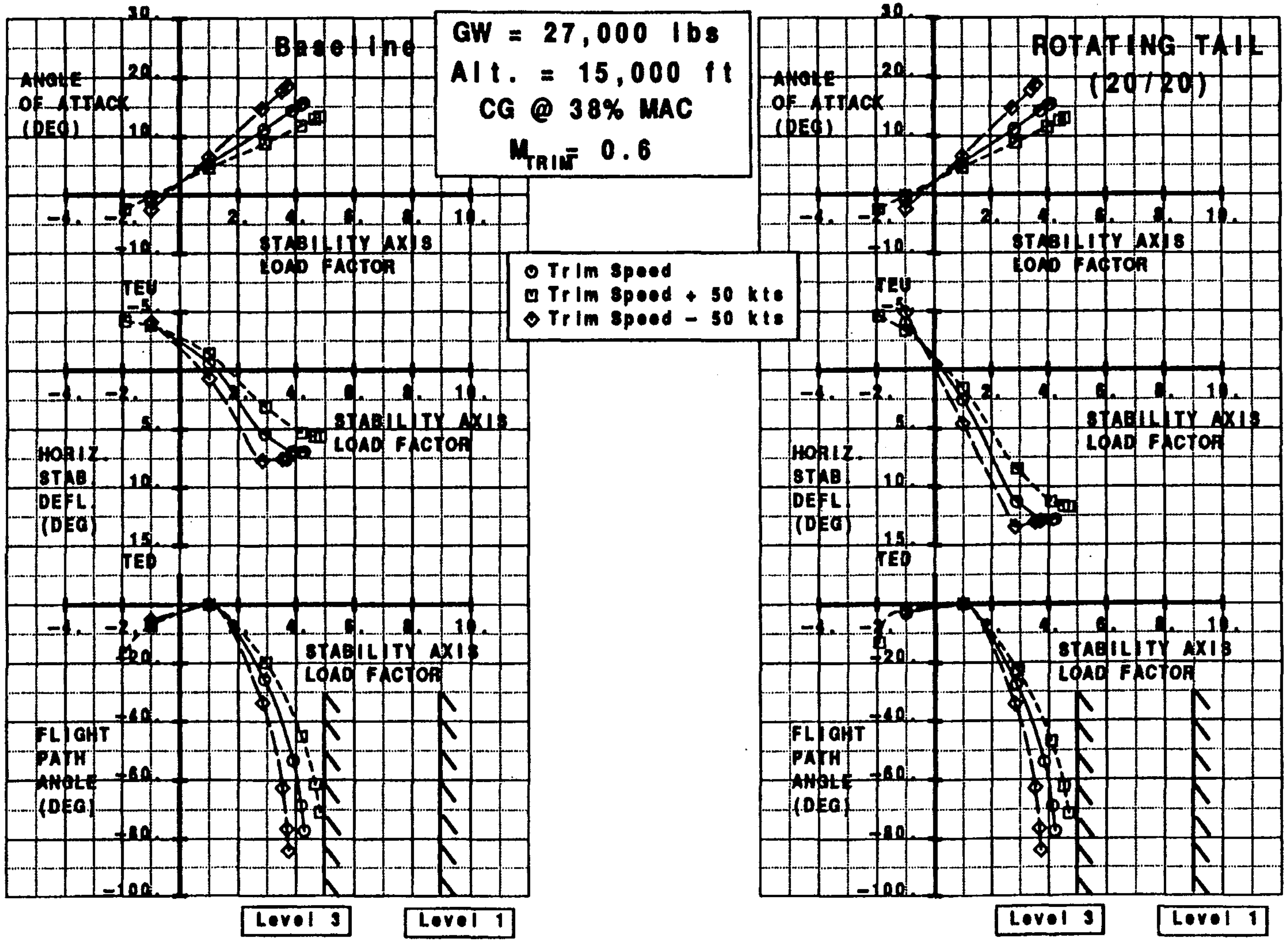

Air Combat Maneuver Corner Point

***Figure 3.4.3-2** Longitudinal Control in Maneuvering Flight - Baseline/Rotating Tail*

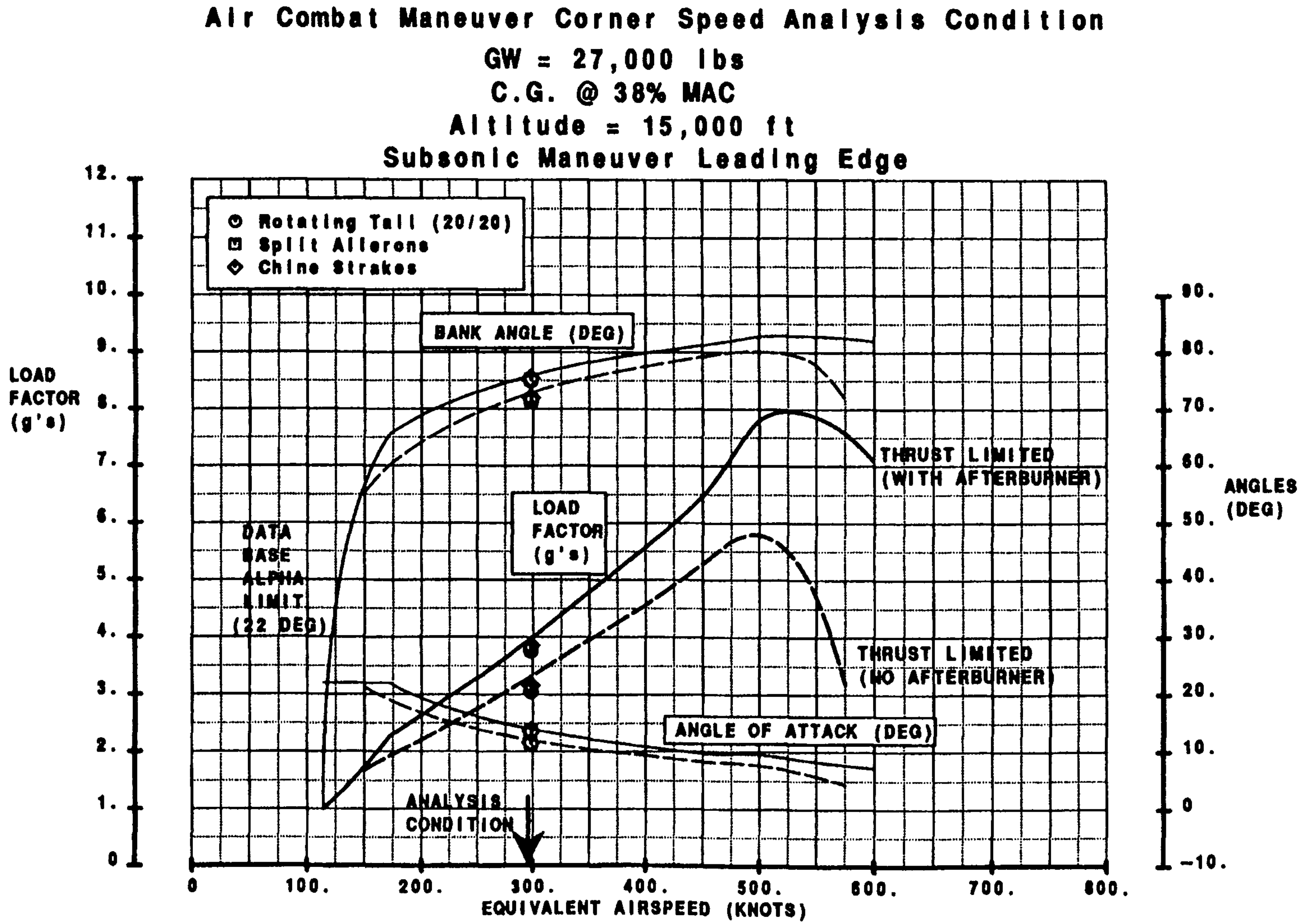

Air Combat Maneuver Corner Point

Figure 3.4.3-3 Maximum Sustained Load Factor at Mid Altitude

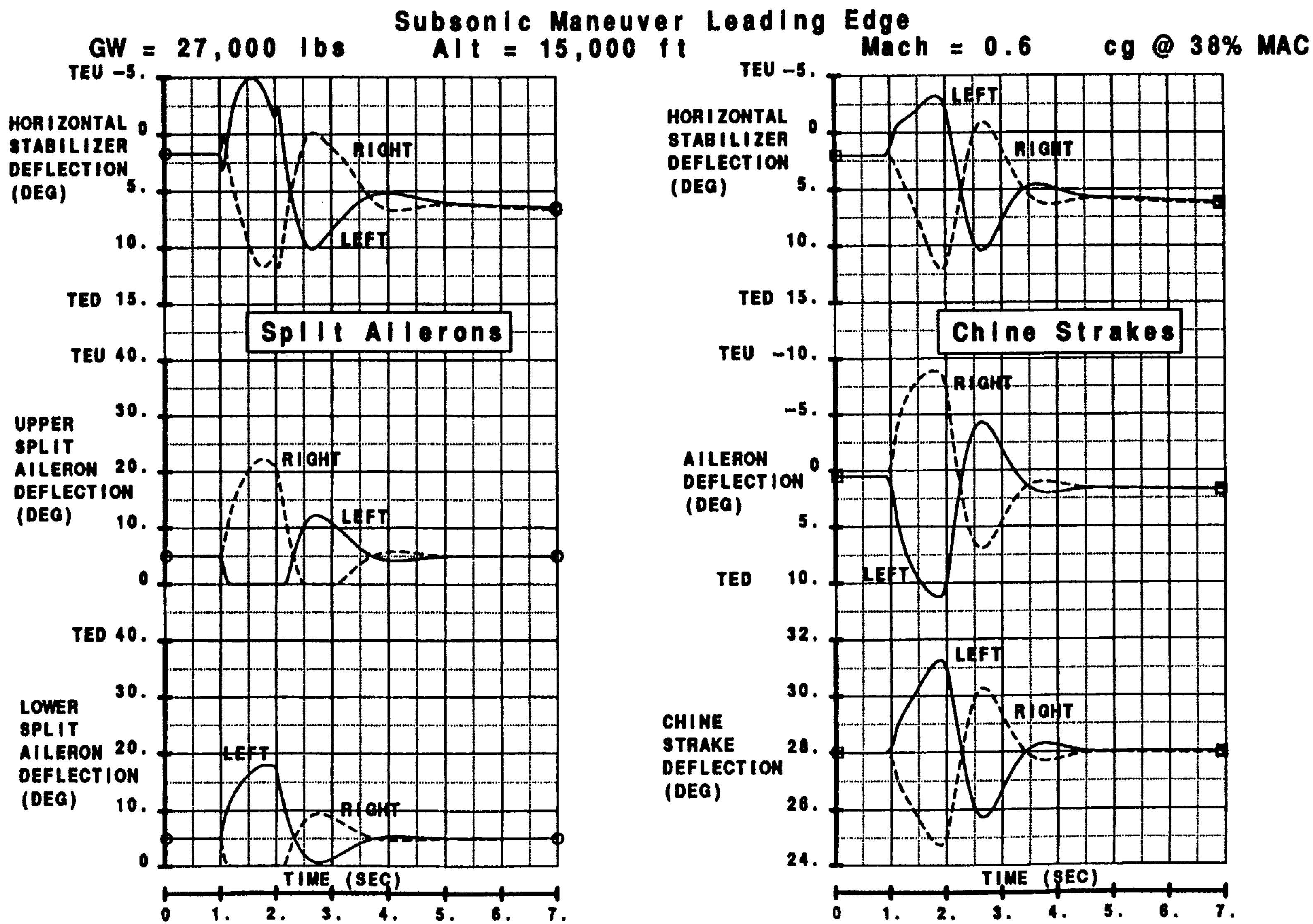

Figure 3.4.3-4 Air Combat Maneuver Corner Speed - Coordinated Turn

3.4.4 Penetration Speed

The assessment of the flying qualities for penetration were conducted for low level flight with the following conditions:

Vehicle gross weight	=	27,000 lb.
Altitude	=	Sea level
Effective velocity v_e	=	600kts

For this flight regime 7 flying qualities were addressed for the 6 configurations (see Figure 3.4.4-1). The flying qualities of the baseline vehicle which includes vertical tail surfaces passes or reaches Level 1 for all but one of the flying qualities assessed. The longitudinal control in level flight condition attaining only Level 3. The origin of the failure for this flying quality is related to the simulation and is consistent with its failure in other conditions. The reader is referred to the previous sections for further discussion.

For the 5 effector configurations, evaluation on many cases could be again determined by inspection. Where pass or Level 1 conditions were satisfied at one level, it is assumed to be achieved with additional effectors operative. The chine strakes and split ailerons configurations are assumed to fail since the data in Appendix B indicate that the control power generated by these effectors will not compensate for the lack of vertical tail control power.

Overall, only 12 of the 42 conditions evaluated failed to achieve pass or Level 1 assessment. The rotating tail being again very effective.

GW = 27,000 lbs V_e = 600 kts   Altitude = Sea Level

DESCRIPTION	REQUIRMENTS SOURCE	CONFIGURATIONS					
		Baseline no TV	Split Ailerons no TV	Chine Strakes no TV	Rotating Tail (Γ_H = 20°/20°) no TV	Rotating Tail+ Split Ailerons no TV	Rotating Tail+ Split Ailerons with TV
Longitudinal control in unaccelerated flight	MIL-F-8785C § 3.2.3.1 MIL-STD-1797A § 4.2.7.1	Pass	Pass	Pass	Pass	Pass*	Pass*
Longitudinal control in maneuvering flight	MIL-F-8785C § 3.2.3.2 MIL-STD-1797A § 4.2.7.2	Level 3	Fail*	Fail*	Level 3	Level 3*	Level 3*
Lateral-directional oscillations Dutch roll	MIL-F-8785C § 3.3.1.1 MIL-STD-1797A § 4.1.11.7 § 4.6.1.1	Level 1	Fail*	Fail*	Level 1	Level 1*	Level 1*
Roll mode	MIL-F-8785C § 3.3.1.2 MIL-STD-1797A § 4.5.1.1	Level 1	Fail*	Fail*	Level 1	Level 1*	Level 1*
Spiral mode	MIL-F-8785C § 3.3.1.3 MIL-STD-1797A § 4.5.1.2	Level 1	Fail*	Fail*	Level 1	Level 1*	Level 1*
Turn coordination	MIL-F-8785C § 3.3.2.6 MIL-STD-1797A § 4.5.9.5.1 § 4.6.7.2	Pass	Pass	Pass	Pass	Pass*	Pass*
Roll control effectiveness	MIL-F-8785C § 3.3.4 MIL-STD-1797A § 4.5.8.1	Level 1	Level 1	Level 1	Level 1	Level 1*	Level 1*

* **Evaluated by Inspection**

Figure 3.4.4-1 Penetration Speed

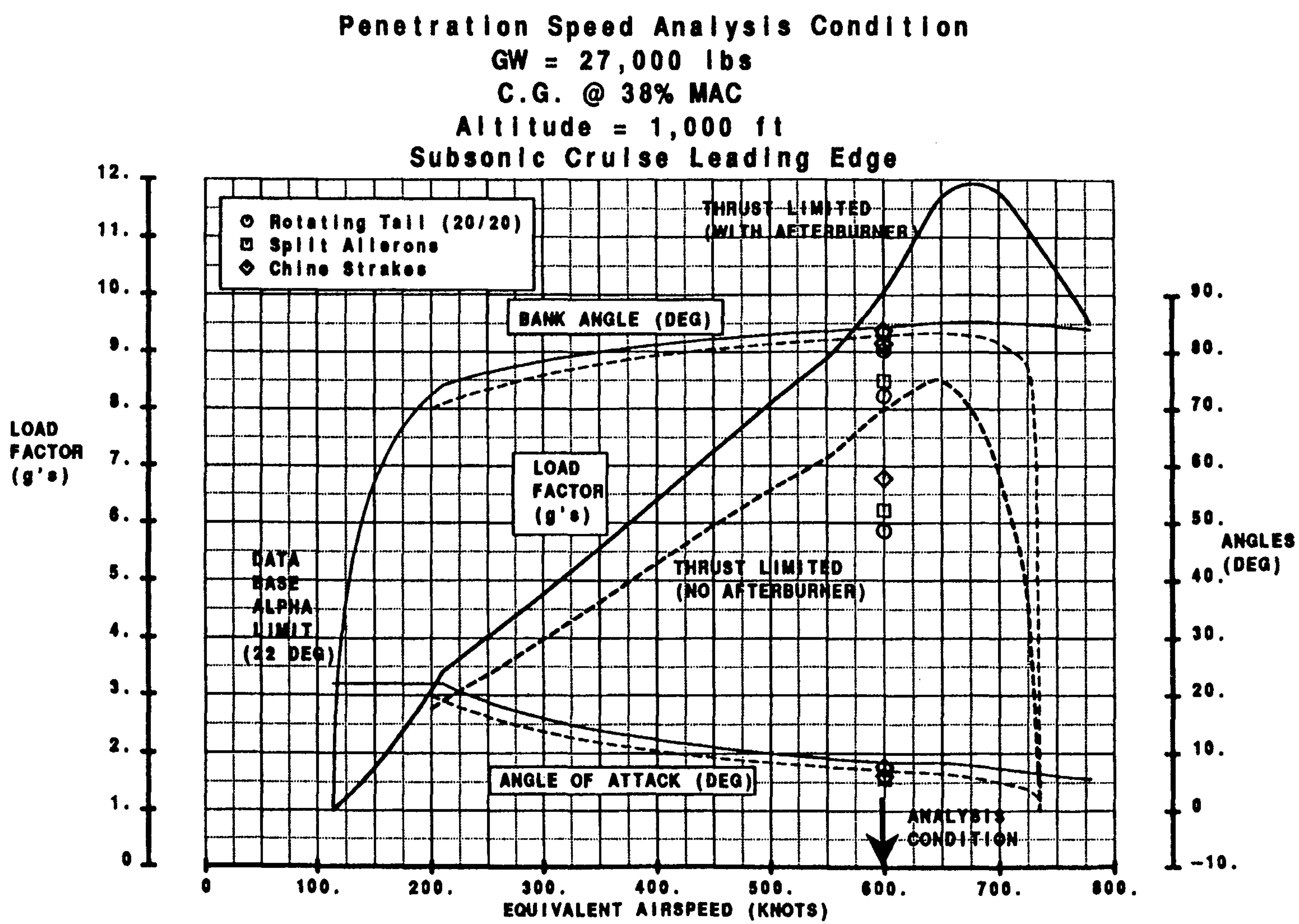

Figure 3.4.4-2 Maximum Sustained Load Factor - Penetration

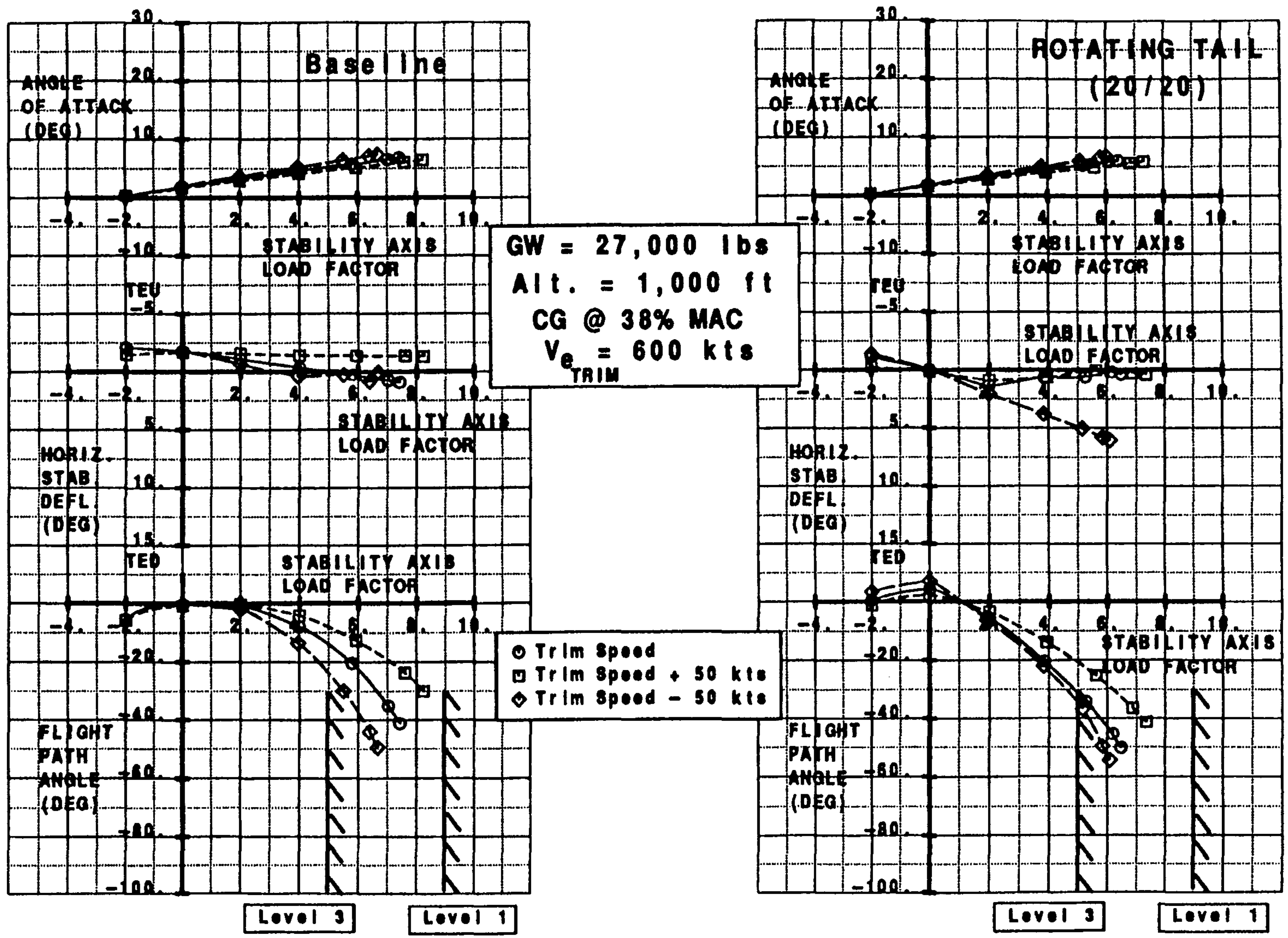

Figure 3.4.4-3 Longitudinal Control in Maneuvering Flight-Penetration Speed

3.4.5 Maximum Sustained Load Factor

The maximum sustained load factor flying qualities assessment was conducted for the following conditions:

Vehicle gross weight	=	27,000 lb.
Altitude	=	30,000 ft
Mach number	=	0.9

In total, for this flight condition, seven flying qualities items were addressed for five configurations in addition to the baseline configuration with the results summarized in the performance summary sheet of Figure 3.4.5-1. Illustrative data are shown in Figures 3.4.5-2 and 3.4.5-3.

The majority of the analysis concentrated on the baseline vehicle or the rotating tail configuration since the other effectors did not generate the required control power.
The baseline Model-24F configuration with vertical tails but without thrust vectoring, as tested, meets the Level 1 or pass criteria of the Military Specification, MIL-F-8785C, reviewed above, for six of the seven conditions and fails for one flight quality item. The failure is again due to the simulation. The reader is referred to the discussion in Section 3.4.3.

The rotating tail meets or exceeds Level 1 for all items except longitudinal control in maneuvering flight. Failure to meet this requirement is again mainly due to the way the simulation analysis is performed in the simulation code RPAS as discussed in Section 3.4.3.

The split ailerons and chine strakes (without vertical tails) fail to meet the lateral-directional dynamics requirements. They do not generate required control power for important flying qualities conditions.

The reader can summarize the remaining elements of the summary sheet of Figure 3.4.5-1, in a similar fashion. The rotating tail shows the overall best performance among the effectors. The reader is to keep in mind that only the baseline configuration had a vertical tail. For more details, see the data collected in Appendix B.

GW = 27,000 lbs M = 0.9 Altitude = 30,000 ft

DESCRIPTION	REQUIRMENTS SOURCE	CONFIGURATIONS: Baseline no TV	Split Ailerons no TV	Chine Strakes no TV	Rotating Tail (Γ_H = 20°/20°) no TV	Rotating Tail+ Split Ailerons no TV	Rotating Tail+ Split Ailerons with TV
Longitudinal control in unaccelerated flight	MIL-F-8785C § 3.2.3.1 MIL-STD-1797A § 4.2.7.1	Pass	Pass	Pass	Pass	Pass*	Pass*
Longitudinal control in maneuvering flight	MIL-F-8785C § 3.2.3.2 MIL-STD-1797A § 4.2.7.2	Fail	Fail*	Fail*	Fail	Fail*	Fail*
Lateral-directional oscillations Dutch roll	MIL-F-8785C § 3.3.1.1 MIL-STD-1797A § 4.1.11.7 § 4.6.1.1	Level 1	Fail*	Fail*	Level 1	Level 1*	Level 1*
Roll mode	MIL-F-8785C § 3.3.1.2 MIL-STD-1797A § 4.5.1.1	Level 1	Fail*	Fail*	Level 1	Level 1*	Level 1*
Spiral mode	MIL-F-8785C § 3.3.1.3 MIL-STD-1797A § 4.5.1.2	Level 1	Fail*	Fail*	Level 1	Level 1*	Level 1*
Control of sideslip in rolls	MIL-F-8785C § 3.3.2.5 MIL-STD-1797A § 4.6.7.1	Pass	Pass	Pass	Pass	Pass*	Pass*
Roll control effectiveness	MIL-F-8785C § 3.3.4 MIL-STD-1797A § 4.5.8.1	Level 1	Level 1	Level 1	Level 1	Level 1*	Level 1*

* Evaluated by inspection

Figure 3.4.5-1 Maximum Sustained Load Factor

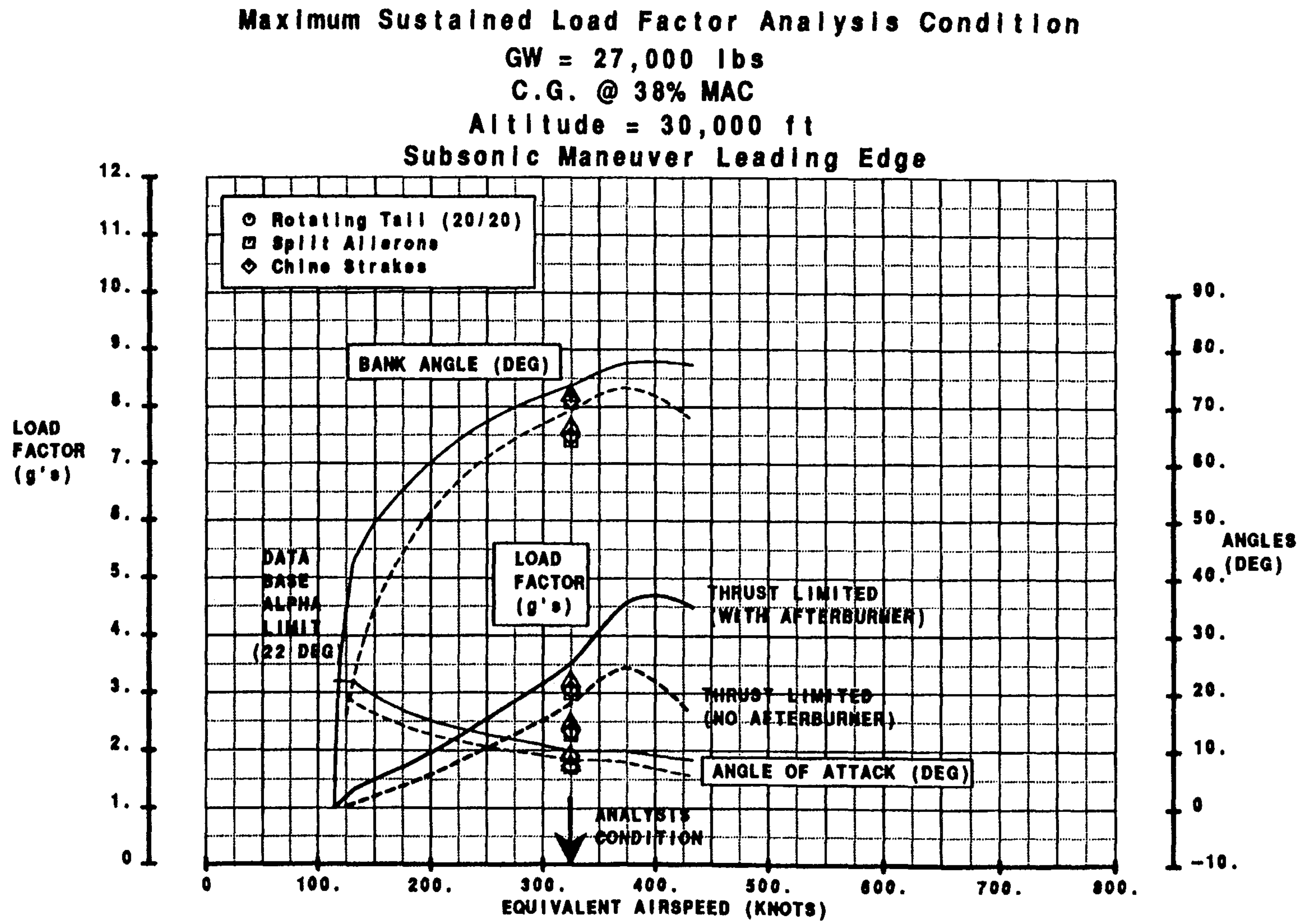

Figure 3.4.5-2 Maximum Sustained Load Factor at High Altitude - Subsonic

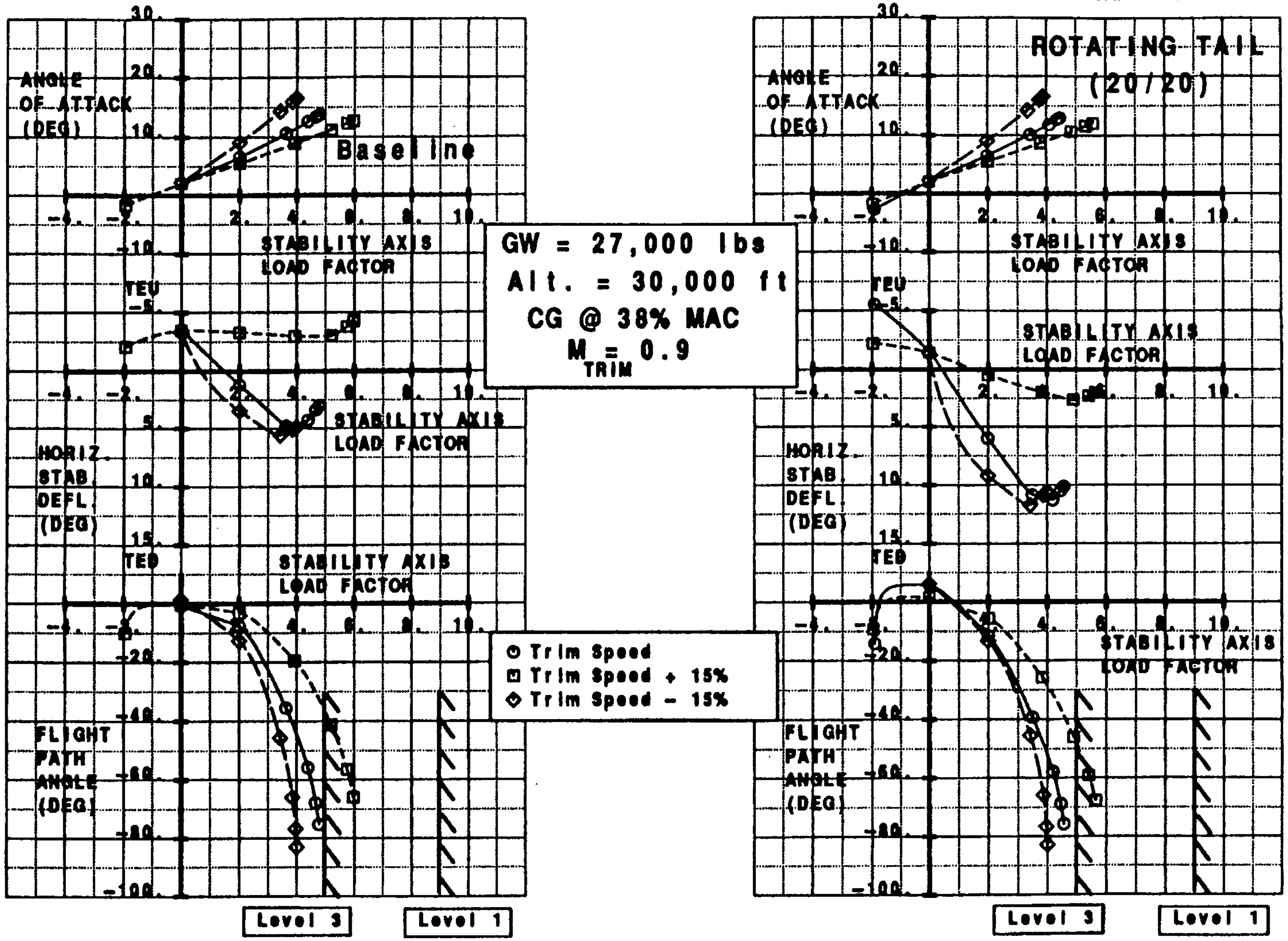

Figure 3.4.5-3 Longitudinal Control in Maneuvering Flight-Maximum Sustained Load Factor

3.4.6 Supersonic Condition

The supersonic condition flying qualities assessment was conducted for the following conditions:

Vehicle gross weight	=	27,000 lb.
Altitude	=	35,000 ft
Mach number	=	2.0

In total, for this flight condition seven flying qualities items were addressed for five configurations in addition to the baseline configuration with the results summarized in the performance summary sheet of Figure 3.4.6-1 based on data as illustrated in Figures 3.4.6-2 and 3.4.6-3..

The majority of the analysis concentrated on the baseline vehicle or the rotating tail configuration since the other effectors did not generate the required control power. The baseline Model-24F configurations with vertical tails but without thrust vectoring, as tested, meets the Level 1 or pass criteria of the Military Specification, MIL-F-8785C, reviewed above, for six of the seven conditions and meets Level 3 quality for one flying quality item, longitudinal control in maneuvering flight. The failure is again due to the simulation and the reader is referred to Section 3.4.3.

The rotating tail meets or exceeds Level 1 for all items except longitudinal control in maneuvering flight where it attains only Level 3. Failure to meet this requirement is again mainly due to the way the simulation analysis is performed in the simulation code RPAS as discussed in Section 3.4.3.

The split ailerons (without vertical tails) fail to meet the lateral-directional dynamics requirements as they do not generate the required control power for important flying quality conditions. The chine strakes are most useful at high angles of attack which is not part of this flight regime.

The reader can summarize the remaining elements of the summary sheet, Figure 3.4.6-1, in a similar fashion. The rotating tail shows the overall best performance among the effectors. The reader is to keep in mind that only the baseline configuration had a vertical tail. For more details, see the data collected in Appendix B.

GW = 27,000 lbs M = 2.0 Altitude = 35,000 ft

DESCRIPTION	REQUIRMENTS SOURCE	CONFIGURATIONS: Baseline no TV	Split Ailerons no TV	Chine Strakes no TV	Rotating Tail (Γ_H = 20°/20°) no TV	Rotating Tail+ Split Ailerons no TV	Rotating Tail+ Split Ailerons with TV
Longitudinal control in unaccelerated flight	MIL-F-8785C § 3.2.3.1 MIL-STD-1797A § 4.2.7.1	Pass	Pass	Pass	Pass	Pass*	Pass*
Longitudinal control in maneuvering flight	MIL-F-8785C § 3.2.3.2 MIL-STD-1797A § 4.2.7.2	Level 3	Fail*	Fail*	Level 3	Level 3*	Level 3*
Lateral-directional oscillations Dutch roll	MIL-F-8785C § 3.3.1.1 MIL-STD-1797A § 4.1.11.7 § 4.6.1.1	Level 1	Fail*	Fail*	Level 1	Level 1*	Level 1*
Roll mode	MIL-F-8785C § 3.3.1.2 MIL-STD-1797A § 4.5.1.1	Level 1	Fail*	Fail*	Level 1	Level 1*	Level 1*
Spiral mode	MIL-F-8785C § 3.3.1.3 MIL-STD-1797A § 4.5.1.2	Level 1	Fail*	Fail*	Level 1	Level 1*	Level 1*
Turn coordination	MIL-F-8785C § 3.3.2.6 MIL-STD-1797A § 4.5.9.5.1 § 4.6.7.2	Pass	Pass	Pass	Pass	Pass*	Pass*
Roll control effectiveness	MIL-F-8785C § 3.3.4 MIL-STD-1797A § 4.5.8.1	Level 1	Level 1	Level 1	Level 1	Level 1*	Level 1*

* Evaluated by Inspection

Figure 3.4.6-1 Supersonic Condition

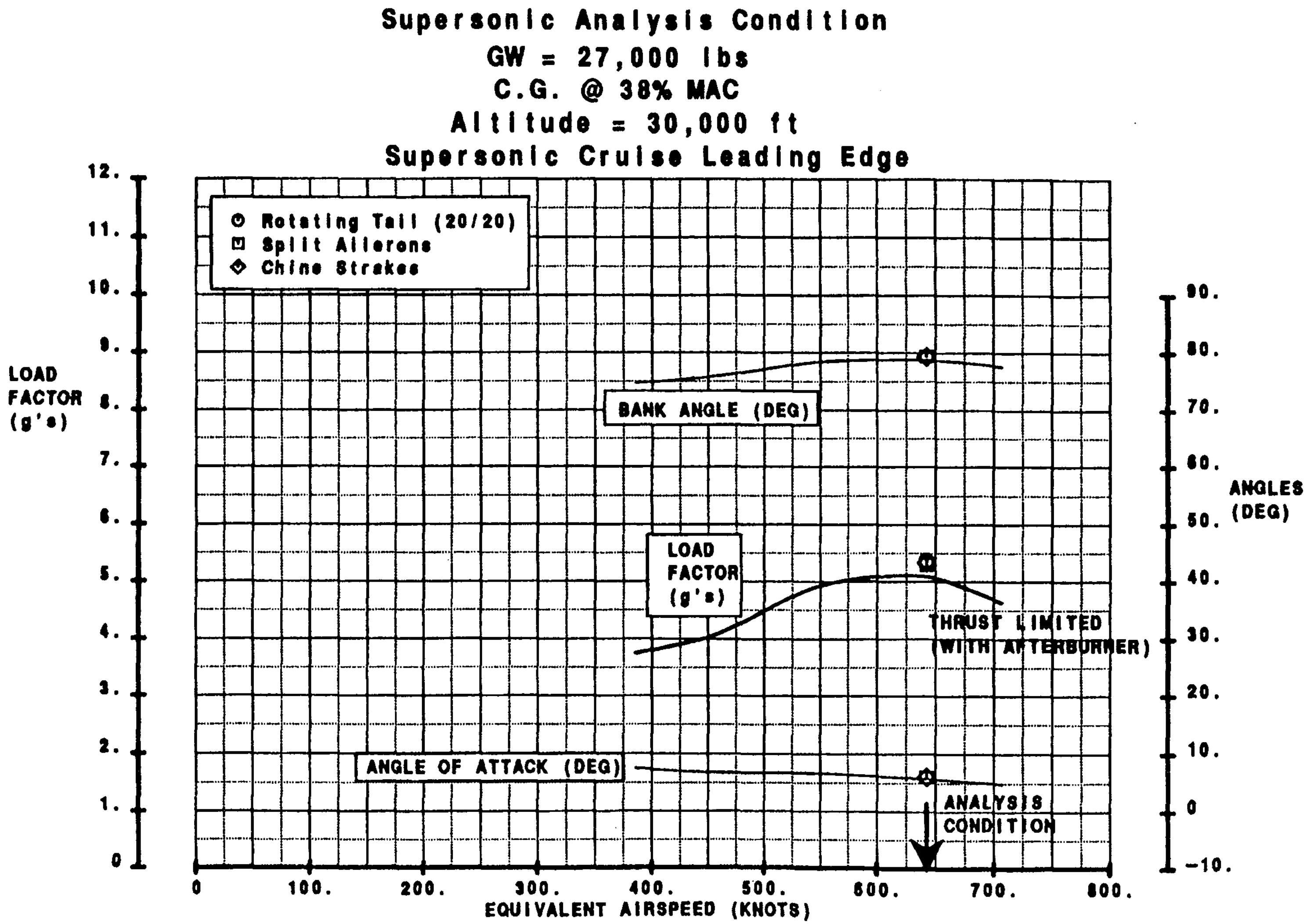

Figure 3.4.6-2 Sustained Load Factor at High Altitude - Supersonic Penetration

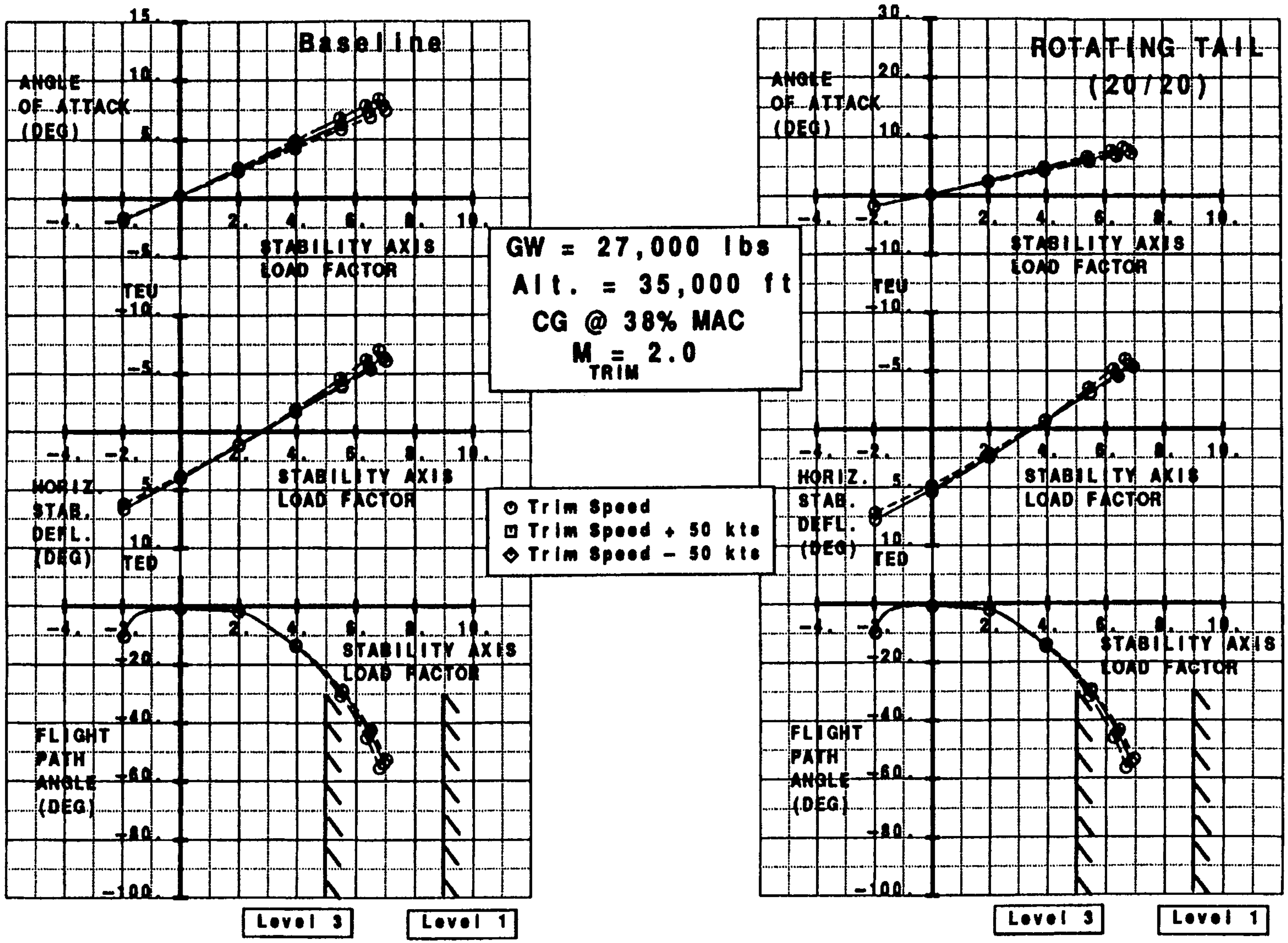

Figure 3.4.6-3 Longitudinal Control in Maneuvering Flight-Supersonic Condition

3.5 Carrier Suitability Performance

The landing and takeoff carrier suitability assessment of three navalized versions of Model-24F were done using RPAS, MEATBALL and CAT2 analysis tools. RPAS is a Boeing product that was developed to provide a fully functional 6 degree of freedom simulation for testing, analysis and real time simulation in minimum time. MEATBALL is a 3 degree of freedom carrier approach performance program designed for the Navy by LTV Aerospace and Defense Company. All the carrier approach criteria studied were analyzed using either RPAS or MEATBALL and in some cases both were used and then compared. RPAS and MEATBALL are not capable of analyzing carrier launch criteria.

A conceptual design tool called CAT2 was used to estimate carrier launch wind over deck for the baseline and rotating tails configurations. It simplifies catapult launch by making approximations of landing gear and control system effects. The effect of nose wheel pitch off is accounted for and it estimates launch performance with minimum inputs. The same geometry, weights, force and moment coefficient data were supplied as applicable to each analysis tool.

The three configurations studied were the Navy baseline, a rotating tail version of the Navy baseline and the rotating tail configuration with split ailerons and thrust vectoring. The Navy Model-24F is a scaled-up version of the baseline Air Force Model-24F. The following table shows the differences between the two aircraft:

	Basic Model -24F	Navalized Model -24F
Wing Area ~ ft^2	465	650
MAC ~ ft	17.408	20.583
Span ~ ft	31.98	37.82
Ixx ~ slug-ft^2	22,000	33,000
Iyy ~ slug-ft^2	85,000	175,000
Izz ~ slug-ft^2	101,000	179,000
Landing Weight ~ lb.	25,000	31,950
Normal Approach Speed ~ kts	132	135

Table 3.5-1

The same aerodynamic database was used for all three Navy configurations. The Model-24F aerodynamic coefficient database is a combination of wind tunnel data and predicted estimates.

Ten landing maneuvers were assessed for all three configurations. Vision over the nose, pop-up, wave-off, longitudinal acceleration and flight path stability were evaluated using both MEATBALL and RPAS. Pitch control power, cross wind landing, roll performance, minimum control speed with one engine out, dutch roll frequency and damping for Level 1 flying qualities were all analyzed with RPAS. The criteria assessment was done using only RPAS for the thrust vectoring model. The assumptions made for all analyses were as follows:

	RPAS	MEATBALL
ALTITUDE	600 FT	600 FT
ATMOSPHERE	STANDARD DAY	TROPICAL DAY
GLIDE SLOPE/MIRROR ANGLE ~ DEG.	-4°	-4°
PILOT RESPONSE TIME (WAVE-OFF)	0.7 SECONDS	0.7 SECONDS
CG LOCATION	38% MAC	38% MAC
LANDING GEAR	DOWN	DOWN
LE FLAPS	30°	30°
TE FLAPS	30°	30°
DIHEDRAL ~ ROTATING TAILS	20°/20°	20°/20°

Table 3.5-2

In MEATBALL, each analysis is initiated with the aircraft trimmed at 1.1 times the power-on stall speed. MEATBALL iterates to find the lowest approach airspeed which meets the specific maneuver requirement. There is an option to specify approach speed in MEATBALL for the pop-up and wave-off maneuvers. Unfortunately, the program did not always converge to a solution at the user specified speed. The trim speed is chosen by the user in RPAS. All RPAS runs were all done at an approach speed of 135 knots.

The pilot must see the carrier stern (waterline) in level flight while intercepting a 4 degree glide path at an altitude of 600 feet to meet the vision over the nose requirement. The nose geometry must be modified from its current pilot view angle of 15 degree to 19.2 degrees to meet this requirement.

The pop-up maneuver requires the aircraft be able to transition 50 feet above the original glide path within 5 seconds with no throttle movement. Both the baseline and the rotating tail configurations were analyzed in MEATBALL and RPAS for this maneuver. Both configurations pass the maneuver but the results between the two programs vary slightly because RPAS includes a 6 degree of freedom control system and a more detailed engine model. Figure 3.5-1 shows the RPAS result and Figure 3.5-2 contains the comparison between the MEATBALL and RPAS solutions. The thrust vectoring configuration was not evaluated for this maneuver or for wave-off.

In a wave-off, the arresting hook point altitude loss can not exceed 30 feet. The MEATBALL wave-off program terminates when the hook sink and glide slope angle changes sign. Figure 3.5-3 shows the RPAS results with varying wind over deck and Figure 3.5-4 contains the comparison between the MEATBALL and RPAS solutions at zero wind over deck. The RPAS solution does not meet the requirement for either configuration at zero knots wind over deck as shown on Figure 3.5-3. However, the wave-off requirement can be obtained with 20 knots wind over deck for both configurations. The MEATBALL result for the baseline just barely meets the requirement and fails badly for the rotating tails as drawn in Figure 3.5-4. The comparisons between the two analysis tools do not agree for the same reasons listed under the pop-up maneuver discussion.

A level flight acceleration of 5 ft/s^2 within 2.5 seconds of throttle movement is required to meet the longitudinal acceleration criteria. The baseline, the rotating tail and the rotating tail with thrust vectoring configurations passed this requirement by a large margin at an approach speed of 135 knots in the RPAS solution, see Figure 3.5-5. MEATBALL does not provide a time history only a single point result at the end of the 2.5 seconds. There is no user specified approach speed capability in MEATBALL for this maneuver. The program uses the lowest speed at which it can meet the requirement. At an approach speed of 104 knots for the baseline, MEATBALL assessed a longitudinal acceleration of 12.76 ft/s^2 after 2.5 seconds. The difference in

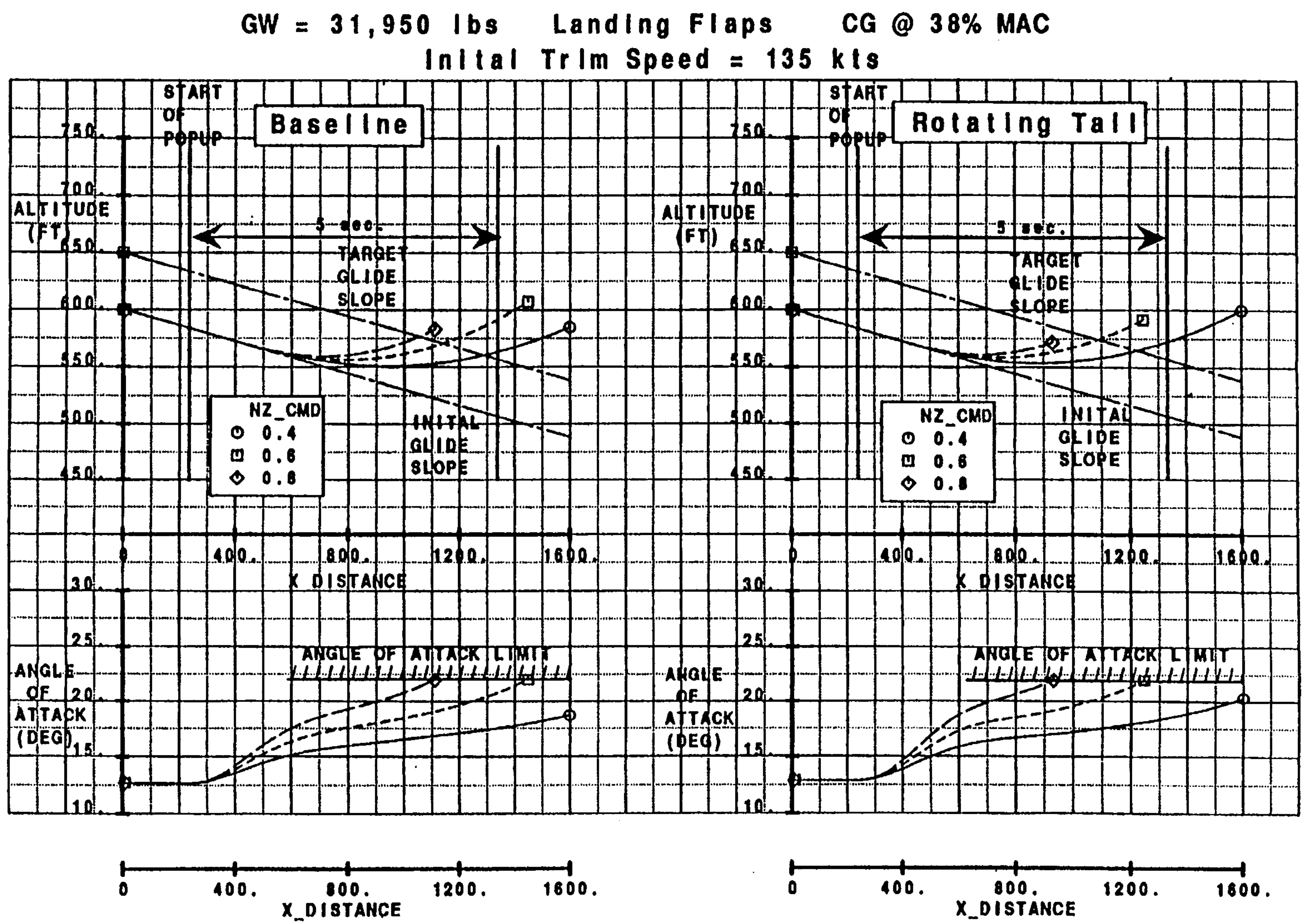

Figure 3.5-1 Pop-up Maneuver - RPAS Simulation results

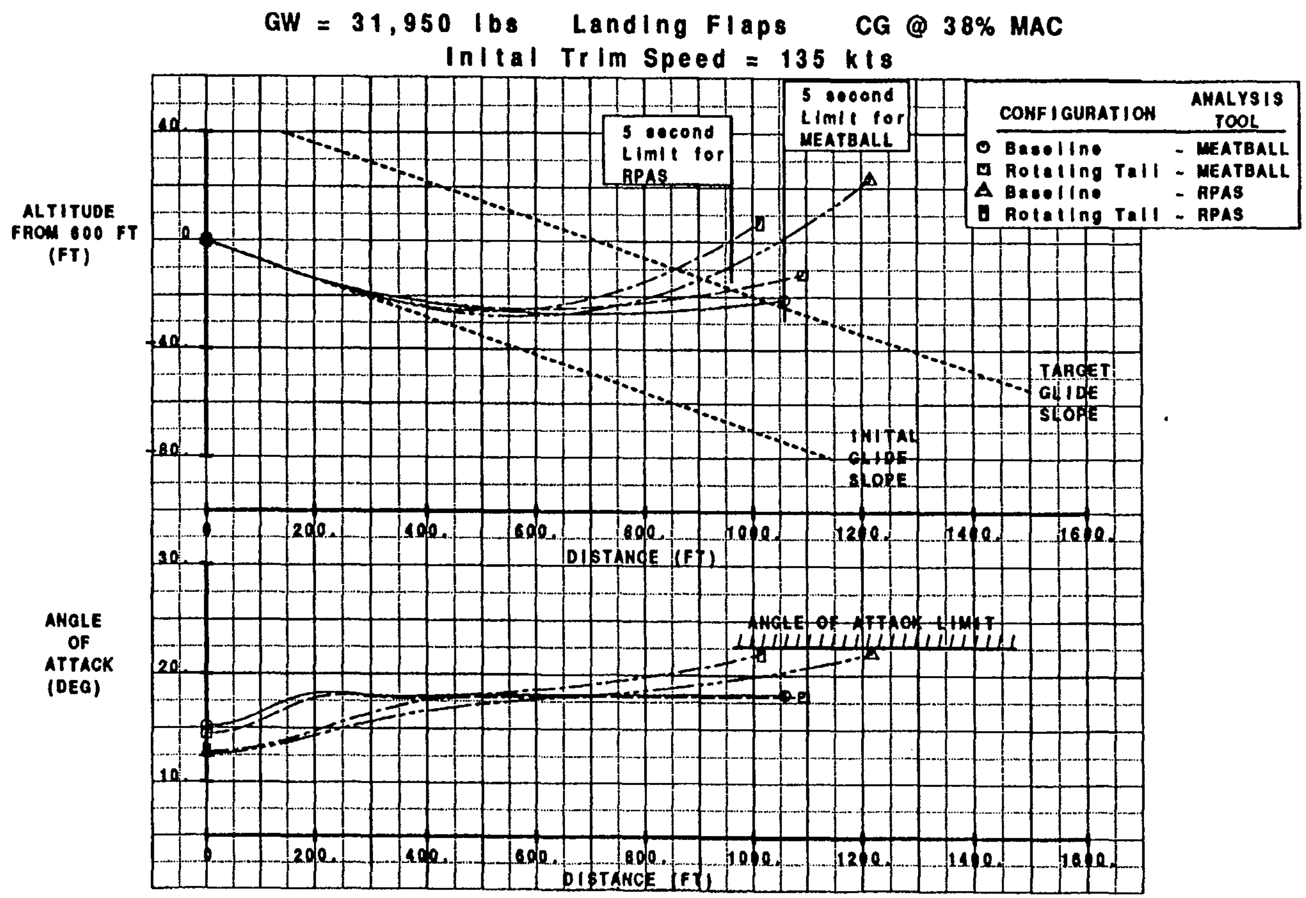

Figure 3.5-2 Pop-up Maneuver - Comparison between RPAS and MEATBALL

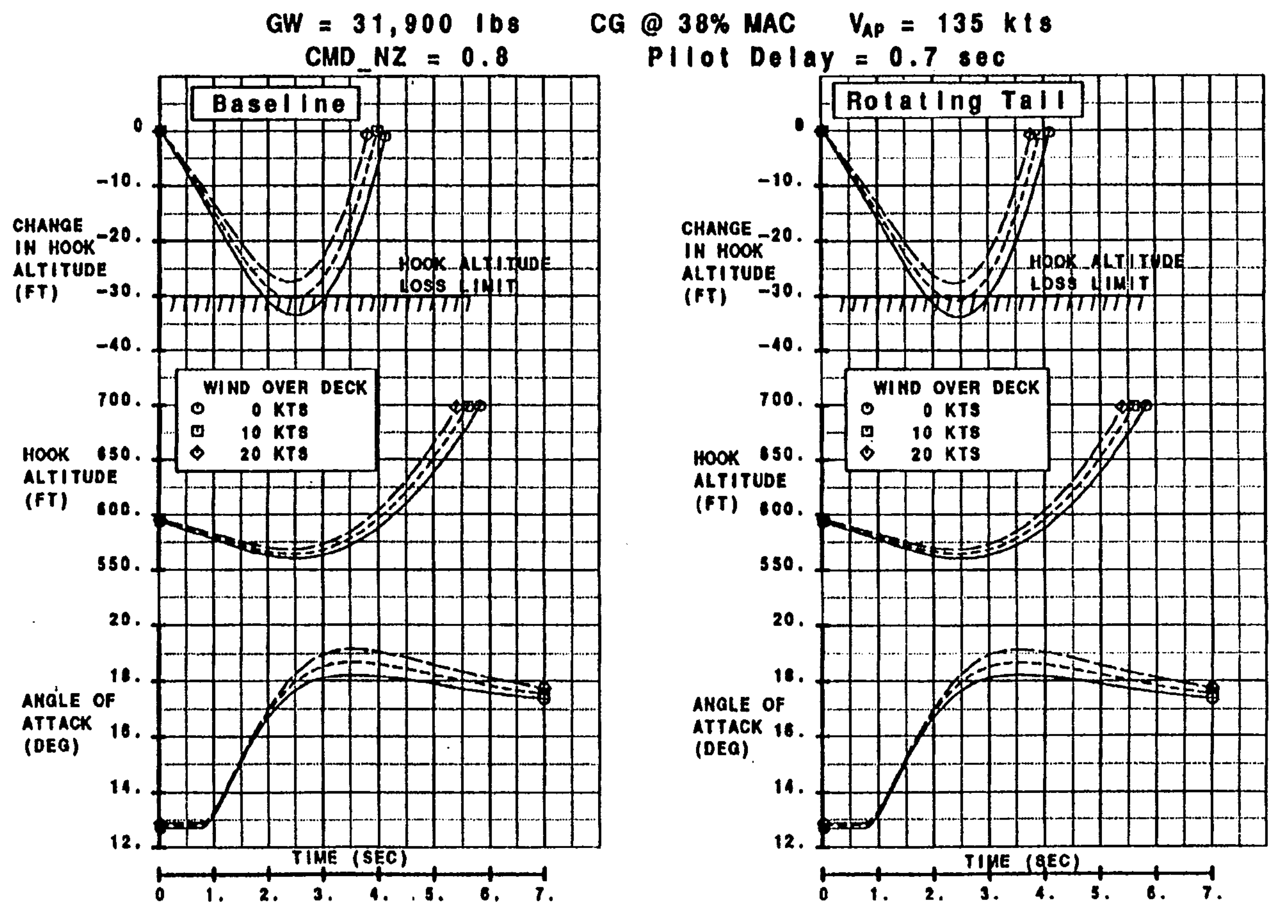

Figure 3.5-3 Wave-off Maneuver - RPAS Simulation data

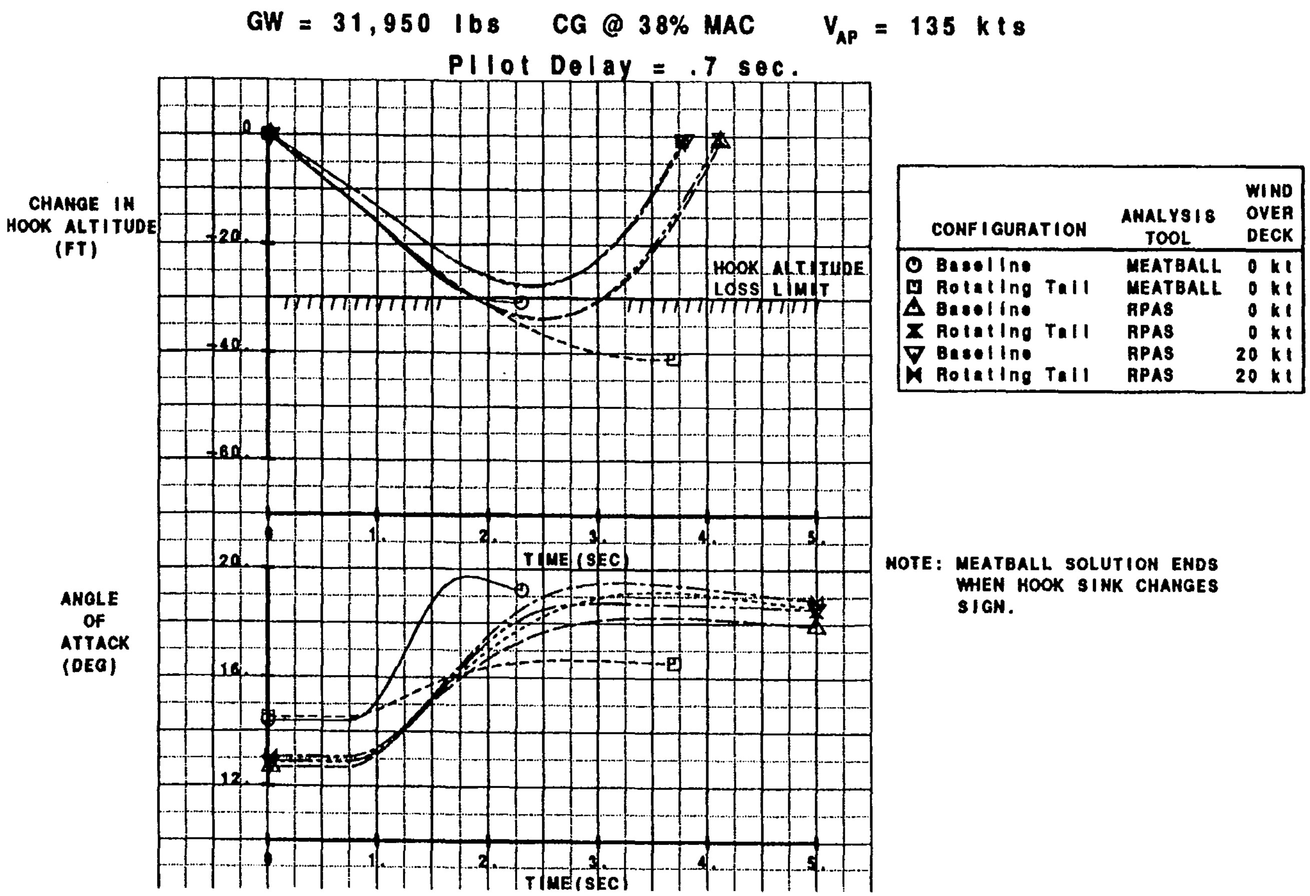

Figure 3.5-4 Wave-off Maneuver - Comparison between RPAS and MEATBALL

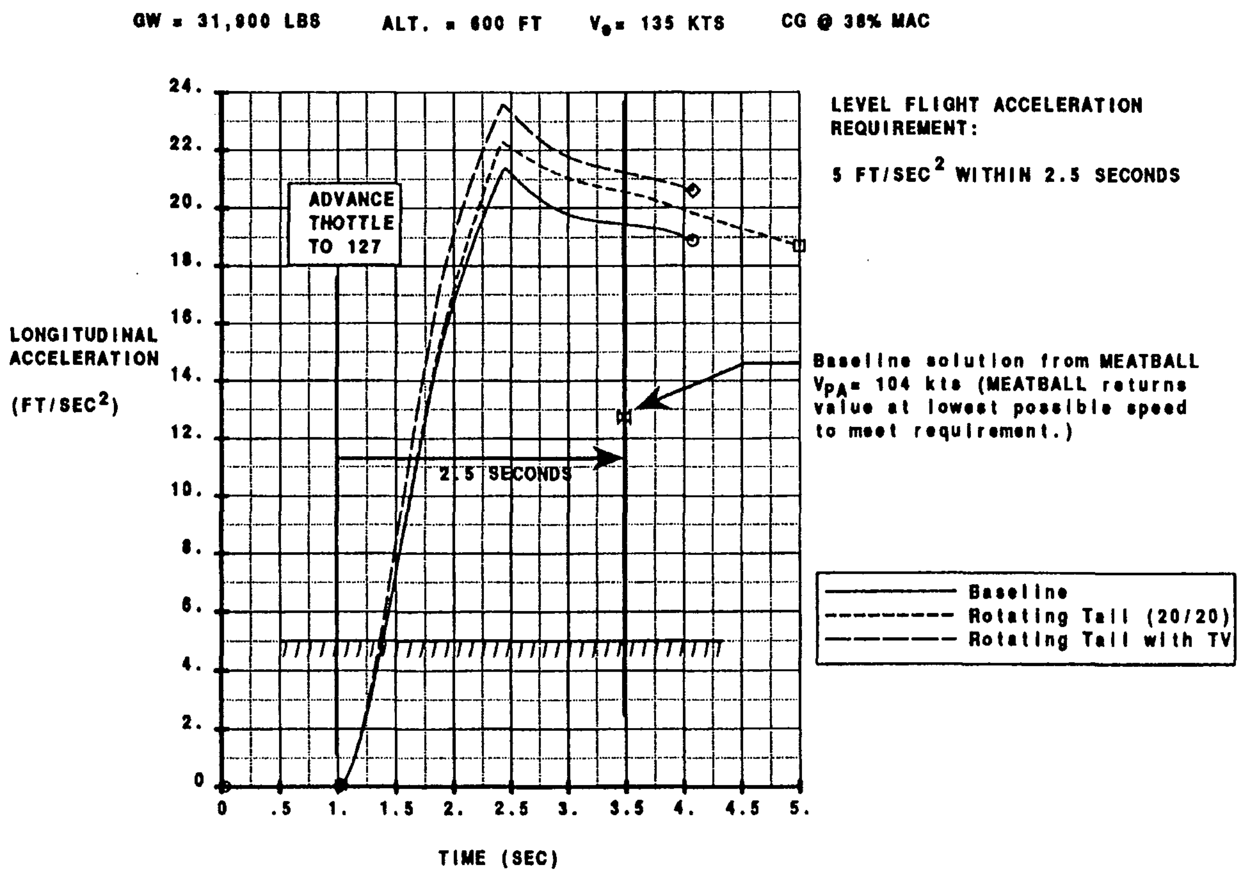

Figure 3.5-5 Level Flight Longitudinal Acceleration

approach speed probably accounts for most of the difference between the two programs solutions. This requirement was not met using MEATBALL for the rotating tail configuration.

If an approach is made on the backside of the thrust required curve or on the unstable portion of the flight path stability curve, then $\Delta\delta\gamma/\delta v$ must be less than 0.05 degrees/knot. It is desirable to land at a speed where $\delta\gamma/\delta v$ is not neutral.

LEVEL 1	$\delta\gamma/\delta v$	< 0.06 deg./kt.
LEVEL 2	$\delta\gamma/\delta v$	< 0.15 deg./kt.
LEVEL 3	$\delta\gamma/\delta v$	< 0.24 deg./kt.

This guideline was analyzed in both RPAS and MEATBALL. Figures 3.5-6 and 3.5-7 contain the flight path stability results for the analyses. MEATBALL gives the minimum approach speed where the criteria are meet for each level. These points are plotted with the RPAS curves for the baseline and rotating tails configuration in Figure 3.5-6. Both configurations pass the criteria using either analysis tool. The MEATBALL points and the RPAS $\Delta\delta\gamma/\delta v$ curves for all three configurations are on Figure 3.5-7. The comparison of $\delta\gamma/\delta v$ for the baseline, rotating tails and rotating tails plus thrust vectoring are also plotted on Figure 3.5-7. The thrust vectoring configuration does meet the requirement and was not analyzed using MEATBALL.

The high angle of attack pitch recovery requirement of $\dot{q}$ = -0.07 rad/sec^2 in 1 second and the NAVAIR Control Power Guideline that a nose-down pitch acceleration ≥ 0.2 rad/sec^2 be obtained within 1 second were analyzed using RPAS. Only the rotating tail thrust vectoring configuration met both criteria as shown on Figure 3.5-8. The baseline and rotating tails configurations fail to meet these criteria.

An aircraft must maintain a steady heading in sideslip for landing in a 90 degree, 30 knot cross wind. No more than 75% of maximum roll authority should be used to achieve landing success for this condition. Figure 3.5-9 shows the baseline configuration passes this requirement for angles of attack under 15.3 degrees. The rotating tails configuration also meets this requirement but only for angles of attack less than 11.9 degrees which is below the approach angle of attack of 12.7 degrees. The thrust vectoring configuration is able to perform this maneuver for all angles of attack analyzed. These results are displayed on Figure 3.5-10.

WEIGHT = 31950 LB CG @ 38% MAC ALT. = 600 FT LANDING FLAPS GEAR DOWN

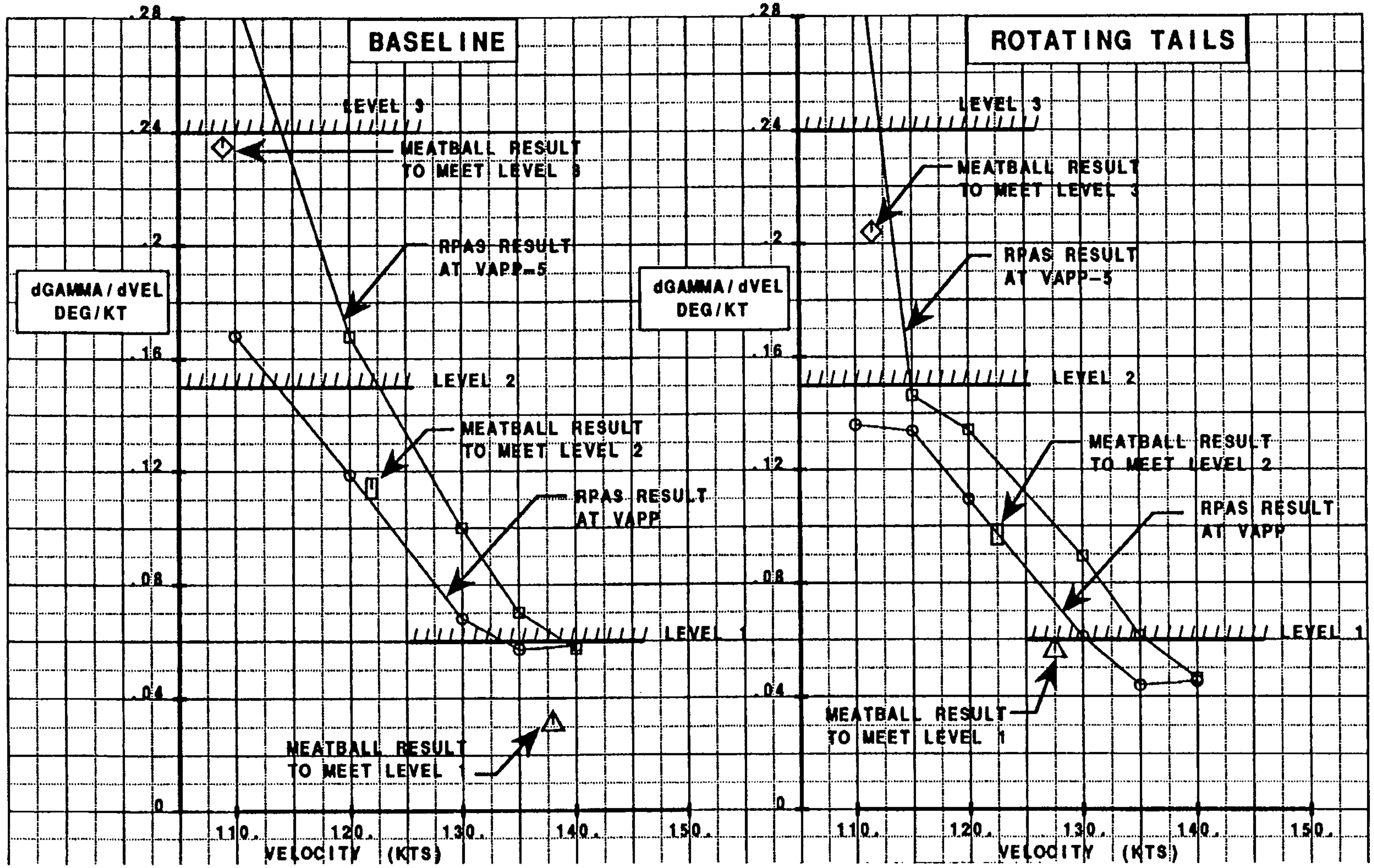

Figure 3.5-6 Flight Path Stability - Comparison between RPAS and MEATBALL

WEIGHT = 31950 LB   CG @ 38% MAC   ALT. = 600 FT   LANDING FLAPS   GEAR DOWN

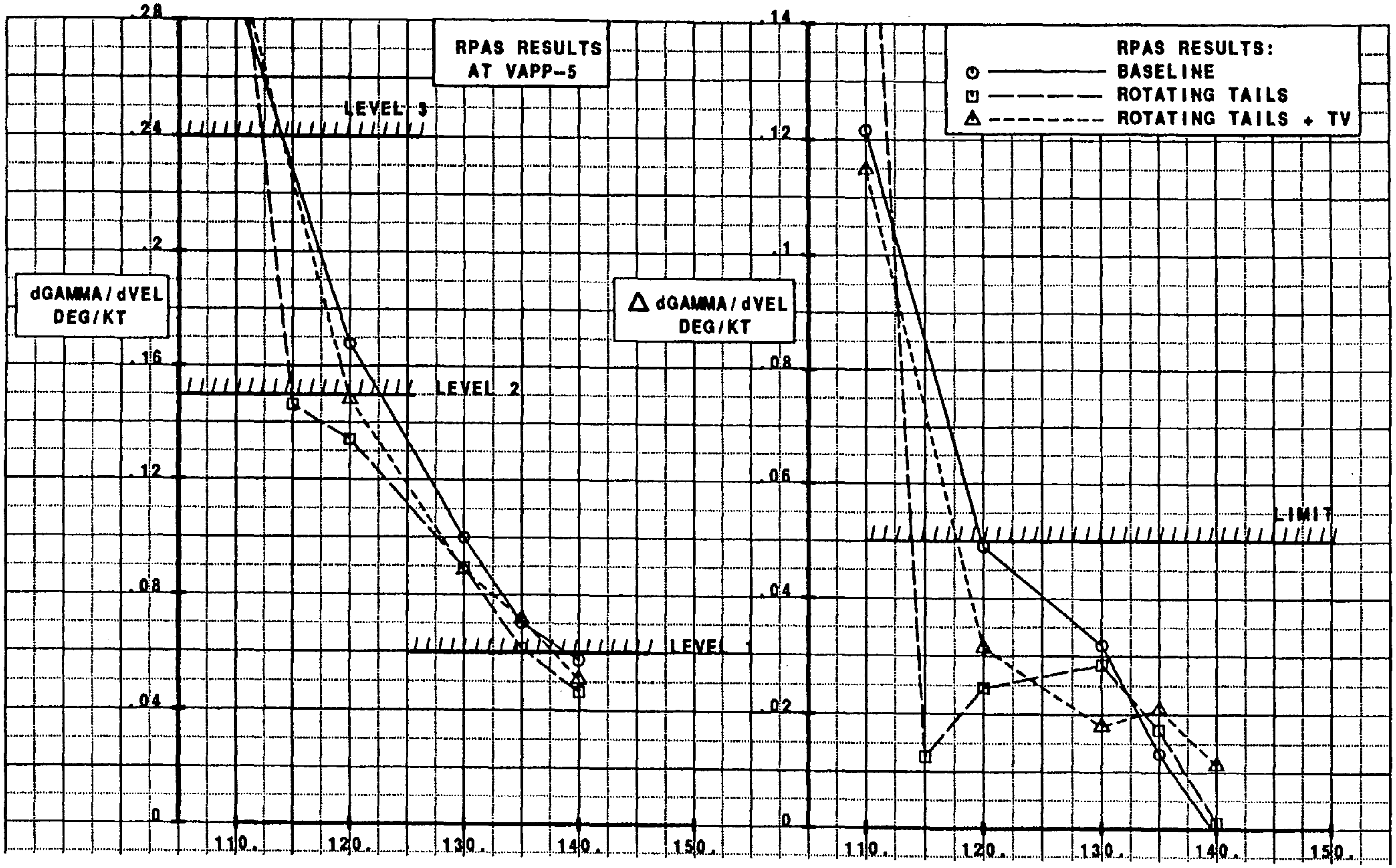

Figure 3.5-7 Flight Path Stability - RPAS Comparison to baseline

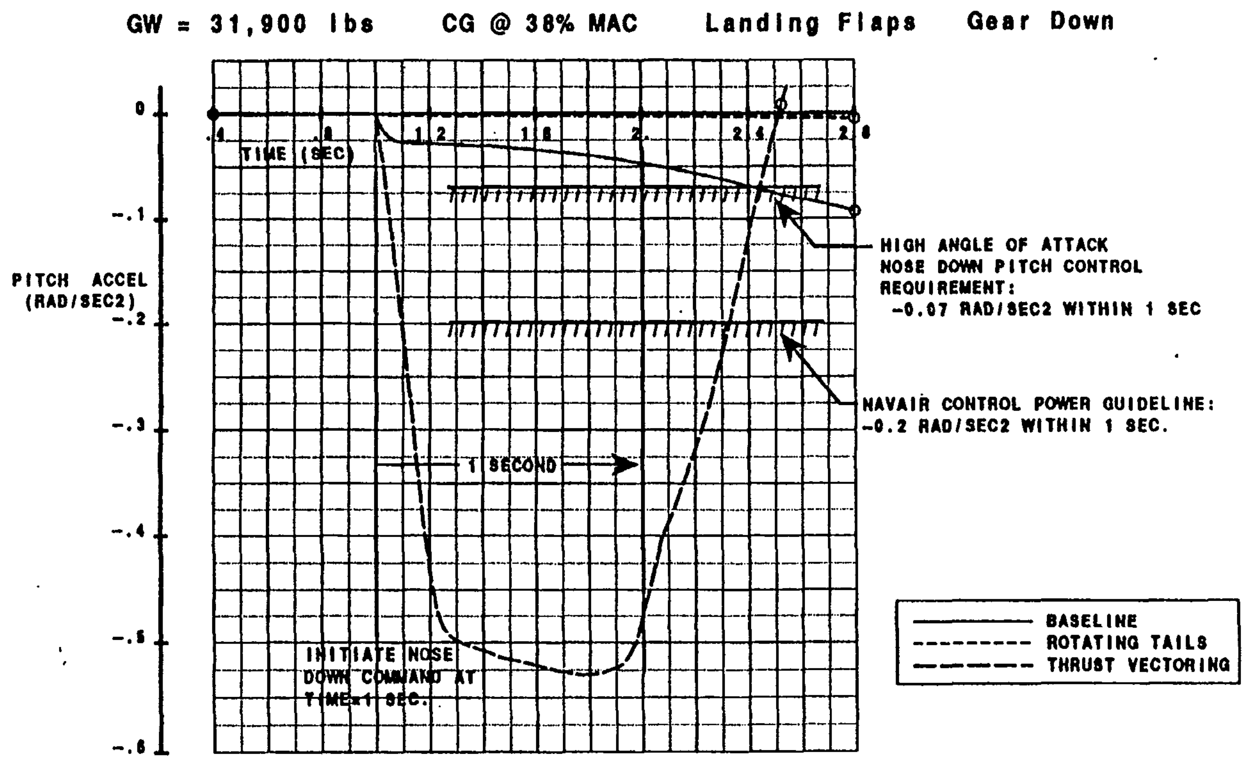

Figure 3.5-8 Landing Approach Nose Down Pitch Acceleration - 22° Angle-of-Attack

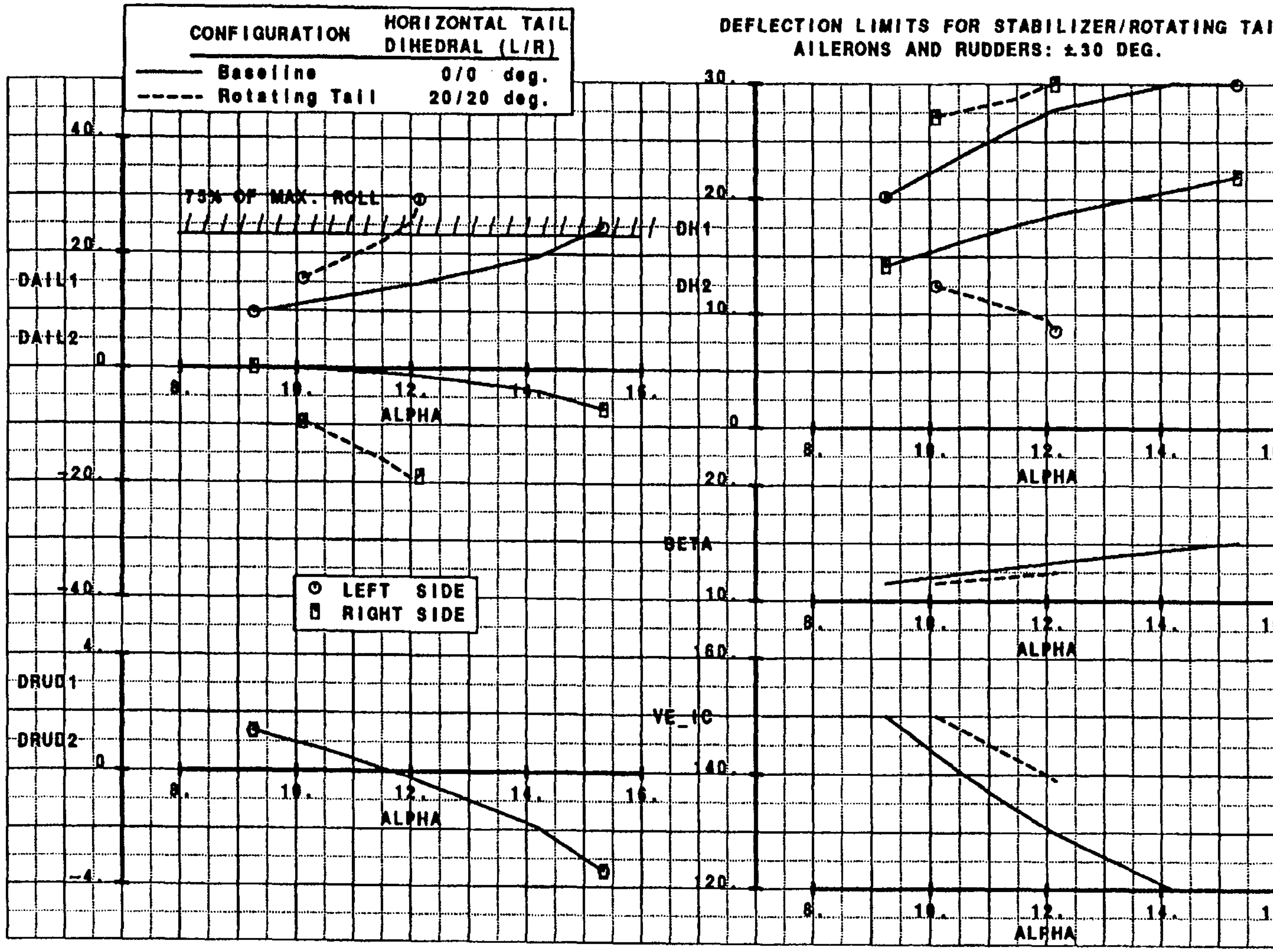

Figure 3.5-9 30 Knot at 90° crosswind

DEFLECTION LIMIT FOR ROTATING TAIL AND SPLIT AILERONS: ±30 DEG.

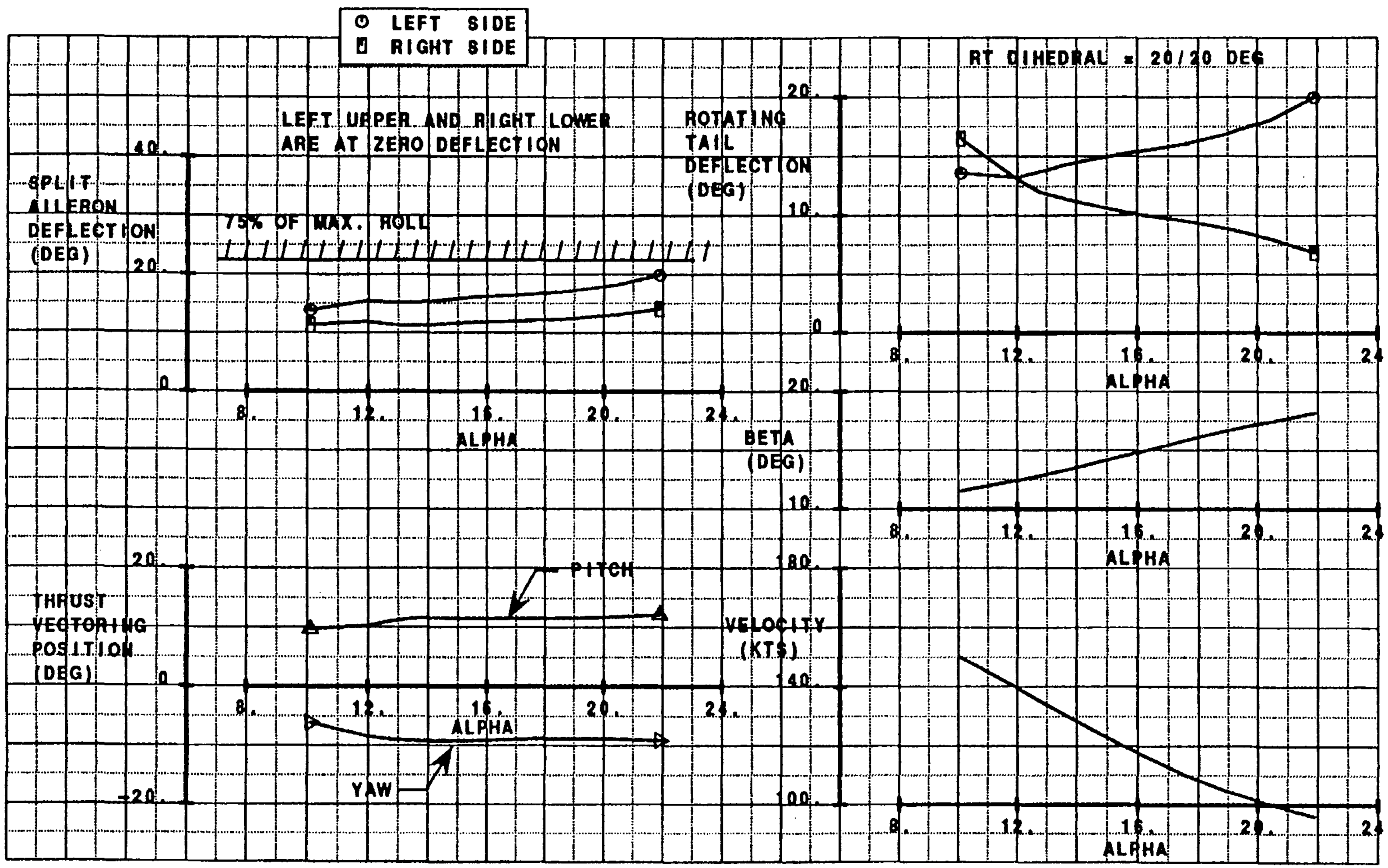

Figure 3.5-10 30 Knot at 90° crosswind - Rotating Tails, Split Aileron with Thrust Vectoring

The expected roll performance for a carrier aircraft is as follows:

30° Bank Angle in 1.1 Second at α_{app}

20° Bank Angle in 1.1 Second at α_{app} plus 4°

10° Bank Angle in 1.1 Second at Maximum Angle of Attack

Roll performance was evaluated using the RPAS tool. The baseline is lacking the roll power to meet this requirement. The baseline barely passes the 10 degree bank angle requirement at 22 degrees angle of attack and fails the 20 and 30 degree requirements. Figure 3.5-11 shows the comparison of the baseline, rotating tails and thrust vectoring configurations time to bank performance. The rotating tails configuration does not meet any of the three criteria. The thrust vectoring model almost meets the 30 degree criteria and does meet the 20 or 10 degree criteria.

The dutch roll frequency, ω_{nd}, shall exceed 0.4 radians/second and the minimum damping, ζ_d, should be greater than 1.0 following a yaw disturbance. This maneuver was done in RPAS at an approach speed of 135 knots with a 3 degree beta release. None of the three configurations had difficulty meeting the dutch roll frequency as shown on Figure 3.5-12. The frequencies and damping terms associated with this plot are as follows:

CONFIGURATION	ω_{nd} rad/sec	ζ_d
Baseline	2.32	0.771
Rotating Tails	2.187	0.796
RT + TV	2.068	0.723

The minimum control speed, V_{mc}, must be at least 5 knots below the powered approach speed with one engine out. The Model-24F baseline has only one engine. For this analysis, it was assumed Model-24F contained two engines located side by side located in the same inlet as the one engine configuration. Each engine center is 19 inches from the aircraft centerline. This analysis was performed using the RPAS simulation. Figure 3.5-13 contains the control surface deflections required to maintain control with one engine out. There is sufficient control with either the baseline or rotating tail configurations at 5 knots below the power approach speed of 135 knots.

This concludes the 10 landing maneuvers evaluated for this study.

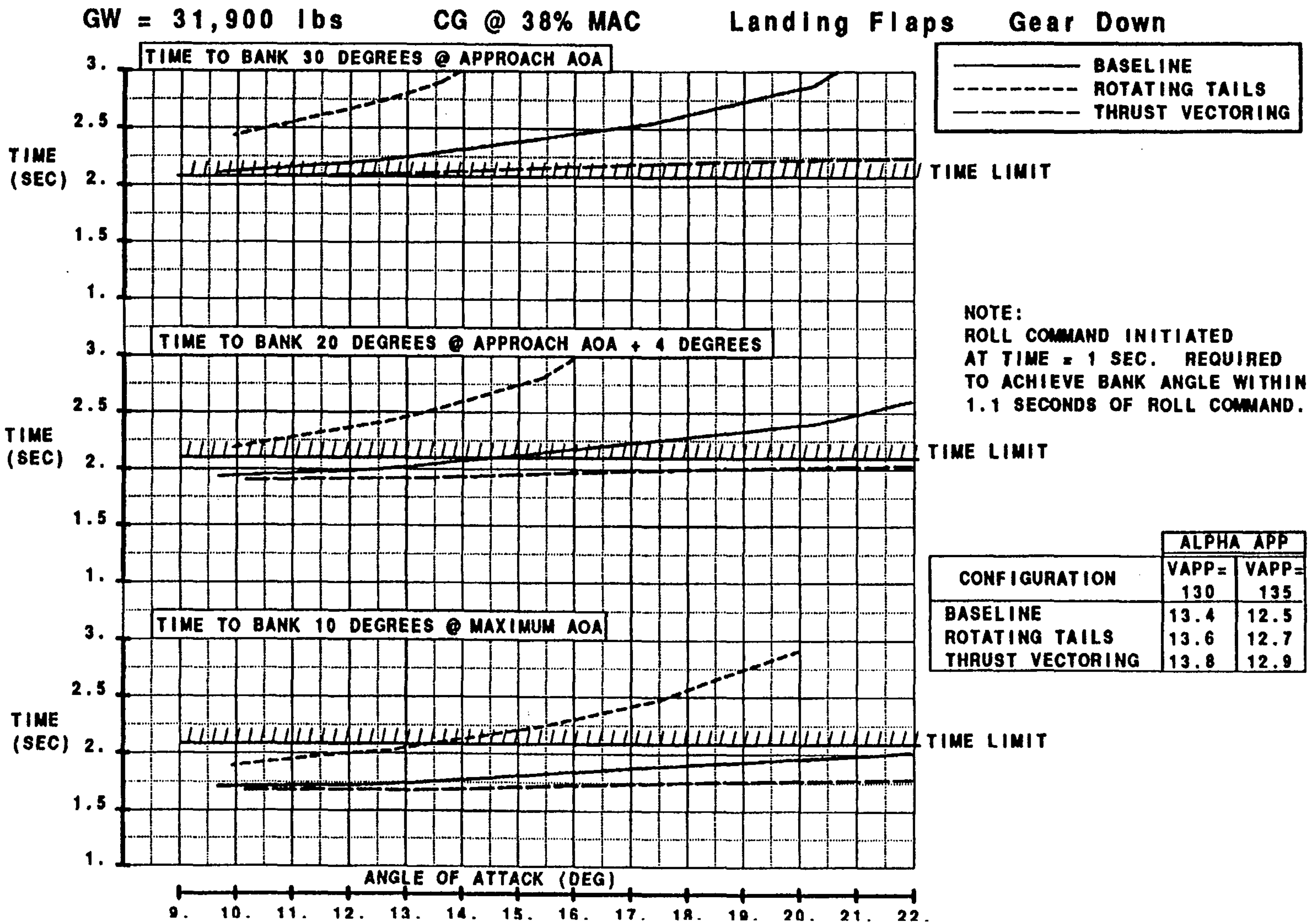

NOTE:
ROLL COMMAND INITIATED AT TIME = 1 SEC. REQUIRED TO ACHIEVE BANK ANGLE WITHIN 1.1 SECONDS OF ROLL COMMAND.

CONFIGURATION	ALPHA APP VAPP= 130	ALPHA APP VAPP= 135
BASELINE	13.4	12.5
ROTATING TAILS	13.6	12.7
THRUST VECTORING	13.8	12.9

Figure 3.5-11 Carrier Suitability Roll Rate Summary

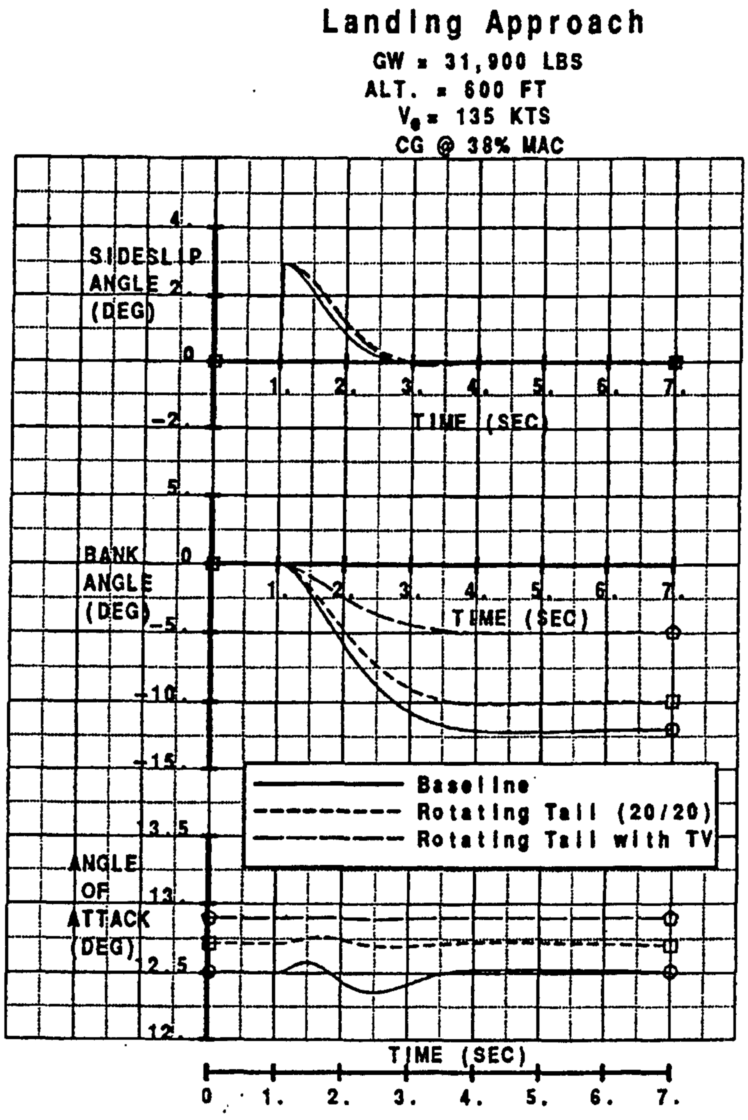

Figure 3.5-12 Dutch Roll Characteristics

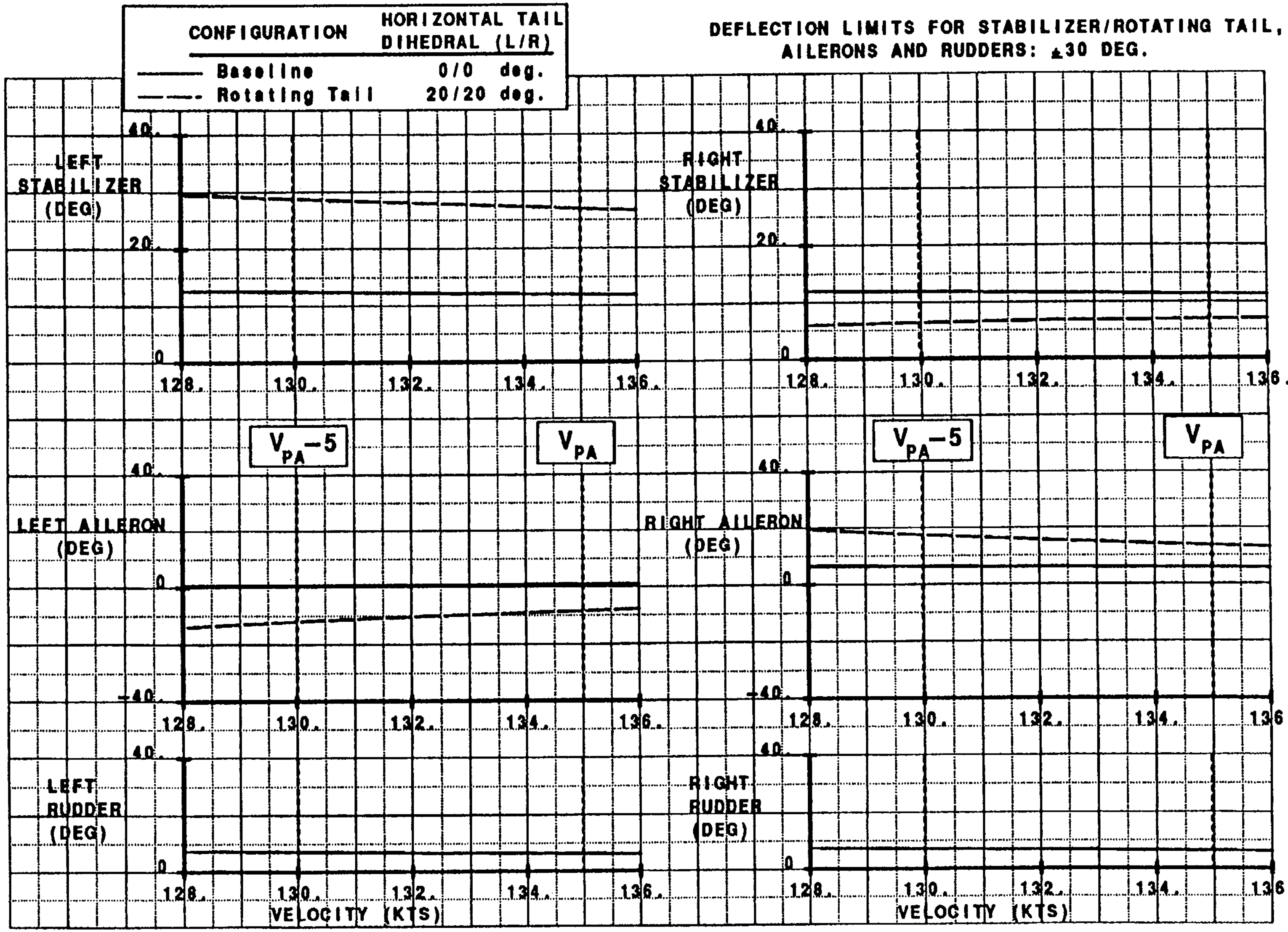

Figure 3.5-13 V_{mc} with Right Engine Out

Two takeoff criteria were estimated with the CAT2 program. The first states the aircraft center of gravity must not sink more than 10 feet off the bow of the carrier after a catapult launch. The second is the aircraft longitudinal acceleration should be greater than 0.065 g at the end of a catapult stroke. Figure 3.5-14 presents the time history results obtained from CAT2 analysis tool. The center of gravity does not sink below 10 feet off the deck at takeoff gross weight for either configuration. Level acceleration is greater than 0.065 g at the minimum end airspeed. The speed at launch is 157.4 knots for the baseline and 159.8 knots for the rotating tails configuration.

The original Model-24F was not designed for carrier use nor was it intended to fly without vertical tails. This study shows that none of the three configurations are acceptable for carrier operations. All the configurations would require geometric changes to the nose and cockpit for the vision over the nose criterion. The rotating tail configuration does meet most of the carrier suitability items evaluated, but, it needs thrust vectoring to meet the pitch down and roll rate requirements. A carrier suitable aircraft can be achieved by further modifying either the baseline or the rotating tails configurations by resizing the horizontal tails to meet the requirements where they currently fail. Resizing the tail surface will reduce the stabilizer deflection required to trim, provide more pitch down capability and increase the yaw and roll control available for roll performance.

Results are summarized in Figure 3.5-15

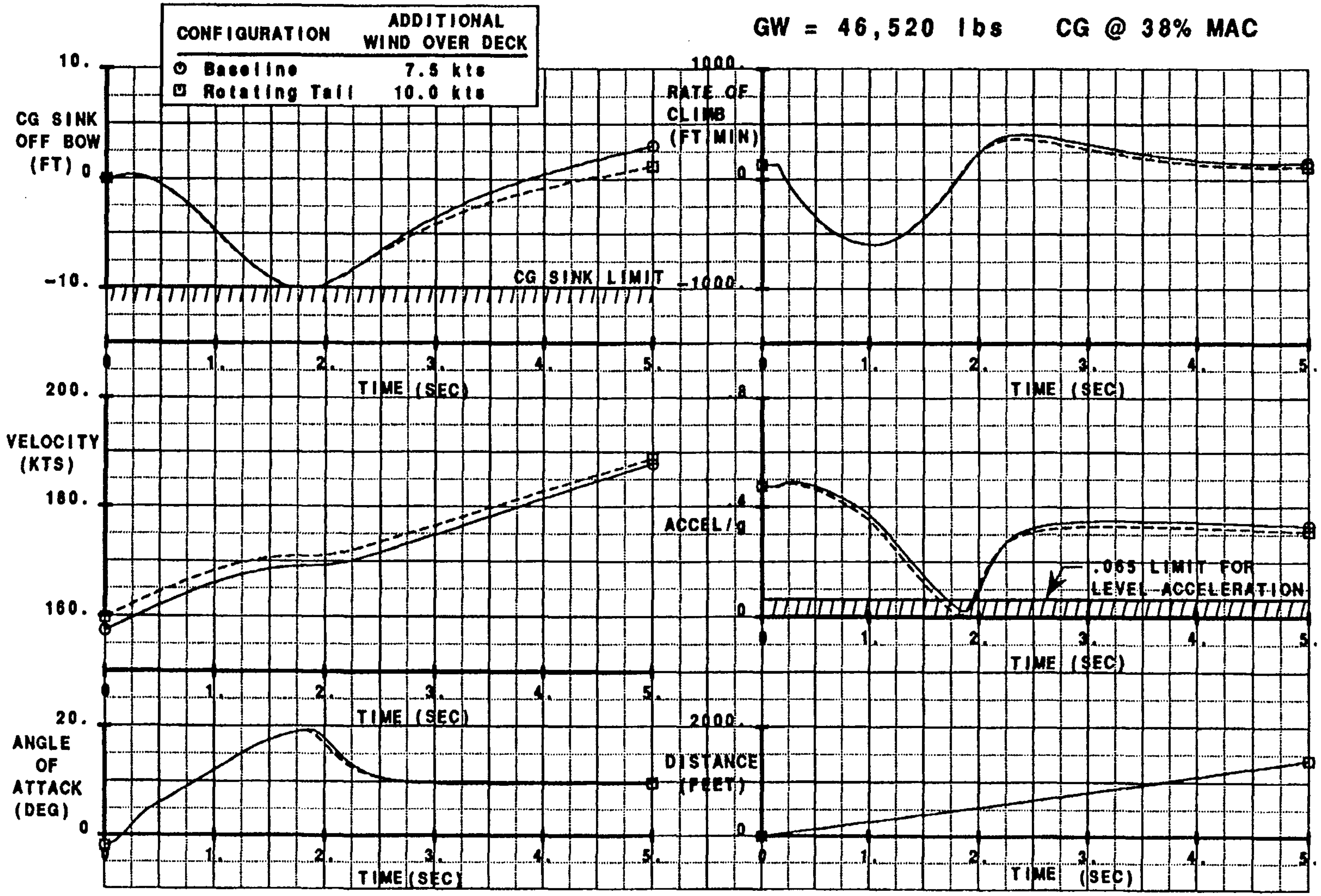

Figure 3.5-14 Catapult Launch

CRITICAL REQUIREMENTS IDENTIFIED FOR CARRIER TAKEOFF AND LANDING

CRITERIA	SOURCE	ANALYSIS METHOD	BASELINE	ROTATING TAILS	TV + ROTATING TAILS + SPLIT AILERONS
Carrier Suit Pitch Control Power Requirements High-α Pitch Recovery Requirement: $\dot{q}$ = -0.07 rad/sec^2 in 1 second Nose-down pitch acceleration ≥ 0.2 rad/sec^2 within 1 second	High Angle of Attack Nose Down Pitch Control Requirements Study 27 April 1993 NAVAIR Control Power Guidelines 27 April 1993	RPAS	**FAILED** Data shown on $\dot{q}$ vs. Time chart	**FAILED** Data shown on $\dot{q}$ vs. Time chart	**PASS** Data shown on $\dot{q}$ vs. Time chart
Must Maintain A Steady Heading In Sideslip For Landing In A 90°, 30-Knot Cross Wind. Use Lowest Approach Speed With No More Than 75% Of Maximum Roll Authority.		RPAS	**PASSES** for α < 15.3° See plots	**PASSES** for α < 11.9° See plots	**PASSES** for α's See plots
Roll Performance: 30° Bank Angle in 1.1 Second at α_{app} 20° Bank Angle in 1.1 Second at α_{app} plus 4° 10° Bank Angle in 1.1 Second at Max. AOA Unofficial Navy Requirement is Bank Angle Achieved in 1 Second	NAVAIR Control Power Guidelines 27 April 1993	RPAS	30° **FAIL** 20° **FAIL** 10° **PASS**	30° **FAIL** 20° **FAIL** 10° **FAIL**	30° **FAIL** 20° **PASS** 10° **PASS**
V_{mc} at least 5 knots below minimum V_{PA}.	NAVAIR Control Power Guidelines 27 April 1993	RPAS	**PASS**	**PASS**	**PASS**
Catapult ~ CG sink off bow < 10 ft, Level acceleration. at min. end airspeed (A/G) > .065 g	NAVAIR Control Power Guidelines 27 April 1993	CAT2	**PASS** End speed = 157.4	**PASS** End speed = 159.8	Not Analyzed
Visibility: Pilot must see carrier stern (Waterline) in level flight while intercepting 4° glide path at 600 ft altitude.	Carrier Suitability Testing Manual 30 Sept. 1994 Page 6-38	Geometry MEATBALL	**Geometry:** Model -24F pilot eye over nose angle is 15°. Solution: Modify nose to obtain more of pilot eye over nose angle. **MEATBALL Result using modified nose:** VON = 19.2° α_{app} = 14.42° and V_{app} = 134.8 knots **RPAS Result:** α_{app} = 12.5° and V_{app} = 135 knots		
Minimum Dutch Roll Frequency And Damping for Level 1 Minimum Frequency (ω_{nd}) ~ 0.4 Minimum Damping (ζ_d) ~ 1.0 RPAS: Beta Release = 3° V_e = 135 kt.	MIL-F-1797 MIL-F-8785 PG 21-22	RPAS	**PASS** ω_{nd} = 2.32 ζ_d = 0.771	**PASS** ω_{nd} = 2.187 ζ_d = 0.796	**PASS** ω_{nd} = 2.068 ζ_d = 0.723
Stall Margin: $V_{PA} \geq 1.1V_s$ (power on)	Carrier Suitability Testing Manual 30 Sept. 1994 Page 6-39	MEATBALL	**PASS**	**PASS**	TV not working in MEATBALL

Figure 3.5-15a Critical Requirements for Carrier Takeoff and Landing

CRITICAL REQUIREMENTS IDENTIFIED FOR CARRIER TAKEOFF AND LANDING

CRITERIA	SOURCE	ANALYSIS METHOD	BASELINE	ROTATING TAILS	TV + ROTATING TAILS + SPLIT AILERONS
Pop-Up ~ Able to transition 50 ft. above original glide path within 5 seconds. (No throttle movement). This speed is $V_{PA_{min}}$. $\Delta\alpha$ allowable based on 1/2 Δn_z available at initiation of maneuver.	NAVAIR Control Power Guidelines 27 April 1993 Carrier Suitability Testing Manual 30 Sept. 1994 Page 6-39	MEATBALL RPAS	**MEATBALL ~ PASS** V_{PA} = 128.2 kt. Popup = 49.8 ft. V_{PA} = 135 kt. Popup = Blows Out **RPAS - PASS**	**MEATBALL ~ PASS** V_{PA} = 127.9 kt. Popup = 50.04ft. V_{PA} = 135 kt. Popup = 67.5ft. **RPAS - PASS**	TV not working in MEATBALL **RPAS - PASS**
Wave-Off: An arresting hook point altitude loss not to exceed 30ft. A time to zero sink speed ≤ 3 seconds with a longitudinal acceleration of 3.0 kts/sec.	Carrier Suitability Testing Manual 30 Sept. 1994 Page 6-74	MEATBALL	**MEATBALL ~ PASS** V_{PA} = 120 kt. H-Sink = -29.27 ft. V_{PA} = 135 kt. H-Sink = -30.7 ft. **RPAS - FAILS FOR** 0 AND 10 KTS WOD PASS AT 20KTS WOD	**MEATBALL ~ FAIL** V_{PA} = 151.5 kt. H-Sink = -34.7ft. V_{PA} = 135 kt. H-Sink = -41.2 ft. **RPAS - FAILS FOR** 0 AND 10 KTS WOD PASS AT 20KTS WOD	TV not working in MEATBALL **RPAS - NOT ANALYZED**
Longitudinal Acceleration: Level flight acceleration of 5 ft/s^2 within 2.5 seconds of throttle movement.	Carrier Suitability Testing Manual 30 Sept. 1994 Page 6-36	MEATBALL RPAS	<u>RPAS:</u> **PASS** for a V_{PA} range of 95 to 150 knots <u>MEATBALL</u>: **31950 LB. ~ PASS** V_{PA} = 104 kt. Accel = 12.76 ft/s^2	<u>RPAS:</u> **PASS** for a V_{PA} range of 101.5 to 150 knots <u>MEATBALL</u>: Did not meet criteria using MEATBALL	<u>RPAS:</u> **PASS** for a V_{PA} range of 97 to 150 knots <u>MEATBALL</u>: TV not working in MEATBALL
Flight Path Stability If approach is made on backside of thrust req. curve or on the unstable portion of the FPS curve, then $\Delta\delta\gamma/\delta V$ < .05 deg./kt. It is desirable to land at a speed where $\delta\gamma/\delta V$ is not neutral LEVEL 1 $\delta\gamma/\delta V$ < 0.06 deg./kt. LEVEL 2 $\delta\gamma/\delta V$ < 0.15 deg./kt. LEVEL 3 $\delta\gamma/\delta V$ < 0.24 deg./kt.	MIL-F-8785C	MEATBALL	**RPAS: PASS** Level V_{PA} 1 138.2 2 122.5 3 114 **MEATBALL: PASS** Level $\delta\gamma/\delta V$ V_{PA} 1 .031 138 2 .114 122 3 .235 109	**RPAS: PASS** Level V_{PA} 1 135.2 2 114.8 3 112.4 **MEATBALL: PASS** Level $\delta\gamma/\delta V$ V_{PA} 1 .056 127.5 2 .097 122.5 3 .204 111.5	**RPAS: PASS** Level V_{PA} 1 137.6 2 119.7 3 114 **MEATBALL:** TV not working in MEATBALL

Figure 3.5-15b Critical Requirements for Carrier Takeoff and Landing

3.6 Summary of Performance Study

The three effectors studied were split ailerons, chine strakes, and a rotating tail concept. The handling qualities of the baseline Model-24F configuration with vertical tails was evaluated to provide a performance reference. The effectors were then evaluated individually with the vertical tail removed. Additional configurations made up of combinations of effectors, the rotating tail together with the split ailerons (vertical tail removed), the rotating tail together with split ailerons and thrust vectoring (vertical tail removed) were included in the study.

The performance of the effectors was evaluated against MIL-F-8785C and MIL-STD-1797A including a total of 56 flight conditions and flying quality items being evaluated for each configuration. The study was conducted with a flight controls system optimized for each configuration including the baseline. The same basic concept of total integrated control assets was used for all configurations. No control force criteria were evaluated as it is assumed that a tailored artificial feel system will be used.

The study used the Boeing RPAS system using the aerodynamic data base for the baseline Model-24F appropriately modified to include the effectors to be evaluated. Trims and time histories were run at the specific flight conditions chosen for the evaluation. The performance was evaluated with an operational flight control system as the tailless Model-24F configuration is unstable at aft center of gravity longitudinally for subsonic speeds and directionally at all speeds. The aerodynamic data base was limited in angle of attack to the range -4° to 22° and in sideslip to the range -10° to +10°. Simplified engine and mass models were used. Simplified actuator models were also used, however, rate and position limiting were included.

The rotating tail evaluation was conducted for a fixed dihedral (Γ_H = 20°/20°). The aerodynamic data base allows independent positioning of left and right sides of the tail. The inclusion of horizontal tail dihedral angle as a control variable results in complications for trim and control inputs requiring more reources to resolve than is available in this study. Additional wind tunnel testing is required to determine optimal angle settings for various flight conditions.

The rotating tail configuration, the baseline configuration with thrust vectoring, and the rotating tail with thrust vectoring configuration were evaluated for carrier suitability. To approximate a potential Navy aircraft the wing area, span, mean aerodynamic chord, weights and inertias of the Model-24F were modified. However, The aerodynamic data base coefficient data were not modified nor was the flight control systems modified. The carrier suitability study concentrated on takeoff and approach. The Navy configuration was not evaluated for up and away flight conditions. The computer codes MEATBALL, CAT2 and RPAS were used for this evaluation with 13 carrier suitability items investigated. Unfortunately MEATBALL and CAT2 can not handle thrust vectoring. The RPAS program was used to duplicate some MEATBALL calculations and their comparisons are presented.

The Rotating Tail appears to be a viable concept being nearly as effective as the baseline Model-24F. The split ailerons and chine strakes are not viable concepts for this configuration since they produce too little yawing moment. There is just not enough control volume for split ailerons to be effective, and the chine strakes not effective at nominal angles of attack. Thrust vectoring improves overall performance which combined with the rotating tail can produce a tailless configuration with acceptable flying qualities at low thrust levels or with vectoring inoperative.

The findings are summarized in the Figure 3.6-1 below. The lateral-directional dynamics requirements failed badly for the aileron and the chine strake.

Configuration	Level 1 or Pass	Level 2	Level 3	fail	% level 1 or pass
Baseline-no TV	45	3	3	5*	80%
Split Ailerons-noTV	17	3	0	36	30%
Chine Strakes-no T V	17	3	0	36	30%
Rotating Tail (Γ_H=20°/20°) no TV	43	2	0	8*	77%
Rotating Tail + Split Ailerons no TV	43	2	0	8*	77%
Rotating Tail + Split Ailerons with TV	48	1	0	5*	86%

*Majority due to aerodynamic data base limits

Figure 3.6-1 Flight Condition and Flying Qualities Items

4.0 Task 3 - Effector Integration Study

4.1 Effector Integration Overview

The integration aspects of innovative control effectors can significantly affect the results of any overall assessment of a given control device. When assessing the feasibility of a device, the ability of the designer to incorporate innovative control concepts into a design without significantly compromising other aspects of the design must be an achievable goal. Integration technologies may vary in relative importance for any given effector design, but the main players generally include actuation, structures (load path), weight, signature, cost/affordability, and reliability, maintainability, and supportability (RM&S). Any device with significant shortcomings in any of the above mentioned areas may present insurmountable problems for the designer and prevent incorporation into the design. For the devices of interest, the most significant challenge is to integrate the rotating horizontal tail concept so that the penalties associated with it do not offset any potential benefits. For this reason, much of the integration task will be focused on this effector.

The primary objective of this contract is to develop control effectors that will facilitate elimination of the vertical tails. Benefits in weight/range and RCS can be obtained by removing the vertical tails. Figure 4.1-1 summarizes the benefits of removing the vertical tails completely in terms of RCS and vehicle aerodynamic drag. For the baseline Model 24F vehicle, removing the vertical tails would provide a net weight improvement of 645 lbs including the removal of structure, LO treatment, and actuation systems. Additional benefits can also be obtained in terms of cost and RM&S by a reduction in overall part count. These benefits are offset by the addition of control effectors to the configuration. Using a concept such as the rotating horizontal tail may still provide a benefit in some technology areas.

4.1.1 Chine Strake Integration

The challenges to integrating this concept onto the baseline configuration include allowances for radar installations, the proximity to the cockpit area, the large angular motion from retracted to fully deployed positions and the location near the chine line. The problem of location on the forebody is critical to this type of effector because the closer the device can be deployed to the nose, the more effective it will be. Unfortunately, forward looking radar also covets this position and placing control

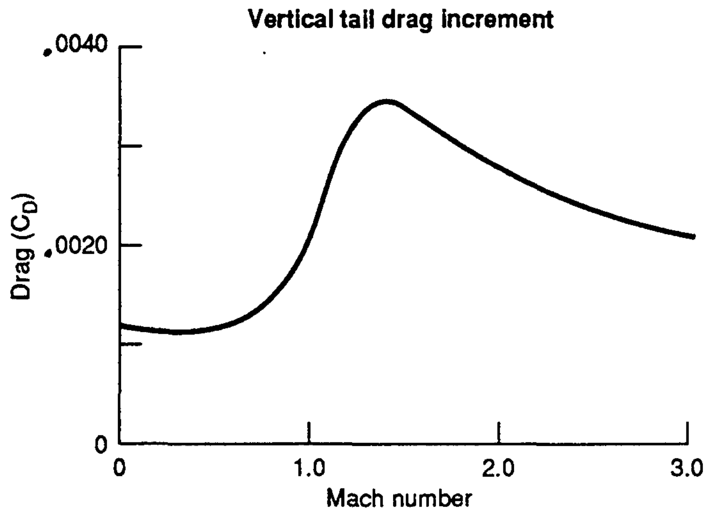

Signature

	P_{50} (v) – db	
Sector	With vertical tail	Without
Forward	-38.3	-40.5
Side	-11.7	-14.2
Aft	-22.4	-23.0

-Ad3

Figure 4.1-1. Benefits From Removing Vertical Tail

devices forward of the radar will have significant adverse effects on the performance of the radar. Moving the device location back from the nose along the chine line will reduce control effectiveness, and placing them alongside the cockpit will either displace other equipment best located near the pilot, or increase the volume in the cockpit area, impacting wave drag. The problem with the chine line itself is that of locating a hinge line that will still place the deployed surface close to the chine and meet any setback requirements to accommodate signature technology. This device significantly affected the forward sector signature characteristics which are summarized in Figure 4.5-1. As shown in Figure 4.1.1-1, the location selected for this effector compromises the aerodynamic performance in order to accommodate these integration concerns. Since the effect on performance in the flight regime studied was deemed to be significantly below desired capabilities for inclusion in future fighters, this concept was not fully studied beyond this conceptual integration.

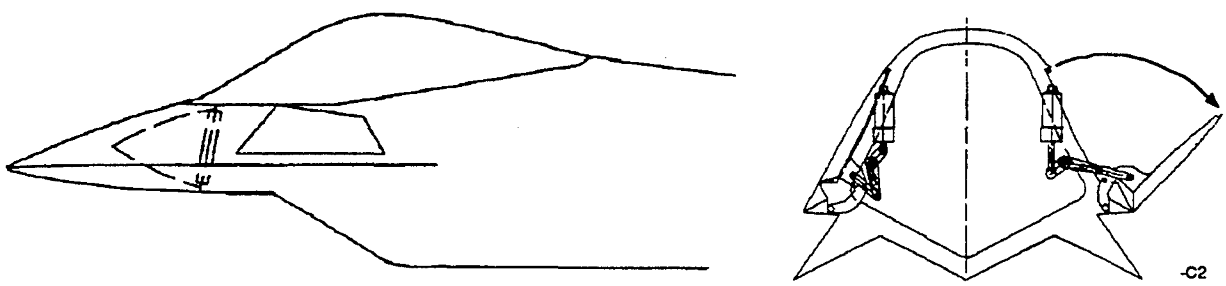

-C2

Figure 4.1.1-1. Chine Strake Installation

4.1.2 Split Aileron Integration

In integrating the split ailerons onto the baseline vehicle, the major concerns were the thickness of the outboard wing and the actuation concept. Several actuation concepts were proposed, including a torque tube extended into the body, rotary actuators, and the design shown in Figure 4.1.2-1, a bank of linear actuators to deploy the surfaces. The torque tube concept had several potentially fatal flaws. The major problem was that the response characteristics required for this system to operate correctly would have required stiffening the tube, a sizeable weight penalty, and moving the aft spar forward to accommodate the tube, reducing the size of the spar box and again resulting in a weight penalty. However, this arrangement could be made to fit within the current wing surface definition. The rotary actuator concept had a serious flaw in that the hinge moment requirements resulted in an actuator with a diameter that was over twice that of the wing at the inboard aileron location. The bump fairing that would be required to accommodate this arrangement would create a significant "deadband" in the actuation of these devices and also increase aerodynamic drag considerably. The design chosen, the linear actuators, still required a significant fairing to provide the necessary clearance for the system. This fairing will reduce the effectiveness of this device but not as severely as the rotary concept. An additional 483 lbs. is required to integrate this concept onto the baseline vehicle, including allowances for additional structure and actuators. This device significantly affected the overall signature of this vehicle as shown in Figure 4.5-1.

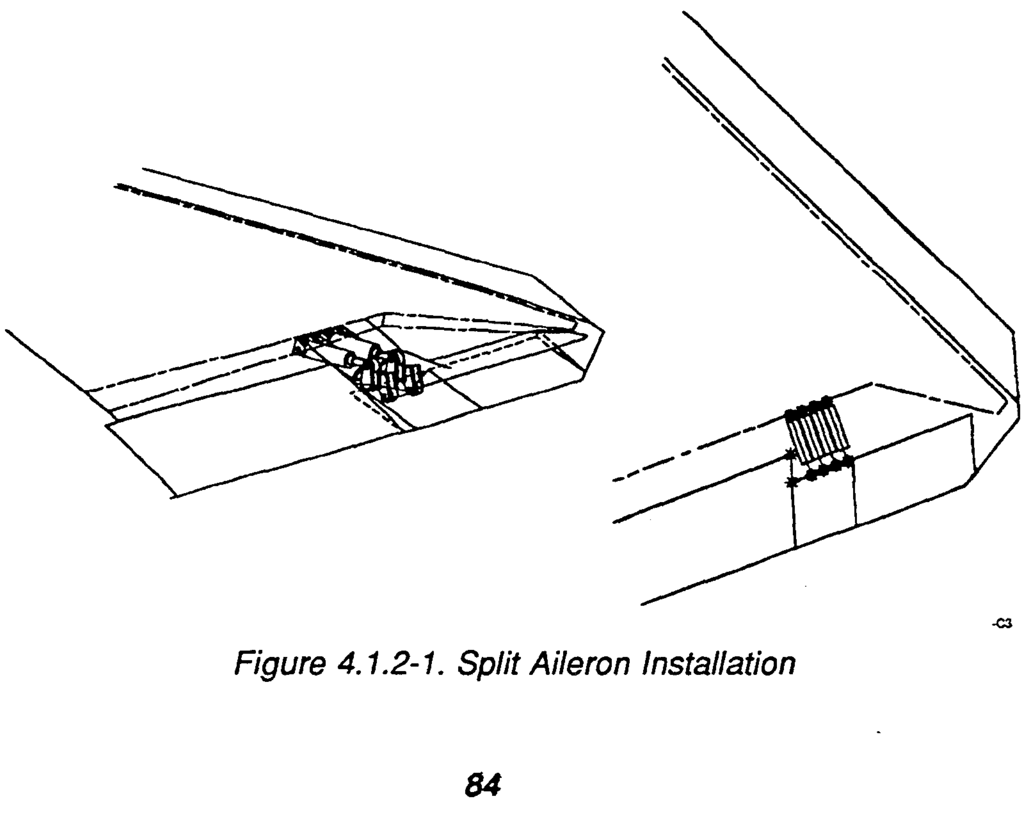

Figure 4.1.2-1. Split Aileron Installation

4.1.3 Rotating Horizontal Tail Integration

The rotating horizontal tail also presents significant challenges to the designer to integrate this concept successfully onto the baseline vehicle. Two integration concepts were studied, the first concept included three rotary actuators to pivot the entire horizontal tail, and resulted in a weight increase of 1457 lbs., for a net increase (allowing for removal of the vertical tails) of 812 lbs. For illustrations of the early attempts to integrate the rotating tail, see Appendix D, Figure D-10. The second concept, shown in Figure 4.1.3-1, included a redesign of the internal pivoting arrangement and a single rotary actuator. This installation concept resulted in a net increase in vehicle weight of 72 lbs., a significant improvement over the first concept. The primary reason for this weight improvement is in the actuator design philosophy. The structure must still be designed to accept the ultimate design loads, but an actuator can be replaced when it reaches its design cycle life. When sizing a rotary actuator to take a load, the frequency of occurrence of that load significantly affects the actuator size and therefore weight. For the range of loads anticipated for this design, the sizing chart is presented in Figure 4.1.3-2. If the actuation system is designed to hold the load of 3,000,000 in-lbs for 8000 cycles, the actuators would have to weigh 572 lbs/side. If the actuators are sized to hold the design load one time, then the actuators can be reduced in weight to 250 lbs/side. This reduced size actuator could still accommodate a load of 1,000,000 in-lbs approximately 20,000 times. Designing to a philosophy allowing for periodic actuator replacement can result in significant weight benefits. For aircraft that have low utilization rates, or are infrequently operated at the ultimate design load for the actuator, significant benefits can be achieved by invoking this philosophy. Many advanced fighter designs are using this philosophy to improve overall system performance. A more detailed analysis of both of these integration concepts is included in Appendix D. The signature aspects of this effector are summarized in Figure 4.5-1.

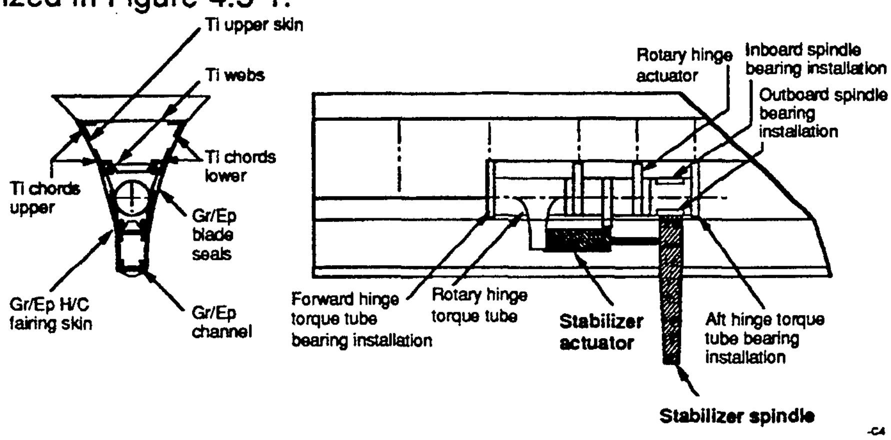

Figure 4.1.3-1. Rotating horizontal Tail Installation

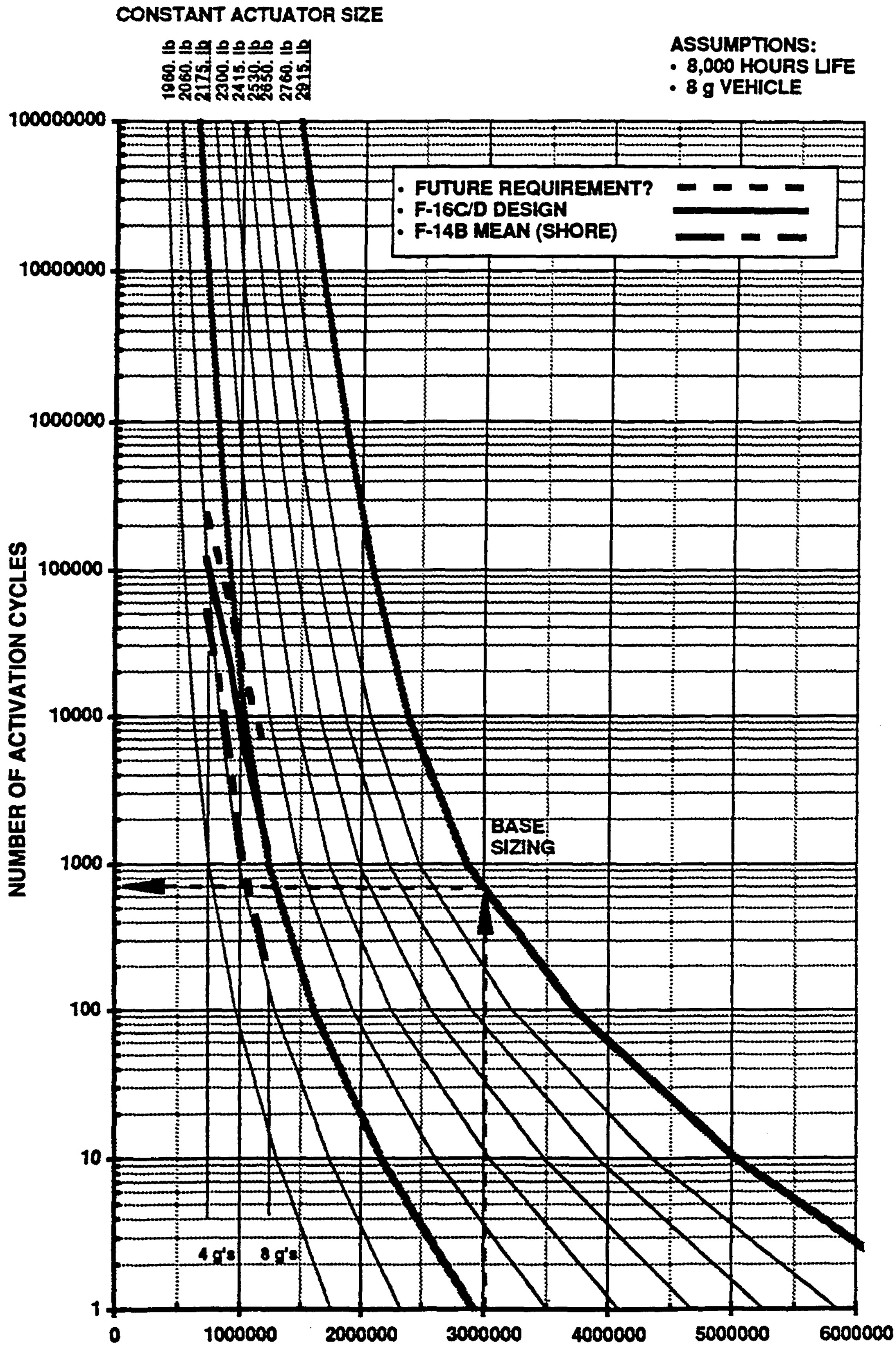

Figure 4.1.3-2. Cycles vs. Hinge Moment

4.2 Actuation Study

The problems of actuating a device include consideration for the type of power source(s) available, the range, type, and rate of motion required, and the design load. Understanding the options available will allow the designer to select an actuation scheme which best fits his design. Various types of actuators are described in this section.

Power Source The form of power supplied to any of these actuators can be electrical, hydraulic, mechanical power-take-off (i.e. shaft from engine) or pneumatic. Present day fighter aircraft utilize distributed electrical and hydraulic-power systems. When required, mechanical power is generated at the location needed (i.e. not distributed) by conversion of power from the electrical or hydraulic systems. Pneumatic power systems have not found wide use or acceptance as a source of power for actuation of flight control surfaces found on fighter aircraft.

Pneumatic Power Reservoir-type pneumatic systems are usually utilized for "blow down" systems (e.g., landing gear extension for emergencies) or are utilized for powering of functions having low or short duration duty-cycle requirements. Hence, the reservoir-type of pneumatic system is not suitable for the duty-cycle requirements that are anticipated relative to the subject of ICE.

Bleed-air type pneumatic systems, which utilize bleed air from the engine, were not found to be acceptable because of reduced performance in the following areas:

Engine To maximize engine thrust, present day aircraft designers prefer to minimize or eliminate the use of bleed air by other systems. Pneumatic systems utilize a percentage of bleed air from the main engine powerplant for driving pneumatic systems. Hence, pneumatic systems represent a degradation of engine performance.

R&M Reliability and maintainability are degraded because of high-temperature operation and poor lubricating qualities of bleed air. These two characteristics work together to produce an erosive, wear-prone environment for pneumatic system components. Consequently, electrical and hydraulic systems are more reliable and require less maintenance than pneumatic systems.

Dynamics The dynamic response and stability of pneumatic systems are less than electrical or hydraulic systems because of the compressibility of air.

Hence, flutter requirements anticipated for flight controls would far exceed the capabilities of a pneumatic-driven system.

In summary, pneumatically-powered actuators were considered an unacceptable alternative to electrically or hydraulically-powered actuators.

Mechanical Power Distributed mechanical power (i.e., shaft) transmitted by the use of torque shafts and gear-boxes from the main engine powerplant was not considered a practical option for driving the subject ICE. The rationale include:

Packaging The physical envelope required for routing, placement, and operation of torque-shafts and gearboxes does not provide for physically compact system installations or acceptable systems integration within the small outer mold lines which are characteristic of fighter aircraft.

R&M The reliability and maintainability of these systems are less than the alternative power systems. The degraded R&M is primarily due to the reliability and servicing requirements associated with poorly accessible components such as torque shafts and couplings utilized in these mechanical systems.

In summary, mechanically-powered actuators driven by distributed mechanical systems are an unacceptable option for the tail mounted ICE application.

Electrical Power Any of the actuators listed in Figure 4.2-1 can be driven by the aircraft electrical power systems. The required power conversion is accomplished by one or more electrical motors which drive gearing elements that provide power to the actuator. Electrical actuators can be placed into the following three categories:

EHA Electrohydrostatic Actuators consist of a bi-directional, variable speed electrical motor, constant-displacement hydraulic pump, fluid, accumulator, valves, and a hydraulically powered actuator. Hence, the EHA is an actuator combined with a self contained hydraulic system. This self-contained hydraulic system operates with variable-pressure and variable-flow to efficiently match the load and rate requirements needed for moving an actuator to a commanded position.

No.	Category	Power source	Output motion	Conversion device
1	Hydraulic	Hydraulic	Rotary	Vane
2	EHA	Electrical	Rotary	Vane
3	Hydraulic	Hydraulic	Rotary	Helically-splined piston
4	EHA	Electrical	Rotary	Helically-splined piston
5	Hydraulic	Hydraulic	Rotary	Recirculating ball
6	EHA	Electrical	Rotary	Recirculating ball
7	Mechanical	Hydraulic	Rotary	Motor-driven planetary
8	EMA	Electrical	Rotary	Motor-driven planetary
9	Hydraulic	Hydraulic	Linear	Piston
10	EHA	Electrical	Linear	Piston
11	Mechanical	Hydraulic	Linear	Motor-driven ball-nut
12	EMA	Electrical	Linear	Motor-driven ball-nut
13	Mechanical	Hydraulic	Linear	Motor-driven ball-screw
14	EMA	Electrical	Linear	Motor-driven ball-screw
15	Mechanical	Hydraulic	Linear	Motor-driven roller-screw
16	EMA	Electrical	Linear	Motor-driven roller-screw

-W2

Figure 4.2-1. Electrical and Hydraulic Actuator Candidates

EMA Electromechanical Actuators consist of a bi-directional, variable speed electrical motor, reduction gearing, brakes, clutches, and a mechanically-driven actuator. Hence, the EMA is an actuator and mechanical power system in one package.

IA An integrated actuator consists of many components similar to those found in an EHA. Hence, the IA is an actuator combined with a self-contained hydraulic system. This system utilizes a unidirectional, constant speed motor in conjunction with a constant-pressure, variable-flow pump to generate hydraulic power for the actuator. This constant-pressure, variable flow hydraulic system is very similar in operation to the conventional hydraulic systems found in present day aircraft.

Only the EHA and EMA were considered as viable electrical actuation candidates for driving the rotating horizontal tail control effector. Generally, the utilization of integrated actuators in lieu of conventional hydraulically powered actuators does not provide for the significant benefits found by using EHA and EMA technologies. The rationale for excluding IA technology in favor of EHA and EMA technologies are:

Weight The EHA and EMA provide a lighter weight solution than the integrated actuator.

Efficiency The EHA and EMA require less energy for positioning a load than an IA. The EHA and EMA output loads and rates provide a better match to required loads and rates for positioning of a load. Also, the EHA and EMA are on-demand systems as opposed to the continuous operating integrated actuator. Hence, the IA requires more energy during quiescent operation than an EHA or EMA.

Thermal The on-demand operation of the EHA and EMA generates less heat than the continuously operating integrated actuator.

Reliability Generally, the EMA is the most reliable of the three electrical actuators. However, special operating features (e.g., bypass, blowback, locking) require additional mechanisms such as clutches and brakes. Consequently, the reliability of the general EMA has been reduced to a level slightly higher than that of an EHA. Reliability of the EHA is somewhat higher than the IA. However, the IA may require more frequent servicing for replacement of fluid and seals.

Maintenance The EHA and EMA are each estimated to require less servicing than the integrated actuator because the more efficient, on-demand functioning results in less heat generation and less operational time.

Hydraulic Power Any of the actuators listed in Figure 4.2-1 can be driven by the aircraft hydraulic power systems. Some of these actuators directly utilize hydraulic power for operation and some require the use of a hydraulic motor to convert hydraulic power into mechanical shaft power. Subsequently, this mechanical power is utilized for driving the actuator.

Actuator Summary For the devices proposed in this study, mechanical actuation provides the best alternative to the aircraft designer. Pneumatic actuation schemes simply cannot provide the response characteristics necessary, and the electrical devices, while suitable for some applications to control devices, still create significant challenges to the designer because of electro-magnetic interference and actuator size constraints.

4.3 Carrier Suitability Requirements

A separate aircraft was defined for the USN carrier specific requirements. The primary requirements were: an approach speed goal of 135 knots; achieve the glide slope transfer or "pop-up" maneuver at this approach speed; and, meet the arresting engine limitations at "0" wind-over-deck. These design requirements resulted in a significantly larger aircraft for the USN analysis. Specifically, the baseline aircraft wing area was resized from 465 ft^2 to 650 ft^2 to meet the carrier specific design goals. Corresponding changes to the fuselage and subsystems are described below and indicated in the weight build up in Figure 4.3-3.

The USN carrier sized aircraft was determined by using the design charts shown in Figures 4.3-1 and 4.3-2. As shown in these charts, the required minimum wing area to meet the design goals is 650 ft^2. This size allowed the USN version of the baseline vehicle to meet the approach speed requirement with a 10,000 bring-back payload. The pop-up and arresting engine requirements are also met with this larger vehicle.

In addition to the resizing, several additional requirements in terms of vehicle structural modifications were also required to meet the USN specifications, which are considerably different from the USAF versions. For example, to achieve a reasonable spotting factor, a wing fold mechanism was incorporated into the design to reduce the folded span to 25 feet. The single wheel nose gear was replaced by a dual tire arrangement, and the nose gear structure was strengthened to meet the catapult loads and the higher sink rate loads for landing. The overall airframe structure was also strengthened to meet the higher design takeoff and landing loads. In addition to the above, bladders were added to the fuel tanks and the USAF LO Inflight refueling (IFR) receptacle was replaced by a retractable USN IFR probe. These changes, and the accompanying weight penalties are summarized in Figure 4.3-3.

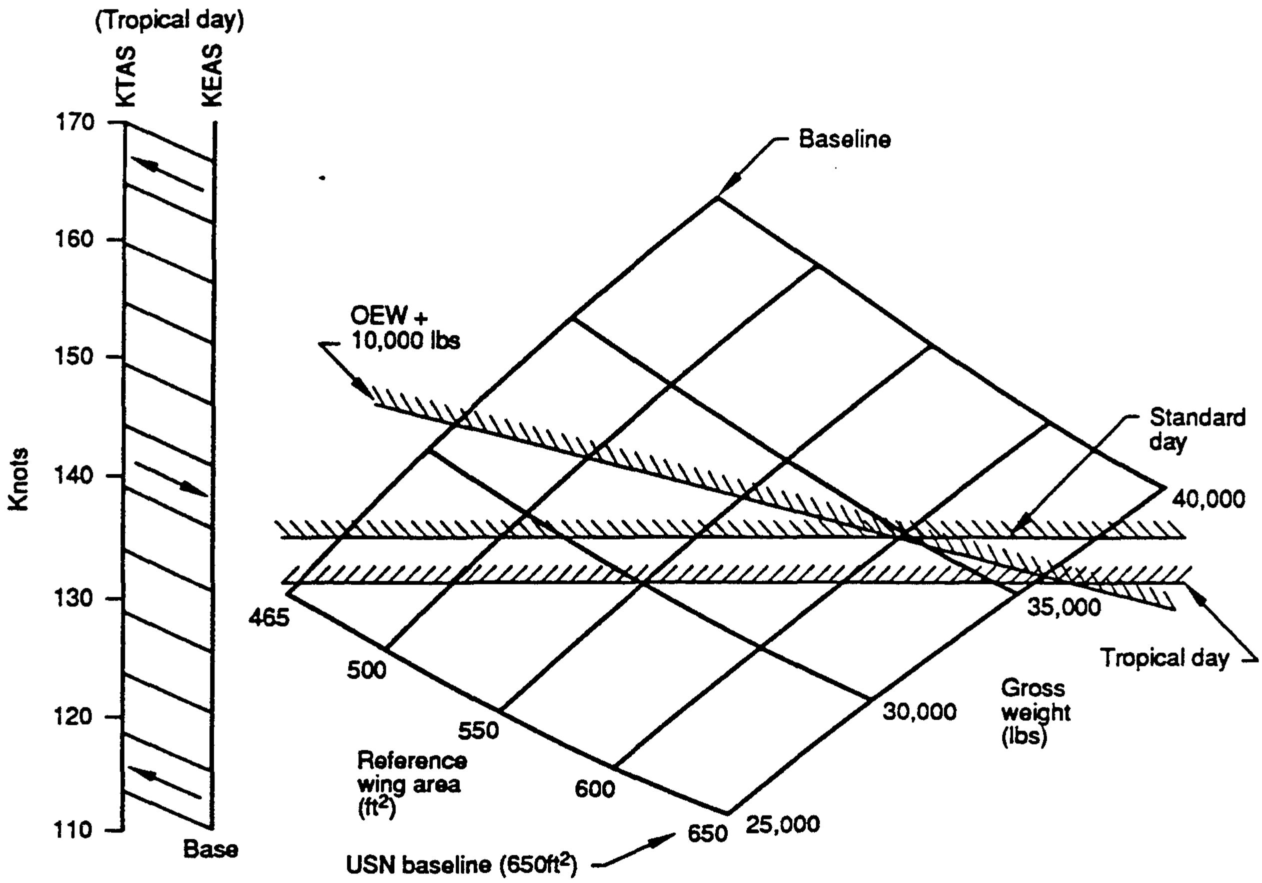

Figure 4.3-1. Approach Speed

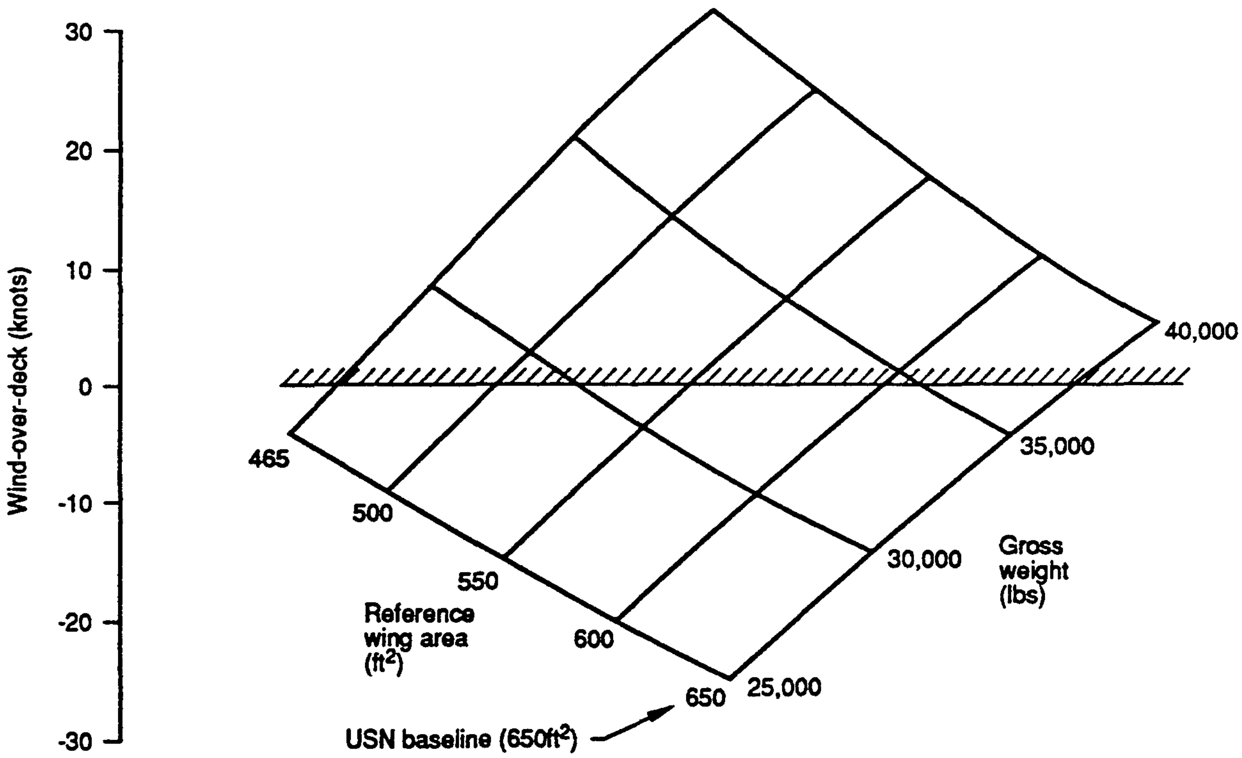

Figure 4.3-2. Mark 7 Mod 3 Arresting Engine

-Ad4

GROUP WEIGHT STATEMENT MISSION: AIR-TO-GROUND MODEL: 120% SCALE MODEL MRF-24F-GE2	USAF A/G WEIGHT (LBS)	Δ WT (USN DESIGN FEATURES) (LBS)	WEIGHT (LBS)	Δ WT (USN DES WTS & LD FACTOR) (LBS)	USN A/G WEIGHT (LBS)
WING (AREA = 650 SQ. FT.)	2621	425	3046	-93	2953
HORIZONTAL TAIL	750		750	-9	741
VERTICAL TAIL	396		396		396
BODY	5838	397	6235	-123	6112
MAIN GEAR	1087	274	1361	48	1409
NOSE GEAR	211	326	537	8	545
ARRESTING GEAR	0	184	184	8	192
AIR INDUCTION	764		764		764
ENGINE SECTION	201		201		201
SPECIAL FEATURE (RAM/RAS)	1256		1256		1256
TOTAL STRUCTURE	13124	1606	14730	-161	14569
ENGINES	4800		4800		4800
AMADS	197		197		197
ENGINE CONTROLS	25		25		25
STARTING SYS. (INCL W/APU)	0		0		0
FUEL SYSTEM	633	66	699		699
TOTAL PROPULSION	5655	66	5721	0	5721
FLIGHT CONTROLS	727	6	733		733
APU	242		242		242
INSTRUMENTS	30		30		30
HYDRAULICS & PNEUMATICS	436	14	450		450
ELECTRICAL	515		515		515
AVIONICS	1598		1598		1598
FURNISHINGS & EQUIP	390		390		390
AIR CONDITIONING	563		563		563
ANTI-ICE	37		37		37
HANDLING EQ	5		5		5
TOTAL FIXED EQUIPMENT	4543	20	4563	0	4563
WEIGHT EMPTY	23322	1692	25014	-161	24853
CREW	200		200		200
CREW EQUIPMENT	15		15		15
OIL & TRAPPED OIL	125		125		125
TRAPPED FUEL	268		268		268
LAUNCHERS/EJECTORS	422		422		422
NON-EXP USEFUL LOAD	1030	0	1030	0	1030
ROUND OFF	8	-2	6	-9	-3
OPERATING WEIGHT	24360	1690	26050	-170	25880
A/G WEAPON	2000		2000		2000
A/A WEAPONS	690		690		690
FUEL (JP-8)	17900	-1690	16210	1690	17900
GROSS WEIGHT	44950	0	44950	1520	46470

Ex1

Figure 4.3-3. USN Baseline Weight Buildup

4.4 Thrust Vectoring Integration

The thrust vectoring study for this contract was focused on the integration and performance issues, and what gains could be achieved by incorporating thrust vectoring onto the baseline vehicle. The performance results are reported in the performance Section 3.0 of this report. This section addresses the integration issues.

Airframe-Nozzle Integration Integrating thrust vectoring onto the baseline vehicle was considered by looking at three different concepts. The thrust vectoring nozzle can be mounted directly onto the engine, the nozzle can be mounted directly to the airframe, or the nozzle can be structurally integrated with the airframe. Figure 4.4-1 illustrates each of these concepts and includes several figures-of-merit showing the relative merits of each of the concepts. As shown in the figure, each of these concepts exhibit its own strengths and weaknesses. For the engine mounted concept, reliability should be higher because of the lower part count. However, maintenance on this nozzle concept will require removal of the entire engine. For the airframe mounted concept, one advantage is that the nozzle can be removed without removing the engine and the engine can be removed and replaced without removing the nozzle. The structurally integrated (SI) nozzle has the advantage of offering potentially lower weight, but at a price. The SI concept will likely have a higher part count and therefore have lower reliability than the other concepts and maintainability will be more difficult.

Thrust Vectoring Nozzle Type Comparison. Another factor considered in the thrust vectoring (TV) study was the type of vectoring scheme to be used. Three vectoring concepts are shown in Figure 4.4-2 that include both yaw and pitch vectoring capability. The baseline Model 24F vehicle was originally designed with a Spherical Convergent Flap Nozzle (SCFN) that had pitch only thrust vectoring; however, this was not considered as part of the baseline aircraft for most of the performance studies herein.

For purposes of this Phase I ICE study, a brief evaluation of a 2-axis thrust vectoring system was assumed in combination with the "best" 2 effectors - namely the split ailerons and the rotating tail. The TV was limited to 30 degrees of vectoring angles, with a rate of 100 degrees/second. All of the above concepts can achieve these capabilities.

Engine mounted nozzle	Airframe mounted nozzle	Structurally integrated nozzle

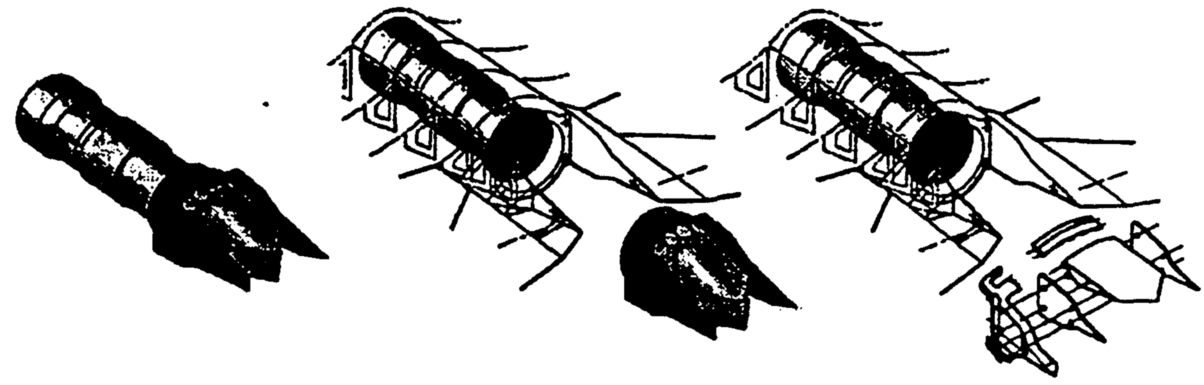

Engine mounted nozzle

- No load sharing between engine nozzle assembly and empennage

Airframe mounted nozzle

- Dual load path between nozzle sub-assembly and empennage

Structurally integrated nozzle

- Single load path between nozzle components and empennage
- Stressed skin joint, multiple fasteners

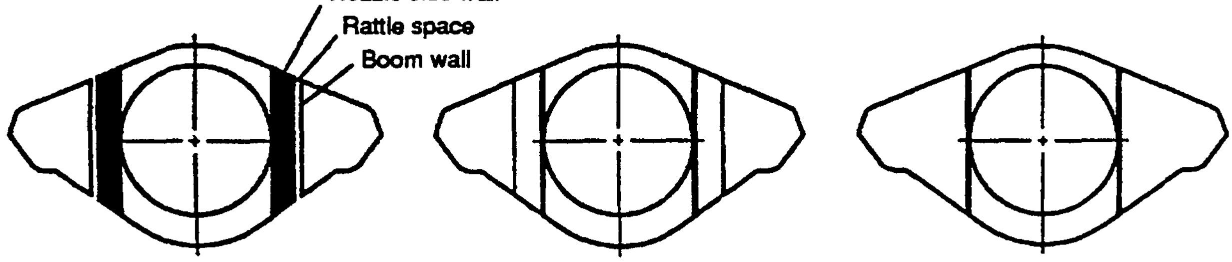

Engine mounted nozzle

- Nozzle is integrally mounted to engine
- Airframer installs engine-nozzle assembly
- Engine manufacturer assembles and tests the engine and nozzle
- Propulsion system responsibility, one source

Airframe mounted nozzle

- Nozzle is a line replaceable unit (sub-assemble)
- Airframer installs nozzle sub-assembly
- Engine manufacturer assembles and tests the engine and nozzle
- Propulsion system responsibility, one source
- Direct subsystems/hardware accessibility

Structurally integrated nozzle

- Nozzle components are separately assembled on the structure
- Airframer assembles and tests nozzle
- Propulsion system responsibility shared between two sources
- Direct subsystems/hardware accessibility

Installed weight (lb)	Higher	Ref	May be lighter
Aft body drag	Higher	Ref	Same
Internal performance	Sam	Ref	Same
Maintainability (accessibility)	Difficult	Ref	Difficult
Reliability	May be higher	Ref	Lower
Supportability	Difficult	Ref	Difficult
Manufacturing	No interfaces	Minimum interfaces	Multiple interfaces, difficult tolerancing
Vulnerability	Higher	Ref	Higher
RCS	Higher	Ref	Ref
IR	Higher	Ref	Ref

Nozzle remove and replace	Entire engine (87 min.)	Reference (20 min.)	•A9 actuator (79 min.)
Reliability	Higher	Reference	Lower
Maintainability	Difficult	Reference	Difficult
Complexity	Lower part count	Reference	Higher part count

•Nozzle maintenance done at LRU level. A9 actuator most frequent maintenance activity.

-C5

Figure 4.4-1. Thrust Vectoring Nozzle Mounting Concepts

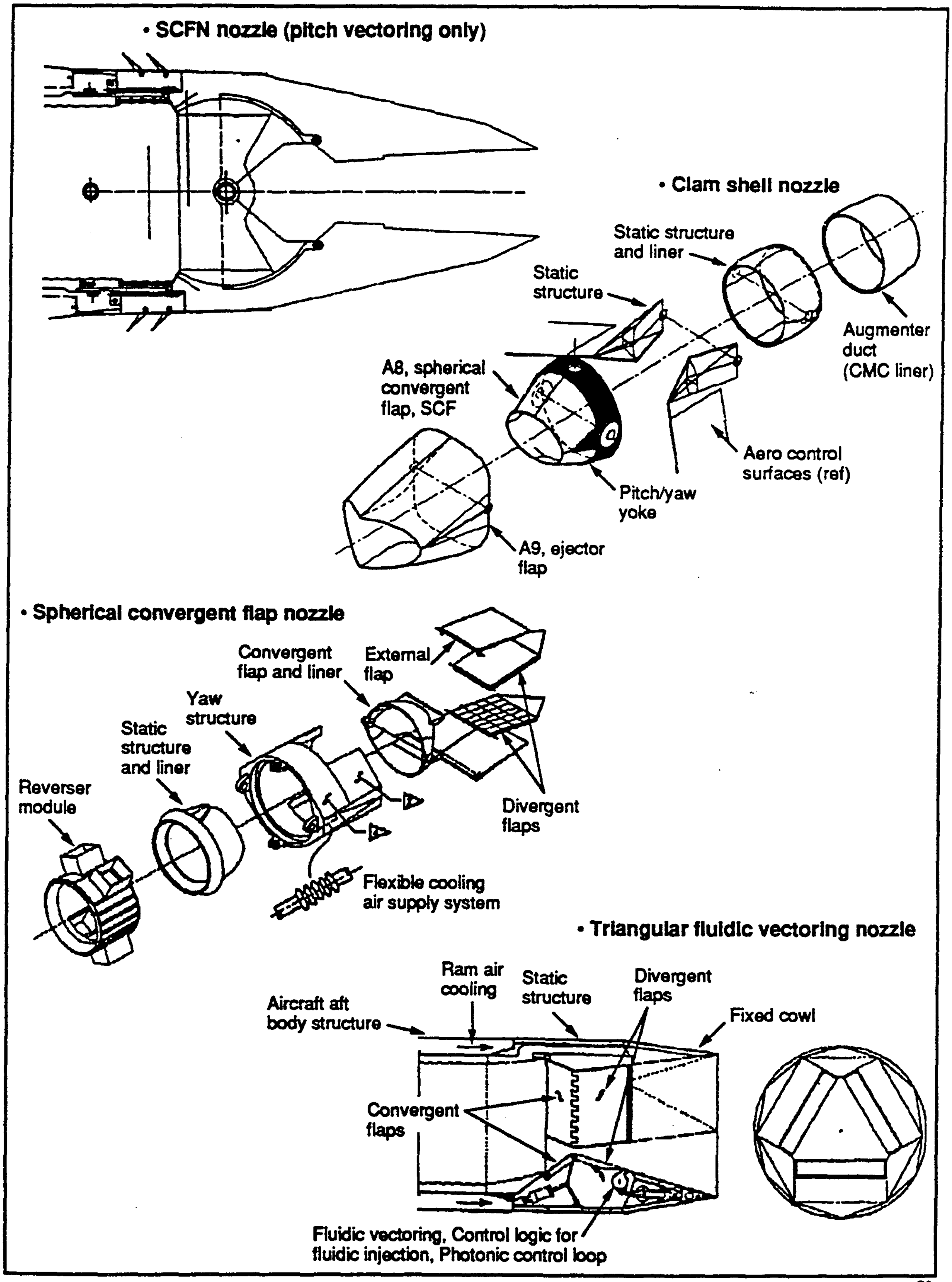

Figure 4.4-2. Thrust Vectoring Nozzle Concepts

Thrust Vectoring Integration Evaluation In evaluating the concepts, several figures-of-merit were taken in account. Figure 4.4-3 shows the weight, cost, and range factor performance of the various concepts. These values are for airframe mounted nozzle concepts. In addition to the above, the relative merits of the four candidate configurations are summarized in Figure 4.4-4. These attributes have all been normalized so that the pitch only thrust vectoring concept was assigned a value of 1.0 for each of the technologies. Using a weighting factor for each of the attributes, and summing the indices, a relative preference and ranking was established for the four concepts. Each of these nozzle concepts has its own merits. The SCFN (pitch only) is the lightest and least complex, offering advantages in several areas. All of the pitch and yaw vectoring concept have a significant edge in maneuvering capability over the pitch only concept. As shown, the SCFN (pitch only) concept is preferred, with the Clamshell concept the preferred pitch and yaw vectoring concept. As shown in the figure, the clamshell concept has advantages over the other two-axis concepts in several areas.

Thrust vectoring concept

		SC FN pitch only	SC FN pitch and yaw	Triangular fluidic	Clamshell
Figures-of-merit	Nozzle weight	1,186	1,253	1,730	1,270
	Life-cycle cost ($1,000)	12,000	12,500	12,300	12,200
	Range factor	4,000	4,000	4,000	4,000

-Ad5

Figure 4.4-3. Thrust Vectoring Figures-of-Merit

The integration issue discussed here are for completeness only. Integration of thrust vectoring into the vehicle was not part of this study.

	Concept attributes (figures of merit)							Concept preference (I)[d]	Concept preference (I)[e]	Concept rank
	Performance index	Maneuver index	Signature index	RMS index	Cost index	Vulnerability index	Risk index			
SCFN pitch only	1	1	1	1	1	1	1	1	0.19	1
SCFN pitch and yaw	1	1.33	0.8	0.97	0.74	0.67	0.67	0.85	0.13	2
Triangular fluidic	1	1.33	0.4	0.92	0.64	0.33	0.33	0.64	0.11	3
Clamshell	1	1.33	1.0	0.97	0.74	1	0.67	0.92	0.15	1-
Importance (I)[a]	0.20	0.10	0.15	0.10	0.30	0.05	0.10			
Variability (V)[b]	0	0.17	0.28	0.03	0.15	0.32	0.27			
Determinance (D)[c]	0	0.02	0.04	0	0.05	0.02	0.03			

a. The attribute importance weights must add up to 1.
b. The variability is measured by the standard deviation of the numbers in each column.
c. The determinance is found by multiplying each importance weight by the corresponding standard deviation. A determinance score of 0 indicates a nondeterminant attributer, and the greater the determinance score, the more determinant the attribute.
d. Concept preference according to the importance weights is found by multiplying each concept's attribute scores by the corresponding importance weights.
e. Concept preference according to the determinance scores is found by multiplying each concept's attribute scores by the corresponding determinance scores.

-Ad6

Figure 4.4-4. Determinant-Attribute Model

4.5 Radar Cross Section Analysis

The Radar Cross Section (RCS) characteristics of the Model-24F configuration have been estimated using high fidelity computational electromagnetic methods. These characteristics have been calculated for several configurations, elevations, frequencies and polarization for the full range of azimuths. Since the main focus of this study was to determine the RCS characteristics of the control effectors, major RCS contributors such as the propulsion system were not included in the computational modeling. The results of this study are summarized in Figures 4.5-1 and 4.5-2 and included in Appendix C.

50% probability sector, 9.0 GHz, 0 elevation

	Forward sector -30 to +30		Aft sector 150 to 210		Side sector 60 to 120	
	H-POL	V-POL	H-POL	V-POL	H-POL	V-POL
Baseline	-37.0	-30.0	-22.0	-22.4	-10.3	-11.7
No vertical tails	-40.4	-40.5	-23.0	-23.0	-11.7	-14.2
No verticals, horizontal tails @ +20° dihedral	-38.6	-39.3	-21.7	-22.9	-11.4	-13.3
No verticals, strakes deployed	-36.1	-36.5	-21.3	-22.3	-12.1	-13.9
No verticals, split ailerons deployed	-32.3	-26.8	-9.0	-13.1	-8.9	-6.8

Figure 4.5-1. Signature Comparison - 50%

96% probability sector, 9.0 GHz, 0 elevation

	Forward sector -30 to +30		Aft sector 150 to 210		Side sector 60 to 120	
	H-POL	V-POL	H-POL	V-POL	H-POL	V-POL
Baseline	-31.5	-31.6	4.7	3.7	-1.1	-1.6
No vertical tails	-31.5	-34.1	-1.0	-1.5	4.0	1.2
No verticals, horizontal tails @ +20° dihedral	-31.1	-33.4	4.8	3.4	4.2	1.0
No verticals, strakes deployed	-20.3	-22.9	-1.0	-1.5	4.0	1.0
No verticals, split ailerons deployed	10.8	12.3	8.4	9.5	7.0	15.6

-Ad7

Figure 4.5-2. Signature Comparison - 96%

The computational analysis was performed using the ARBSCAT code to estimate the primary scattering components. This code uses equivalent current sources with input for RCS treatment based on measured data. The analysis shown here is for untreated configurations. The code can also make corrections for edge radii and wedge angle for an accurate representation of the total vehicle signature. Additional RCS contributions such as multi-bounce and cavities were analyzed using a 3-D ray trace, physical optics code, XPATCH. For the data shown, the effects of traveling waves have been ignored. However, contributors that affect the trade study, such as strake deployment doors and the trailing edge control surface gaps have been accounted for. The study was performed by analyzing each component separately and then adding the pieces using the RCS budgeting code PLTSUM to obtain the total vehicle signature.

The results of the RCS study are summarized in Figures 4.5-1 and 4.5-2. The data are presented for 0 degrees elevation, 9.0 GHz, both polarization's, for the five study configurations listed below:

1) Baseline configuration
2) Baseline with vertical tails removed
3) (2) with Horizontal Tails @ 20 degrees dihedral
4) (2) with nose strakes deployed
5) (2) with Split Ailerons deployed @ 45 degrees

Additional analysis for +30 and -30 degrees elevation, 2.0 and 16.0 GHz are included in Appendix C.

4.6 Summary of Integration Results

Incorporating a control effector into an existing design can have significant adverse consequences. Most tactical aircraft do not have the volume available to easily integrate additional systems onto the airframe without degrading performance in other areas. Accommodating innovative devices early in the vehicle design process can preclude integration concerns and result in acceptable design compromises. The devices investigated during this effort may offer significant advantages to future aircraft designers if the devices are included early enough in the design process to preclude many of the problems noted in the previous sections. A quick look summary is included in table 4.6-1.

Summary Table

	Split Aileron	Chine Strake	Rotating Tail
Δ Weight	483 lbs	——	72 lbs
Δ Signature Front Side Aft	 3.7 V 8.1 H 7.4 V 2.8 H 9.9 V 14 H	 4 V 4.3 H .3 V .4 H .7 V 1.7 H	 13.7 V 8.1 H 7.4 V 2.8 H 9.9 V 14 H
Structural Integration	Moderate	Extensive	Extensive
Actuation	Significant Fairing	Moderate Difficulty	Complicated
Reliability	Proven	Proven	Technology similar to other concepts
Subsystem Trades	——	Radar Operation/ Effector Location	Weight/Replacement Schedule

Table 4.6-1

5.0 Task 4 - Risk Assessment and Reduction Plan

Based on the results of the performance and integration efforts, a risk reduction plan has been proposed to minimize the risk of trasitioning any of these concepts to an advanced development project. The major risk elements identified for each of the effector concepts were aerodynamic performance, the integration aspects and the signature contributions for each device. This section evaluates the performance and integration risks associated with these effectors and proposes additional efforts which could reduce the risk in incorporating these devices onto future aircraft. The risk assessment summaries in Figures 5.1-2 and 5.2-1 are based on the risk rating guide shown in Figure 5.0-1.

Factors in probability of failure

Probability of failure level	Attribute		
	Maturity factor	Complexity factor	Dependency (availability) factor
Low	Existing	Simple design	Independent of existing system, facility, or subcontractor
Minor	Minor redesign	Minor increase in complexity	Schedule dependent on existing system, facility, or subcontractor. Less than 1 month delivery slip.
Moderate	Major change feasible	Moderate increase in complexity	Performance/supportability dependent on existing system, facility, or subcontractor. 1-3 months delivery slip.
Significant	Technology available, complex design	Significant increase in complexity	Schedule dependent on new system schedule, facility, or subcontractor. Greater than 3 months delivery slip.
High	Some research complete, never done before	Extremely complex	Performance/supportability dependent on new system, facility, or subcontractor. Delivery slip precludes use at IOC.

Factors in consequence of failure

Impact level	Technical factor	Supportability factor	Cost factor	Schedule factor
Low	Minimal or no consequences	Minimal or no consequences	Budget estimates not exceeded	Negligible impact on program. Slight change compensated by available schedule slack.
Minor	Small reduction in technical performance	Small reduction in supportability performance	Cost estimates exceed budget by 1 to 5 percent	Minor slip in schedule (less than 1 month). Some adjustment in milestones required.
Moderate	Some reduction in technical performance	Some reduction in supportability performance	Cost estimates increased by 5 to 20 percent	Small slip in schedule (1 to 3 months)
Significant	Significant degradation in technical performance	Significant degradation in supportability performance	Cost estimates increased by 20 to 50 percent	Development schedule slip in excess of 3 months
High	Technical goals cannot be achieved	Supportability goals cannot be achieved	Cost estimates increased in excess of 50 percent	Large schedule slip that affects segment

-Ad8

Figure 5.0-1. Risk Rating Guide

5.1 Aerodynamic Performance Risk Assessment

The performance risks are associated with the limited test database associated with each of these effectors, and the interaction with the airframe the device is intended to be installed on. Expanding the knowledge database for each of these effectors will significantly enhance the possibility of success in including any of these designs on future fighter concepts. The greatest potential for exploration is in the low speed high angle-of-attack region. Figure 5.1-1 shows the current configuration test database and the region of proposed testing that should enhance the understanding of these devices. Of particular interest is the post-stall flight region, where improvements in control technology could provide future aircraft with advantages in air combat.

The performance risk assessment for each of the final study effectors is summarized in Figure 5.1-2. For each of the selected devices the risk rating reflects the concerns inherent in the device. For the forebody nose strake, the geometry of the forebody can significantly affect the performance of the device. The ability to locate the device close to the nose will directly affect the resulting vehicle capability. The split ailerons, while posing little risk, have significant disadvantages that may pose problems when incorporated onto future aircraft. For low aspect ratio vehicles, performance of these devices at low speed could fall well below requirements. The rotating horizontal tails have not been explored throughout the entire flight envelope, and may need to be larger than originally anticipated in order to achieve the acceptable results throughout the entire flight envelope.

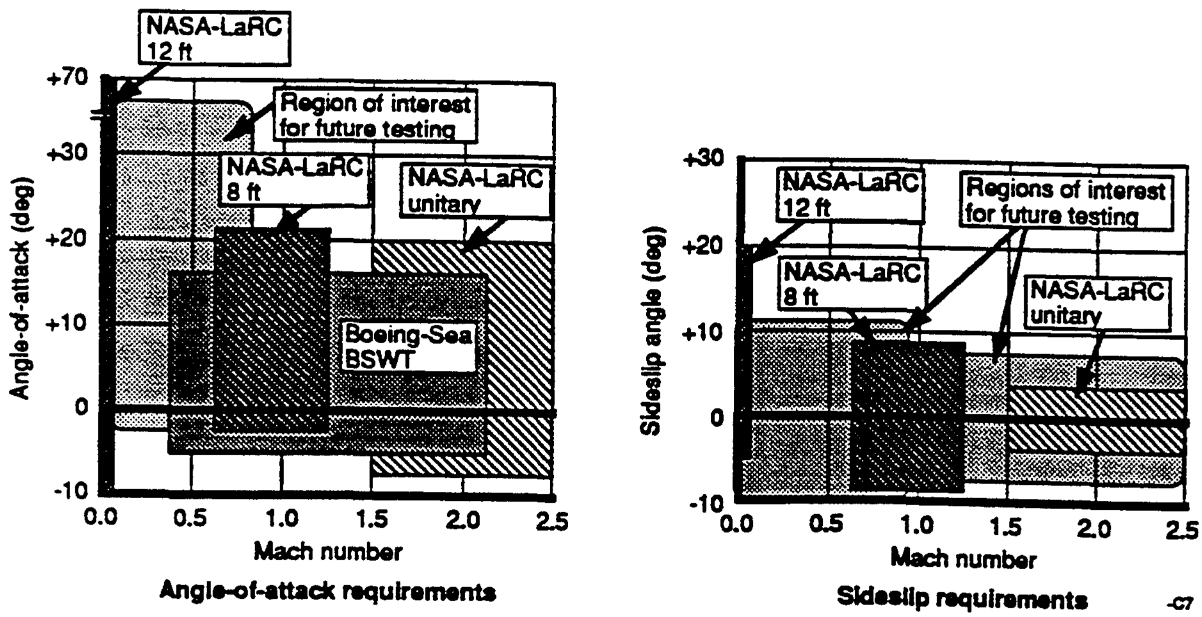

Figure 5.1-1. Future Testing

	Probability of failure	Consequence of failure	Comments
Nose strake	Moderate	Significant	Need to better define high angle-of-attack performance. Interaction effects need to be understood, concept forebody configuration dependent.
Split aileron	Low	Minor	Control capability fairly well defined. Concept operating on the B-2. Short span limits capability.
Rotating tail	Minor	Significant	"V" tail concepts have been tested before. Current estimation basis is CFD, however.

-Ad9

Figure 5.1-2. Performance Risk Assessment

5.2 Integration Risk Assessment

The integration risk summary is shown in Figure 5.2-1. Because of the nature of each of the selected effectors, the integration risks vary considerably. For the forebody nose strake, placement of the device and accompanying systems could compromise the effectiveness of the antennas which are normally installed in the forebody. Accommodating the antennas could degrade the performance of the device to the point that it is not useful. For the split ailerons, on fighter aircraft the wing thickness outboard poses a significant challenge. Integrating actuators into the outboard wing will probably require a fairing which will adversely affect the drag and thereby the performance of the vehicle. Other installation concepts may also compromise the overall vehicle design by either thickening the wing or reducing the spar box chord. For the rotating horizontal tails, weight and balance could be a consideration, and the proximity to the wing trailing edge could also adversely affect performance.

	Probability of failure	Consequence of failure	Comments
Nose strake	Minor	Moderate	Resizing of actuators could be limited by volume constraints. Interference with radar could be problem.
Split aileron	Minor	Minor	Actuator size is a problem. Fairing likely required. Vehicle moments not well defined.
Rotating tail	Moderate	Moderate	Hinge moments not well defined. Smaller actuator would help the integration problems.

-Ad10

Figure 5.2-1. Integration Risk Assessment

5.3 Risk Assessment and Reduction Summary

Additional wind tunnel testing of these effector concepts will reduce the risk in transitioning them to advanced development projects. Additional integration investigation on a more detailed level of these concepts will also reduce the risk in proposing these effectors as devices on future fighter aircraft. The Boeing model BMA-S-1798-6A shown in Figure 5.3-1 is a 5% scale model of the baseline configuration and accomplishing the additional proposed testing would significantly enhance the database for these effectors and reduce the risks inherent in incorporating these devices onto future aircraft. A description of this model is included in Appendix E.

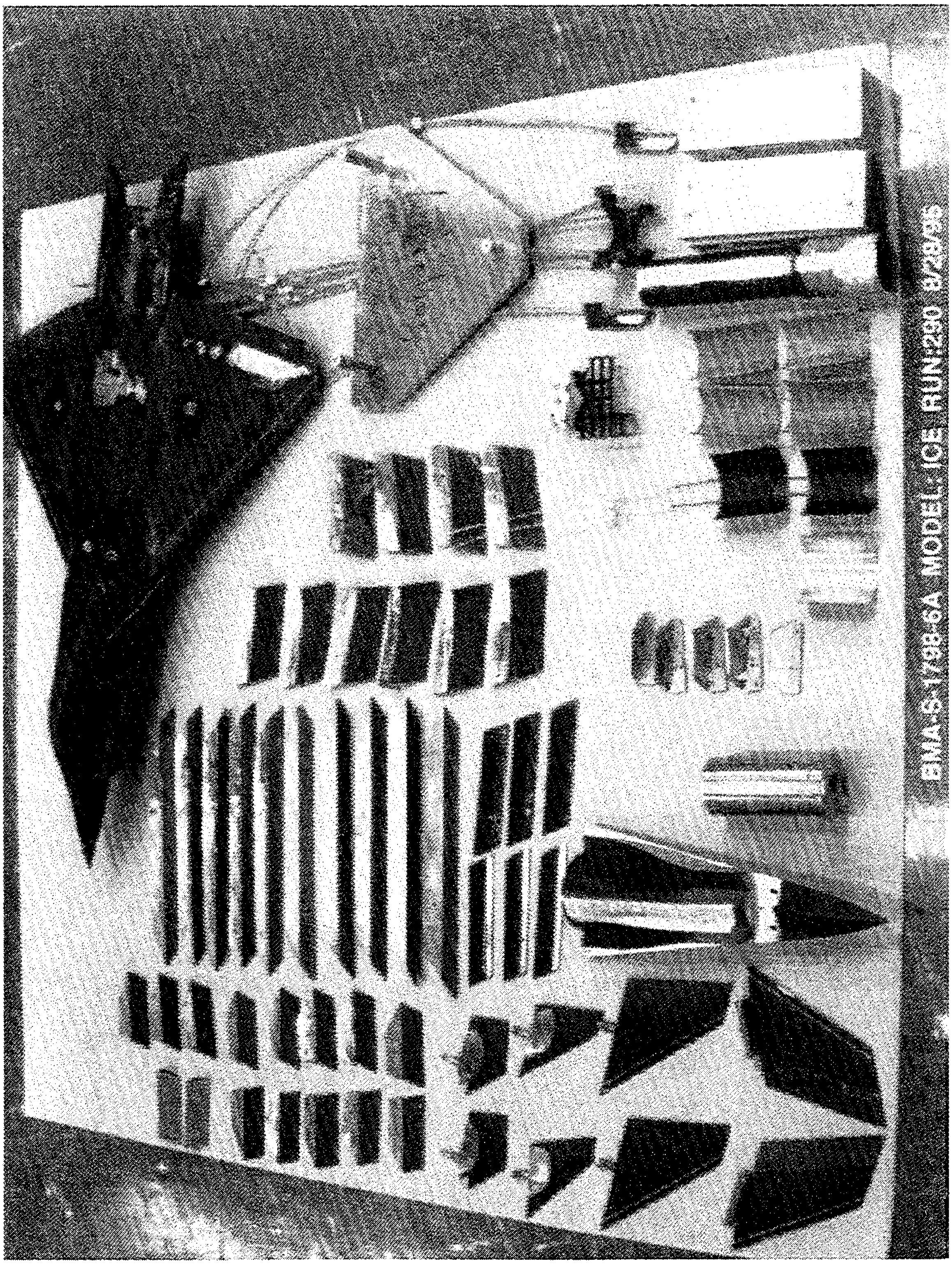

Figure.5.3-1

6.0 - Concluding Remarks

The ICE contract has provided a focus for development and assessment of innovative controls technology that will be relevant to future fighter aircraft studies. The performance and integration efforts undertaken during this study have demonstrated that these devices have the potential for eliminating the vertical tails from future configurations.

The aerodynamic effectors chosen for this study have provided some insight into the performance enhancement capabilities of these devices and their potential for integration into the vehicle flight control system. By the judicious selection of a suite of control devices, and an advanced design control system, the full potential of innovative devices may be exploited.

The integration study has provided additional insight into the challenges associated with incorporating these candidate devices onto future fighter aircraft. The effectiveness of the devices are certainly configuration dependent and must be carefully integrated to achieve desired control power.

An effector such as the rotating tail may buy its way onto a vehicle only with sufficient integration design effort. The design philosophy will effect the relative weight cost thereby impacting the trade-off with other devices.

Retrofit to existing vehicles seems unlikely to have benefit, but incorporation into the design of new vehicles at an early stage offers serious potential. The trade-off between the agility of the vehicle and the observable requirements will be dependent on many factors such as weapon agility and operational strategies for future aircraft.

Aircraft for the Navy have stringent requirements that are best evaluated with a vehicle designed initially for carrier operations, but the estimates made by some scaling and aerodynamic data modifications as done here give reasonable indications of effectiveness. (Control lows)

Clearly thrust vectoring has a great potential for reducing or eliminating the vehicle tail (it is proven technology). Additional operational experience will give more design guidance and confidence.

Further exploration is required to provide confidence for application of new control approaches on weapons systems. The data bases need to be extended through wind tunnel testing of models, and computational methods for stability and control assessment must be matured.

7.0 REFERENCES

1. "Low Speed Wind Tunnel Investigation of a Porous Forebody and Nose Strakes for Yaw Control of a Multirole Fighter Aircraft", S. P Fears, NASA CR4685, August 1995.

2. "High AOA Stability and Control Concepts for Supercruise Fighters," Boalbey, Ely, and Hahne. Report on Cooperative study by McDonnell Aircraft Co. and NASA LaRC (undated-1990?).

3. Unpublished Boeing Aerodynamic Test Data, BTWT 235 and BRWT 241, 1989.

4. "Advanced Fighter Tested for Low-Speed Aerodynamics With Vortex Flaps," G. Gatlin, Vortex Flow Aerodynamics Volume III, NASA CP2417, October 8-10, 1985.

5. "AFTI-F-111 Mission Adaptive Wing, Wind Tunnel Analysis Report, Test Entry, NARC 449-1-12 and NARC 449-1-11T," Boeing D365-10074-1, February, 1983.

6. "An Investigation of a Close-Coupled Canard.as a Direct Side-Force Generator on a Fighter Model at Mach Numbers from 0.40 to 0.90," Re and Capone, NASA TN D-8510, July, 1977.

7. Unpublished Boeing Data, D. Nelson, WSU Wind Tunnel Test, December, 1994.

8. Unpublished Boeing Data, G. Letsinger, BRWT 211 and 198, October, 1986.

9. Unpublished Boeing Data, Merker, February, 1990.

10. "Development of a Mission Adaptive Wing System for a Tactical Aircraft," W. Gilbert, AIAA-80-1886, August, 1980.

11. "Wind Tunnel Test Report, Boeing Model BMAC-T-1549," Boeing D180-30190-1, S. Northcraft, January, 1987.

12. "Controlled Vortex Flows Over Forebodies and Wings", Roberts, et al,.High Angle of Attack Vol 1, NASA CP 3149, Oct.-Nov. 1990.

13. "Subsonic Wind Tunnel Investigation of the High Lift Capability of a Circulation Control Wing on a 1/5 scale T-2C Aircraft Model." R. Englar , NSR&D Center TN AC-299," May, 1973.

14. "Low Speed Investigation of Chined Forebody Strakes and Mechanical Control Effectors," M. Alexander, WL-TR-94-3120, September, 1994.

15. "Nozzle IPD Study," FAPIP Final Review, Contract No. F33657-90-D-0032, E. O'Neill and D. Kirkbride, February, 1992.

16. "ACWFT Summary Technical Report," O'Neill, et al, WL-TR-95-3002, December, 1994.

APPENDIX A

Summary of Candidate Control Effectors

This appendix contains descriptions, diagrams, and summary data for a number of candidate control effectors.

Figure A-1	Porous forebody
Figure A-2	Pneumatic forebody vortex control
Figure A-3	Nose yaw vanes
Figure A-4	Vortex flaps, differential
Figure A-5	Differential horizontal tail
Figure A-6	Differential canard deflections
Figure A-7	Pivoting wing tip fins
Figure A-8	Pivoting fins
Figure A-9	Differential leading edge flaps
Figure A-10	Seamless TEF and LEF
Figure A-11	Wing tip split panel flaps
Figure A-12	Wing leading edge blowing
Figure A-13	Circulation control (wing trailing edge blowing)
Figure A-14	Moving Chine/Strake
Figure A-15	Aftbody flap (upper and lower)

Porous Forebody

Primary control function

Yaw and pitch control.

Benefits

Improves yaw control at moderate and high alphas. This control is used to roll around the velocity vector.

Risks

Operating phenomena not well understood. Supersonic characteristics are unknown. Limited database. Stealth may be poor and this concept may be difficult to integrate with radar.

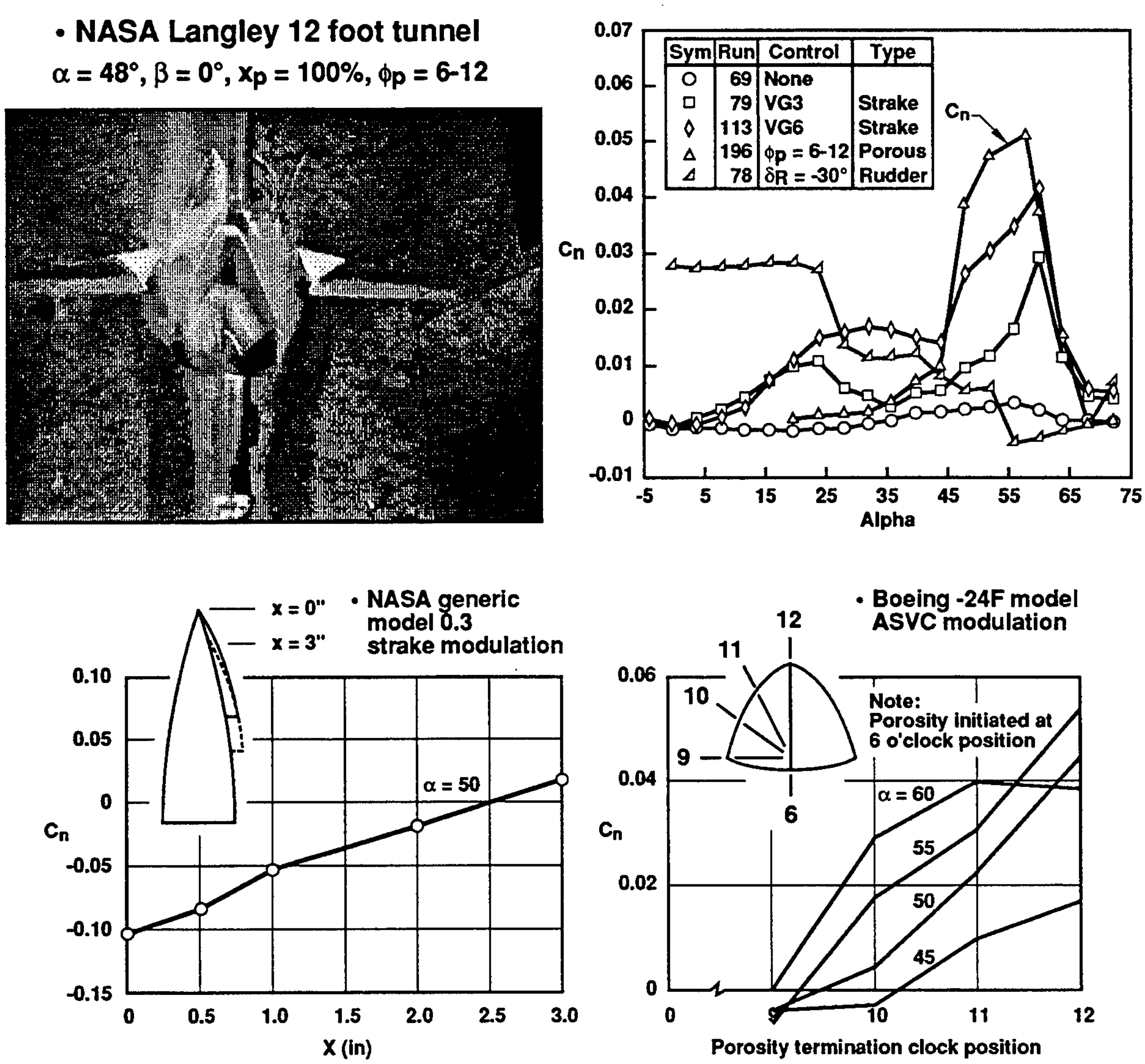

Reference: "Low Speed Wind Tunnel Investigation . . .", NASA CR4685, August, 1995.

Figure A-1 Porous Forebody

Pneumatic Forebody Vortex Control

Primary control function

Yaw and pitch control.

Benefits

Improves yaw control at moderate and high alphas. This yaw control is used to roll around the velocity vector.

Risks

Limited success on chined forebodies. Unknown supersonic characteristics. Signature impact unknown and hard to integrate with radar.

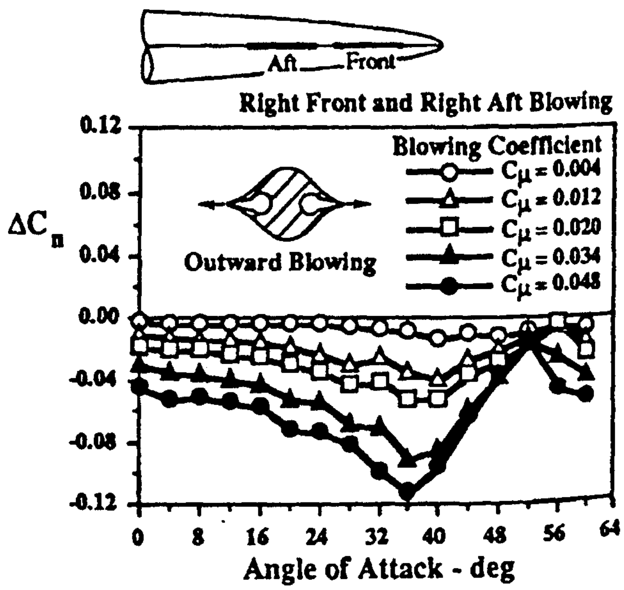

•Effect of blowing momentum coefficient on yaw control

•Effect of blowing direction

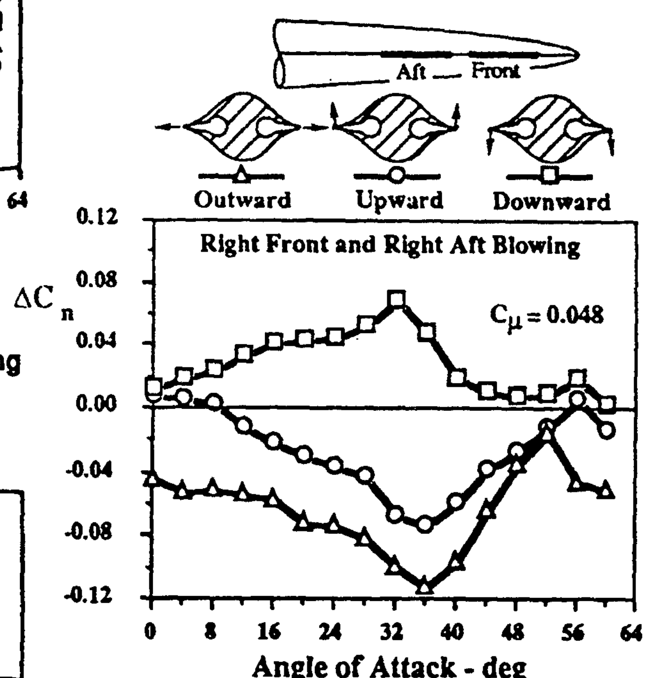

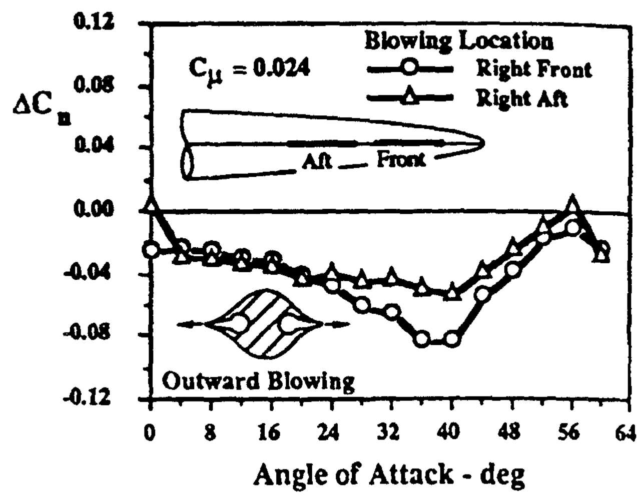

•Effect of blowing location

Reference: "High AOA Stability and Control Concepts for Supercruise Fighters", Boalbey, Ely, and Hahne.

Figure A-2 Pneumatic Forebody Vortex Control

Nose Yaw Vanes

Primary control function

Yaw and pitch control.

Benefits

Improves yaw control at moderate and high angles-of-attack. This control is used to roll around the velocity vector.

Risks

Stealth may be poor, integration with radar is difficult.

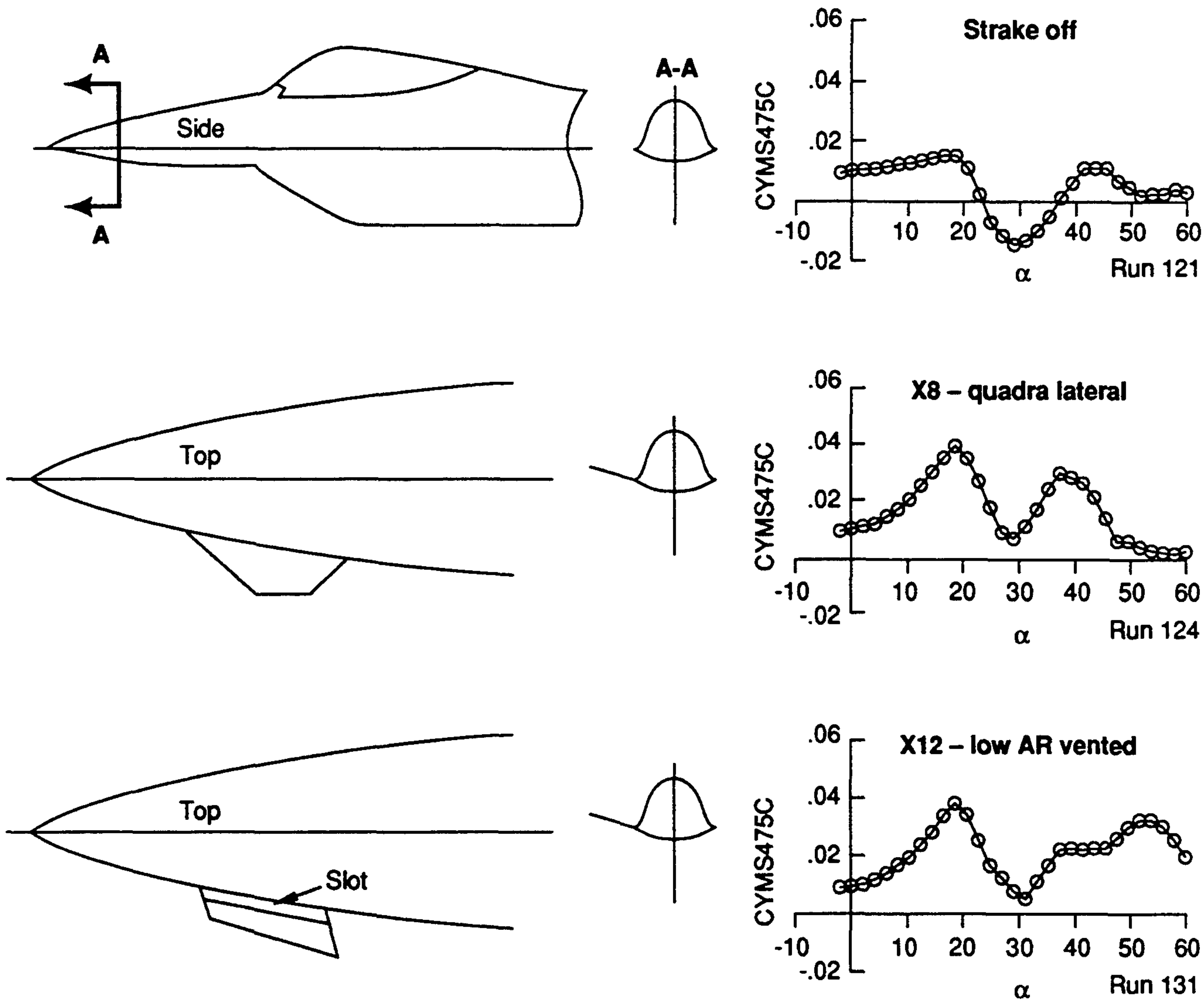

• Slotting the vane improves post stall control power

Reference: Unpublished Boeing Aerodynamic Test Data, BTWT 235 and BRWT 241, 1989.

Figure A-3 Nose Yaw Vanes

Vortex Flaps, Split Inboard/Outboard, Symmetric/Asymmetric

Primary control function

All axis – using combinations of inboard/outboard, symmetric and asymmetric.

Benefits

Exploits features of leading edge vortex on swept wings.

Risks

May not be effective at low angles-of-attack or supersonic region.

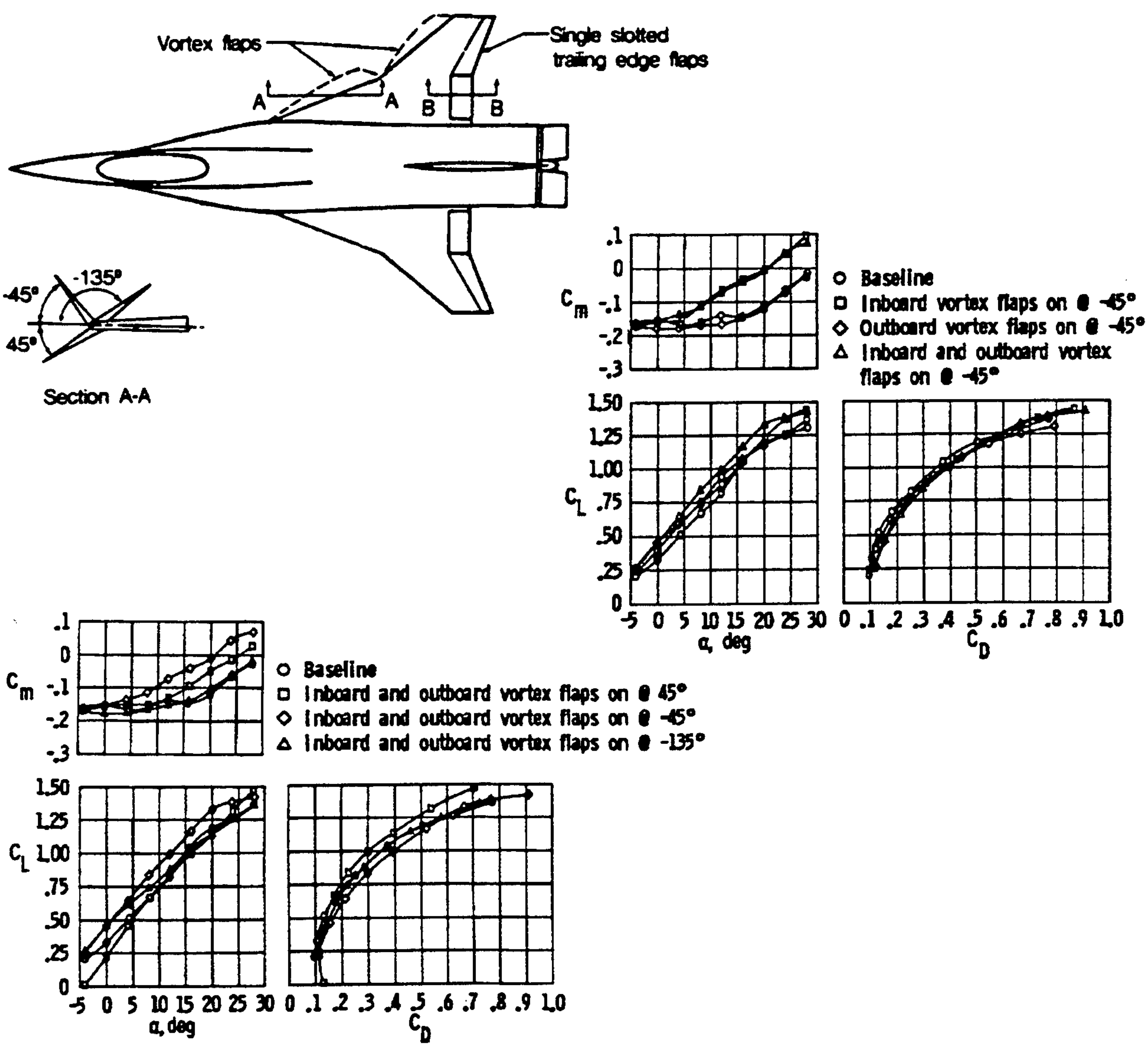

Reference: "Advanced Fighter Tested for Low-Speed Aerodynamics With Vortex Flaps", G. Gatlin, Vortex Flow Aerodynamics Conference, October 8-10, 1985.

Figure A-4 Vortex Flaps, Differential

Differential Horizontal Tail

Primary control function
    Yaw and roll control.

Benefits
    Enhances roll capability, roll around the velocity vector.

Risks
    Large actuator range required. Complex control software problem.

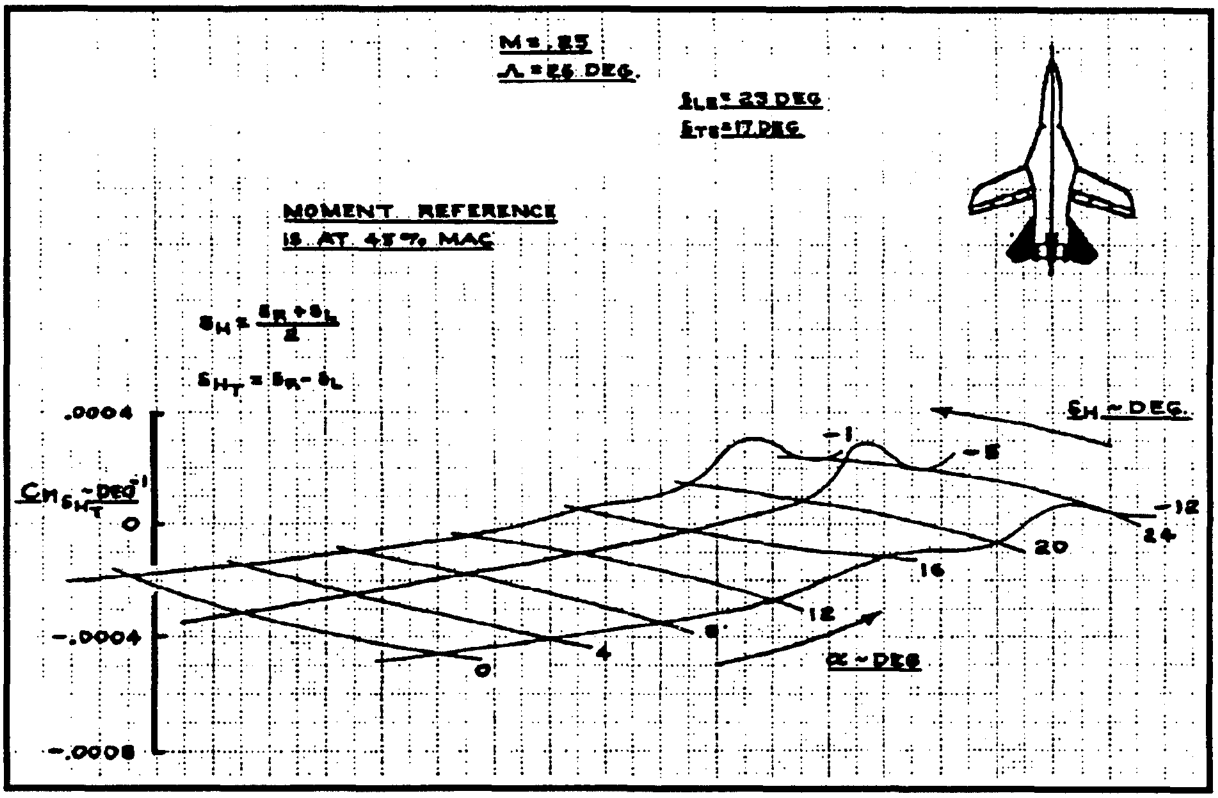

Reference: "AFTI-F-111 Mission Adaptive Wing . . .", F33615-78-C-3027, February, 1983.

Figure A-5 Differential Horizontal Tail

Differential Canard Deflections for Yaw Control

Primary control function
Yaw and roll control.

Benefits
Enhances yaw capability, yaw and roll around the velocity vector.

Risks
Signature levels are higher.

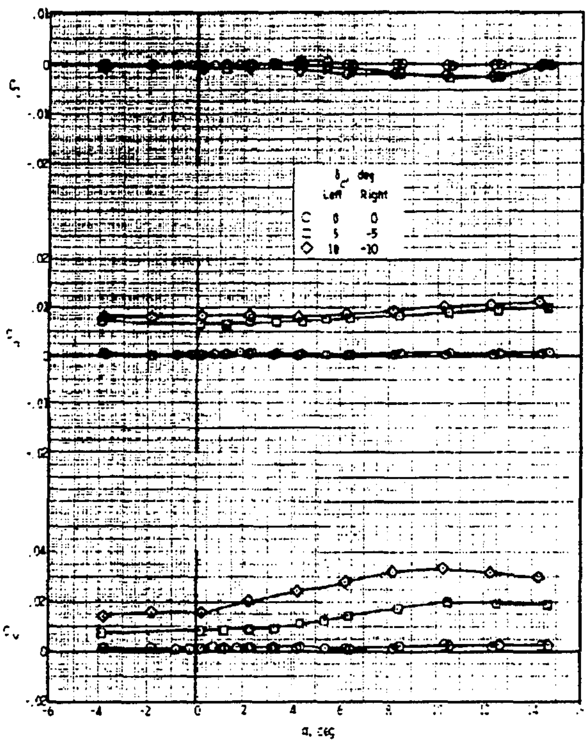

(a) M = 0.40.

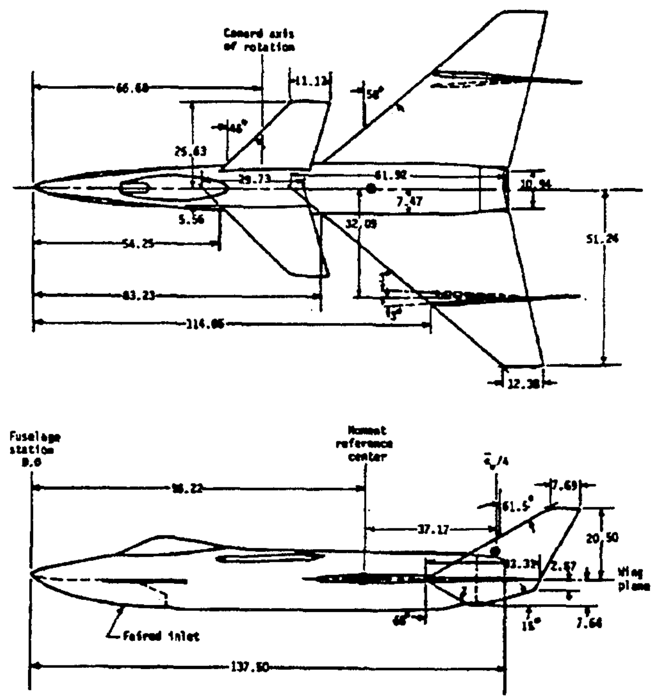

• **Effect of differential canard-panel deflection on model lateral aerodynamic coefficients**

Reference: "An Investigation of a Close-Coupled Canard . . .", Re and Capone, NASA TN D-8510, July, 1977.

Figure A-6 Differential Canard Deflections

Pivoting Wing Tip Fins For Side Force

Primary control function

Side force.

Benefits

Exploit flat turns for heading and alignment agility.

Risks

Heavy, defeats concept.

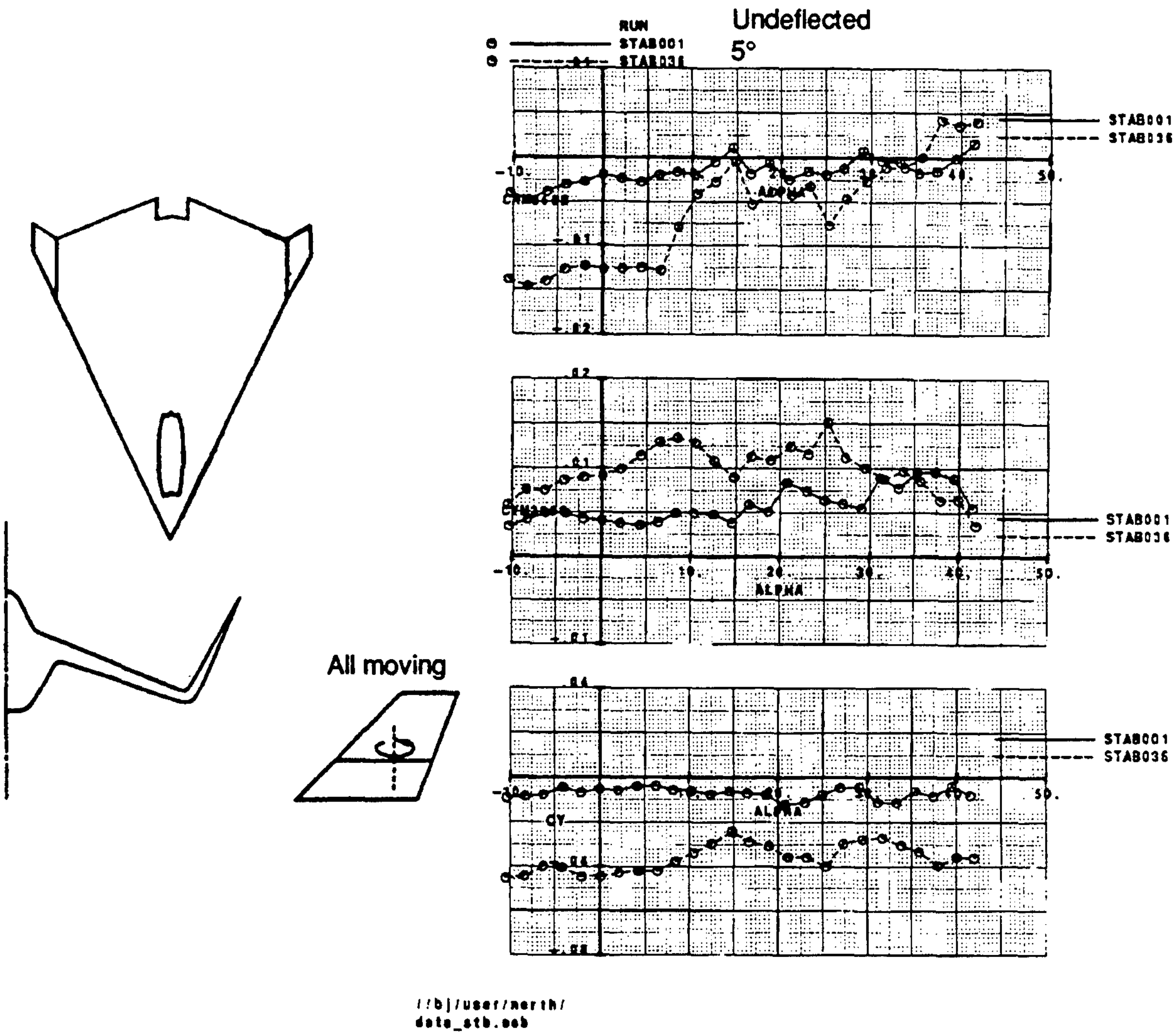

Reference: Unpublished Boeing Data, D. Nelson, WSU Wind Tunnel Test, December, 1994.

Figure A-7 Pivoting Wing Tip Fins

Pivoting Fins for Side Force

Primary control function
Side force.
Benefits
Exploit flat turns for heading agility.
Risks
Heavy, defeats the concept (case shown is for a deflected pair of rudders – side force is shown).

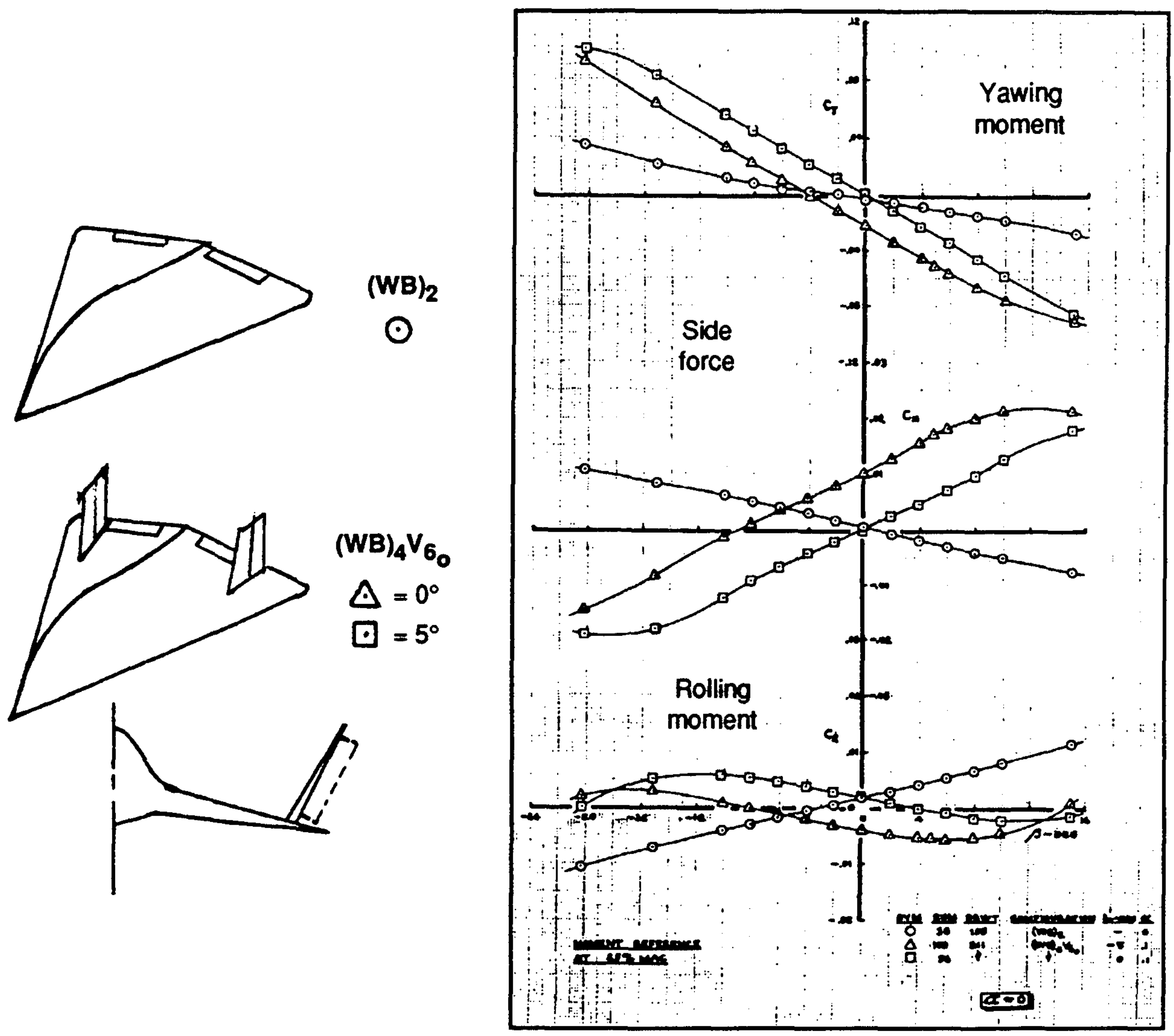

Reference: Unpublished Boeing Data, G. Letsinger, BRWT 211 and 198, October, 1986.

Figure A-8 Pivoting Fins

Differential Leading Edge Flaps

Primary control function

Roll control.

Benefits

Improves roll control.

Risks

Not very effective for highly swept configurations; roll reversal occurs at angles-of-attack approaching stall, requiring a complete database of characteristics to define reversal effects.

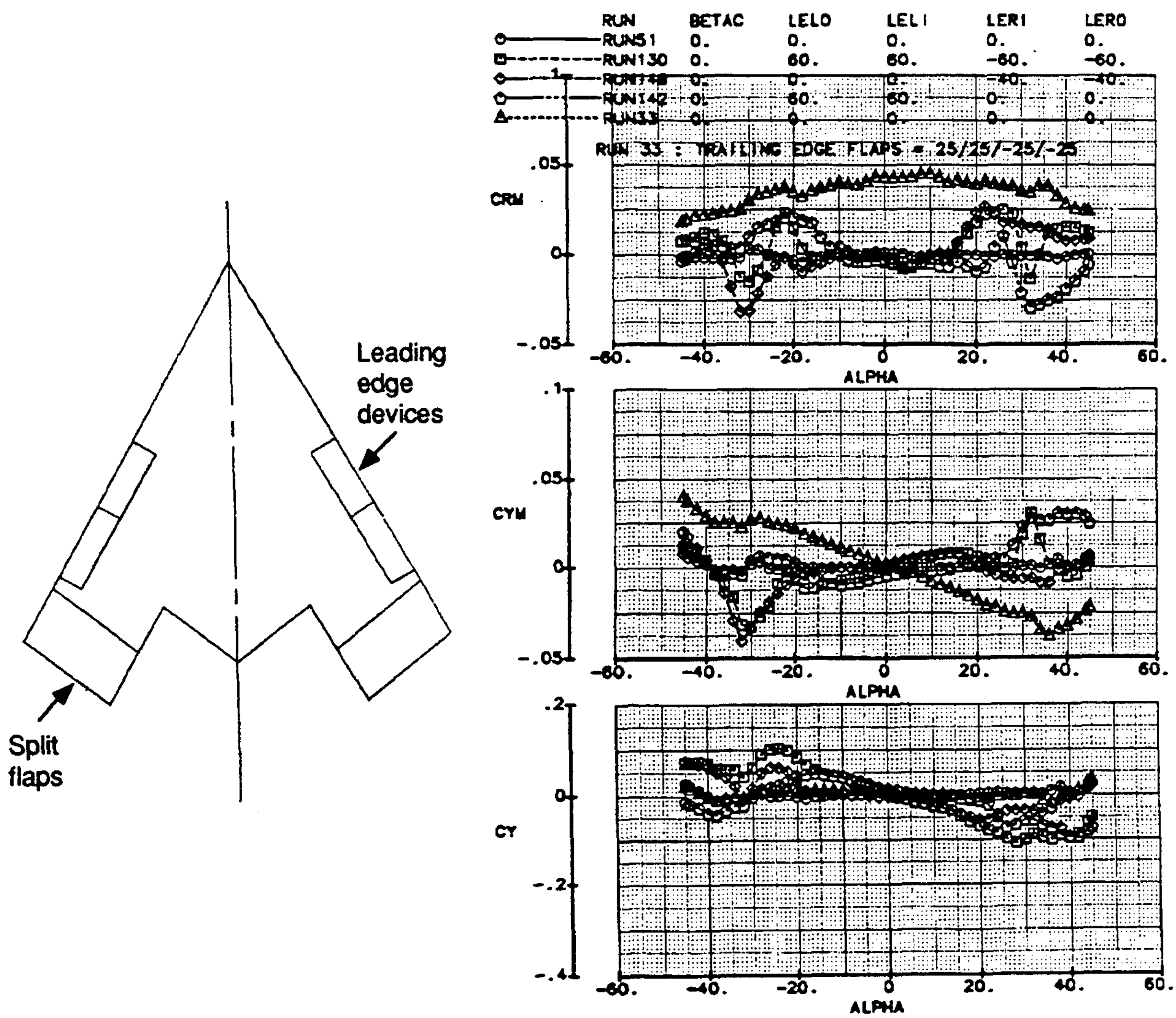

Reference: Unpublished Boeing Data, Merker, February, 1990.

Figure A-9 Differential Leading Edge Flaps

Seamless TEF and LEF Hinges

Primary control function
L/D and stealth improvements.
Benefits
Extrapolation of maw technology. Eliminates the seams associated with conventionally hinged flaps.
Risks
4 bar linkages are heavy and complex.

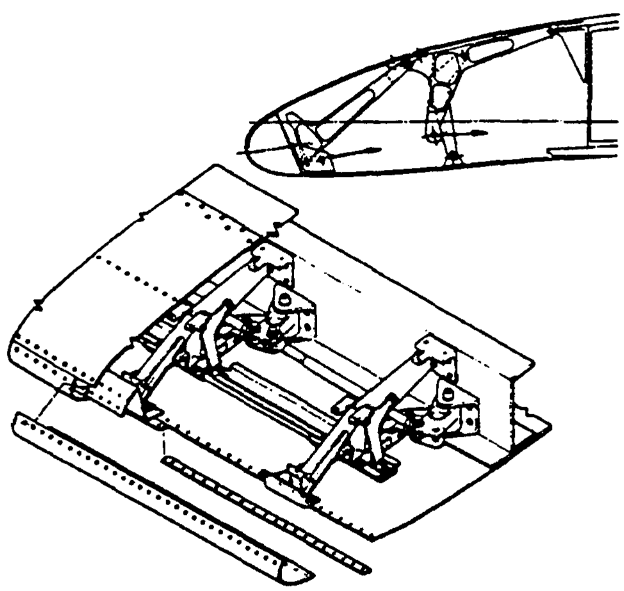

• Leading edge concept

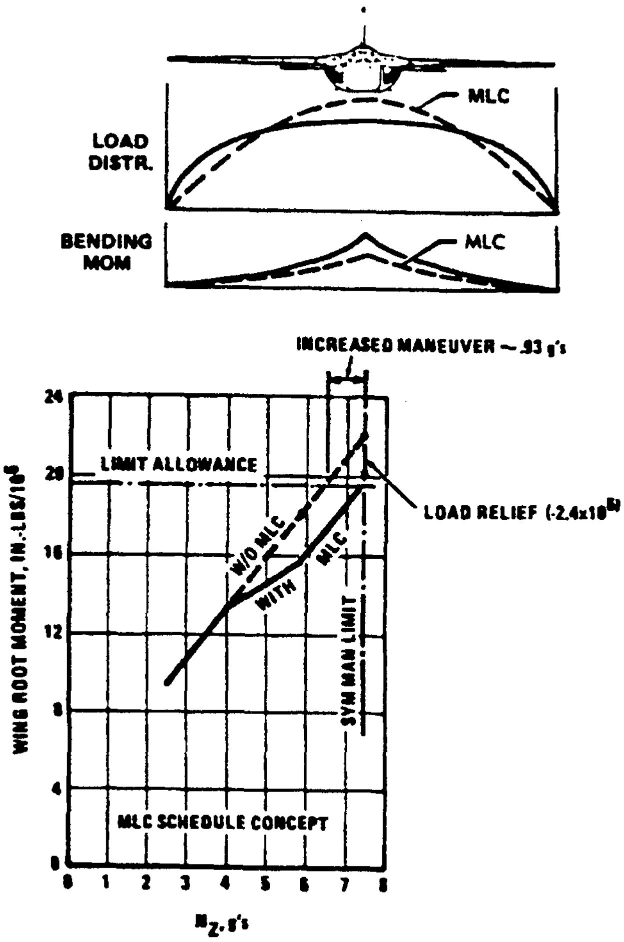

• Maneuver load control benefits

Reference: "Development of a Mission Adaptive Wing System . . .",
W. Gilbert, AIAA-80-1886, August, 1980.

Figure A-10 Seamless TEF and LEF

Wing Tip Split Panel Flaps

Primary control function
: Yaw control.

Benefits
: Can be used to reduce/replace rudders or vertical fins. Good at all alphas. Effective throughout the entire flight envelope.

Risks
: Supersonic characteristics not well known. Defeats stealth benefits when deployed.

• **Planform view of split elevon**

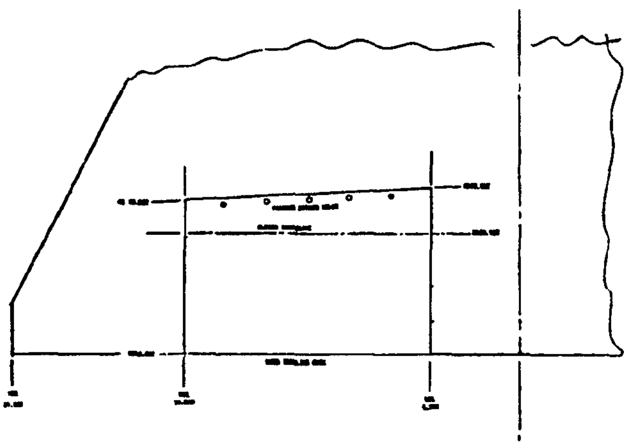

• **Split elevons**

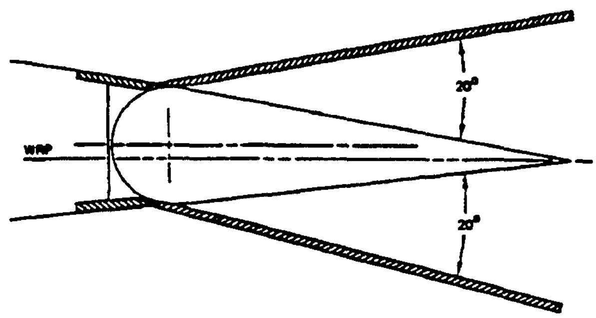

• **Yawing moment coefficient**

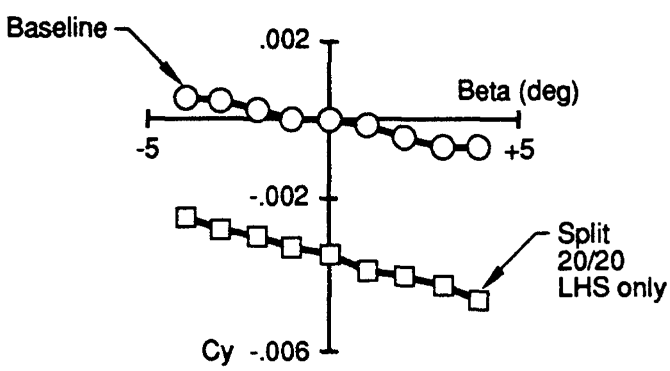

Reference: "Wind Tunnel Test Report, Boeing Model BMAC-T-1549", D180-30190-1, S. Northcraft, January, 1987.

Figure A-11 Wing Tip split Panel Flaps

Wing Leading Edge Blowing

Primary control function
: Lift enhancement and roll control.

Benefits
: Maintain attached vortex flow at high angles-of-attack.

Risks
: Weight/system sizing penalties, interference with high-lift system.

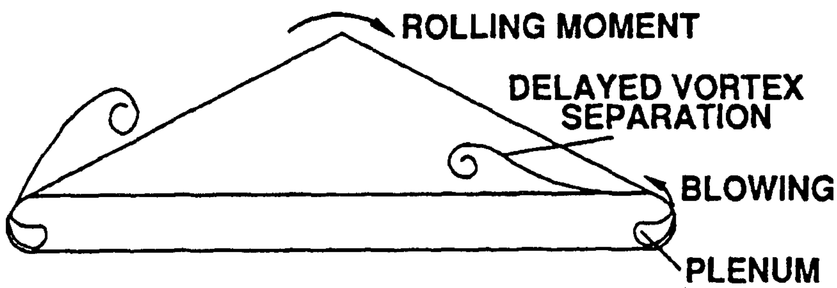

(α = 50 DEG)

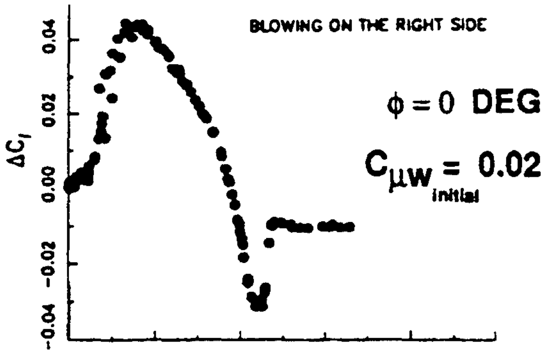

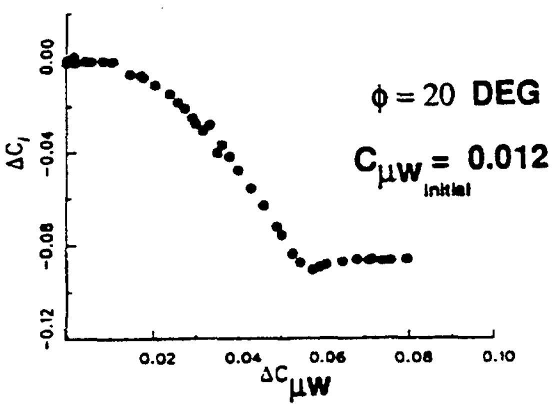

• **Rolling moments produced by differential blowing on a delta wing – as a function of blowing coefficient**

Reference: "Controlled Vortex Flows Over Forebodies and Wings", Roberts, et. al., 1990.

Figure A-12 Wing Leading Edge Blowing

Circulation Control (Wing Trailing Edge Blowing)

Primary control function

Lift enhancement and roll control.

Benefits

Increases wing circulation and lift at a given flight condition.

Risks

Weight penalty, integration with trailing edge flaps.

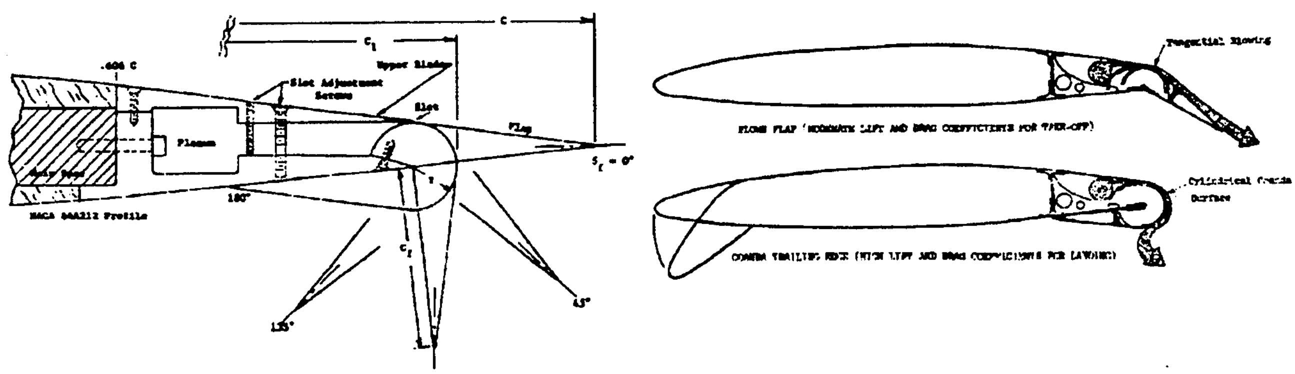

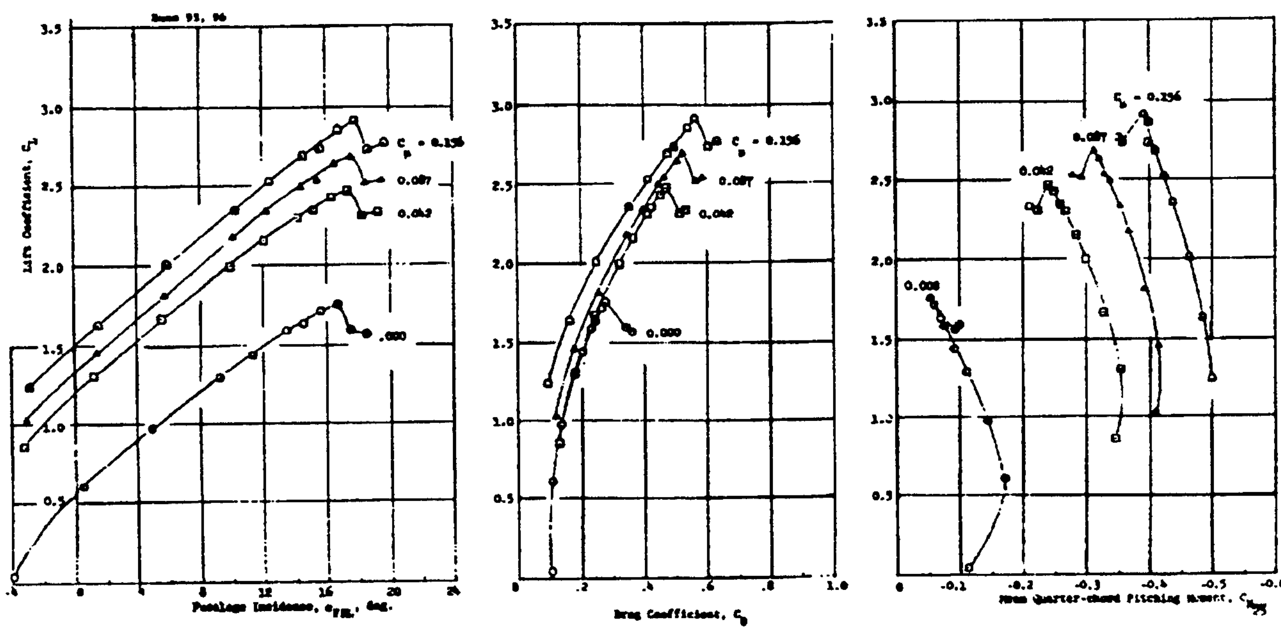

Figure 20 - Effect of Blowing on Longitudinal Characteristics of Configuration 9
($\delta_f = 45°$, $\delta_n = 30°$, $\delta_{n_o} = 10°$, Fences, Tail-Off)

Reference: "Subsonic Wind Tunnel Investigation . . .",
R. Englar, May, 1973.

Figure A-13 Circulation Control (Wing Trailing Edge Blowing)

Moving Chine/Strake

Primary control function

Pitch and yaw.

Benefits

Improve yaw and pitch control at moderate to high angles-of-attack.

Risks

Stealth may be poor.

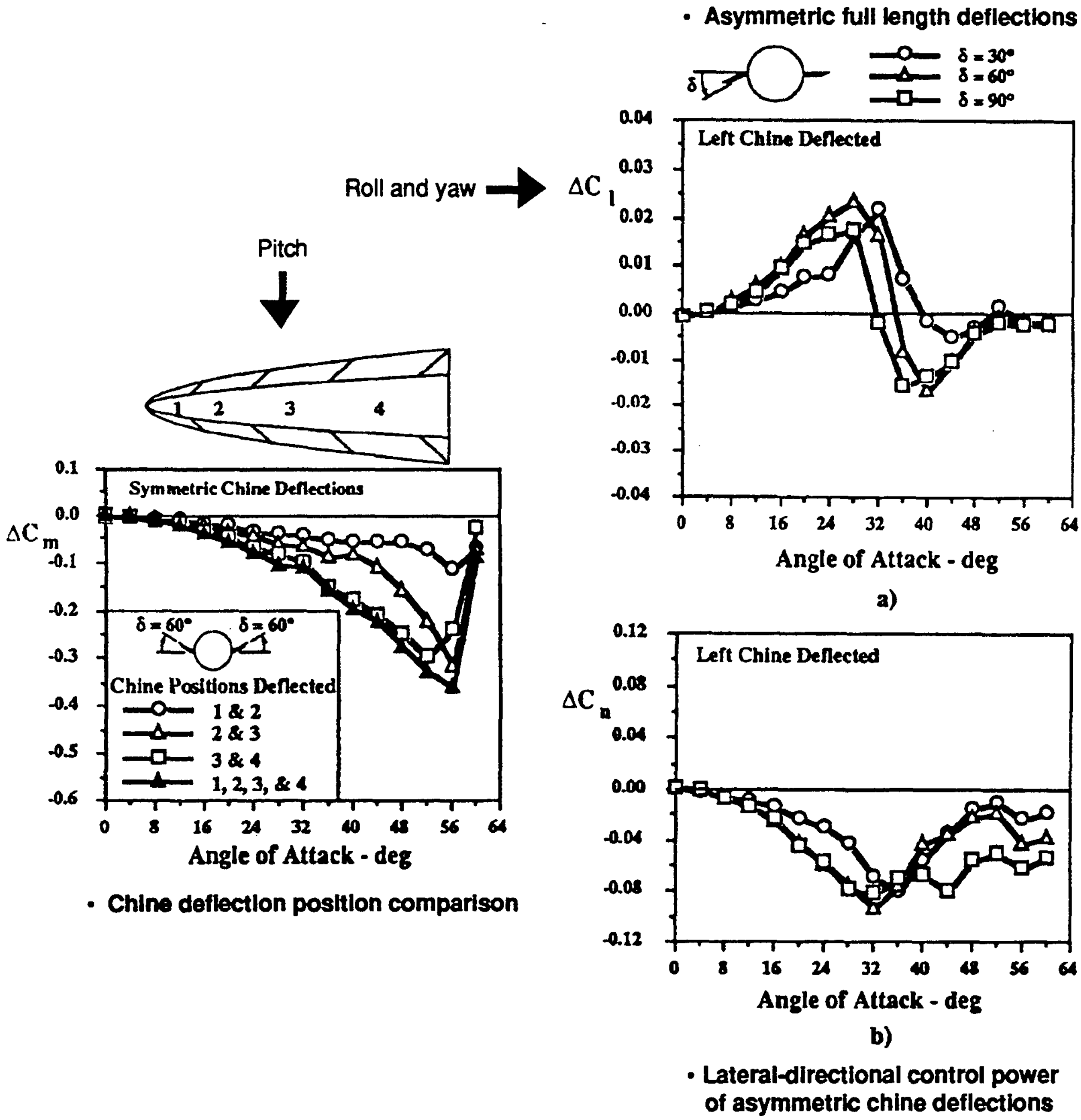

Reference: "High AOA Stability and Control Concepts for Supercruise Fighters", Boalbey, Ely, and Hahne.

Figure A-14 Moving Chine/Strake

Aftbody Flap (Upper and Lower)

Primary control function

Pitch control.

Benefits

Enhances pitch capability.

Risks

Signature, weight, volume required.

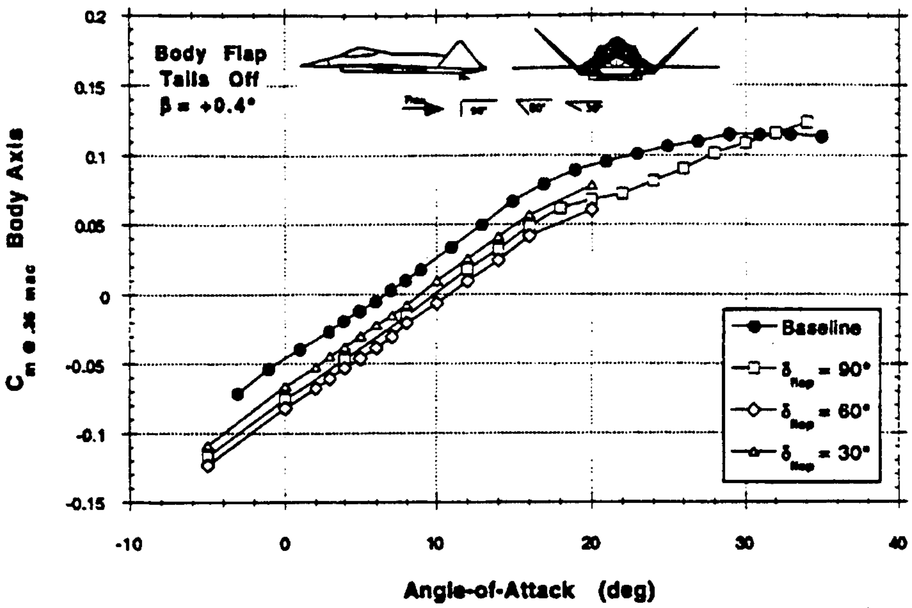

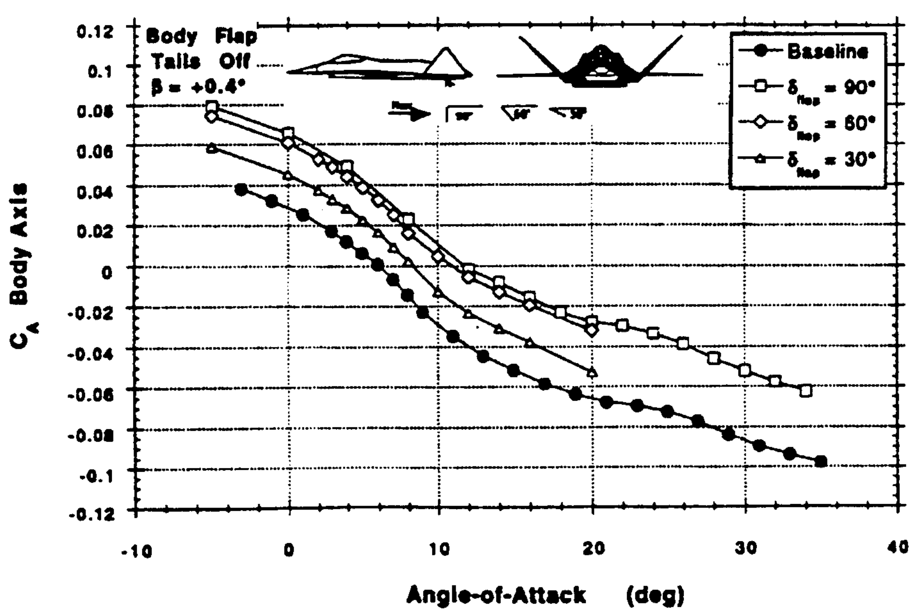

• Body flap, β = +0.4°

Reference: "Low Speed Investigation . . .", M. Alexander, WL-TR-94-3120, September, 1994.

Figure A-15 Aftbody Flap (Upper and Lower)

APPENDIX B

Summary of Performance Results:

This appendix contains a summary of the information used to evaluate the candidate effectors from a stability and flight control performance standpoint:

Figure B-1 Longitudinal Control in Maneuvering Flight-Maximum Sustained Load Factor

Figure B-2 Longitudinal Control in Maneuvering Flight-Penetration Speed

Figure B-3 Longitudinal Control in Maneuvering Flight-Supersonic Condition

Figure B-4 Wave-Off Maneuver

Figure B-5 Air Combat Maneuver Corner Speed

Figure B-6 Maximum Sustained Load Factor

Figure B-7 Wave-Off Maneuver-Simulation Comparison

Figure B-8 Pop-Up Maneuver

Figure B-9 90 Degree ~ 30 Knot Crosswind

Figure B-10 Catapult Launch

Figure B-11 Flight Path Stability

Figure B-12 Carrier Suitability Roll Rate Summary

Figure B-13 Flight Path Stability

Figure B-14 90 Degree ~ 30 Knot Crosswind-Thrust Vectoring

Figure B-15 Dutch Roll Characterics

Figure B-16 Maximum Yawing Moment Coefficient Due to Controls

Figure B-17 Maximum Rolling Moment Coefficient Due to Controls

Figure B-18 V_{mc} *with Right Engine Out*

Figure B-19 Pop-Up Maneuver-Simulation Comparison

Figure B-20 Level Flight Longitudinal Acceleration

Figure B-21 Roll Control Effectiveness Landing Approach

Figure B-22 Roll Control Effectiveness Landing Approach-Thrust Vectoring

Figure B-23 Roll Rate Oscillations

Figure B-24 30 Degree Bank Control Surface Response-Ailerons, Strakes

Figure B-25 30 Degree Bank Control Surface Response-Rotating Tail

Figure B-26 30 Degree Bank Vehicle Response--Rotating Tail

Figure B-27 30 Degree Bank vehicle Response - Ailerons, Strakes

Figure B-28 2-g Coordinated Turn Entry Control Surface Response

Figure B-29 2-g Coordinated Turn Energy Vehicle Response-Rotating Tail

Figure B-30 2-g Coordinated Turn Entry Vehicle Response-Ailerons, Strakes
Figure B-31 Longitudinal and Directional Stability Levels
Figure B-32 Longitudinal Control in Maneuvering Flight
Figure B-33 Maximum Sustained Load Factor at Mid Altitude
Figure B-34 Maximum Sustained Load Factor at High Altitude-Subsonic
Figure B-35 Maximum Sustained Load Factor at High Altitude-Supersonic Penetration
Figure B-36 Maximum Sustained Load Factor-Penetration
Figure B-37 Dutch Roll Characteristics
Figure B-38 Low Speed Lift and Pitching Moment Coefficients
Figure B-39 Level Flight Longitudinal Acceleration
Figure B-40 Landing Approach Nose Down Pitch Acceleration
Figure B-41 Carrier Suitability Roll Rate Summary
Figure B-42 Sideslip Angle Capture
Figure B-43 Departure Stall-Roll Rate Time Constant
Figure B-44 Departure Stall-Roll Performance
Figure B-45 Power on Departure Stall-Lateral-Directional Dynamics

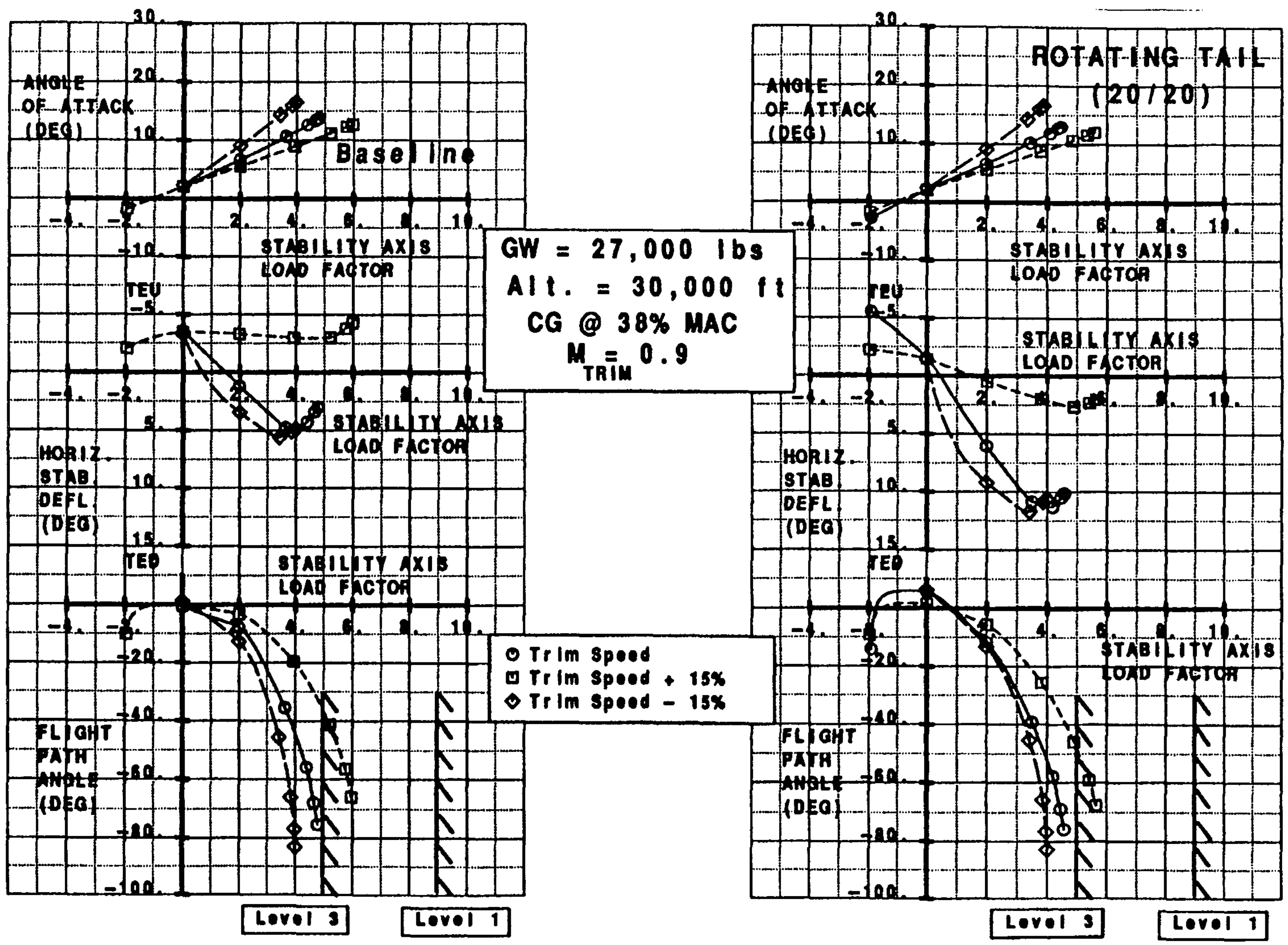

Figure B-1 Longitudinal Control in Maneuvering Flight-Maximum Sustained Load Factor

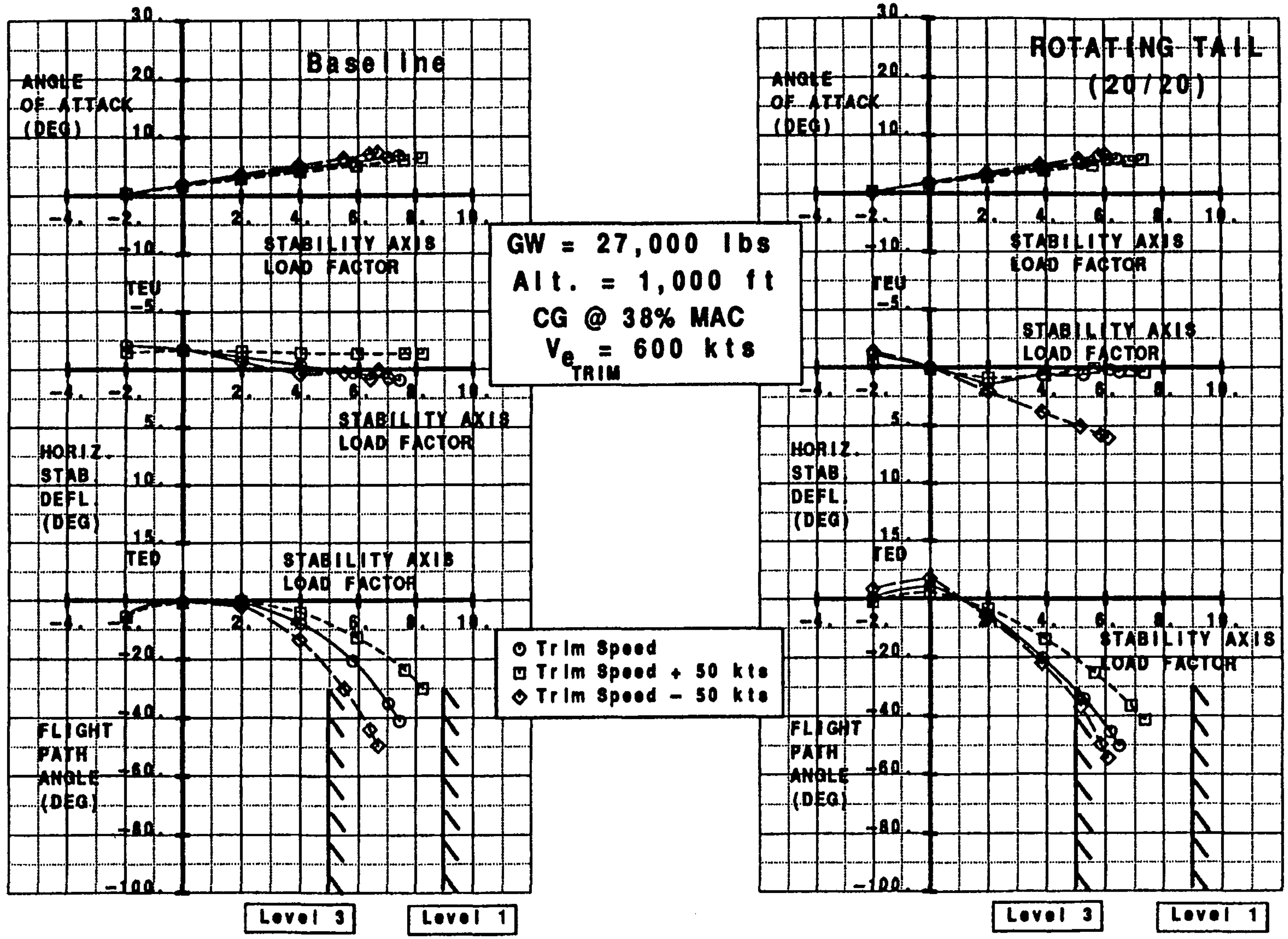

Figure B-2 Longitudinal Control in Maneuvering Flight-Penetration Speed

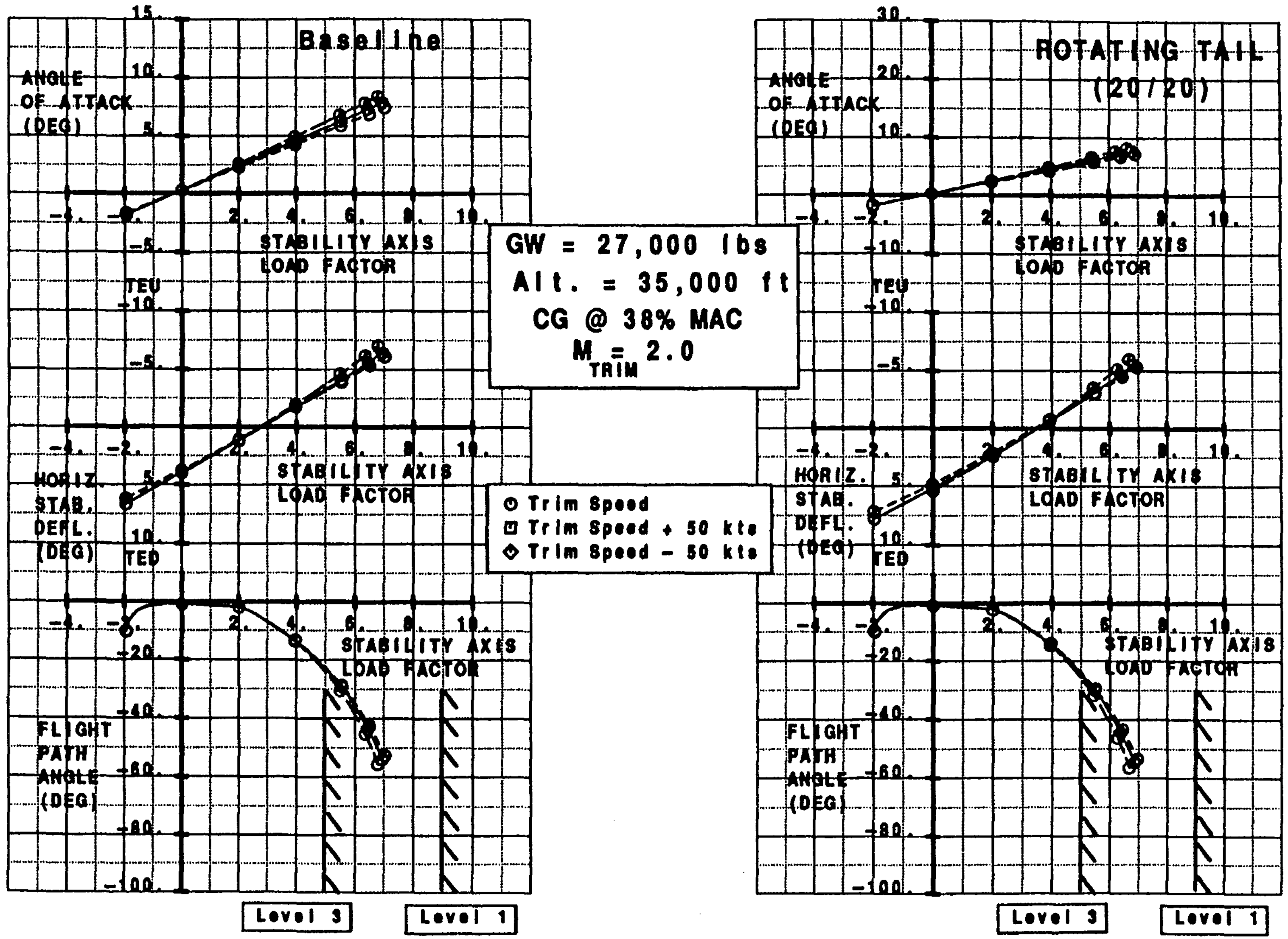

Figure B-3 Longitudinal Control in Maneuvering Flight-Supersonic condition

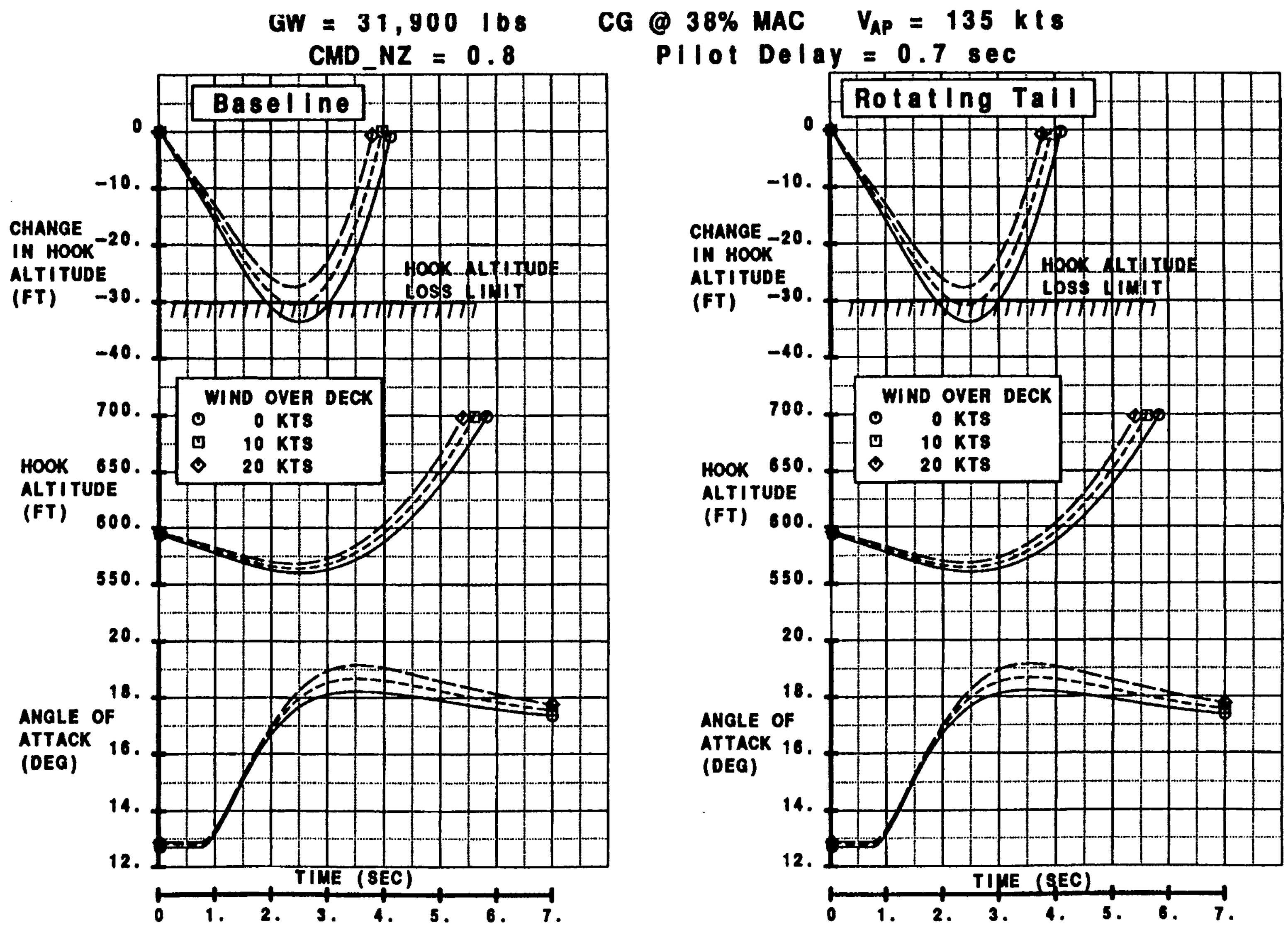

Figure B-4 Wave-Off Maneuver

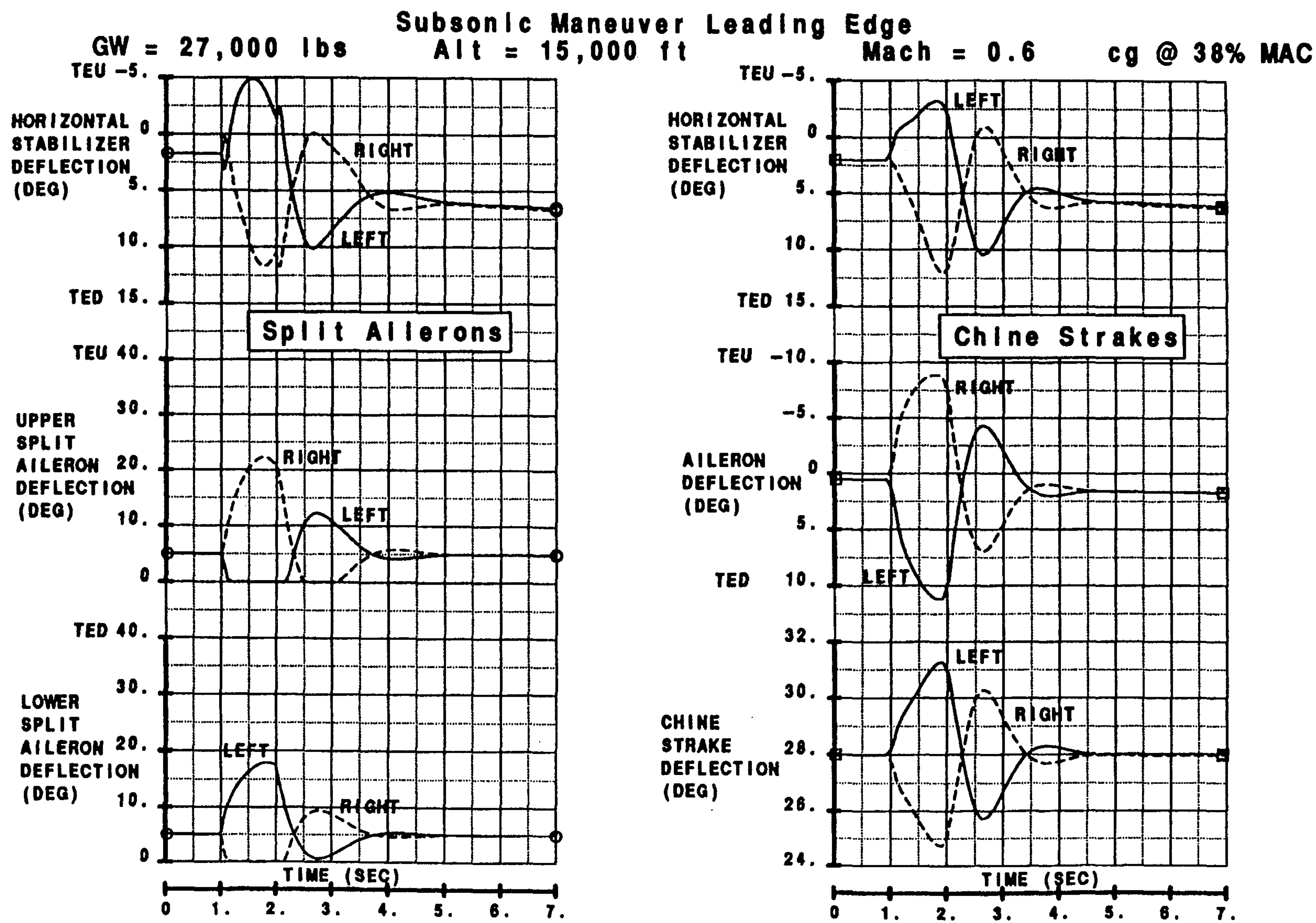

2-g Coordinated Turn Entry - Control Surface Response

Figure B-5 Air Combat Maneuver Corner Speed

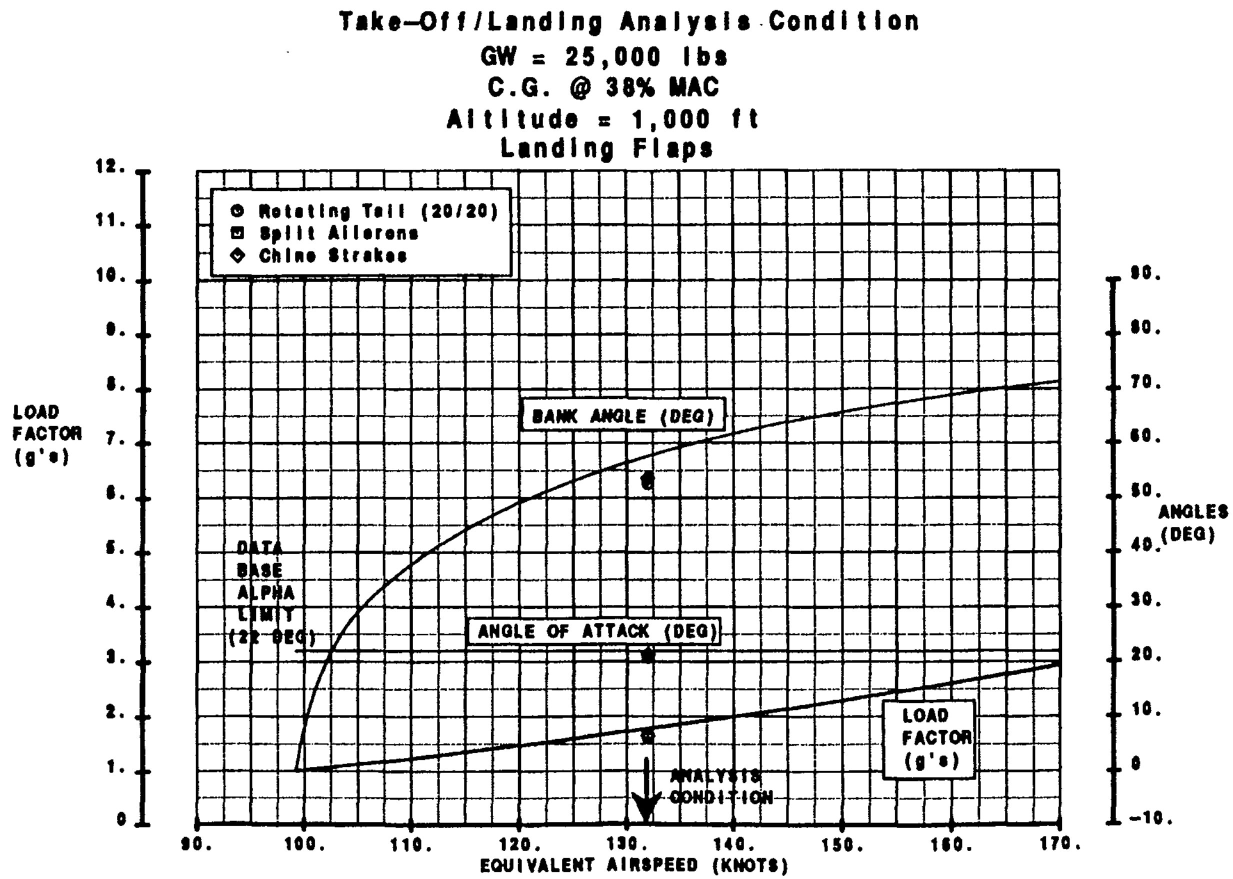

Model - 24F - Capability in Coordinated Turns
Figure B-6 Maximum Sustained Load Factor

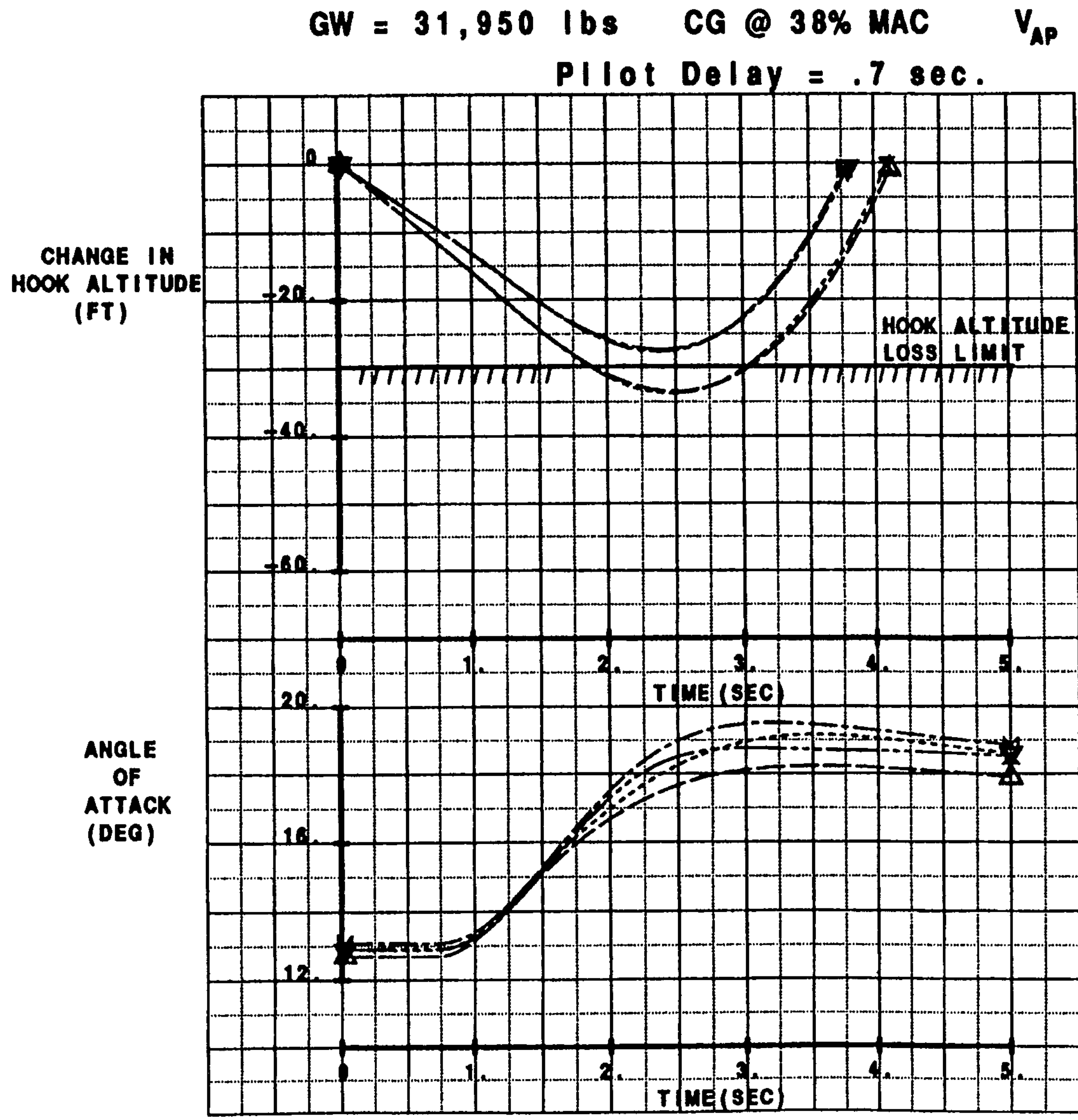

CONFIGURATION	ANALYSIS TOOL	WIND OVER DECK
△ Baseline	MEATBALL	0 kt
⧗ Rotating Tail	MEATBALL	0 kt
▽ Baseline	RPAS	0 kt
⋈ Rotating Tail	RPAS	0 kt
Baseline	RPAS	20 kt
Rotating Tail	RPAS	20 kt

NOTE: MEATBALL SOLUTION ENDS WHEN HOOK SINK CHANGES SIGN.

Figure B-7 Wave-Off Maneuver-Simulation Comparison

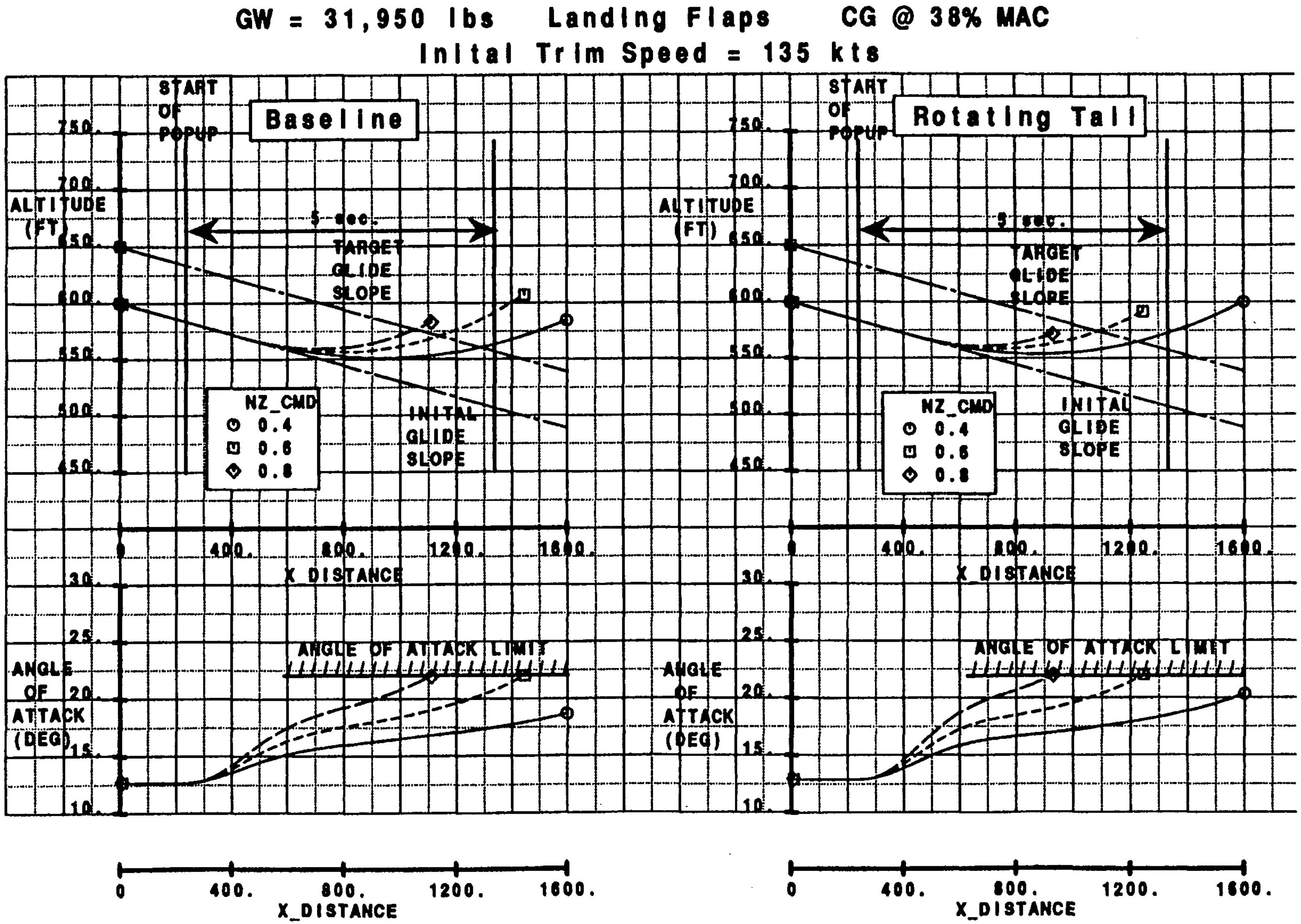

Figure B-8 Pop-Up Maneuver

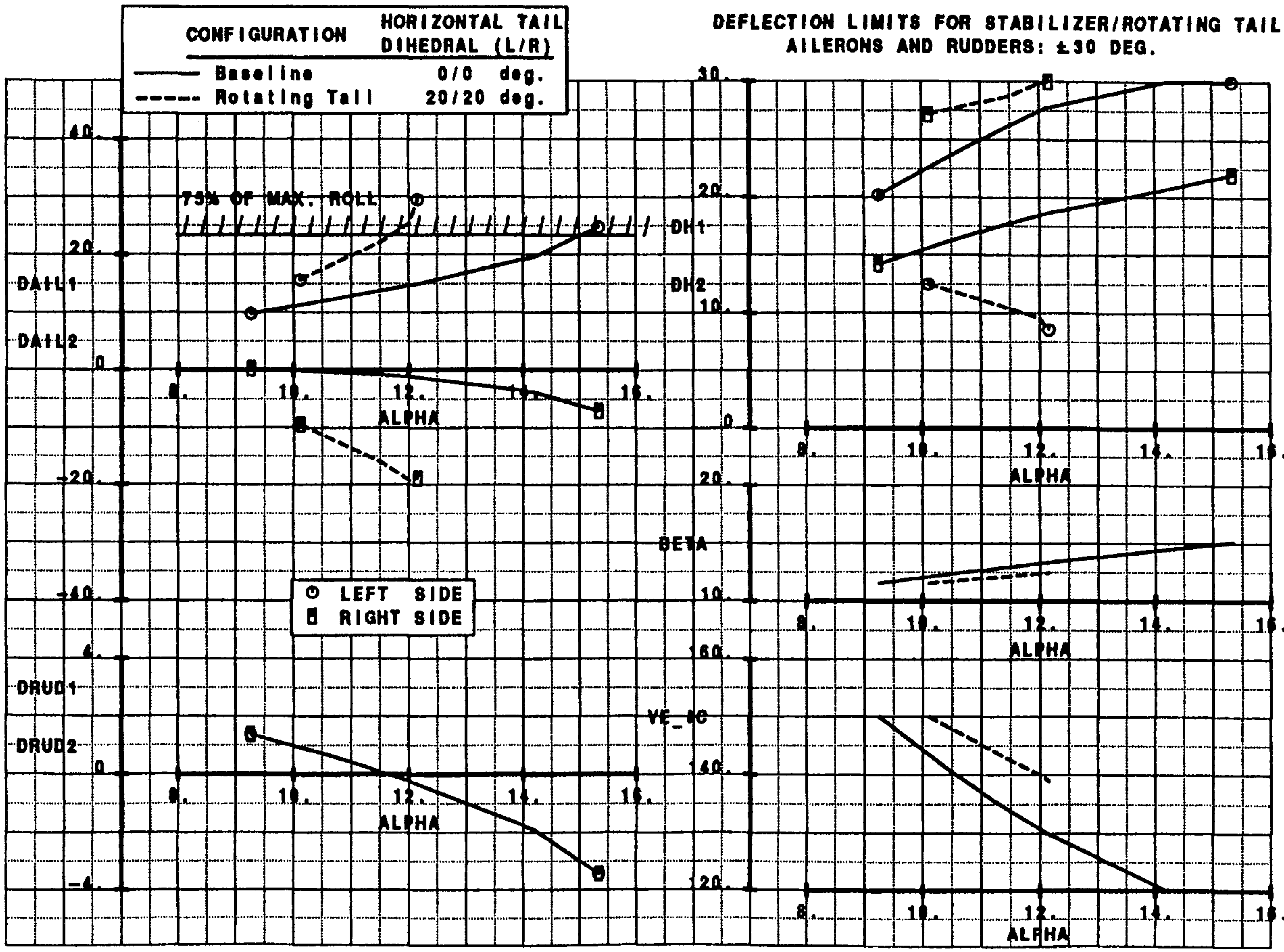

Figure B-9 90 Degree ~ 30 Knot Crosswind

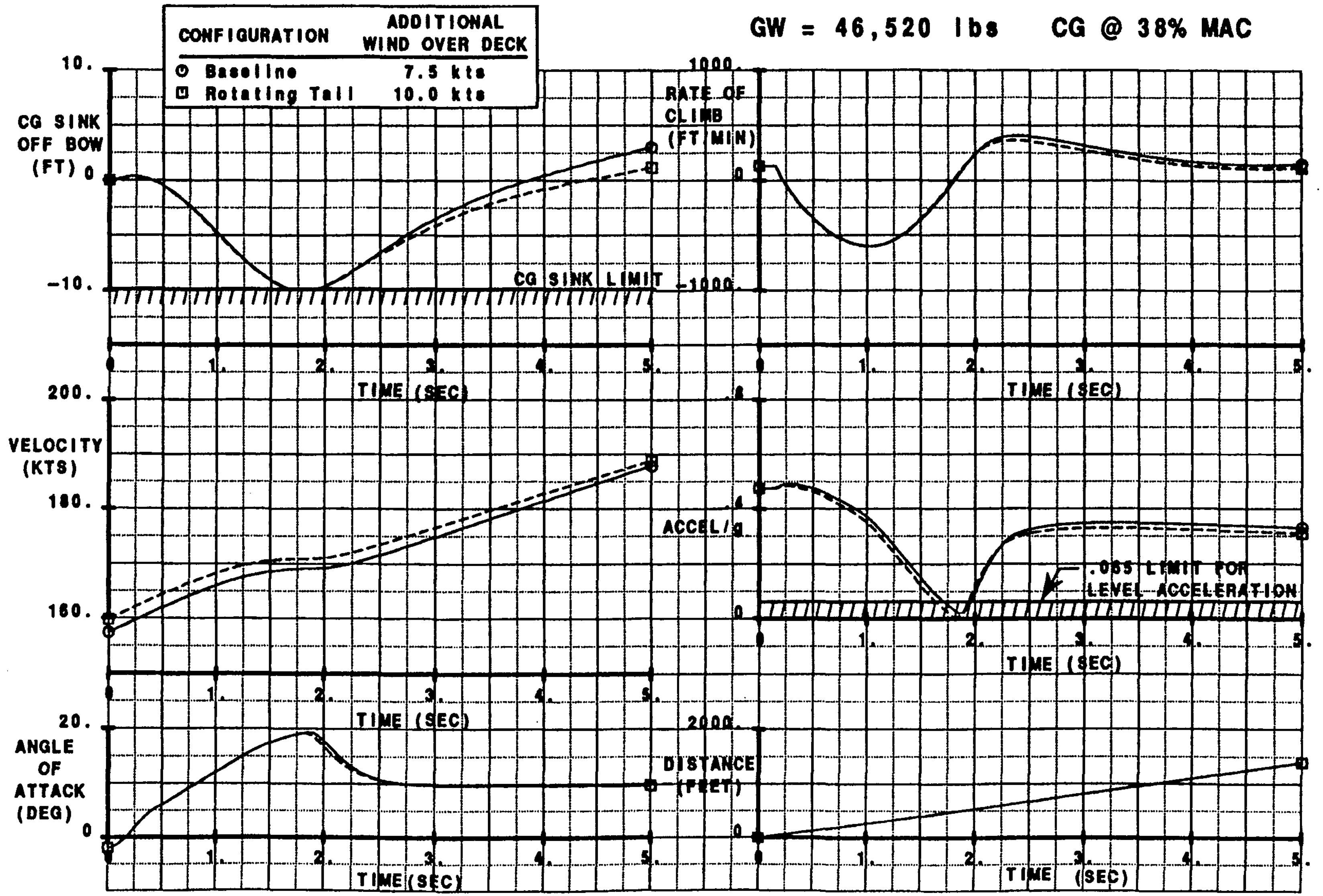

Figure B-10 Catapult Launch

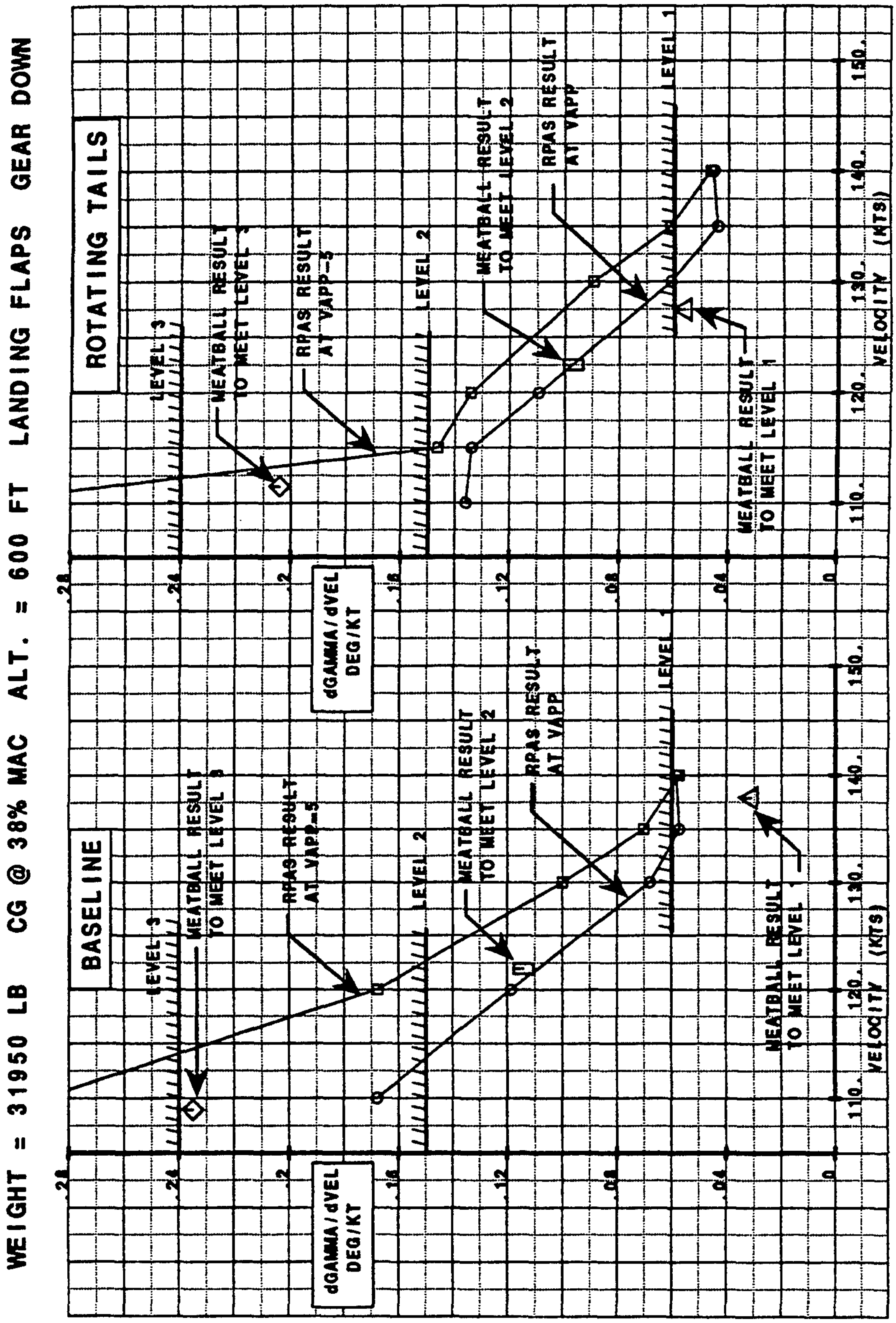

Figure B-11 Flight Path Stability

GW = 31,900 lbs CG @ 38% MAC Landing Flaps Gear Down

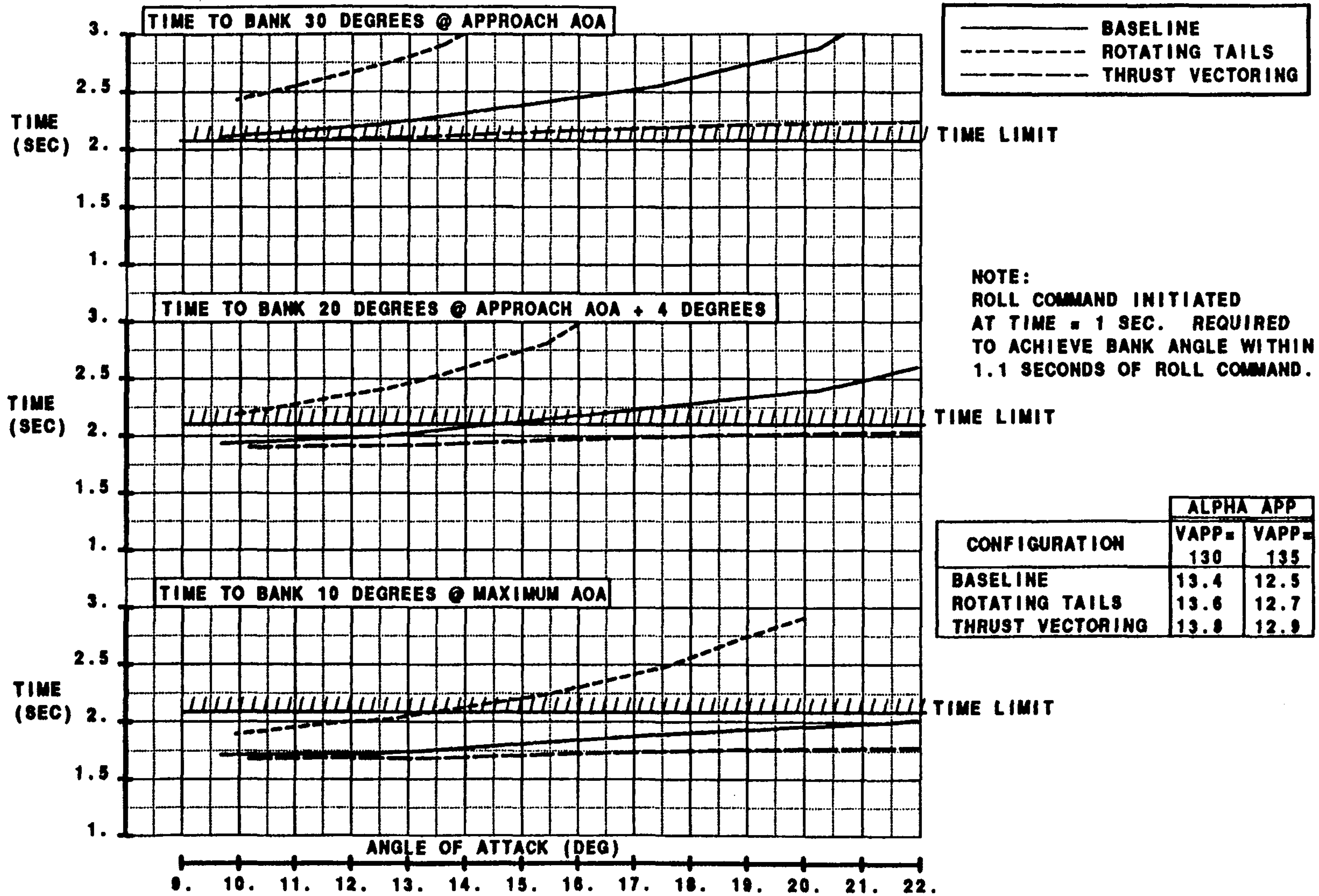

NOTE:
ROLL COMMAND INITIATED AT TIME = 1 SEC. REQUIRED TO ACHIEVE BANK ANGLE WITHIN 1.1 SECONDS OF ROLL COMMAND.

CONFIGURATION	ALPHA APP	
	VAPP= 130	VAPP= 135
BASELINE	13.4	12.5
ROTATING TAILS	13.6	12.7
THRUST VECTORING	13.8	12.9

Figure B-12 Carrier Suitability Roll Rate Summary

WEIGHT = 31950 LB   CG @ 38% MAC   ALT. = 600 FT   LANDING FLAPS   GEAR DOWN

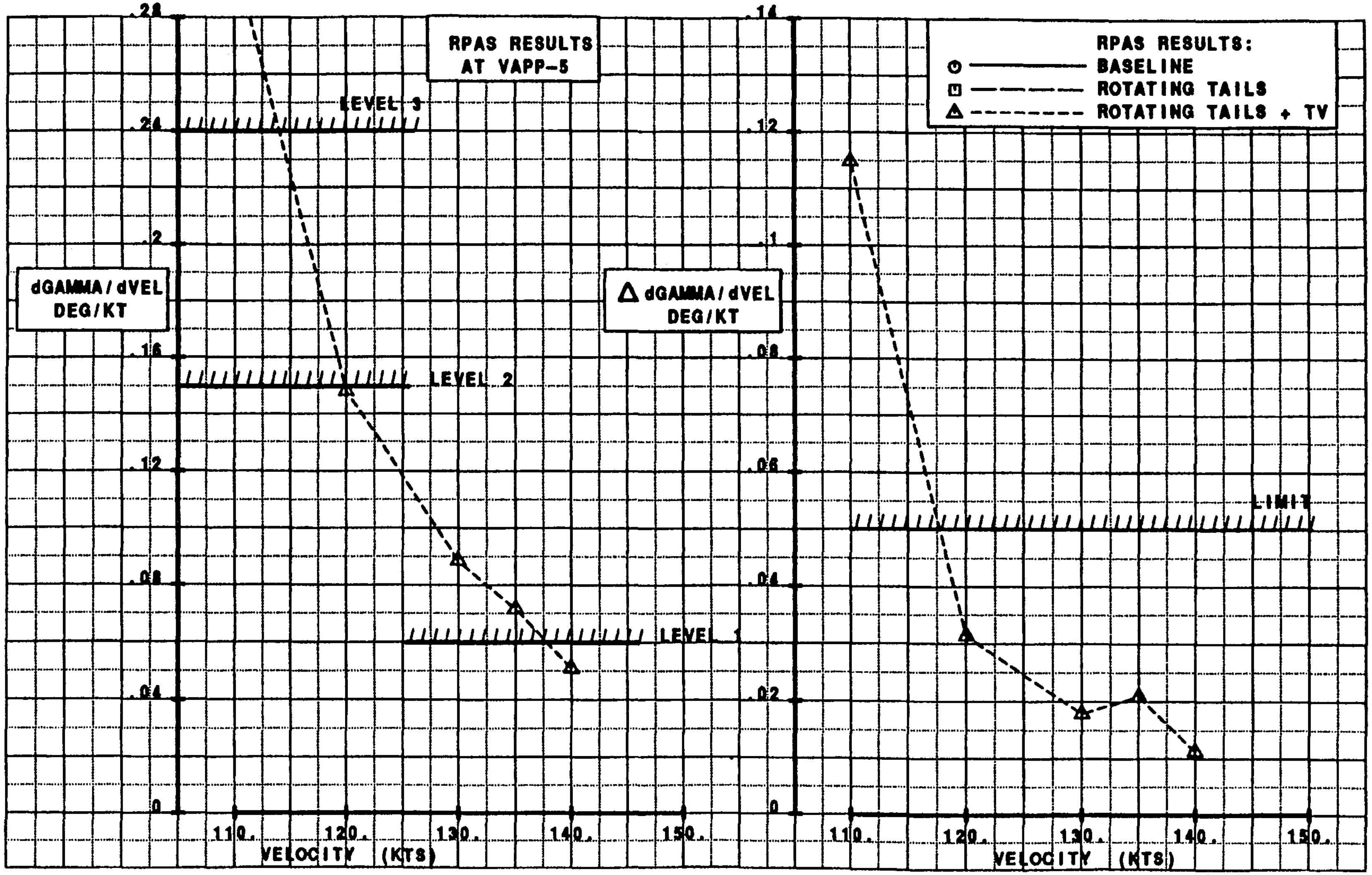

Figure B-13 Flight Path Stability

ROTATING TAILS, SPLIT AILERON WITH THRUST VECTORING

DEFLECTION LIMIT FOR ROTATING TAIL AND SPLIT AILERONS: ±30 DEG.

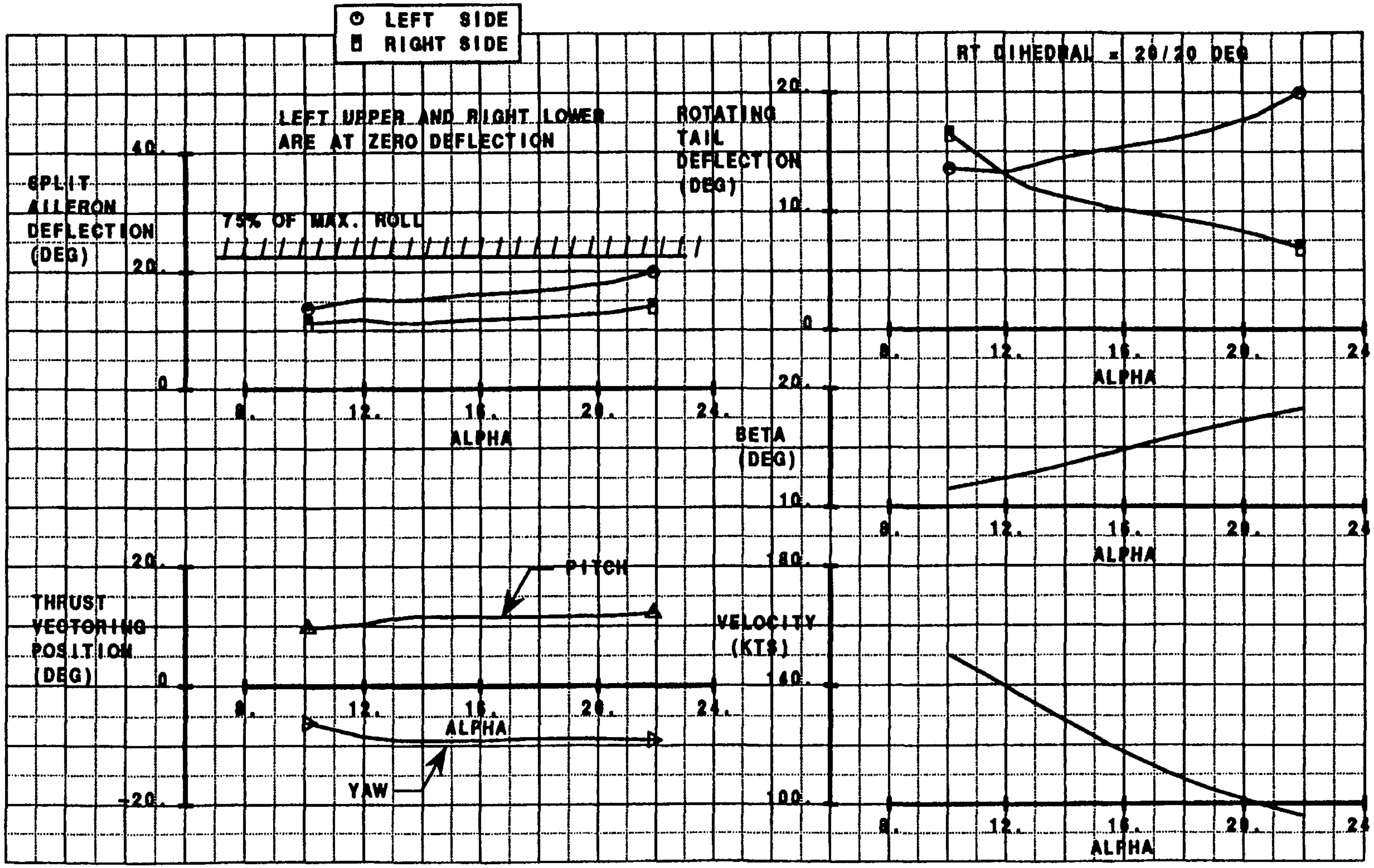

Figure B-14 90 Degree ~ 30 Knot Crosswind-Thrust Vectoring

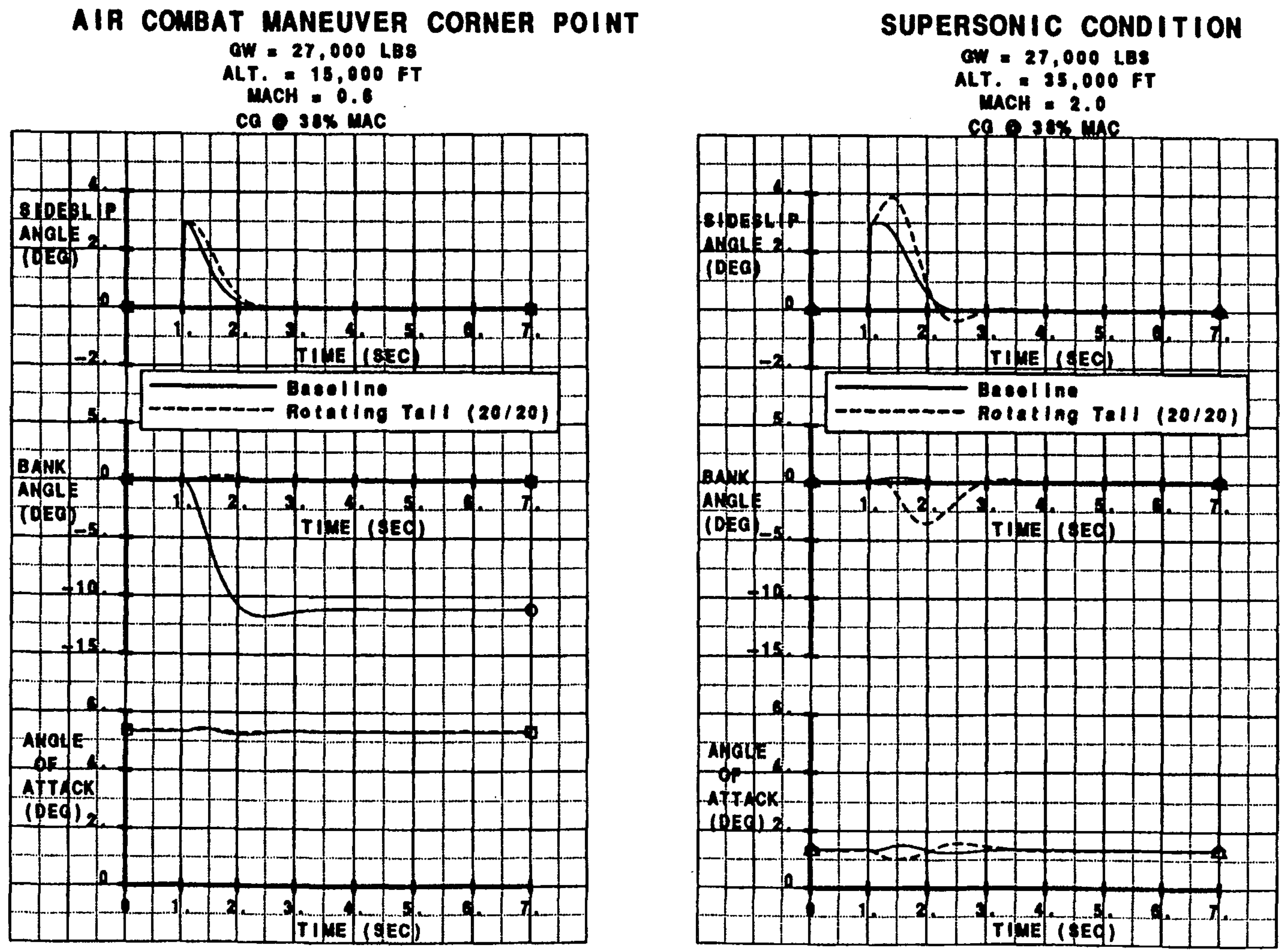

Figure B-15 Dutch Roll Characterics

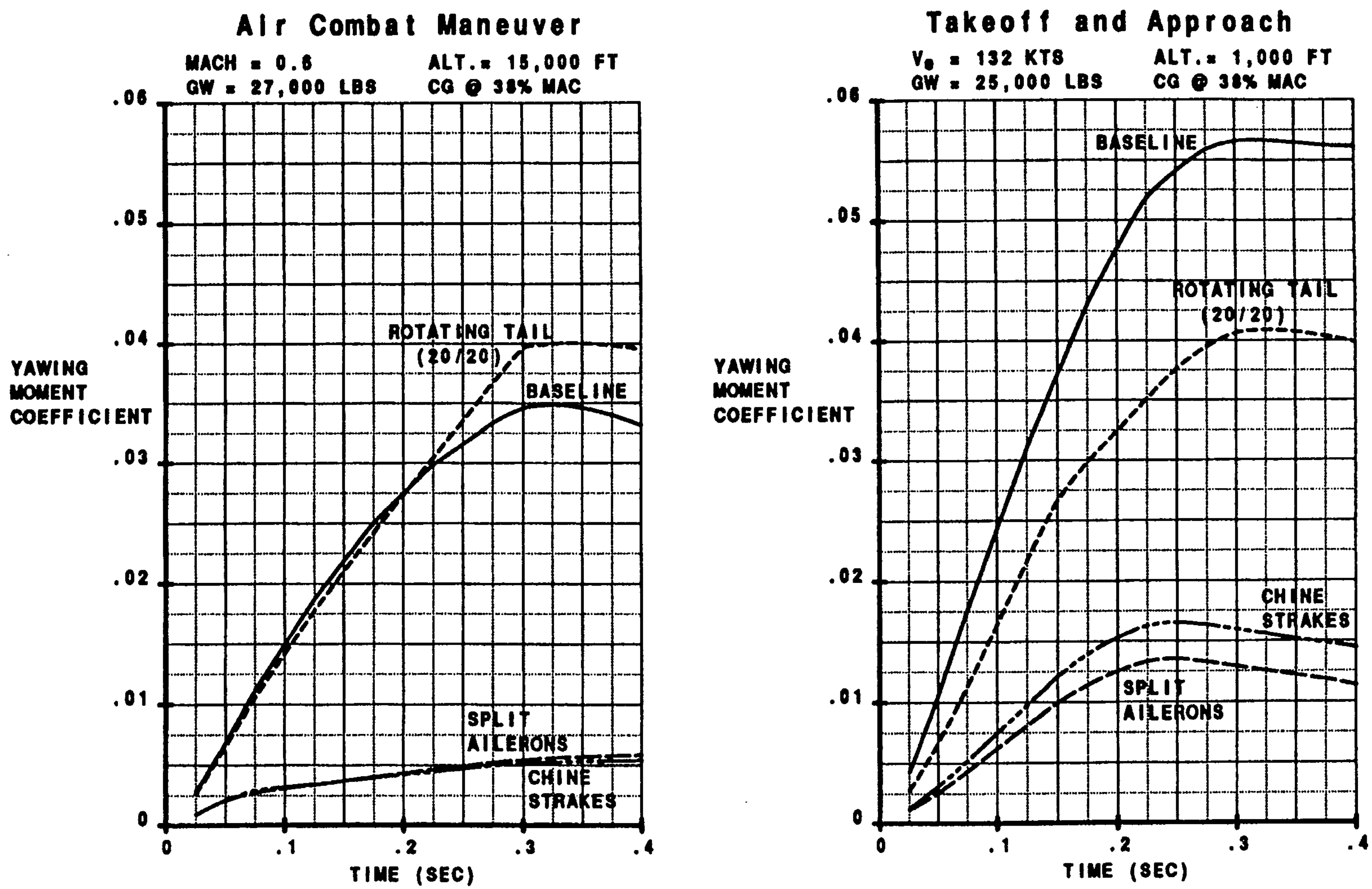

Figure B-16 Maximum Yawing Moment Coefficient Due to Controls

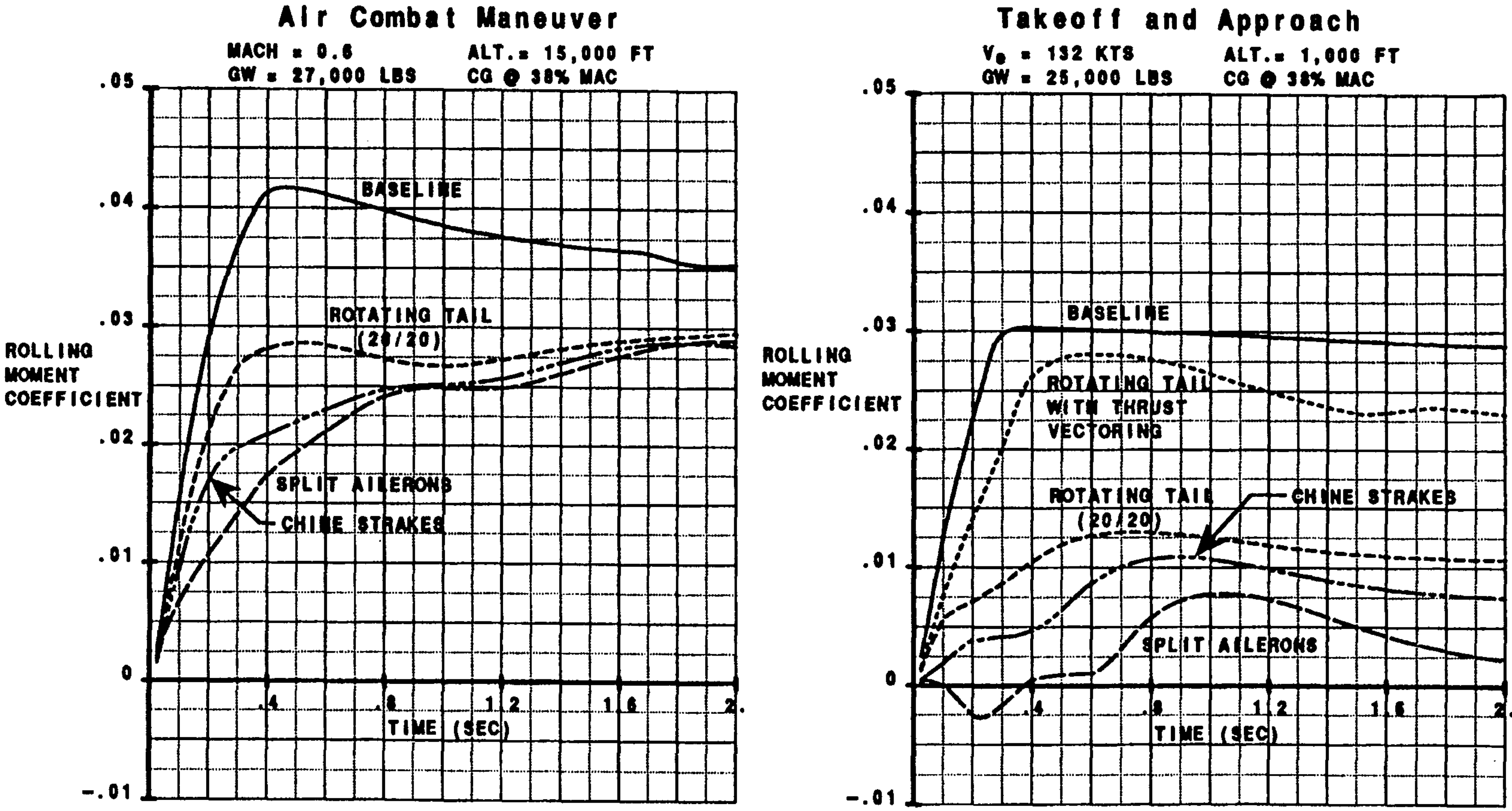

//fred/home/dawdy/
max_roll_control.esb
#MAX_ROLL_CONTOL – ORAL_REVIEW.plb

Figure B-17 Maximum Rolling Moment Coefficient Due to Controls

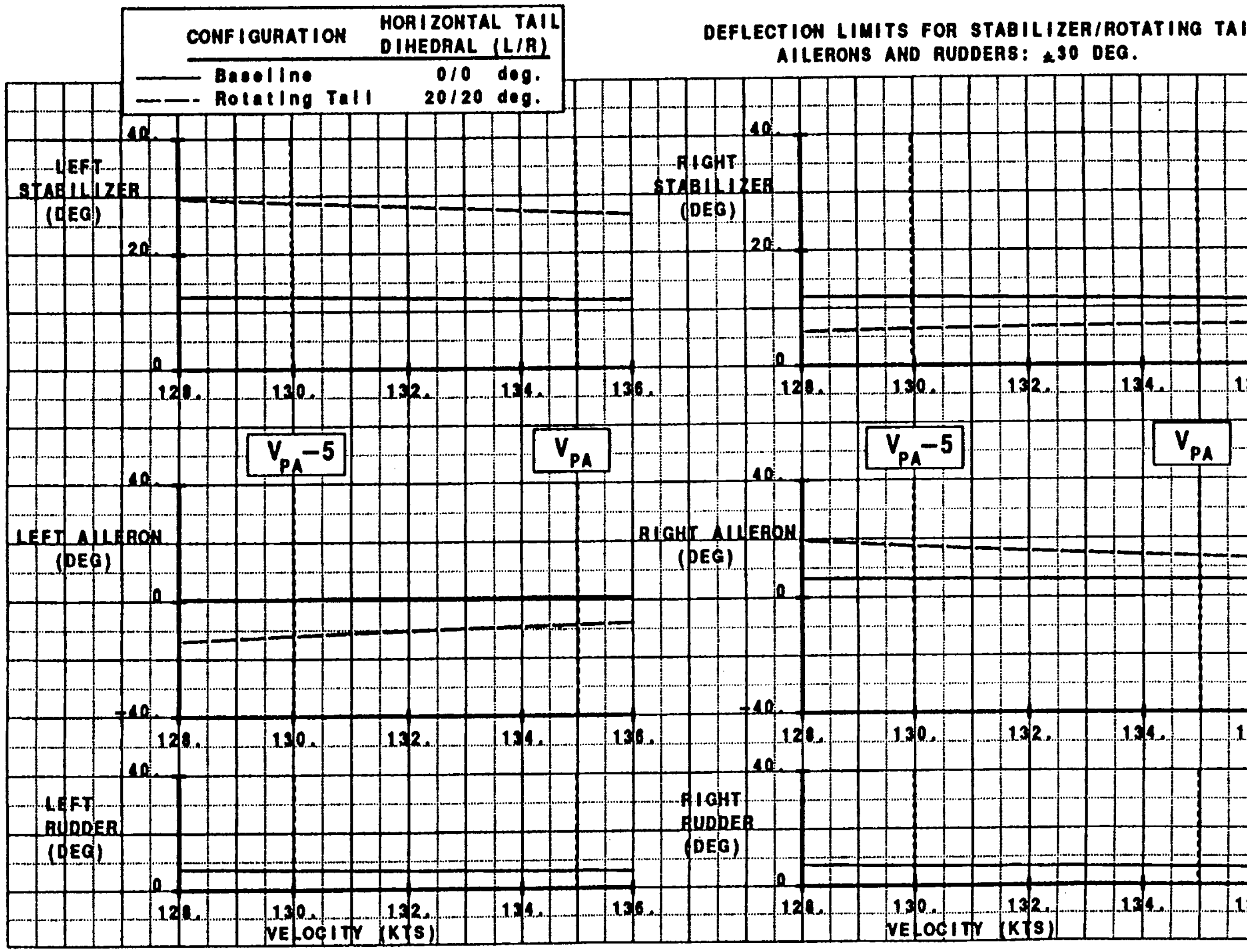

Figure B-18 V_{mc} with Right Engine Out

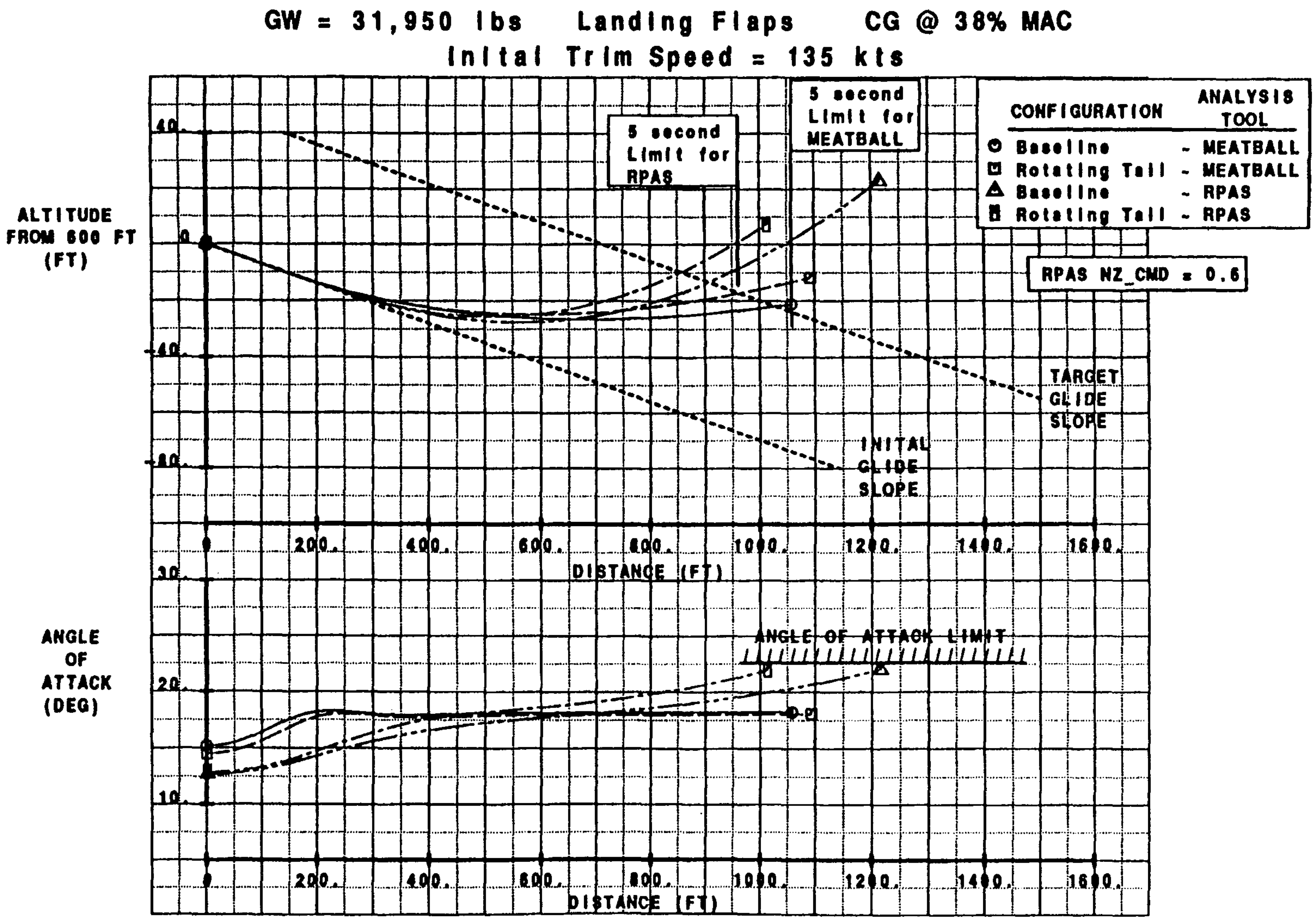

Figure B-19 Pop-Up Maneuver-Simulation Comparison

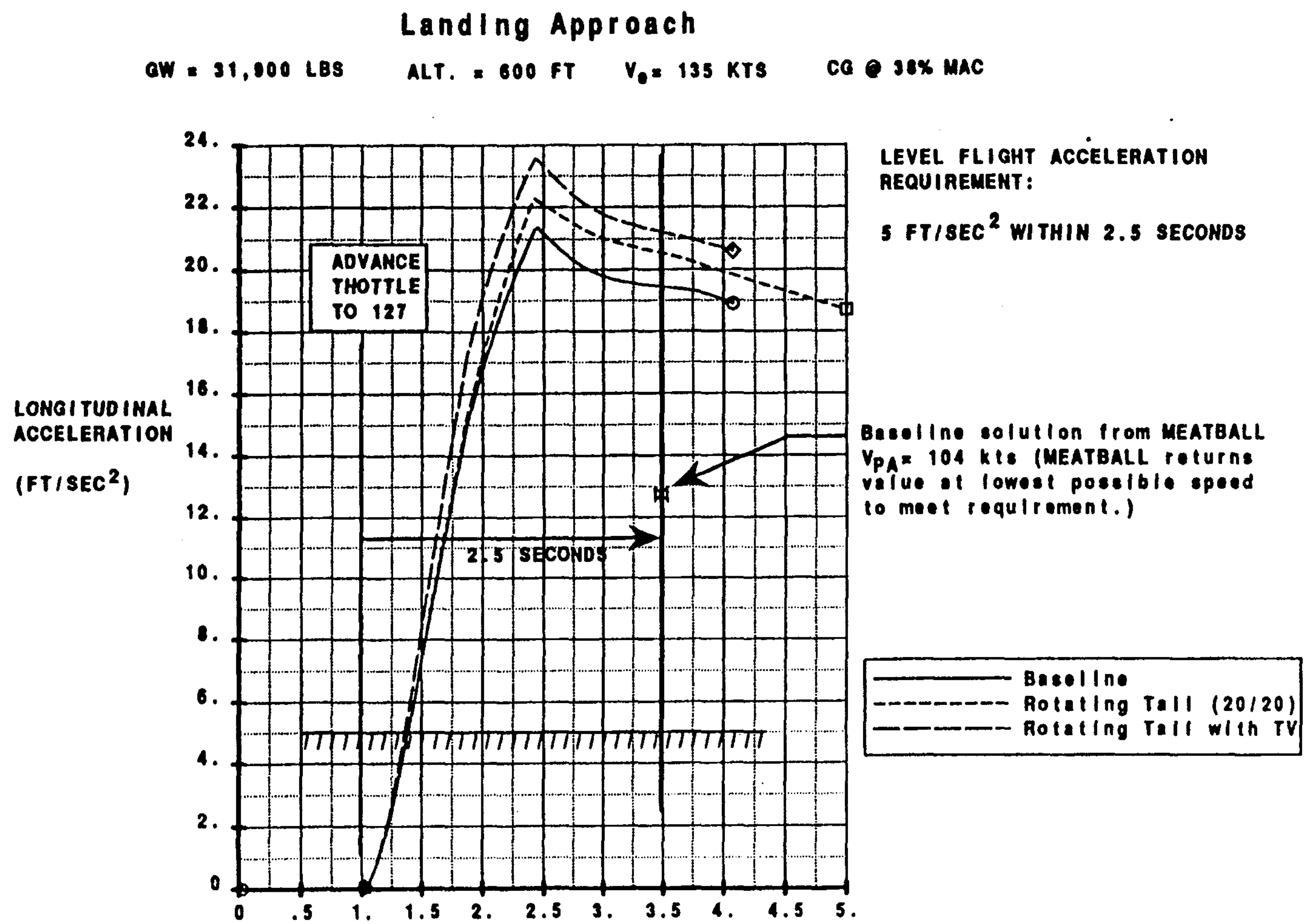

Figure B-20 Level Flight Longitudinal Acceleration

GW = 25,000 lbs   Alt. = 1,000 ft V_e = 132 kts   CG @ 33% mac

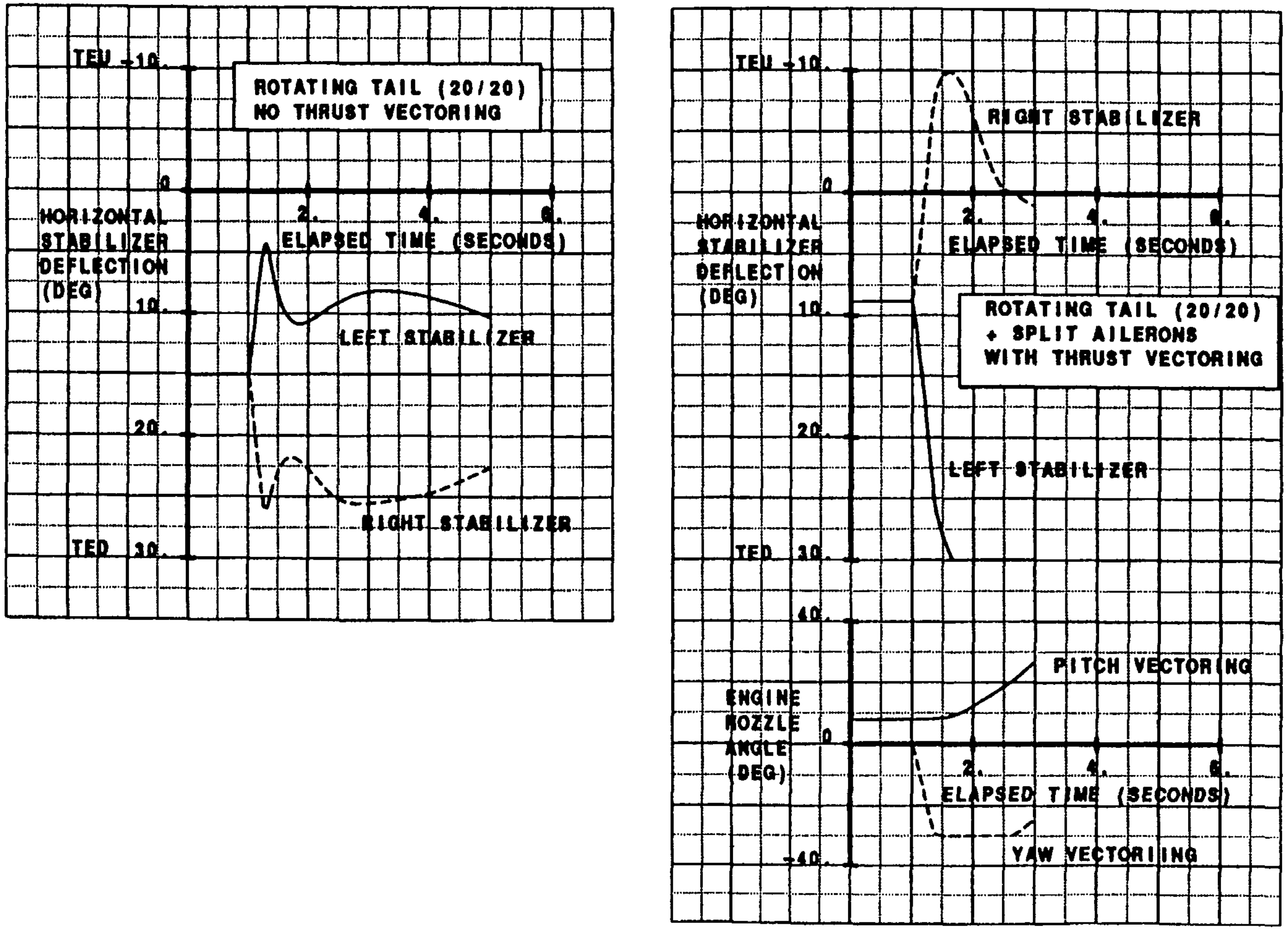

Figure B-21 Roll Control Effectiveness Landing Approach

GW = 25,000 lbs   Alt. = 1,000 ft V_e = 132 kts   CG @ 33% mac

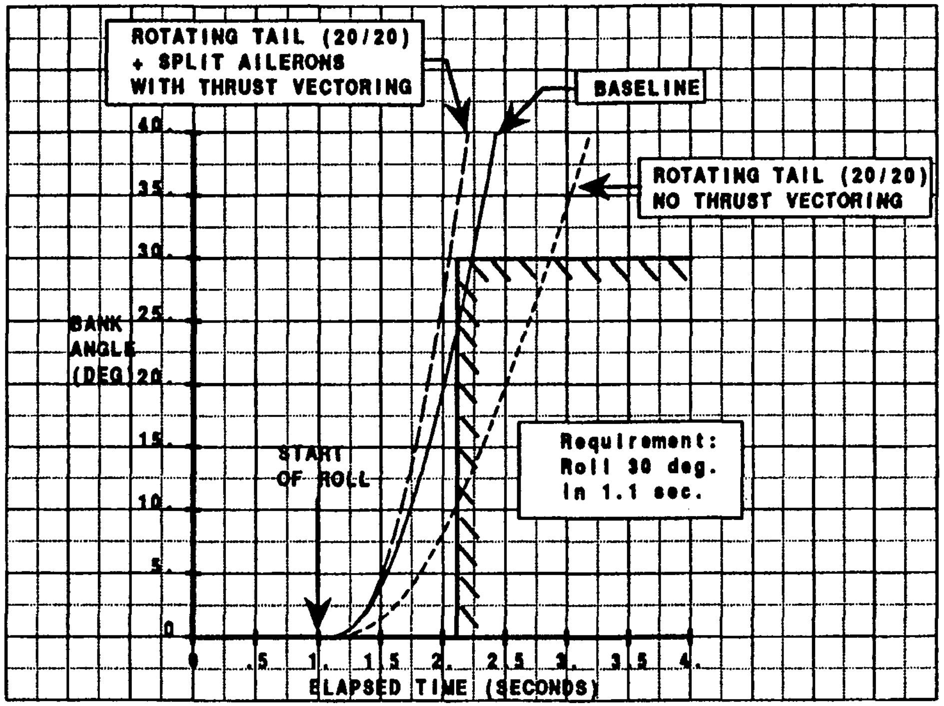

Figure B-22 Roll Control Effectiveness Landing Approach-Thrust Vectoring

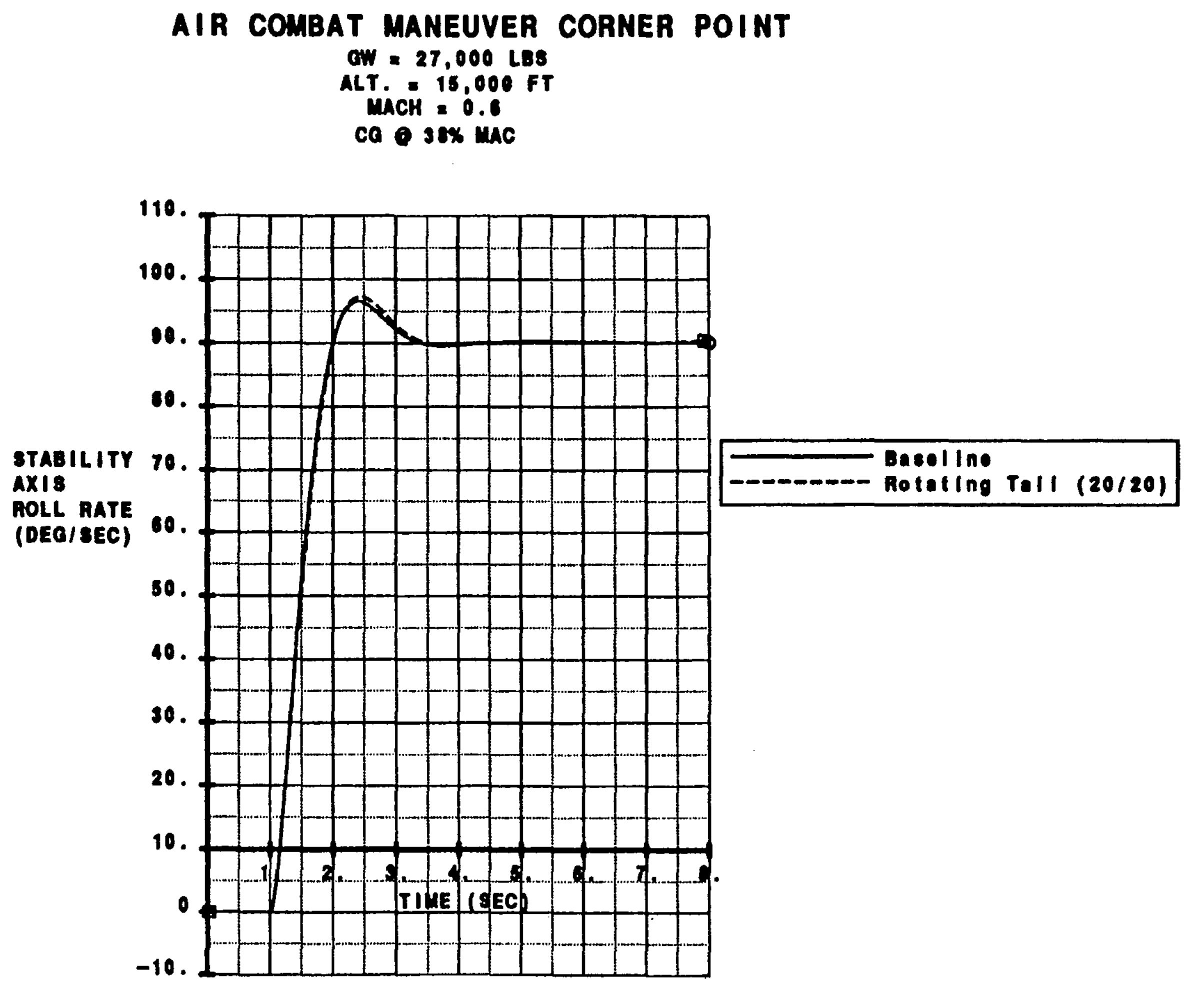

Figure B-23 Roll Rate Oscillations

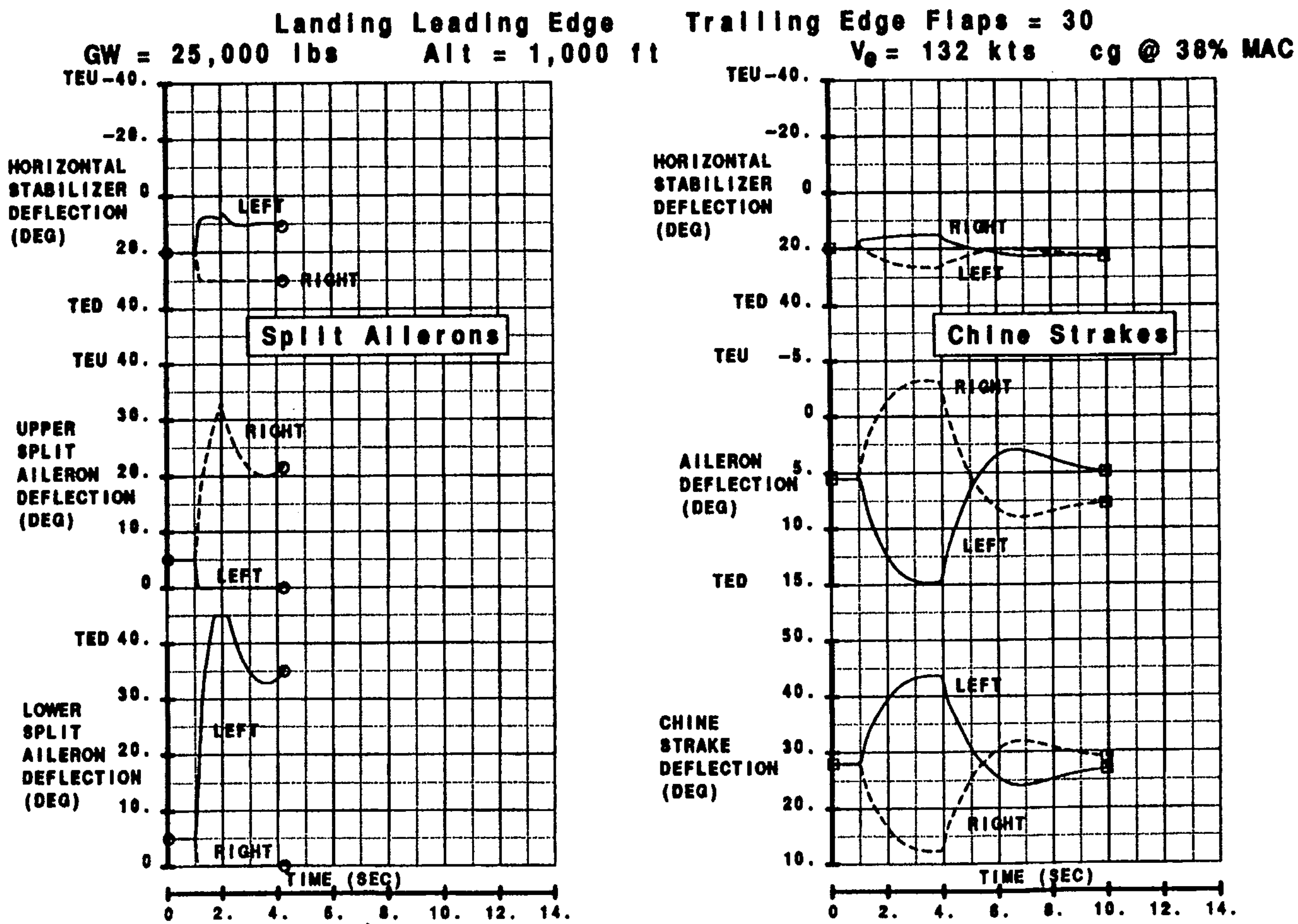

Coordinated Turn Entry for Landing Approach

Figure B-24 30 Degree Bank Control Surface Response-Ailerons, Strakes

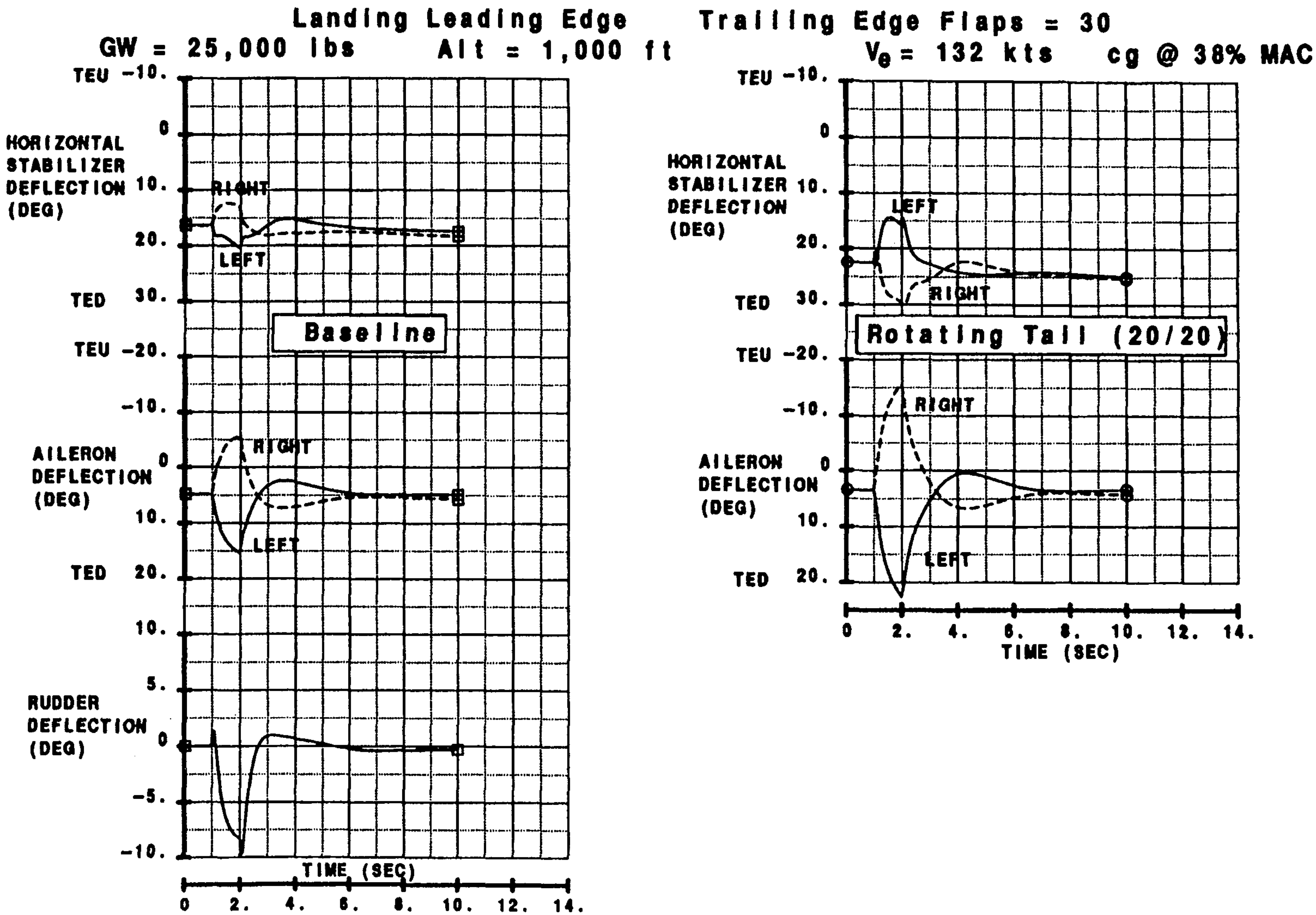

Coordinated Turn Entry for Landing Approach

Figure B-25 30 Degree Bank Control Surface Response-Rotating Tail

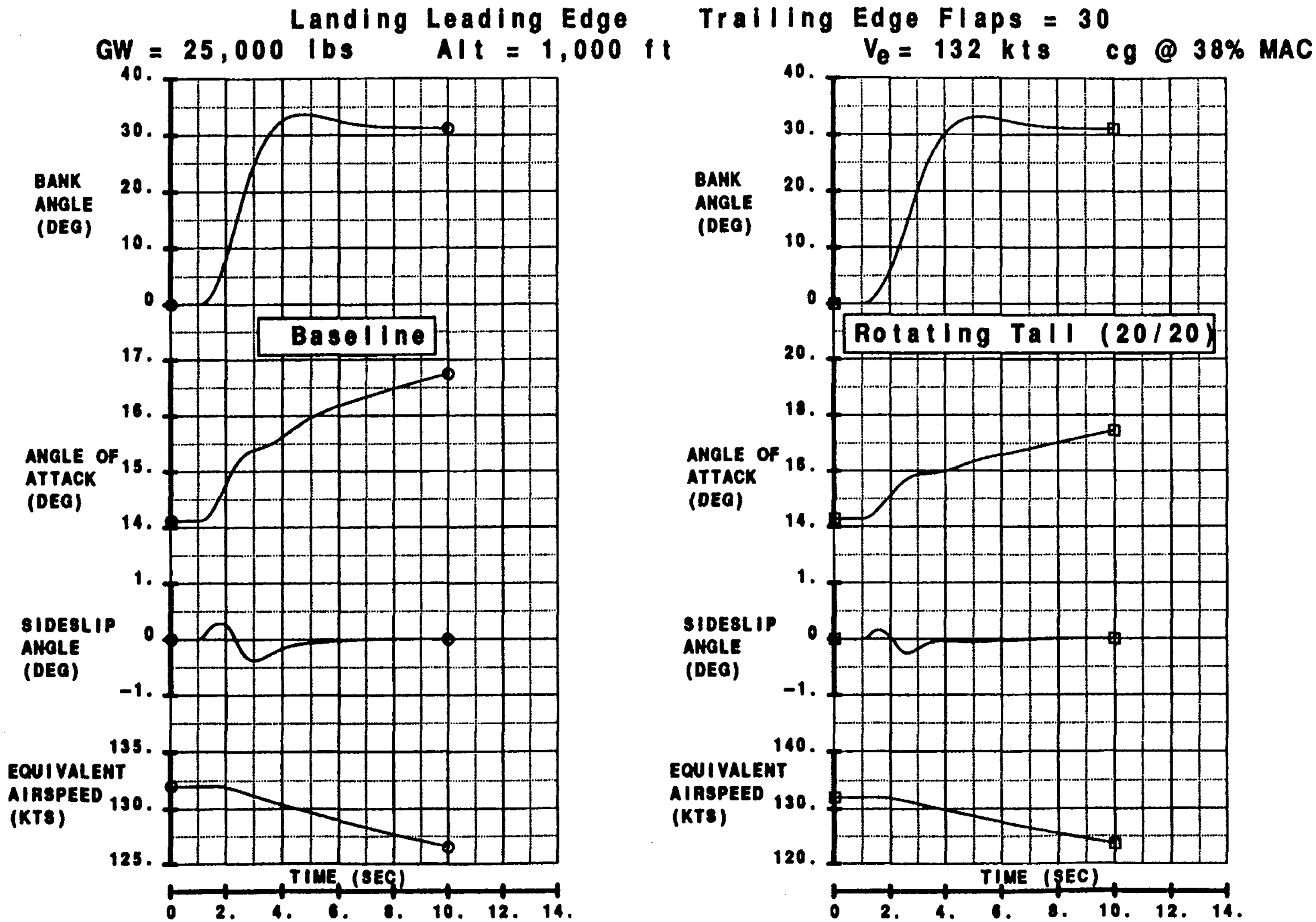

Coordinated Turn Entry Landing Approach

Figure B-26 30 Degree Bank Vehicle Response-Rotating Tail

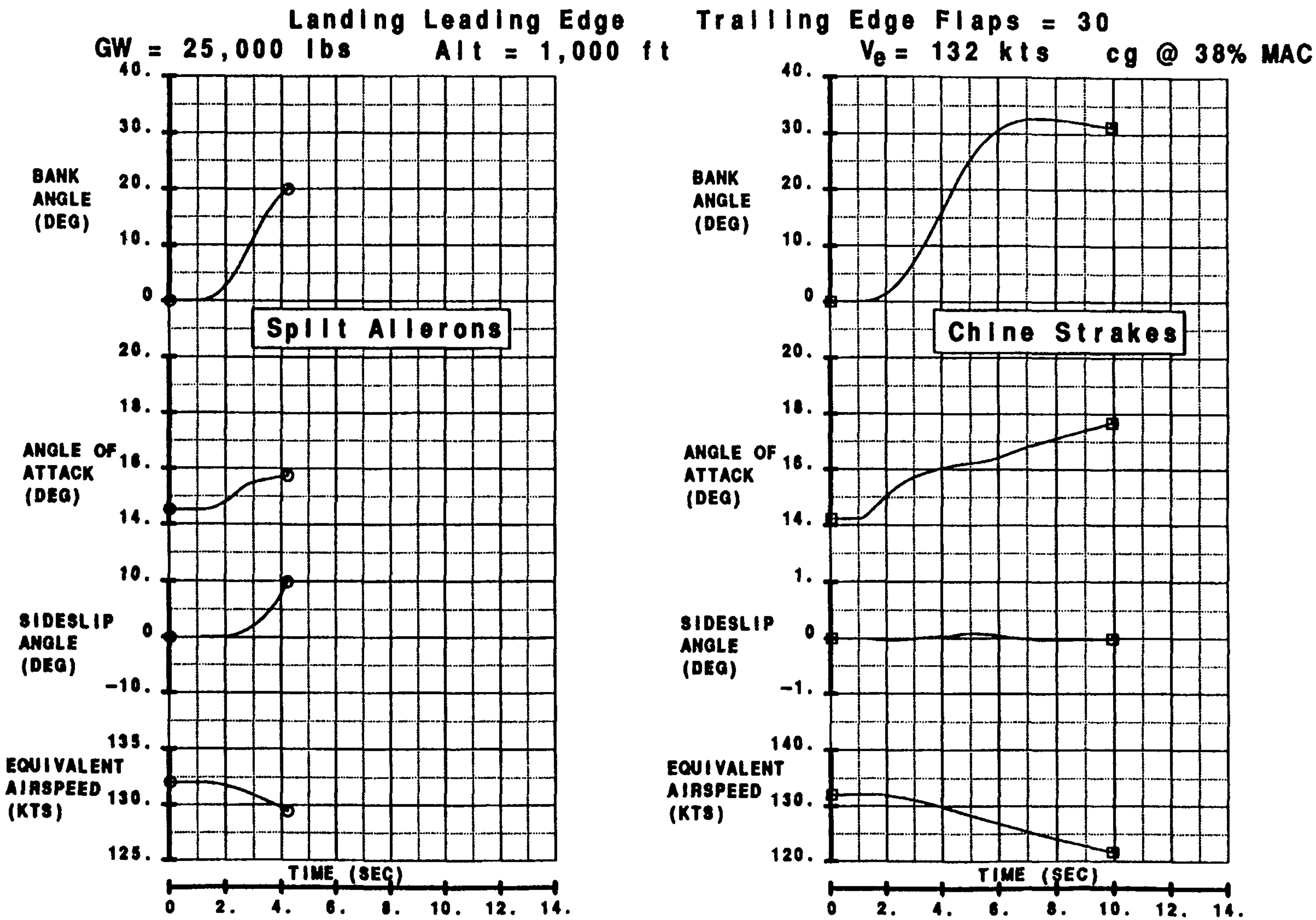

Coordinated Turn Entry Landing Approach

Figure B-27 30 Degree Bank Vehicle Response - Ailerons, Strakes

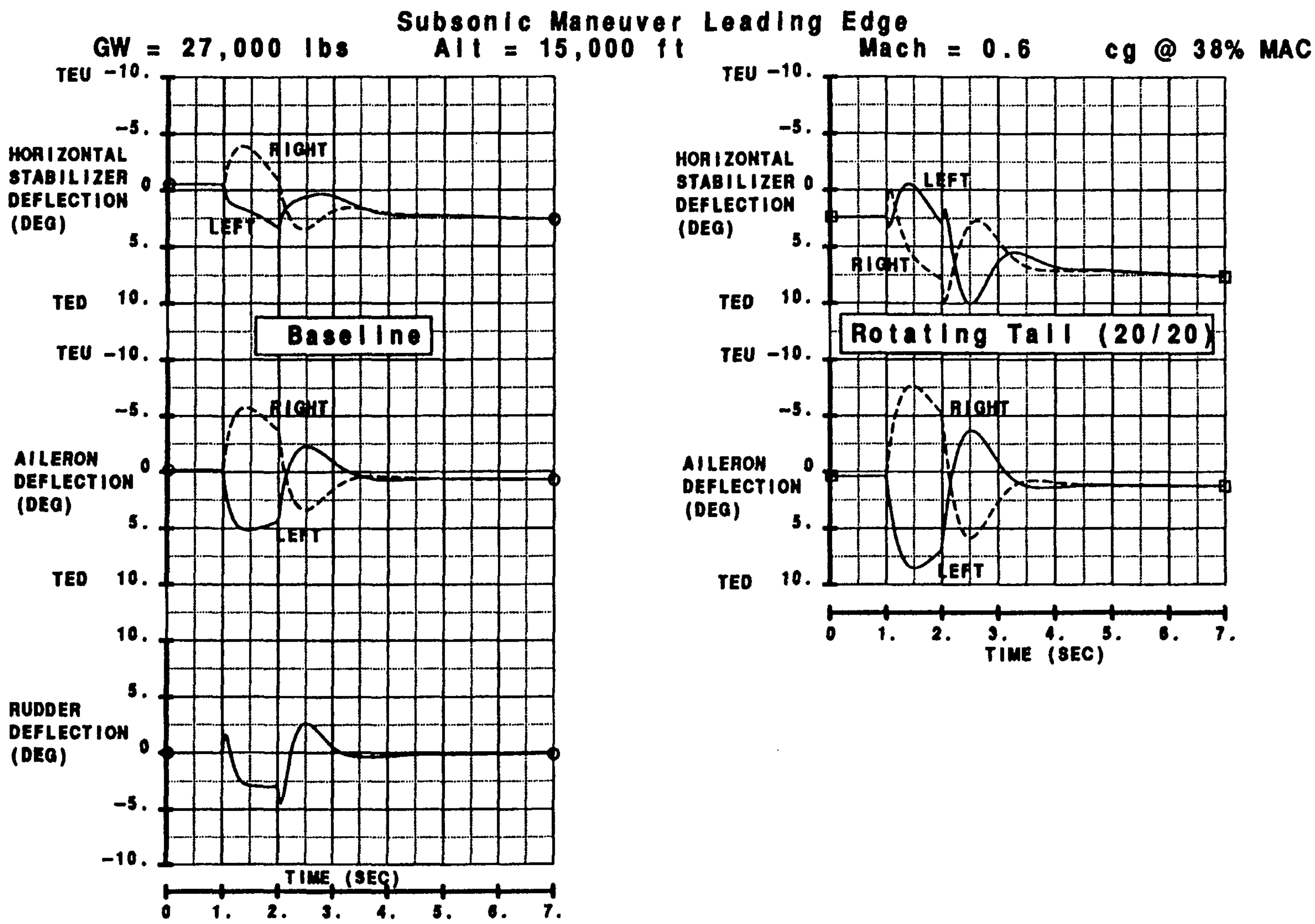

Air Combat Maneuver Corner Speed

Figure B-28 2-g Coordinated Turn Entry Control Surface Response

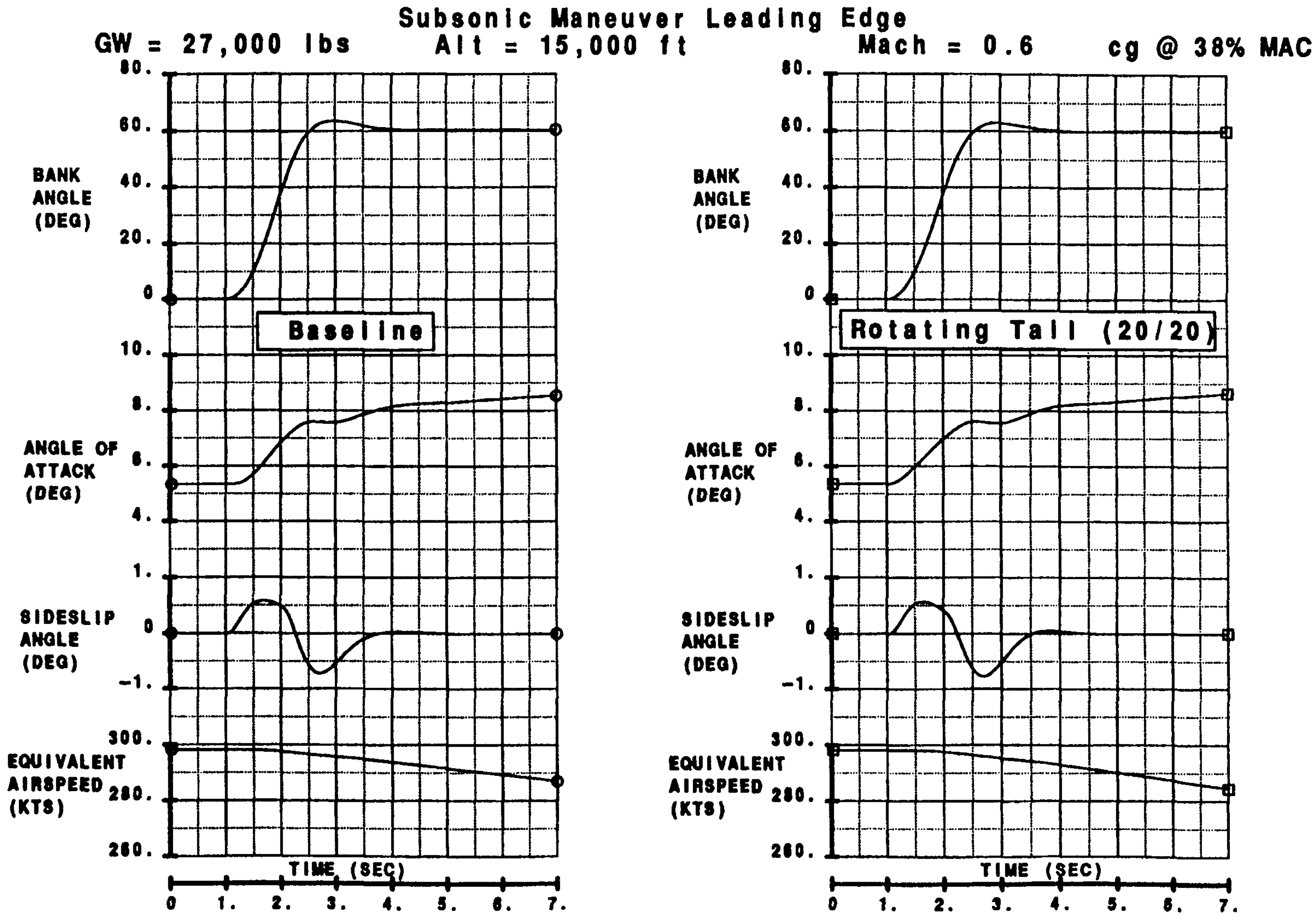

Air Combat Maneuver Corner Speed

Figure B-29 2-g Coordinated Turn Entry Vehicle Response-Rotating Tail

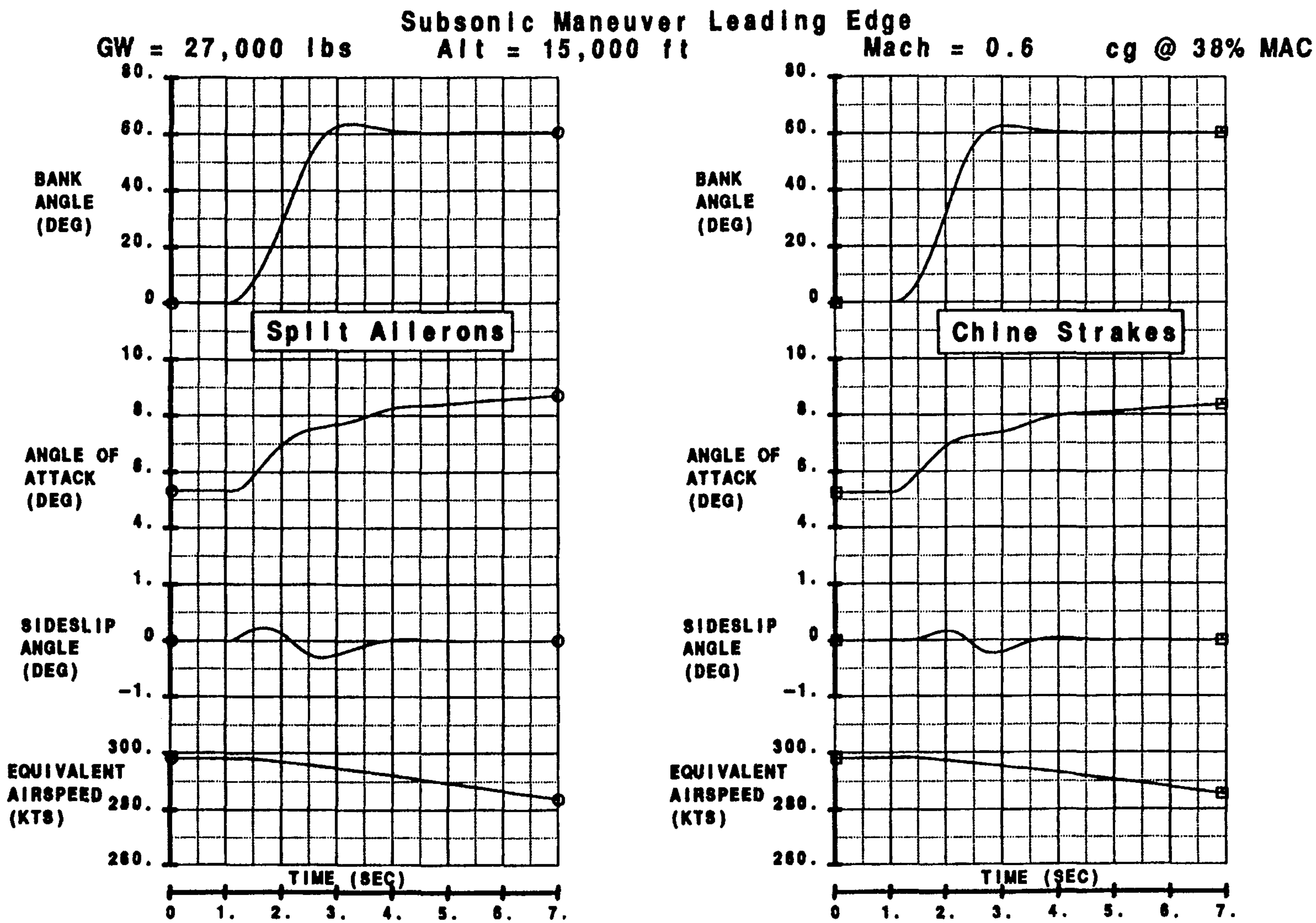

Air Combat Maneuver Corner Speed

Figure B-30 2-g Coordinated Turn Entry Vehicle Response-Ailerons, Strakes

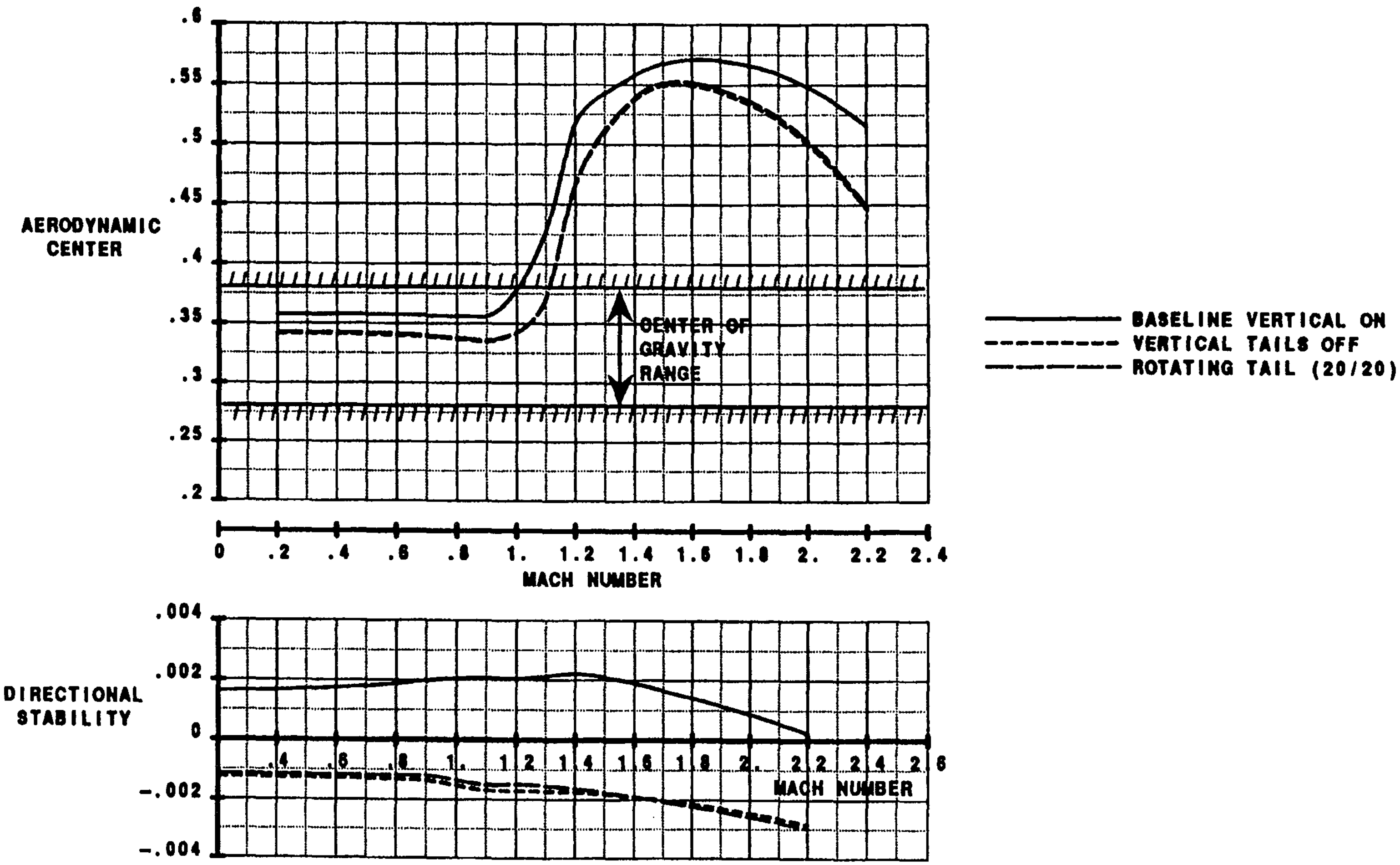

Figure B-31 Longitudinal and Directional stability Levels

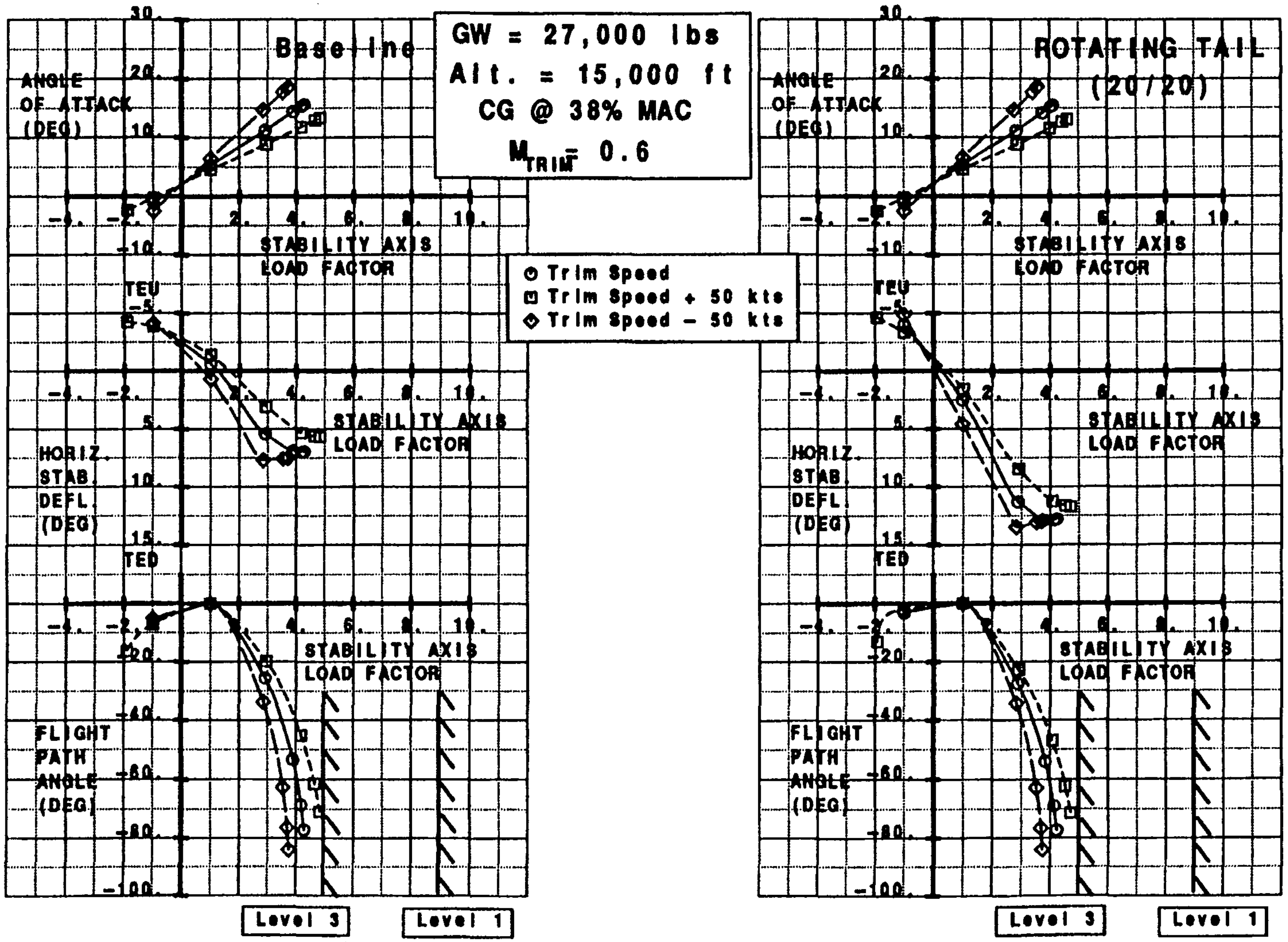

Air Combat Maneuver Corner Point

Figure B-32 Longitudinal Control in Maneuvering Flight

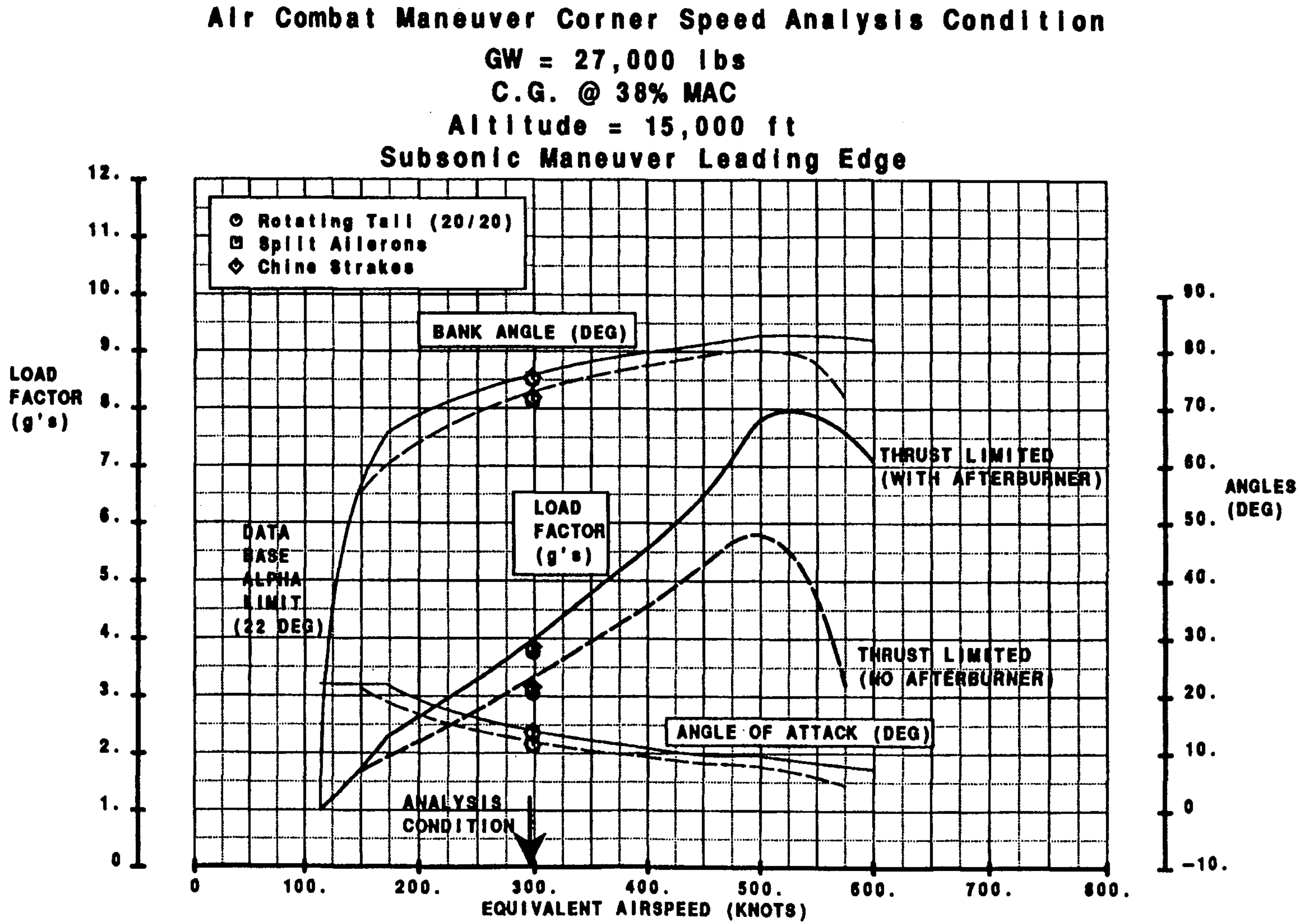

Model -24F Capability in Coordinated Turns

Figure B-33 Maximum Sustained load Factor at Mid Altitude

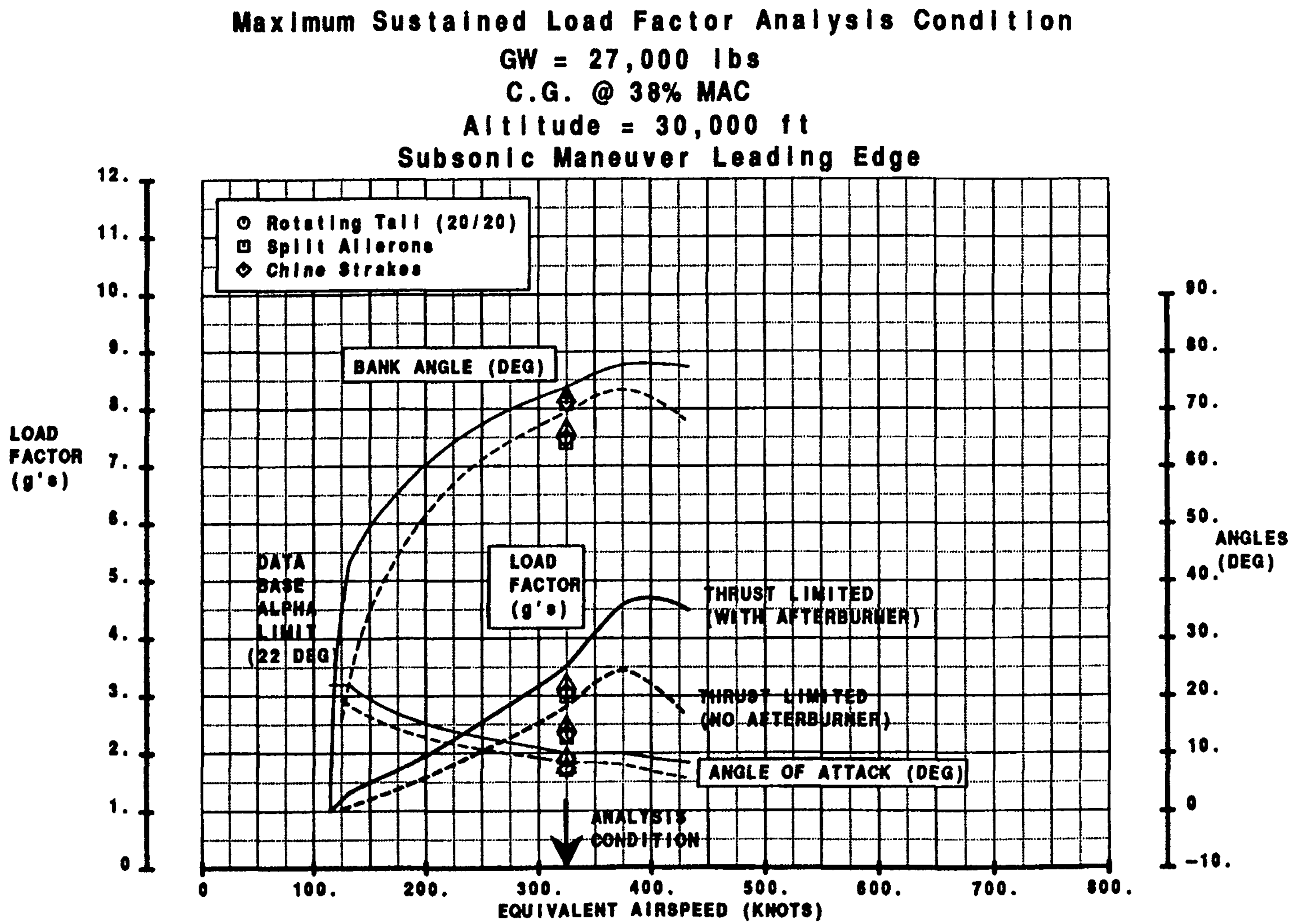

Model -24F Capability in Coordinated Turns

Figure B-34 Maximum Sustained Load Factor at High Altitude-Subsonic

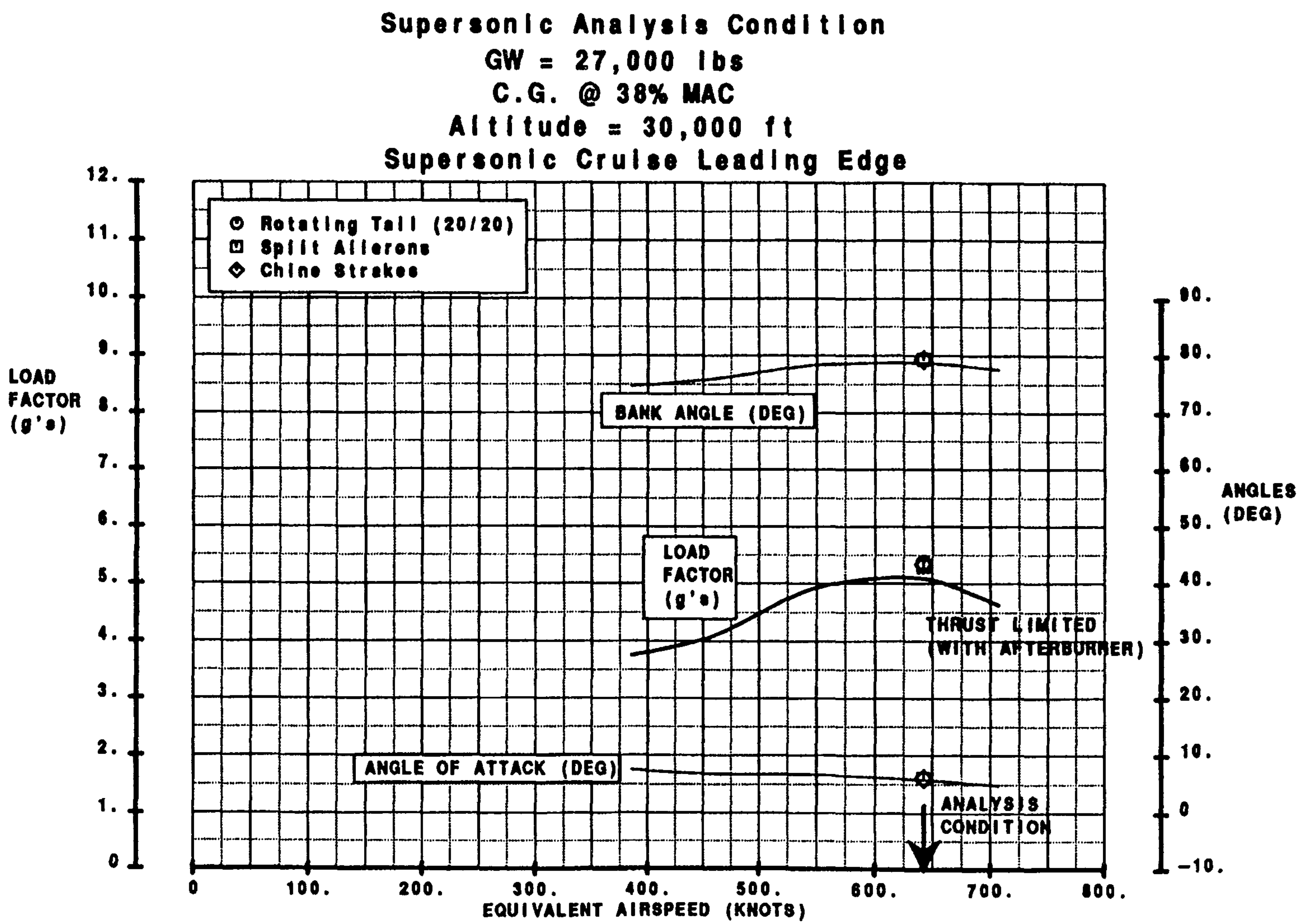

Model -24F Capability in Coordinated Turns
Figure B-35 Maximum Sustained Load Factor at High Altitude-Super Sonic Penetration

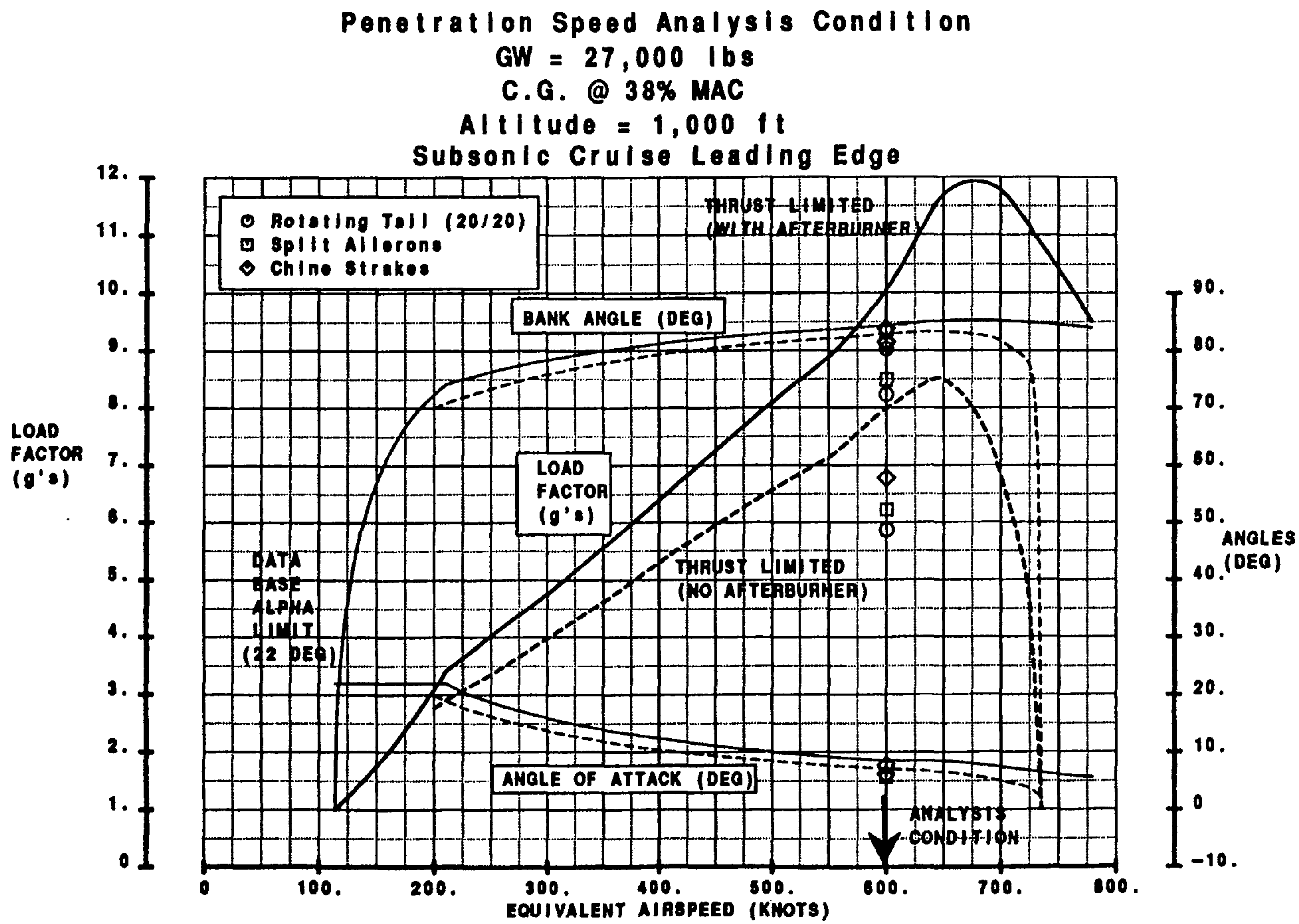

Model -24F Capability in Coordinated Turns
Figure B-36 Maximum Sustained Load Factor Penetration

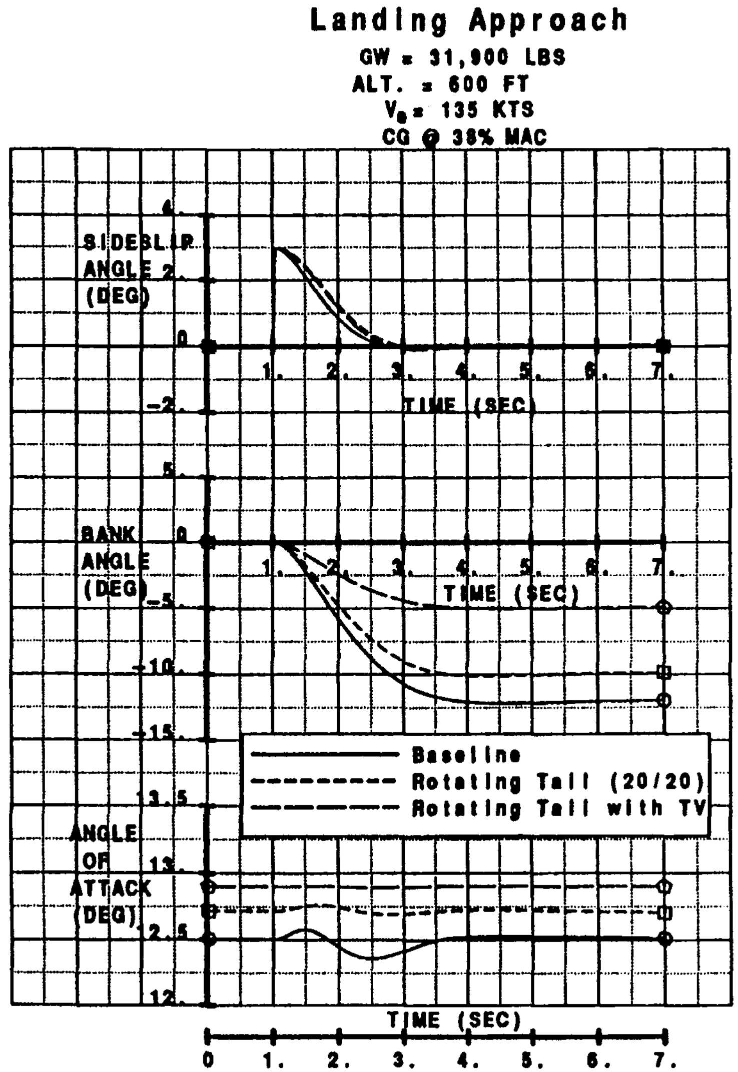

Figure B-37 Dutch Roll Characteristics

Horizontal and Vertical Tail On

Mach = 0.05

Data Source: LaRC 12 ft Wind Tunnel Test (Oct/Nov 1991)

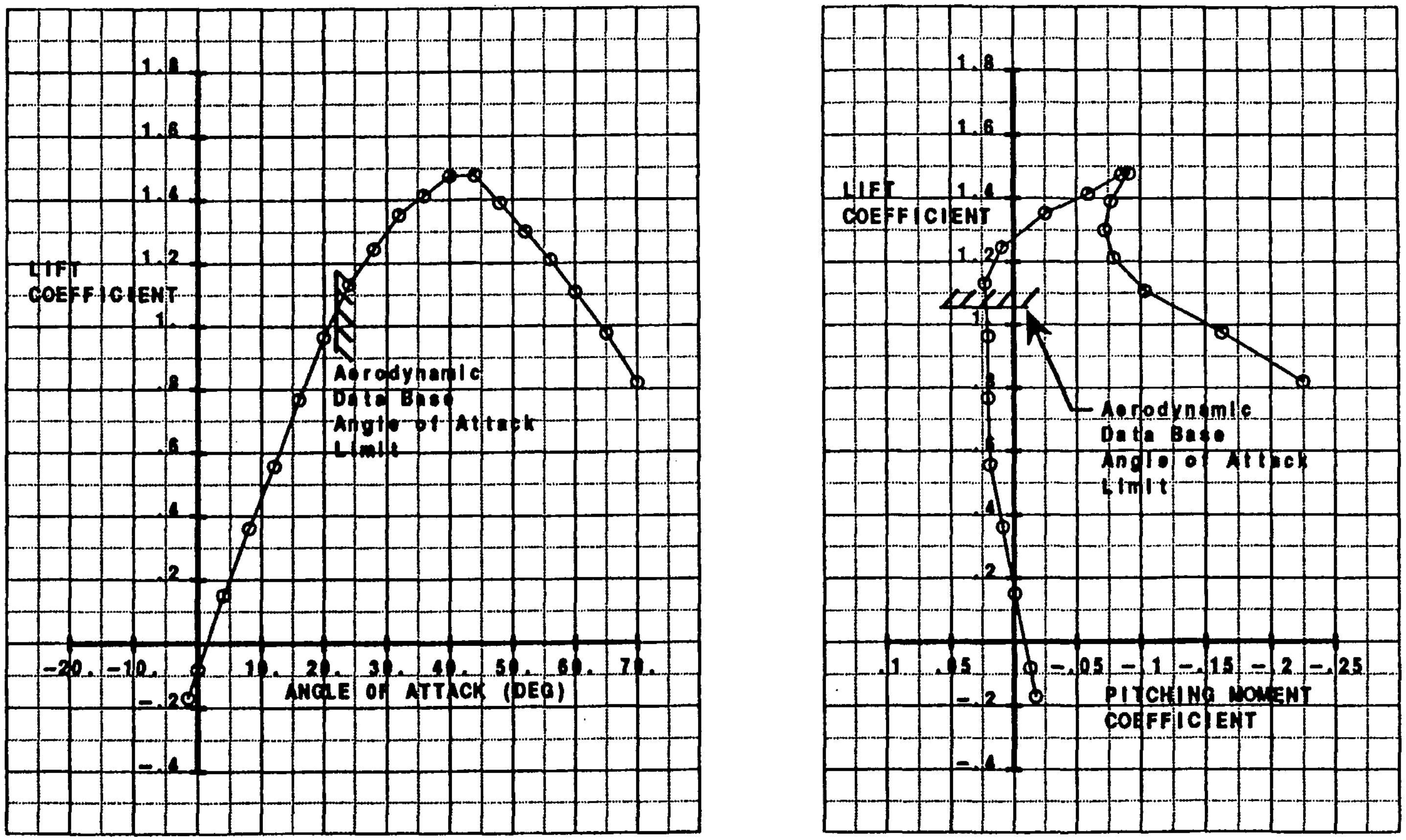

Figure B-38 Low Speed Lift and Pitching Moment Coefficients

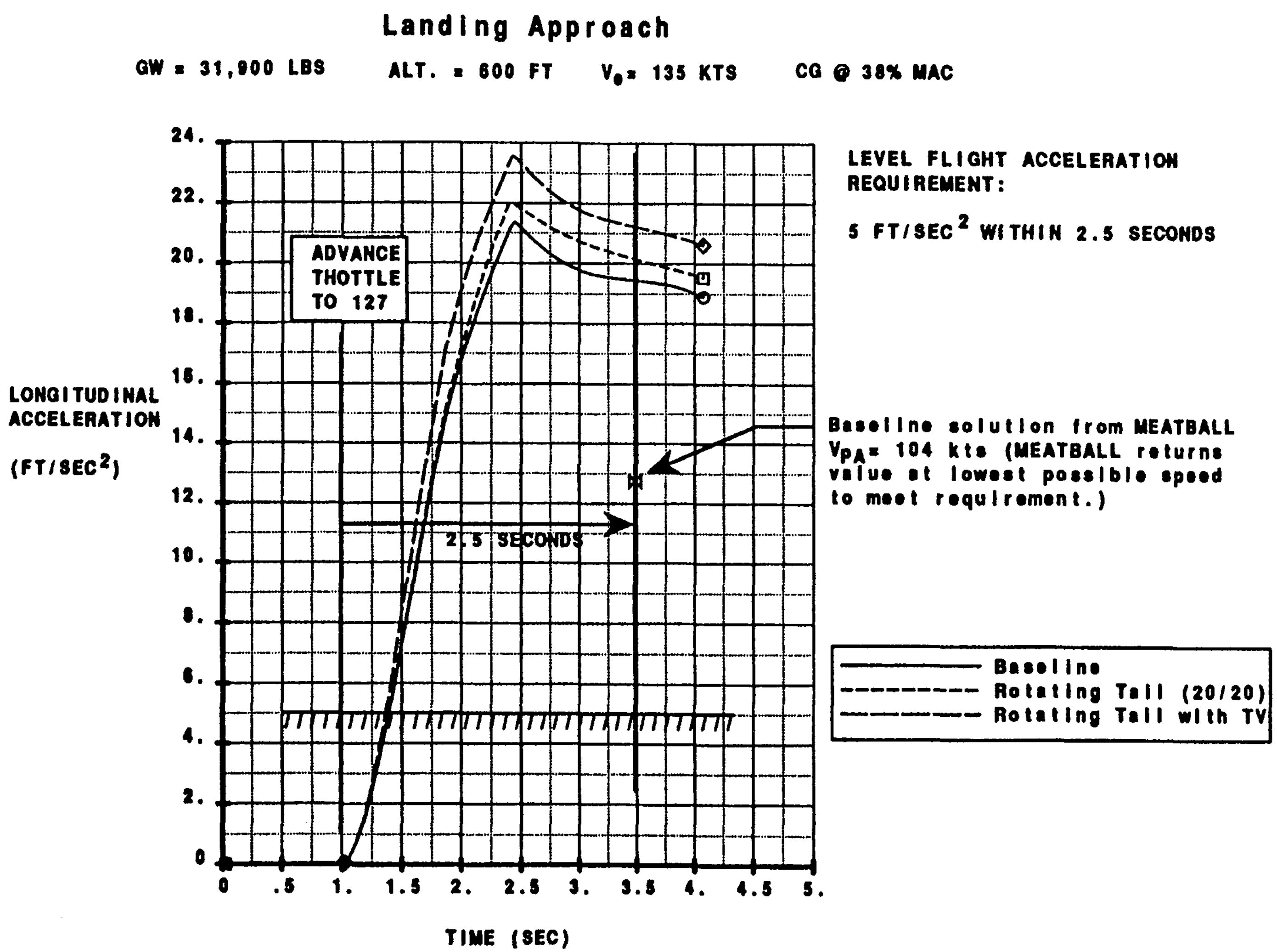

Figure B-39 Level Flight Longitudinal Acceleration

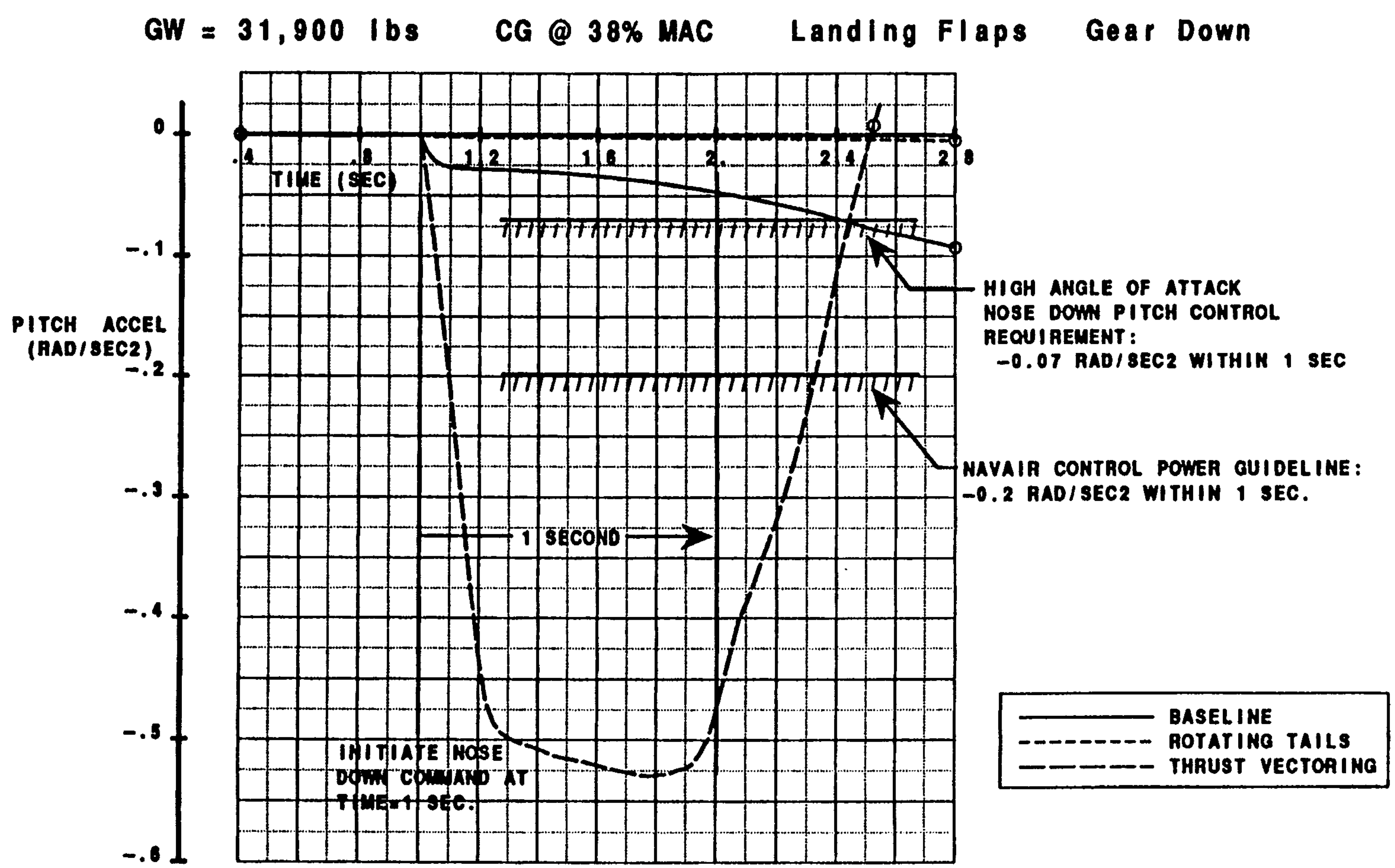

Maximum Data Base Angle of Attack
Figure B-40 Landing Approach Nose Down Pitch Acceleration

GW = 31,900 lbs   CG @ 38% MAC   Landing Flaps   Gear Down

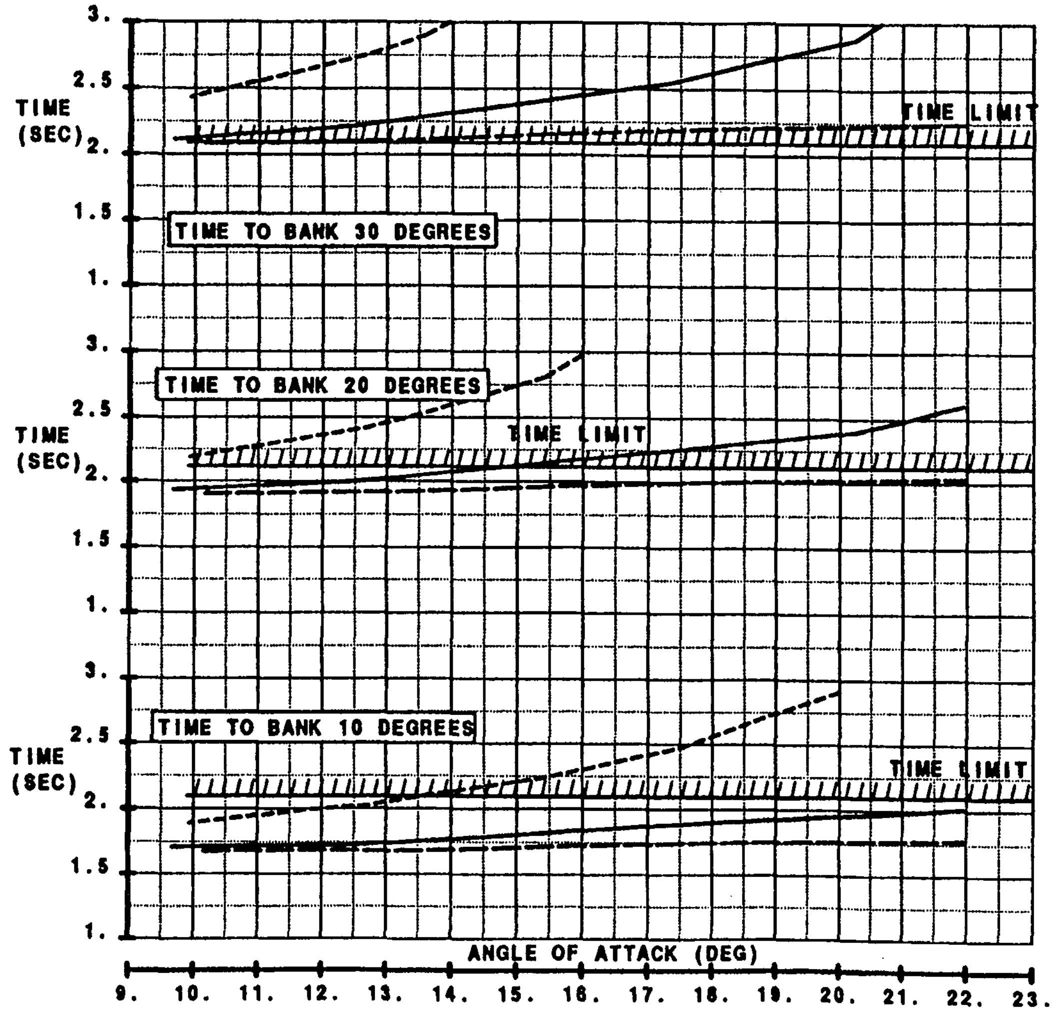

NOTE: ROLL COMMAND INITIATED AT TIME = 1 SEC. REQUIRED TO ACHIEVE BANK ANGLE WITHIN 1.1 SECONDS OF ROLL COMMAND.

CONFIGURATION	ALPHA APP VAPP= 130	ALPHA APP VAPP= 135
BASELINE	13.4	12.5
ROTATING TAILS	13.6	12.7
THRUST VECTORING	13.8	12.9

——— BASELINE
- - - - ROTATING TAILS
— — — THRUST VECTORING

Figure B-41 Carrier Suitability Roll Rate Summary

AIR COMBAT MANEUVER CORNER POINT

GW = 27,000 LBS

ALT. = 15,000 FT

MACH = 0.6

CG @ 38% MAC

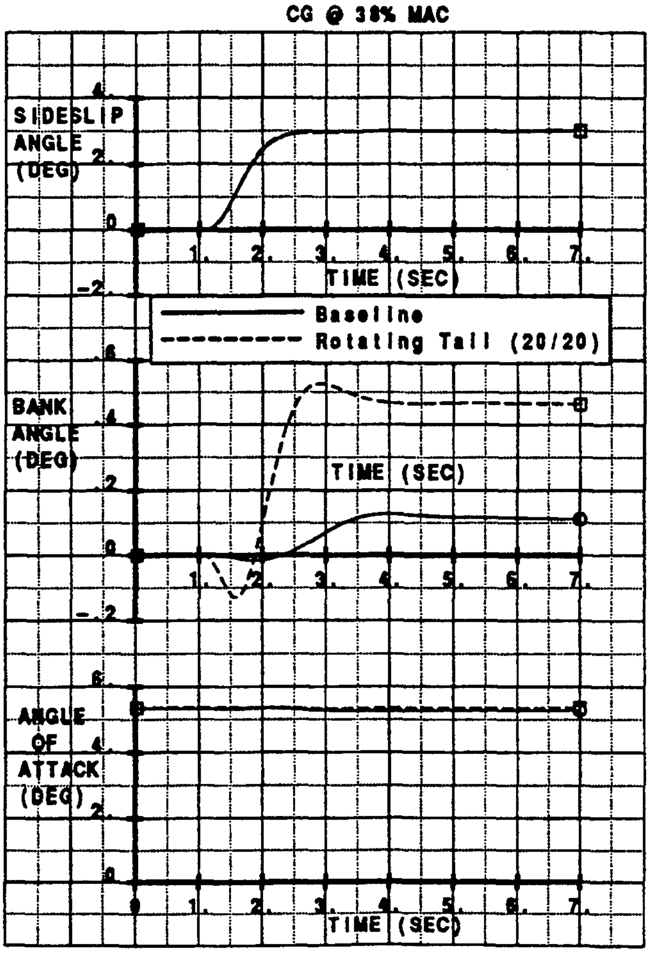

Figure B-42 Sideslip Angle Capture

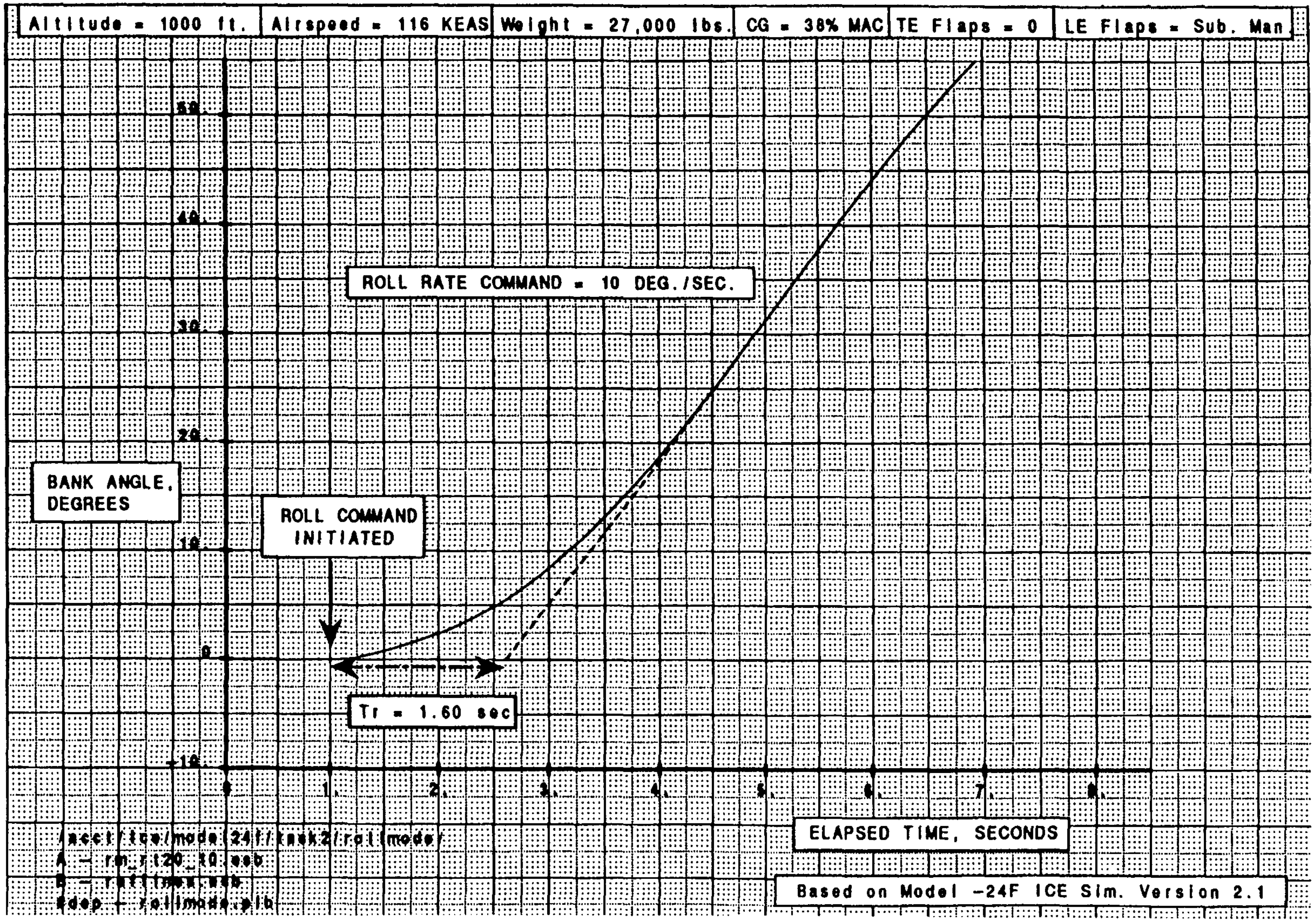

Figure B-43 Departure Stall-Roll Rate Time Constant

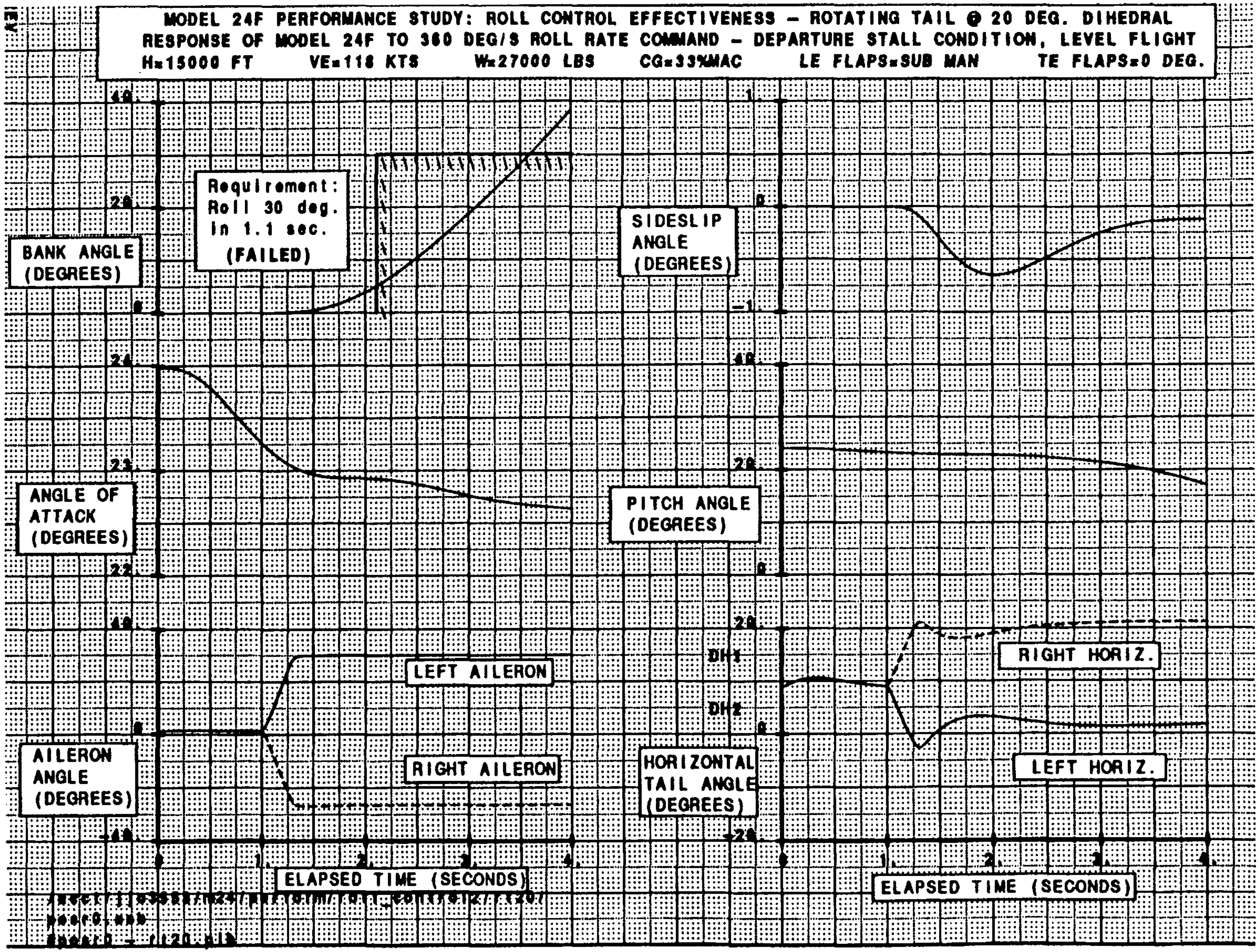

Figure B-44 Departure Stall-Roll Performance

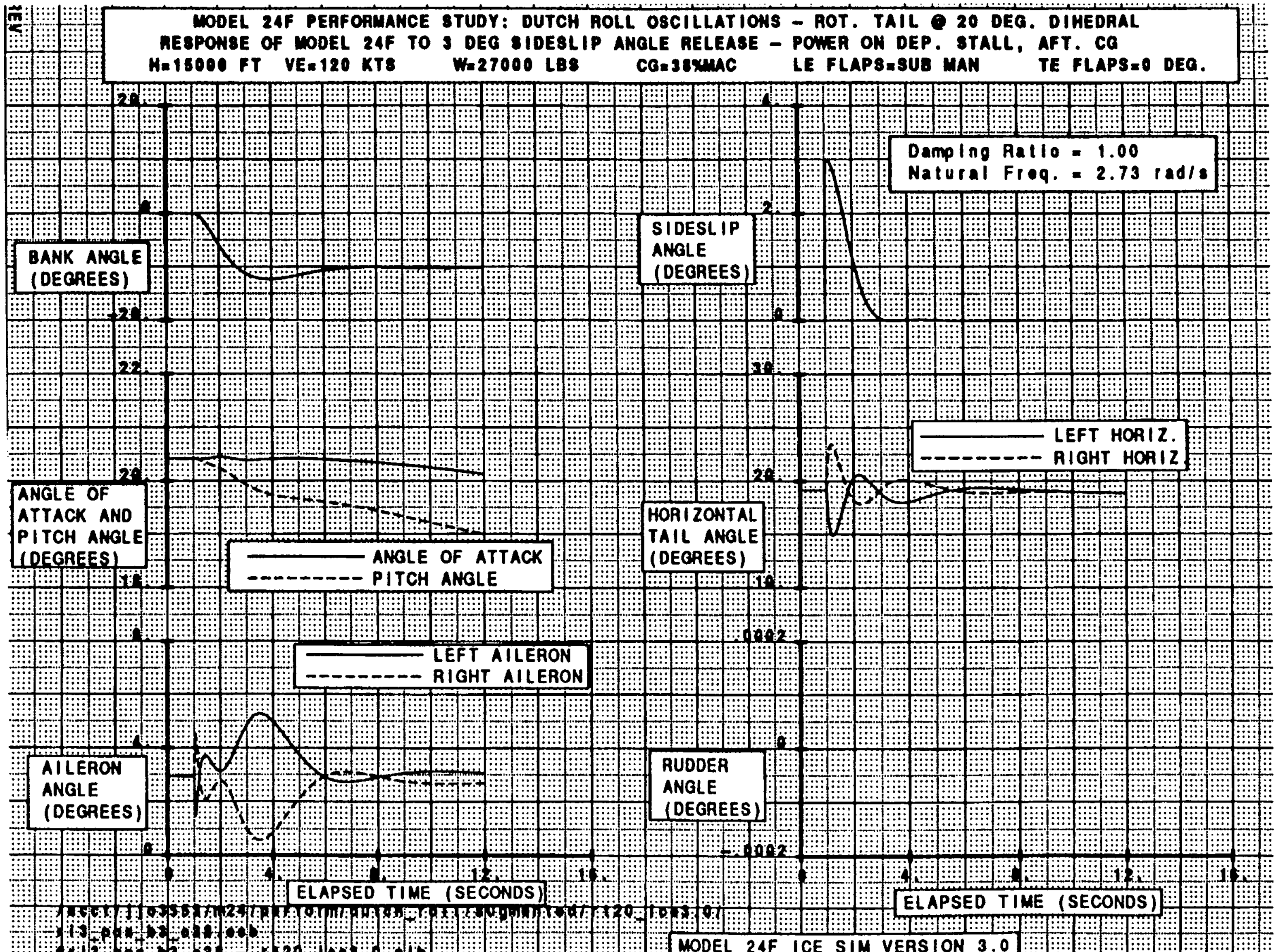

Figure B-45 Power on Departure Stall-Lateral-Directional Dynamics

APPENDIX C

Summary of Signature Data

Configurations are summarized as:

1) Baseline
2) Baseline with vertical tails removed
3) 2) with horizontal tails @ 20 degrees dihedral
4) 2) with nose strakes deployed
5) 2) with split ailerons deployed @ 45 degrees

Figure	Config.	Frequency ~ Ghz			Elevation ~ degrees		
		2	9	16	-30	0	+30
C.1	1		X			X	
C.2	2		X			X	
C.3	3		X			X	
C.4	4		X			X	
C.5	5		X			X	
C.6	1		X				X
C.7	2		X				X
C.8	3		X				X
C.9	1		X		X		
C.10	2		X		X		
C.11	3		X		X		
C.12	1	X				X	
C.13	2	X				X	
C.14	3	X				X	
C.15	1			X		X	
C.16	2			X		X	
C.17	3			X		X	

All figures include both horizontal and vertical polarization.

BaseLine Configuation

9.0 Ghz 0.0 Degrees elevation

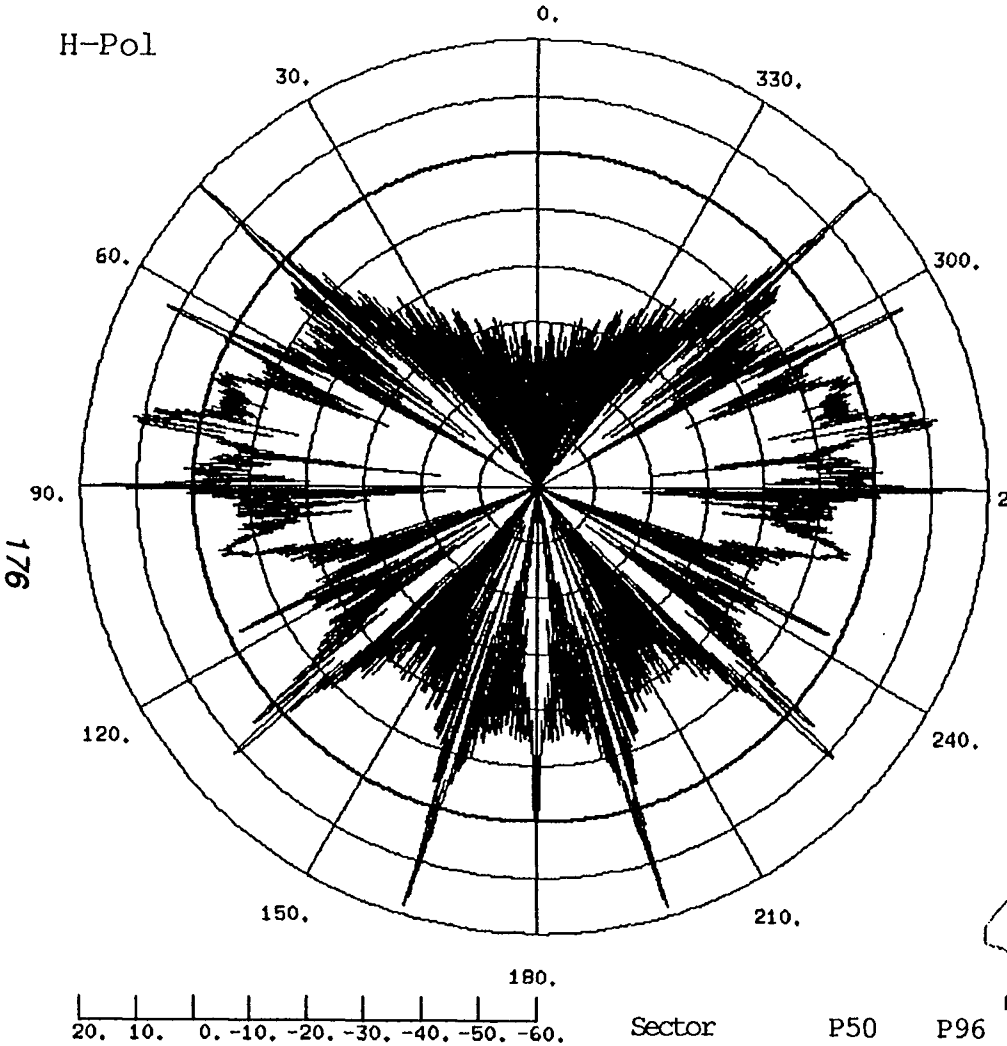

Sector		P50	P96
-30.0	30.0	-37.0	-31.5
60.0	120.0	-10.3	4.7
150.0	210.0	-10.3	4.7
240.0	300.0	-22.0	-1.1

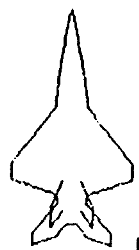

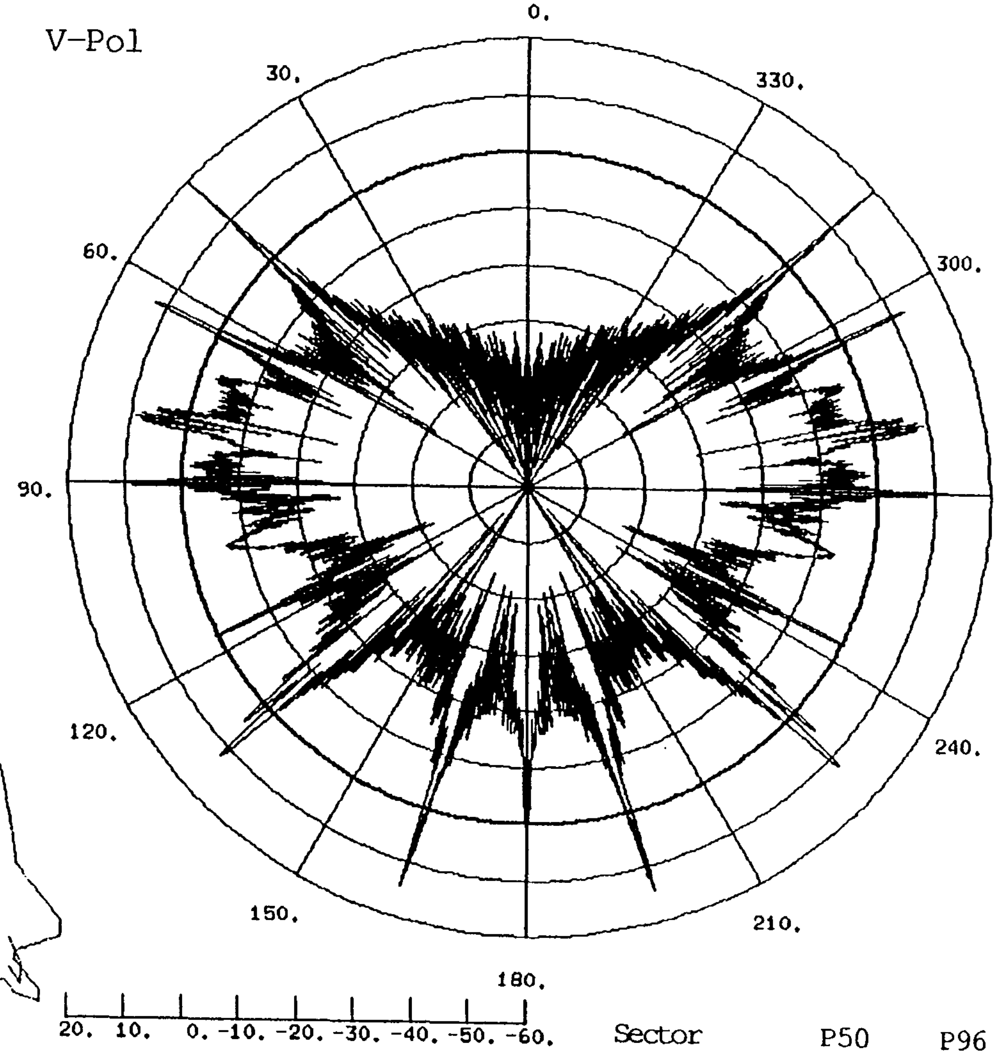

Sector		P50	P96
-30.0	30.0	-38.3	-31.6
60.0	120.0	-11.7	3.7
150.0	210.0	-11.7	3.7
240.0	300.0	-22.4	-1.6

Figure C-1

BaseLine Configuation

Vertical Tails Removed

9.0 Ghz 0.0 Degrees elevation

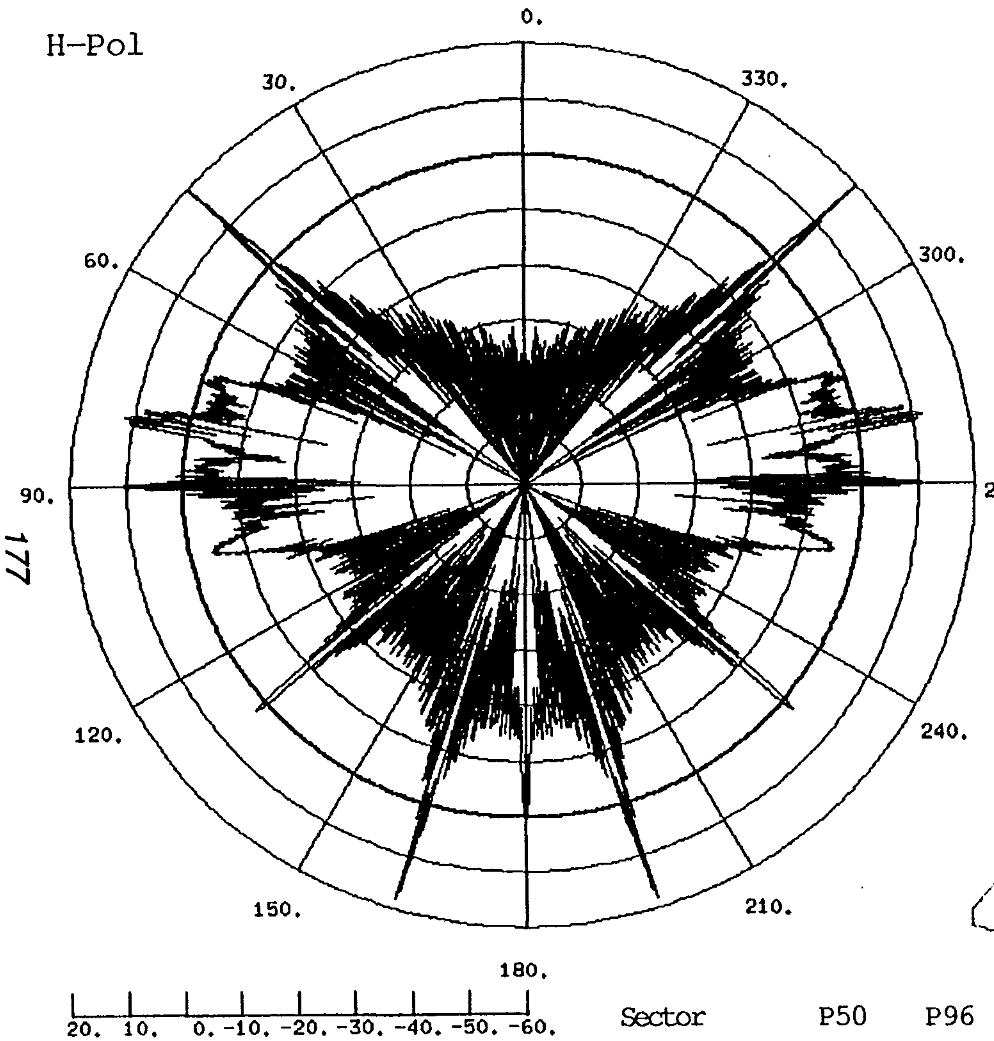

Sector		P50	P96
-30.0	30.0	-40.4	-31.5
60.0	120.0	-11.7	4.0
150.0	210.0	-11.7	4.0
240.0	300.0	-23.0	-1.0

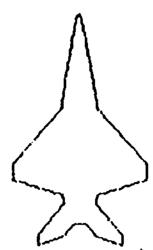

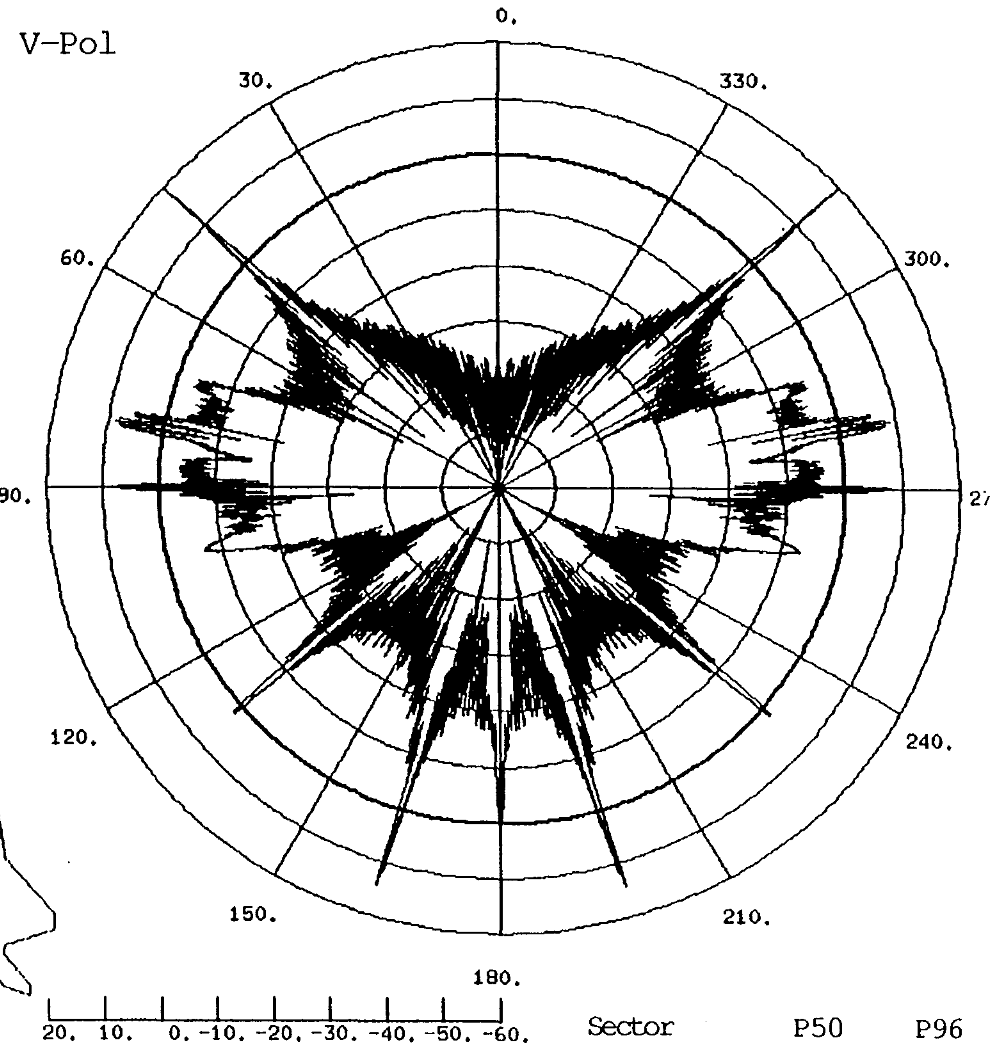

Sector		P50	P96
-30.0	30.0	-40.5	-34.1
60.0	120.0	-14.2	1.2
150.0	210.0	-14.2	1.2
240.0	300.0	-23.0	-1.5

Figure C-2

BaseLine Configuation

Vertical Tails Removed & Aft Wings @ +20 Dihedral

9.0 Ghz   0.0 Degrees elevation

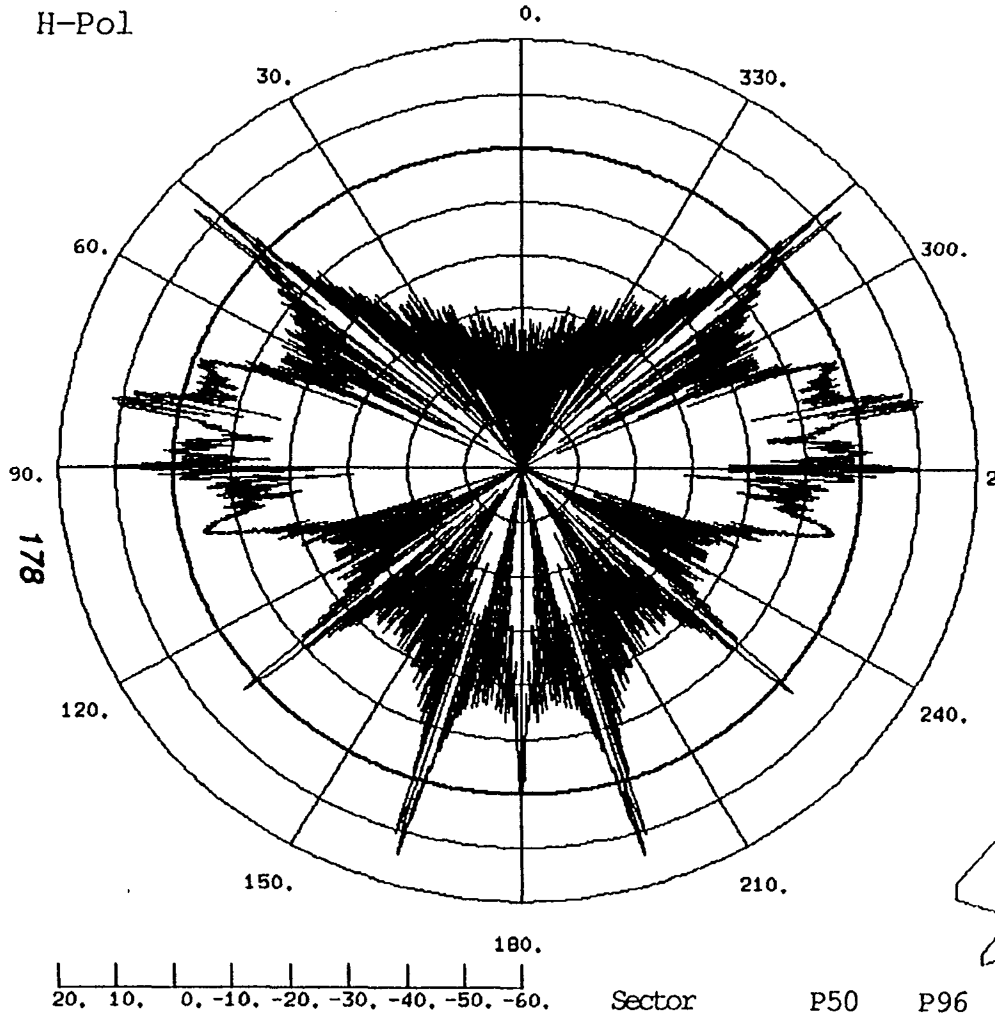

Sector		P50	P96
-30.0	30.0	-38.6	-31.1
60.0	120.0	-11.4	4.2
150.0	210.0	-11.4	4.2
240.0	300.0	-21.7	4.8

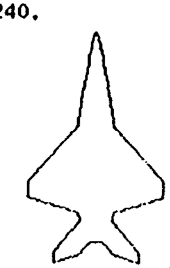

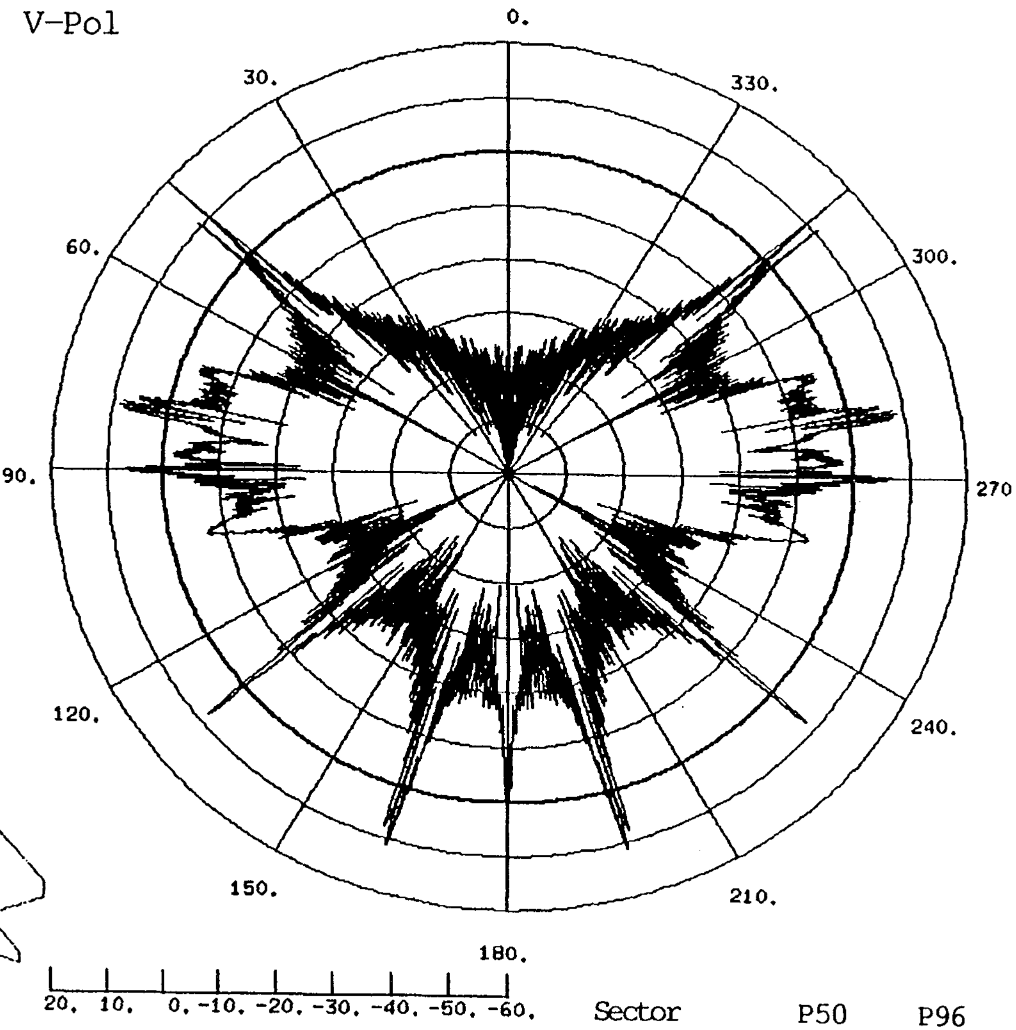

Sector		P50	P96
-30.0	30.0	-39.3	-33.4
60.0	120.0	-13.3	1.0
150.0	210.0	-13.3	1.0
240.0	300.0	-22.9	3.4

Figure C-3

BaseLine Configuation

Vertical Tails Removed & Strakes Added

9.0 Ghz 0.0 Degrees elevation

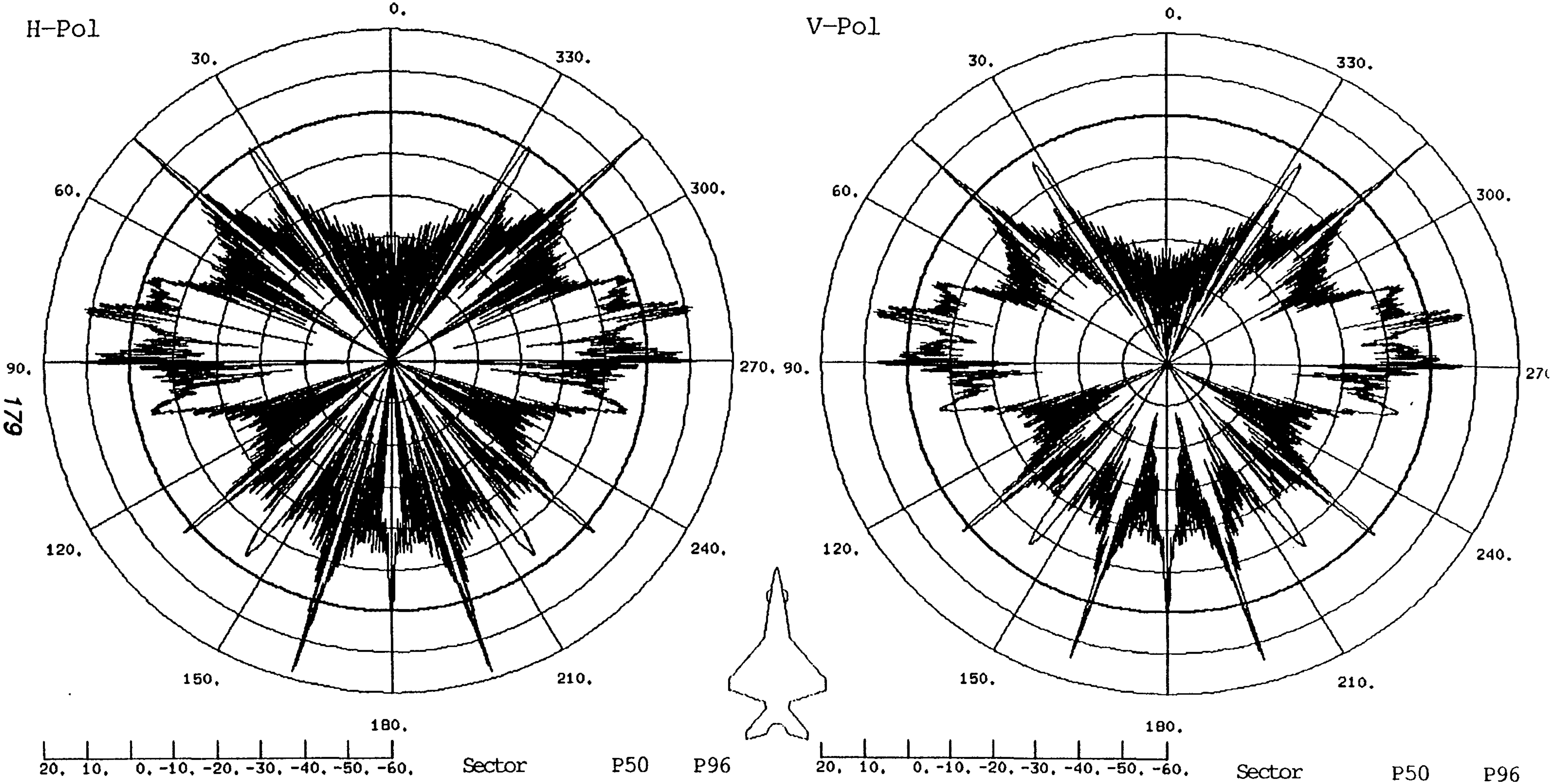

H-Pol

Sector		P50	P96
-30.0	30.0	-36.1	-20.3
60.0	120.0	-12.1	4.0
150.0	210.0	-12.1	4.0
240.0	300.0	-21.3	-1.0

V-Pol

Sector		P50	P96
-30.0	30.0	-36.5	-22.9
60.0	120.0	-13.9	1.0
150.0	210.0	-13.9	1.0
240.0	300.0	-22.3	-1.5

Figure C-4

BaseLine Configuation

Vertical Tails Removed With Split Alerons

9.0 Ghz 0.0 Degrees elevation

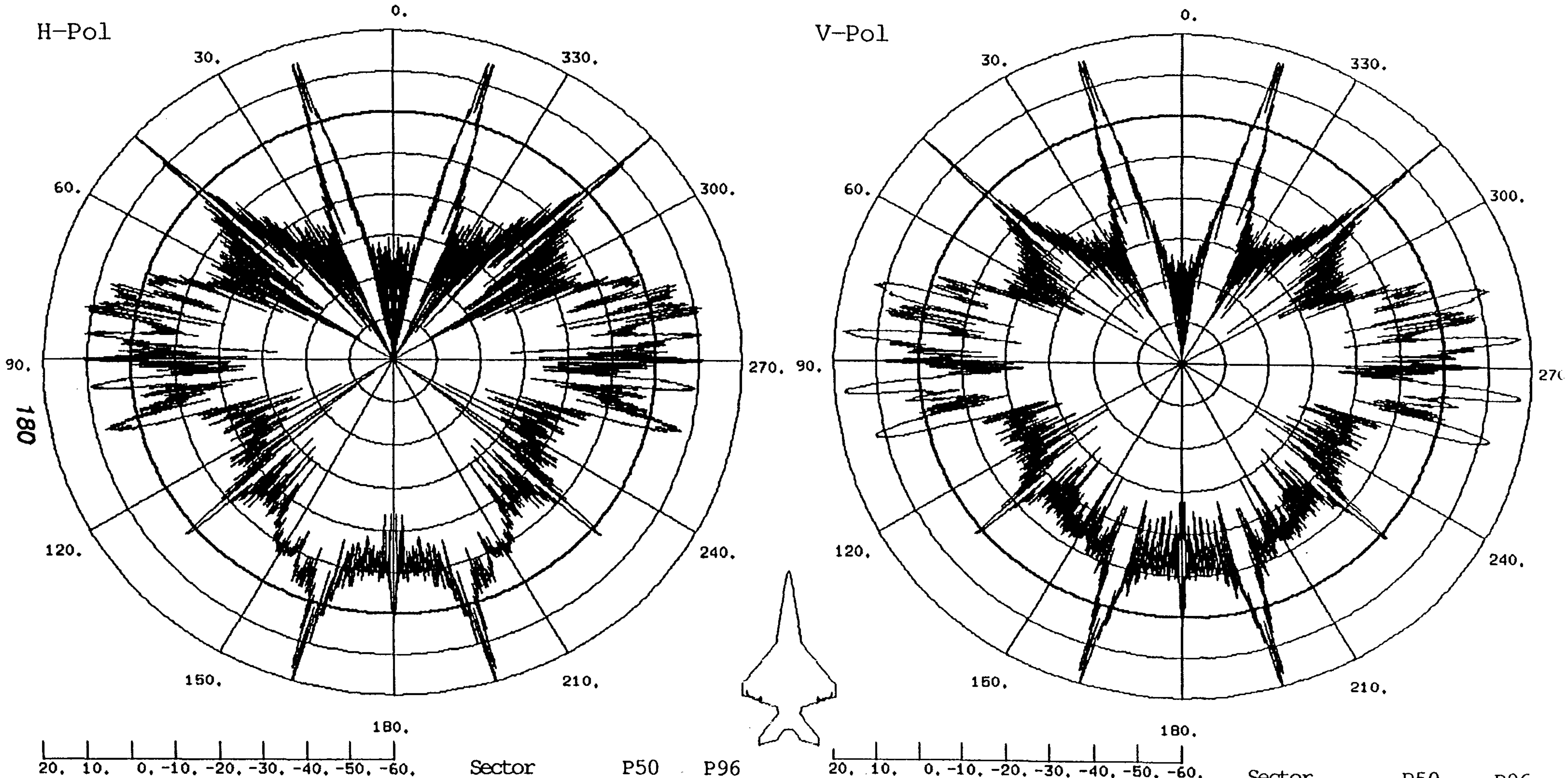

Sector		P50	P96
-30.0	30.0	-32.3	10.8
60.0	120.0	-8.9	7.0
150.0	210.0	-8.9	7.0
240.0	300.0	-9.0	8.4

Sector		P50	P96
-30.0	30.0	-26.8	12.3
60.0	120.0	-6.8	15.6
150.0	210.0	-6.8	15.6
240.0	300.0	-13.1	9.5

Figure C-5

BaseLine Configuation

9.0 Ghz 30.0 Degrees elevation

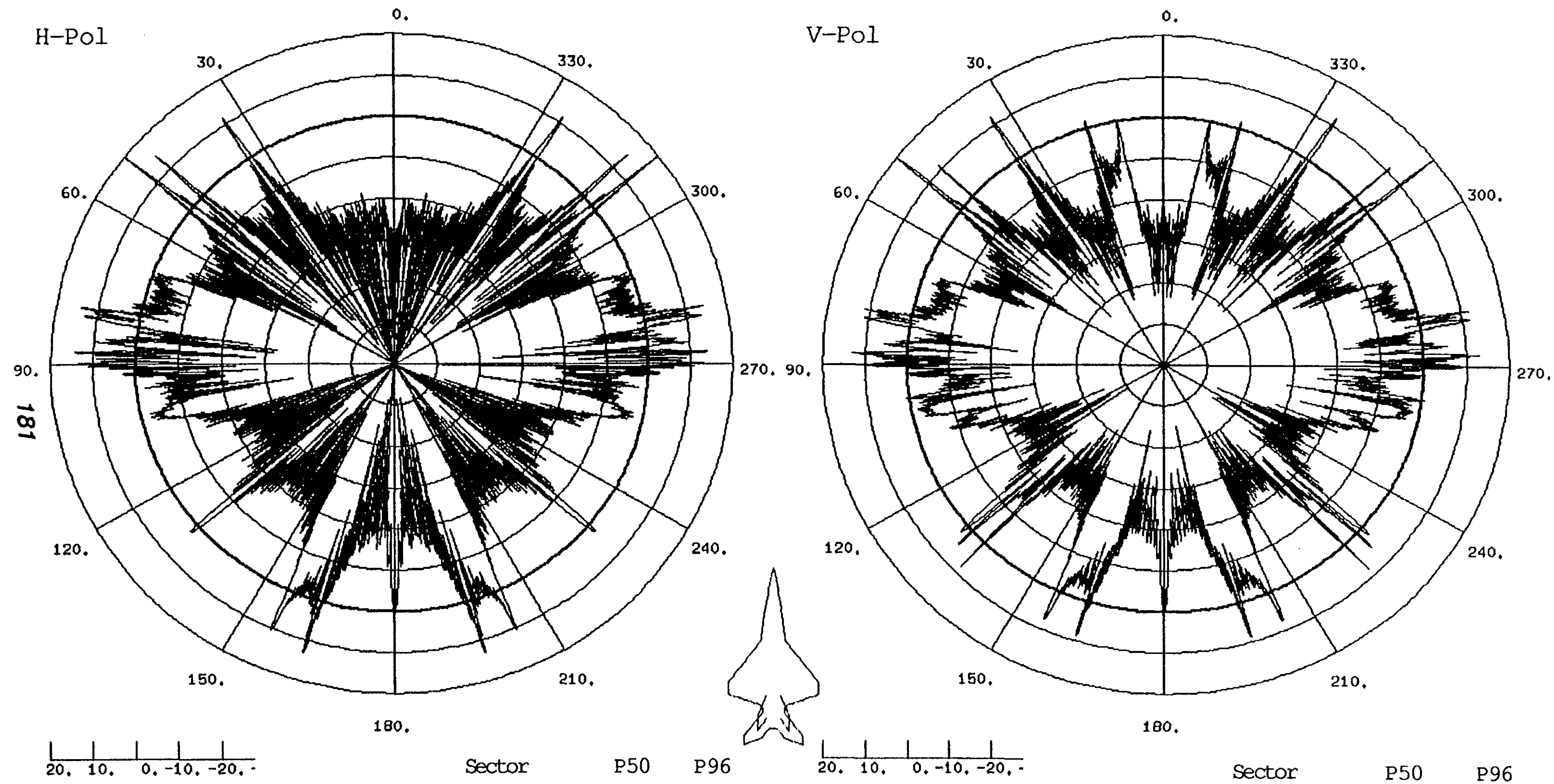

Sector		P50	P96
-30.0	30.0	-26.9	-20.9
60.0	120.0	-9.4	8.6
150.0	210.0	-9.4	8.6
240.0	300.0	-14.0	5.8

Sector		P50	P96
-30.0	30.0	-21.3	-4.2
60.0	120.0	-7.5	7.8
150.0	210.0	-8.8	7.8
240.0	300.0	-16.0	-4.0

Figure C-6

BaseLine Configuation

Vertical Tails Removed

9.0 Ghz 30.0 Degrees elevation

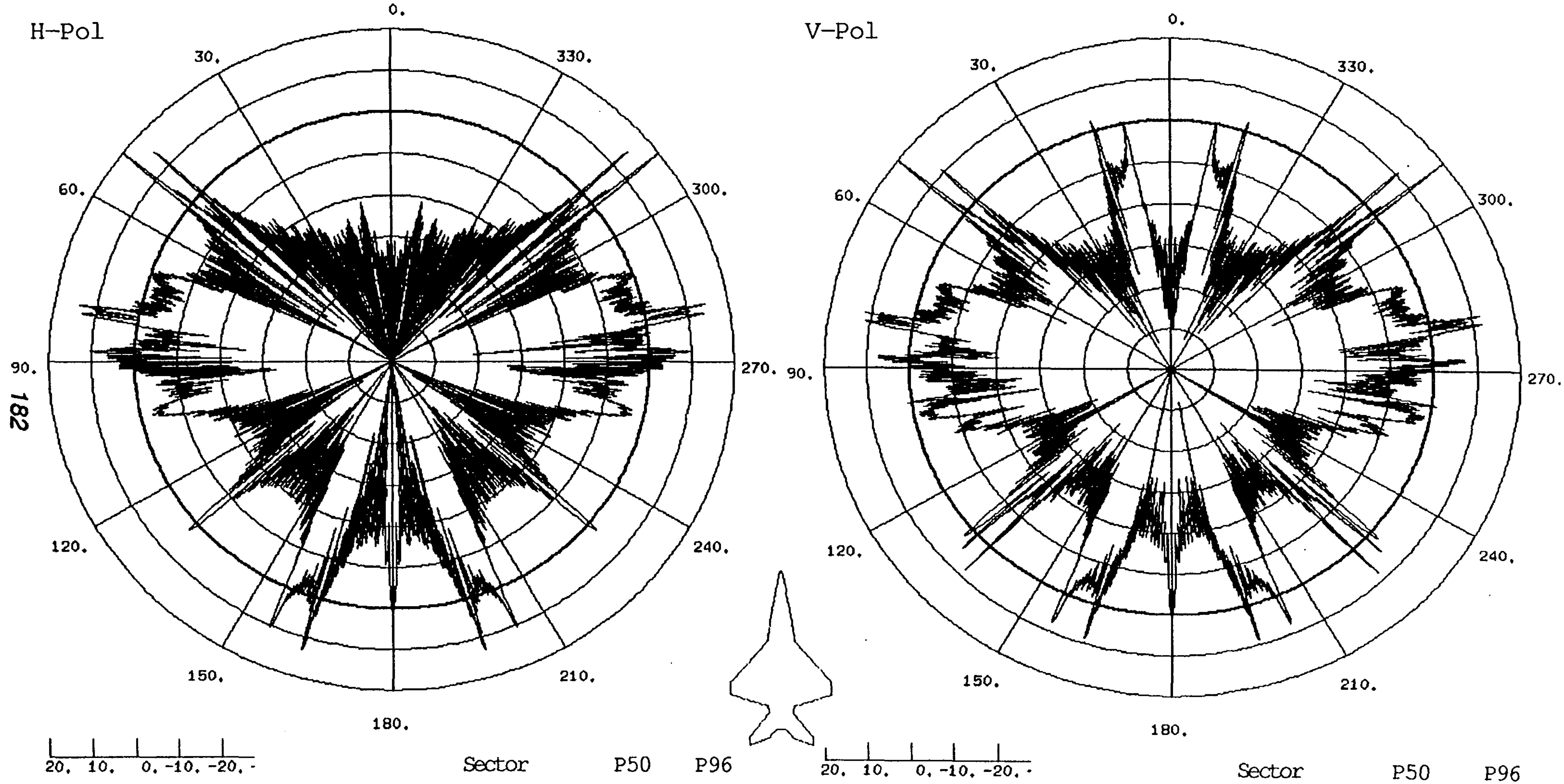

Sector		P50	P96
-30.0	30.0	-34.9	-29.3
60.0	120.0	-8.3	7.8
150.0	210.0	-8.3	8.1
240.0	300.0	-14.4	-5.8

Sector		P50	P96
-30.0	30.0	-28.9	-4.2
60.0	120.0	-8.2	5.1
150.0	210.0	-8.1	4.5
240.0	300.0	-15.9	4.0

Figure C-7

BaseLine Configuation

Vertical Tails Removed & Aft Wings @ +20 Dihedral

9.0 Ghz 30.0 Degrees elevation

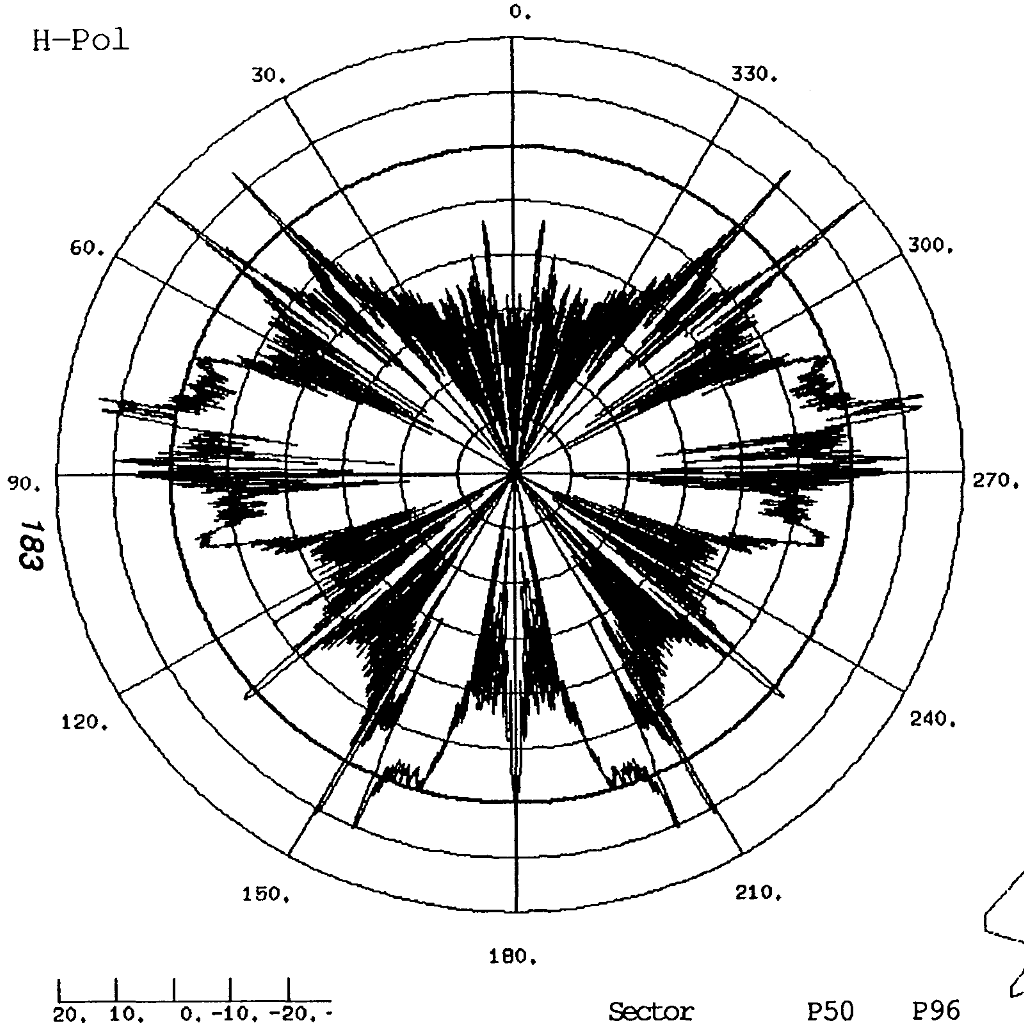

Sector		P50	P96
-30.0	30.0	-32.6	-27.1
60.0	120.0	-10.1	7.9
150.0	210.0	-10.1	7.7
240.0	300.0	-10.6	1.7

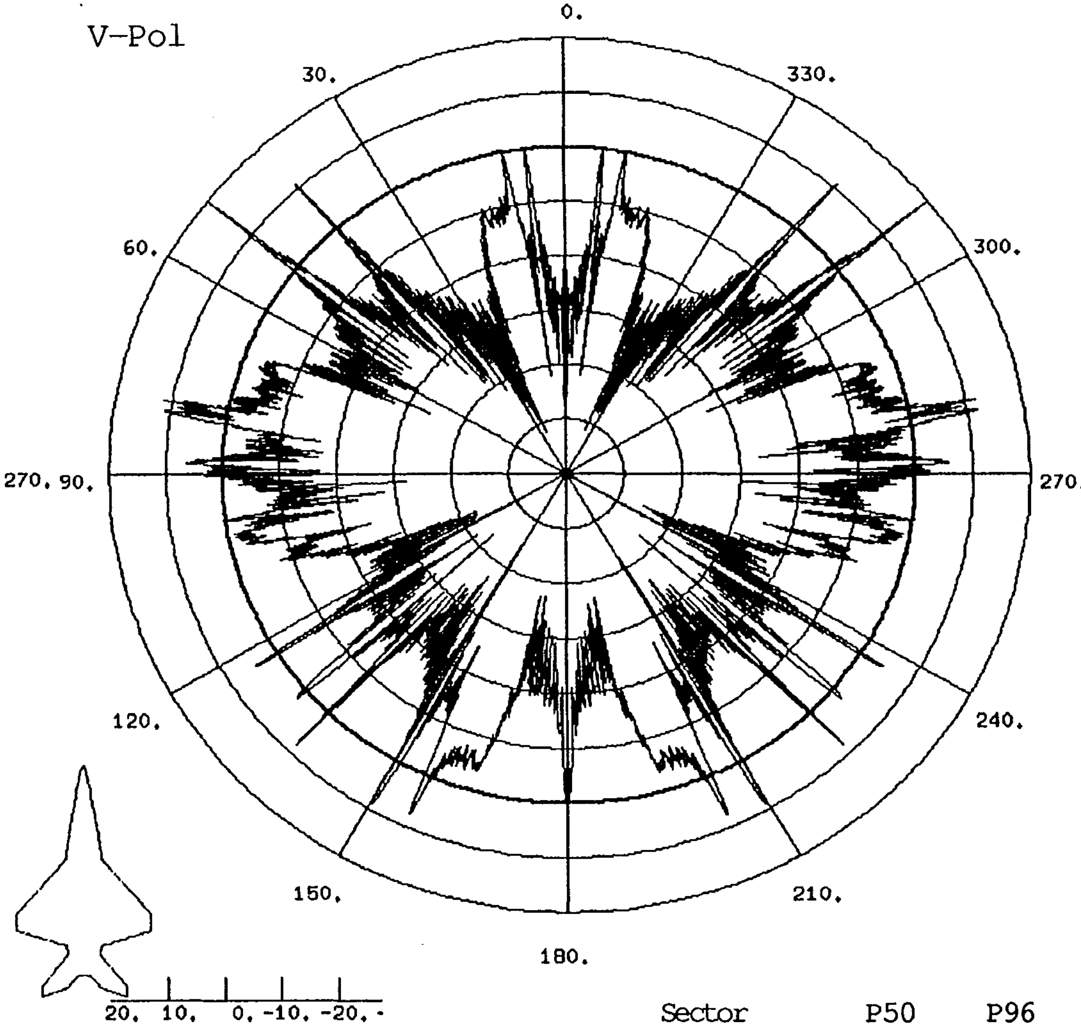

Sector		P50	P96
-30.0	30.0	-23.9	-7.1
60.0	120.0	-9.0	5.0
150.0	210.0	-9.4	4.5
240.0	300.0	-13.6	-1.1

Figure C-8

BaseLine Configuation

9.0 Ghz −30.0 Degrees elevation

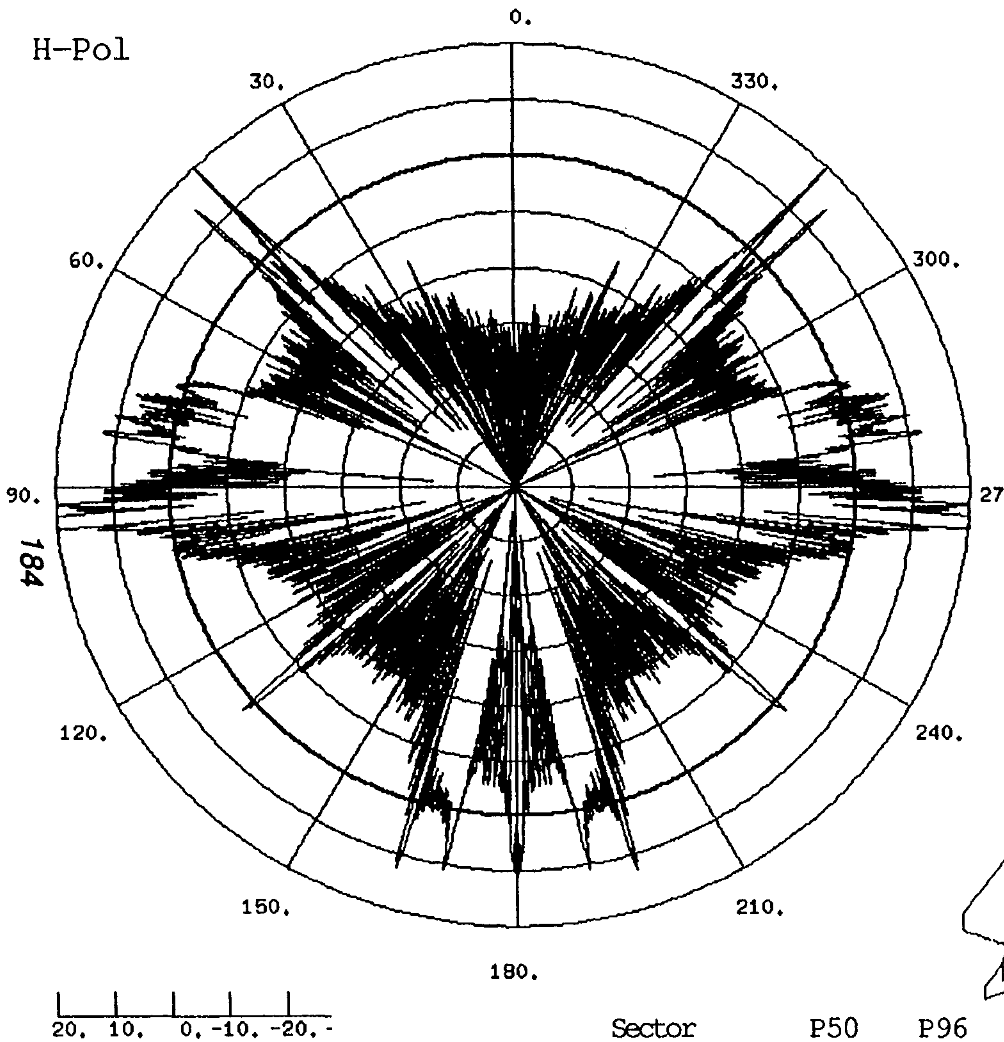

Sector		P50	P96
−30.0	30.0	−33.4	−27.5
60.0	120.0	−6.4	13.1
150.0	210.0	−6.3	13.1
240.0	300.0	−11.8	8.9

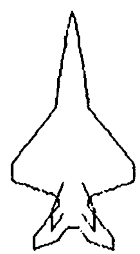

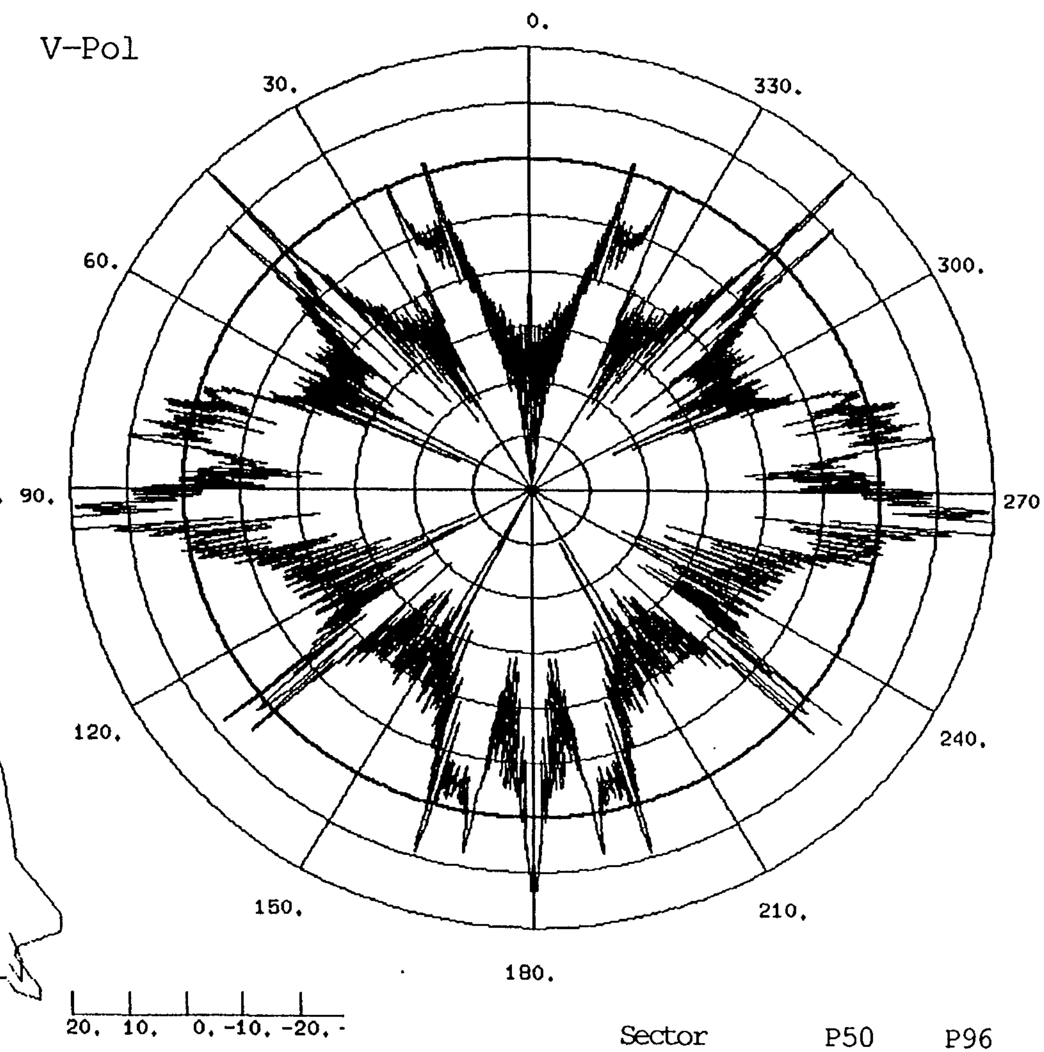

Sector		P50	P96
−30.0	30.0	−26.8	−2.9
60.0	120.0	−8.6	13.2
150.0	210.0	−9.2	13.2
240.0	300.0	−10.0	5.9

Figure C-9

BaseLine Configuation

Vertical Tails Removed

9.0 Ghz −30.0 Degrees elevation

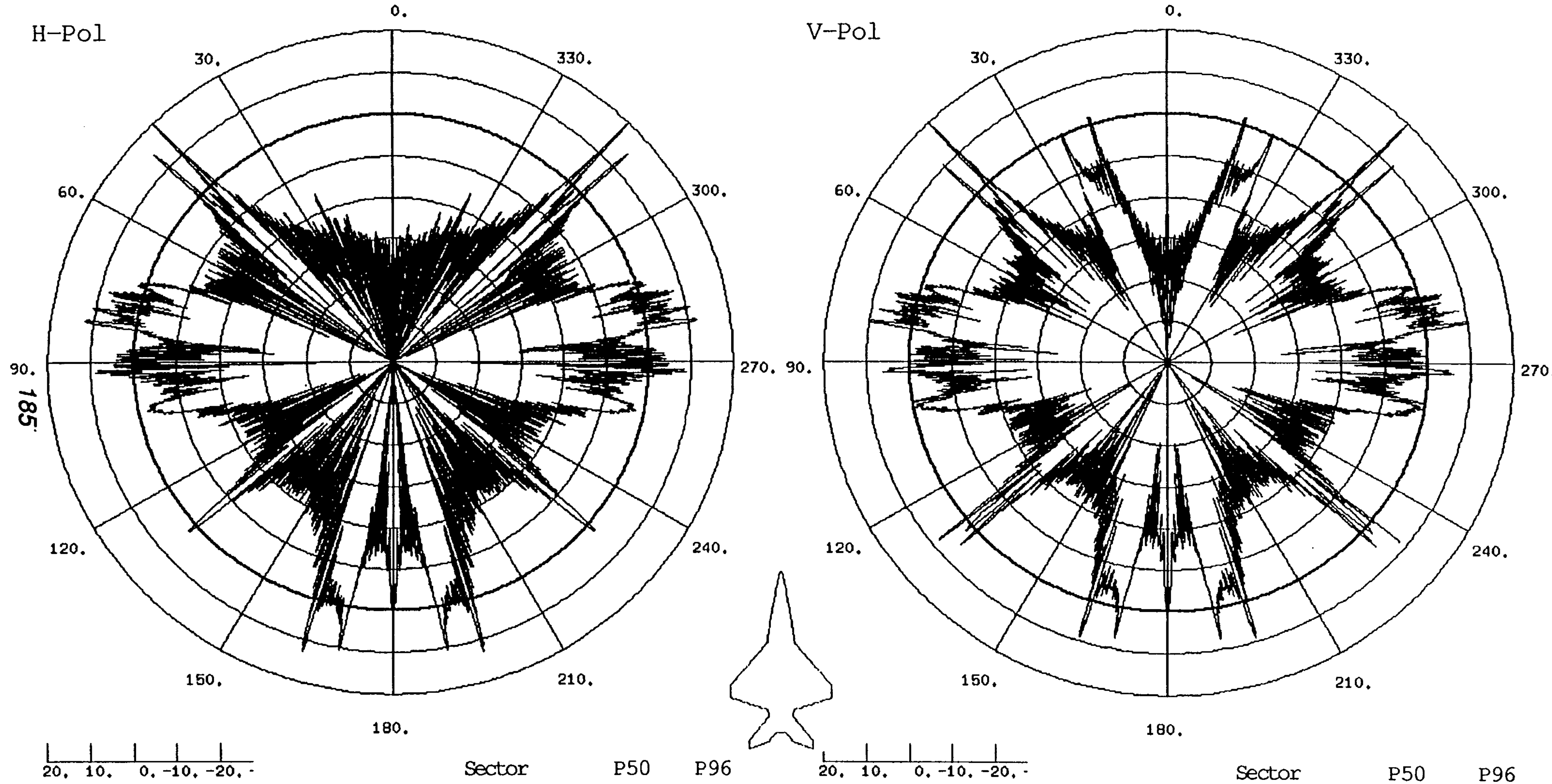

Sector		P50	P96
−30.0	30.0	−33.8	−27.0
60.0	120.0	−10.9	3.9
150.0	210.0	−10.9	3.9
240.0	300.0	−16.9	−5.9

Sector		P50	P96
−30.0	30.0	−27.2	−2.9
60.0	120.0	−10.9	3.2
150.0	210.0	−10.8	3.2
240.0	300.0	−17.5	3.1

Figure C-10

BaseLine Configuation

Vertical Tails Removed & Aft Wings @ +20 Dihedral

9.0 Ghz -30.0 Degrees elevation

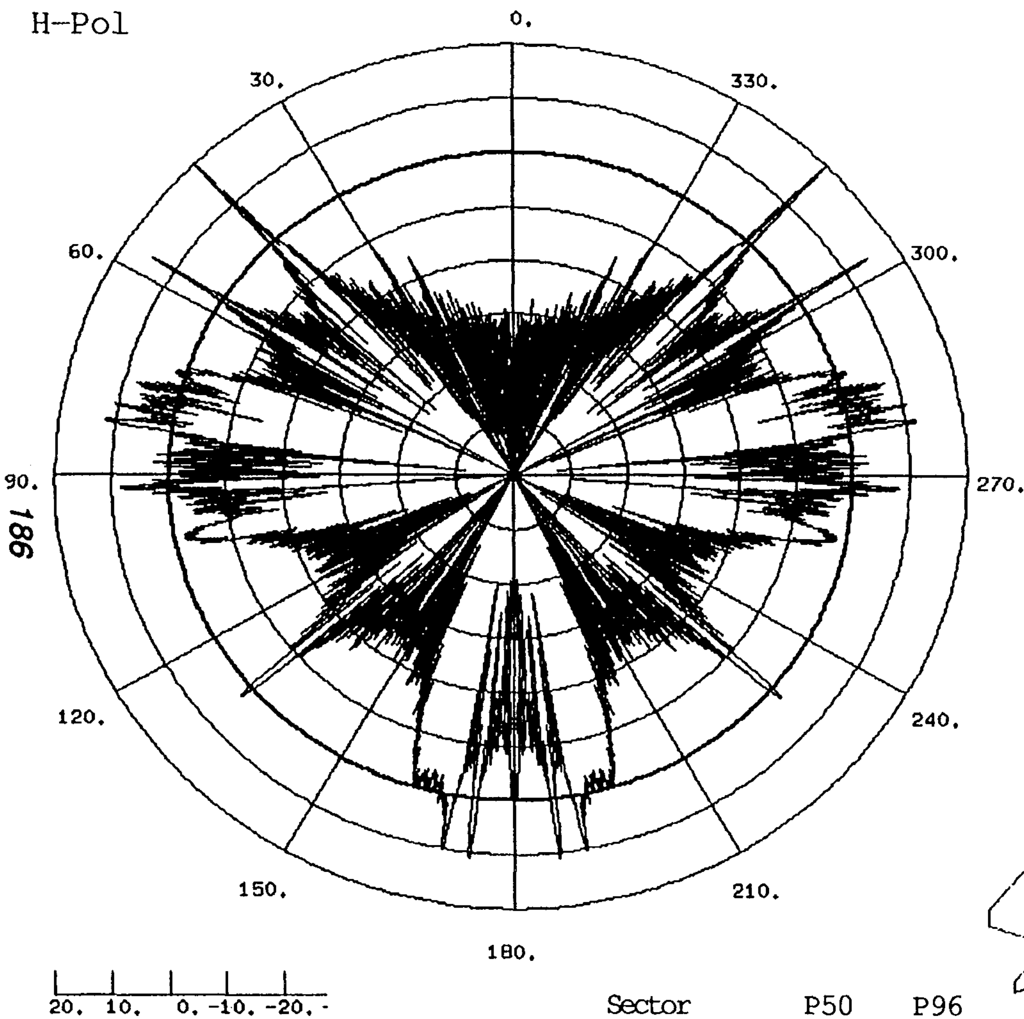

Sector		P50	P96
-30.0	30.0	-34.5	-22.3
60.0	120.0	-12.1	4.3
150.0	210.0	-12.2	4.3
240.0	300.0	-11.6	3.8

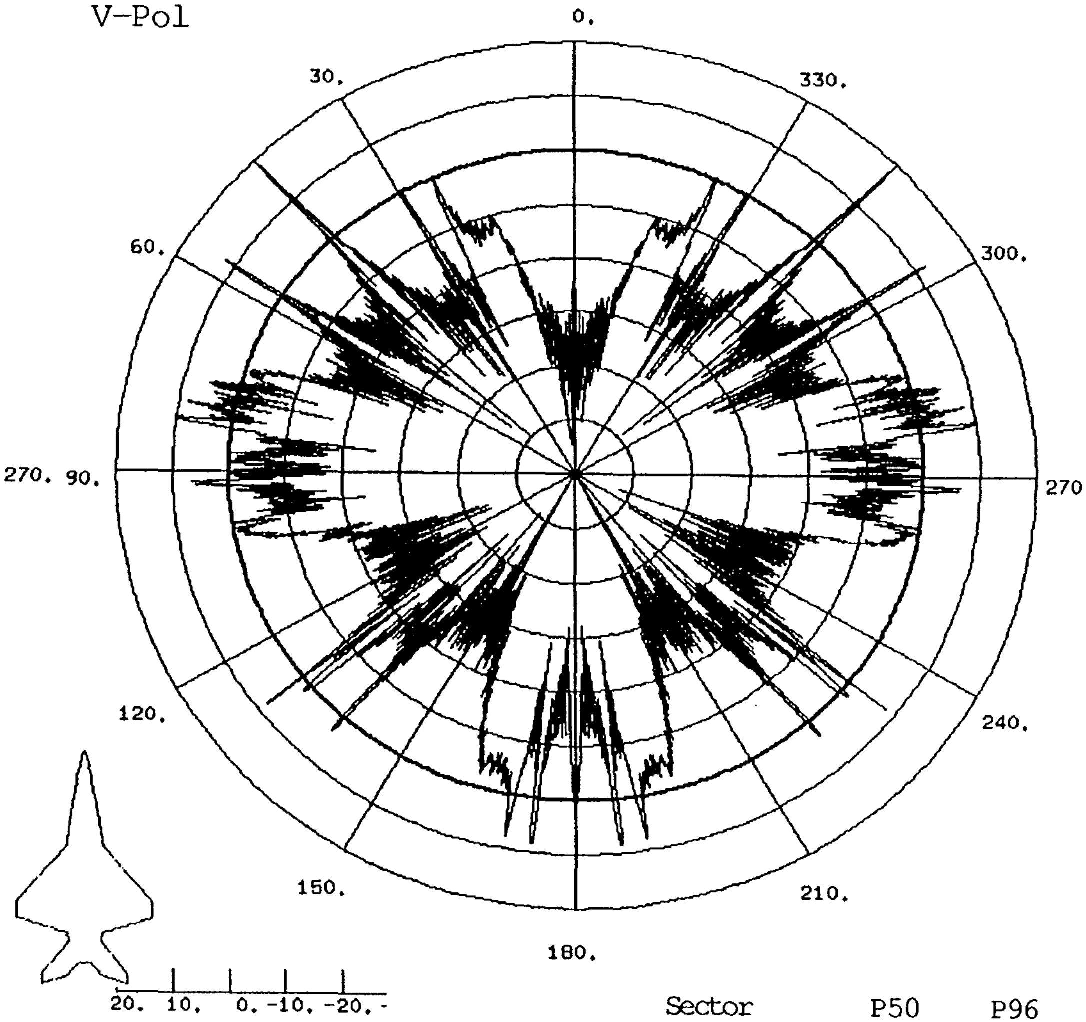

Sector		P50	P96
-30.0	30.0	-21.8	-8.7
60.0	120.0	-10.0	3.5
150.0	210.0	-10.1	3.4
240.0	300.0	-13.2	0.0

Figure C-11

BaseLine Configuation

2.0 Ghz 0.0 Degrees elevation

H-Pol

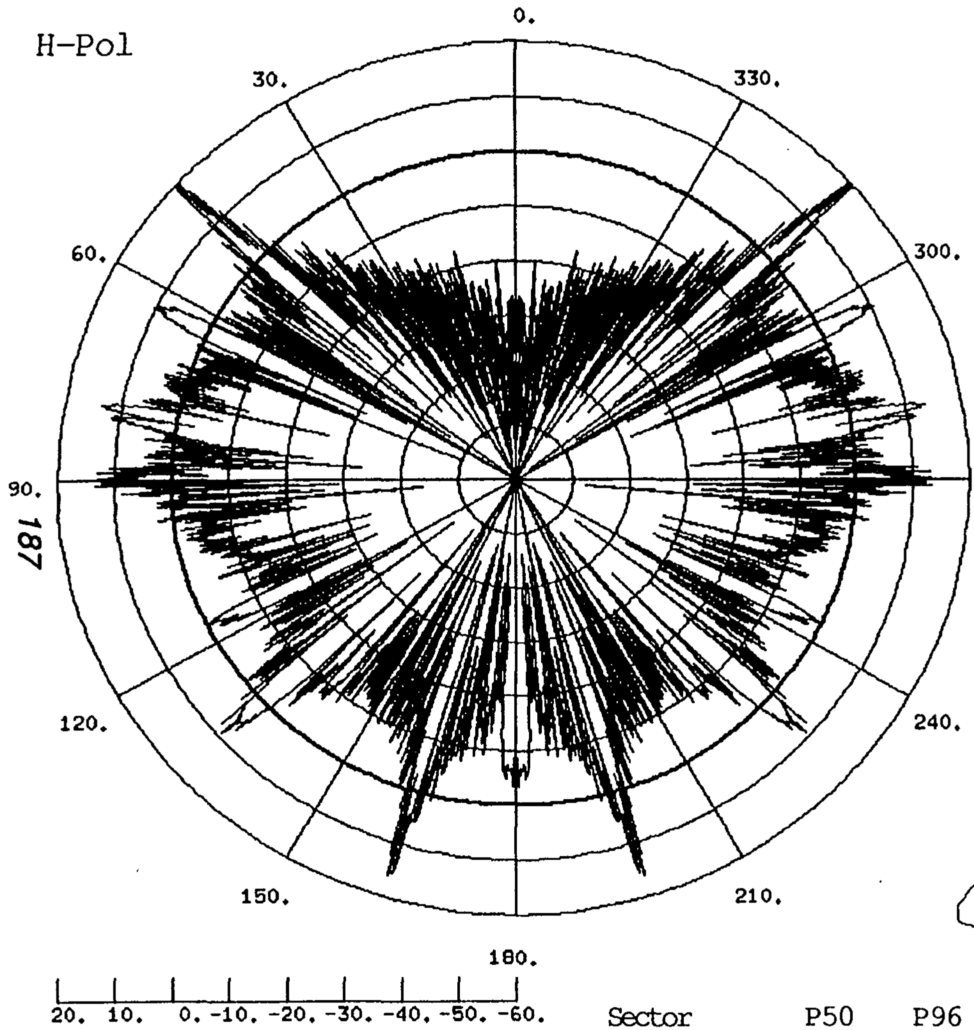

Sector		P50	P96
-30.0	30.0	-27.8	-22.0
60.0	120.0	-3.9	8.7
150.0	210.0	-3.9	8.7
240.0	300.0	-14.9	3.5

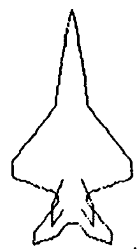

V-Pol

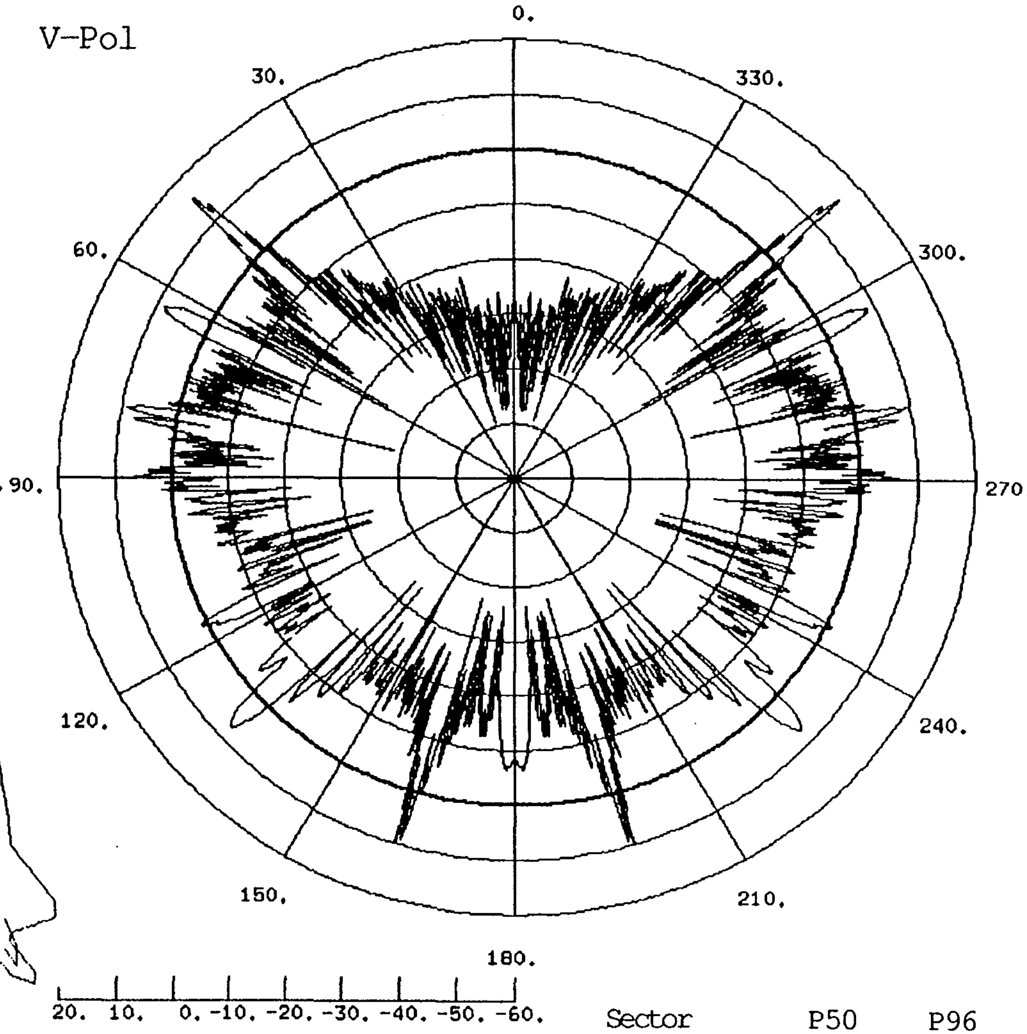

Sector		P50	P96
-30.0	30.0	-29.4	-24.0
60.0	120.0	-6.7	6.1
150.0	210.0	-6.7	6.1
240.0	300.0	-15.8	-2.6

Figure C-12

BaseLine Configuation
Vertical Tails Removed
2.0 Ghz 0.0 Degrees elevation

H-Pol

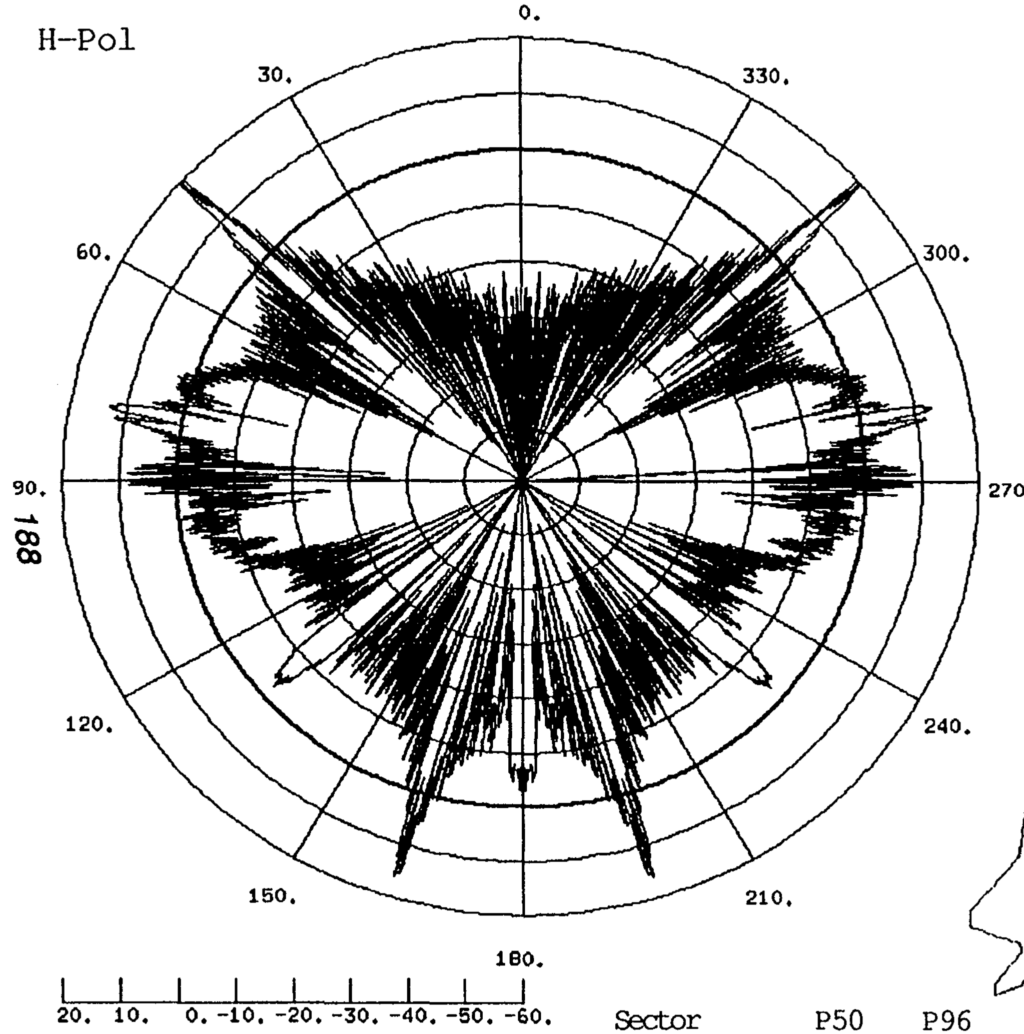

Sector		P50	P96
-30.0	30.0	-29.7	-21.8
60.0	120.0	-6.6	7.7
150.0	210.0	-6.6	7.7
240.0	300.0	-14.8	3.8

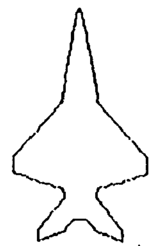

V-Pol

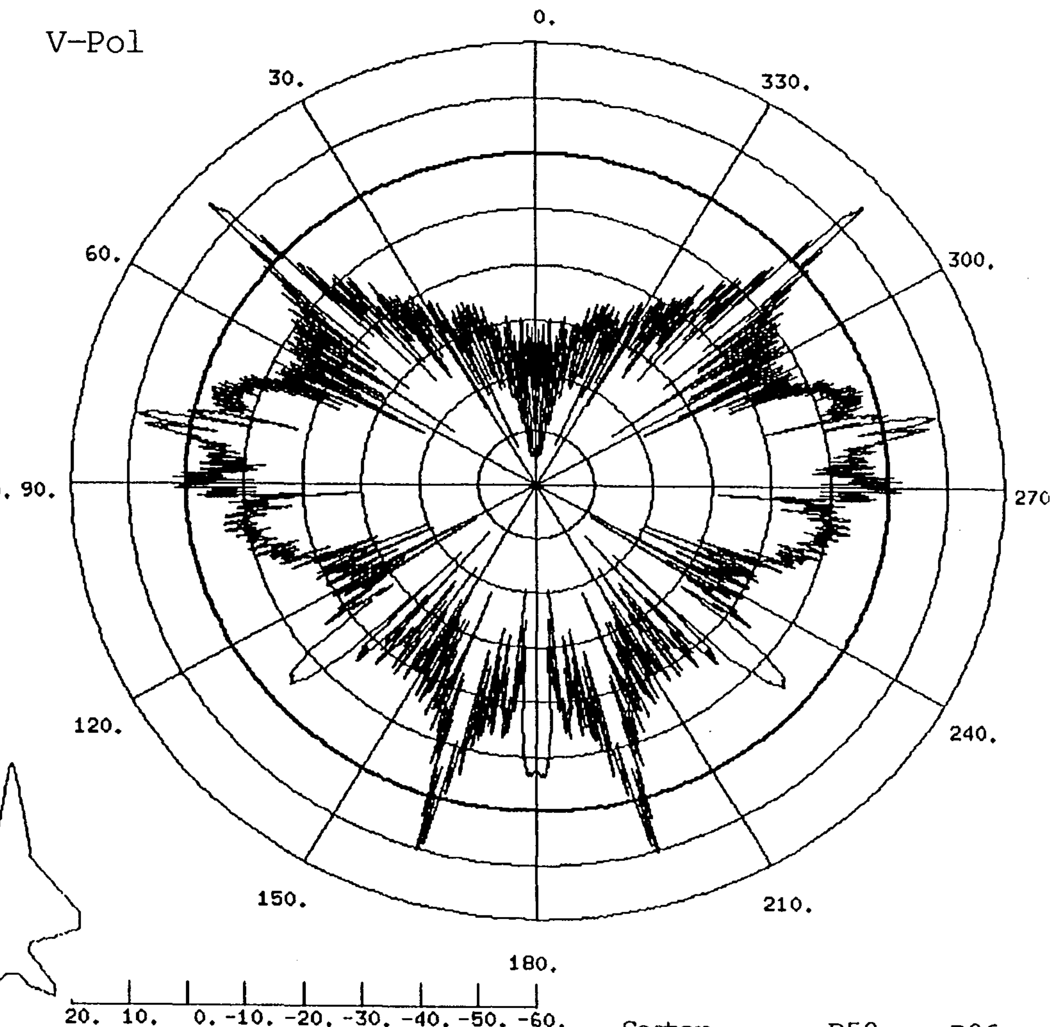

Sector		P50	P96
-30.0	30.0	-31.7	-26.8
60.0	120.0	-11.0	3.2
150.0	210.0	-11.0	3.1
240.0	300.0	-16.7	-1.8

Figure C-13

BaseLine Configuation

Vertical Tails Removed & Aft Wings @ +20 Dihedral

2.0 Ghz 0.0 Degrees elevation

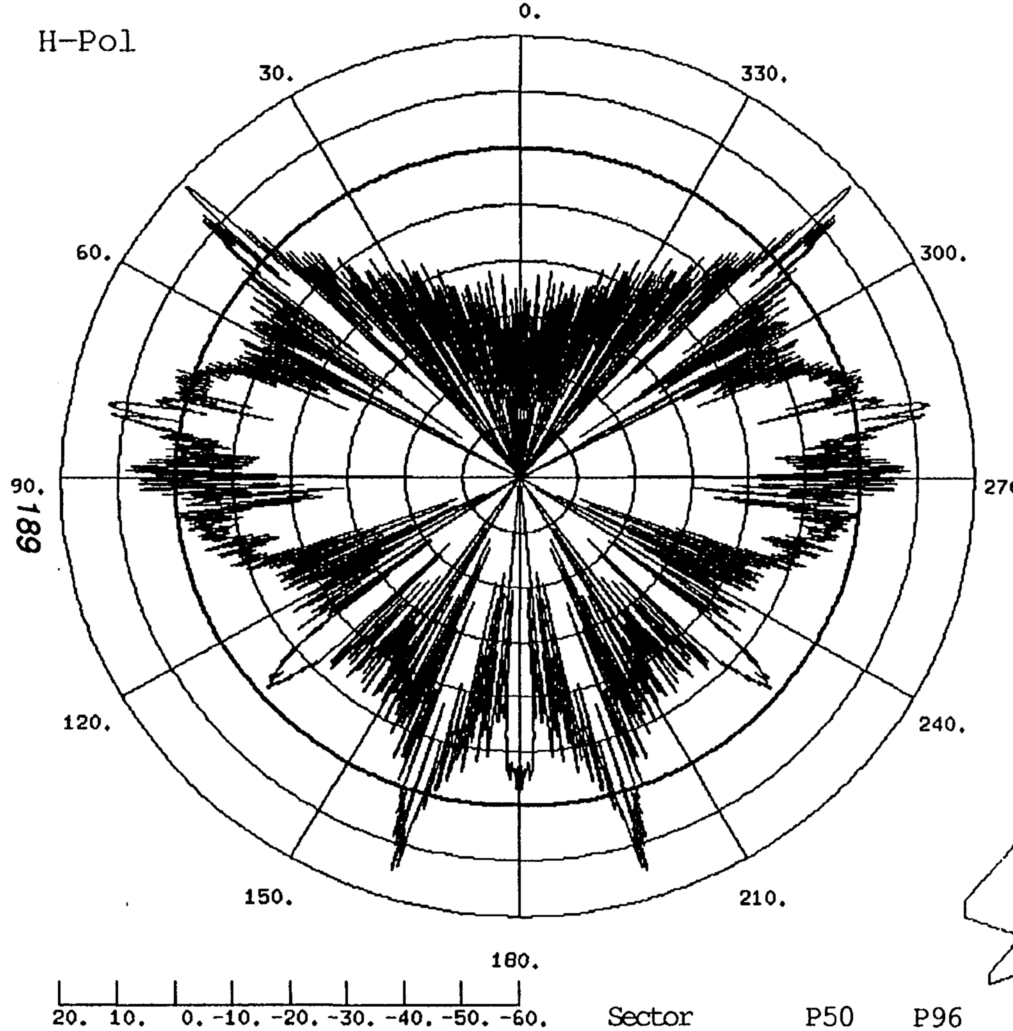

Sector		P50	P96
-30.0	30.0	-31.7	-24.5
60.0	120.0	-5.7	8.2
150.0	210.0	-5.7	8.2
240.0	300.0	-14.9	5.5

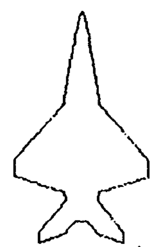

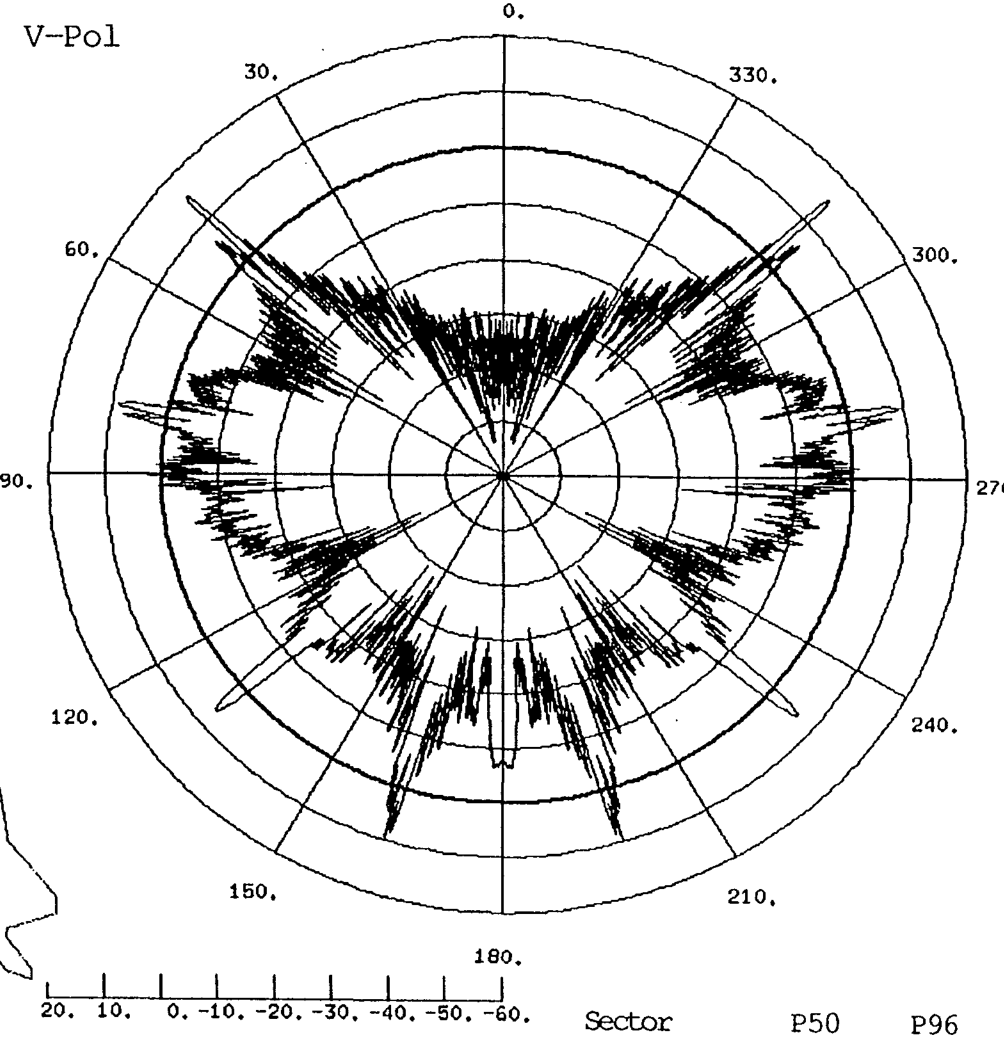

Sector		P50	P96
-30.0	30.0	-32.9	-24.6
60.0	120.0	-10.3	3.1
150.0	210.0	-10.3	3.1
240.0	300.0	-16.5	3.2

Figure C-14

BaseLine Configuation

16.0 Ghz 0.0 Degrees elevation

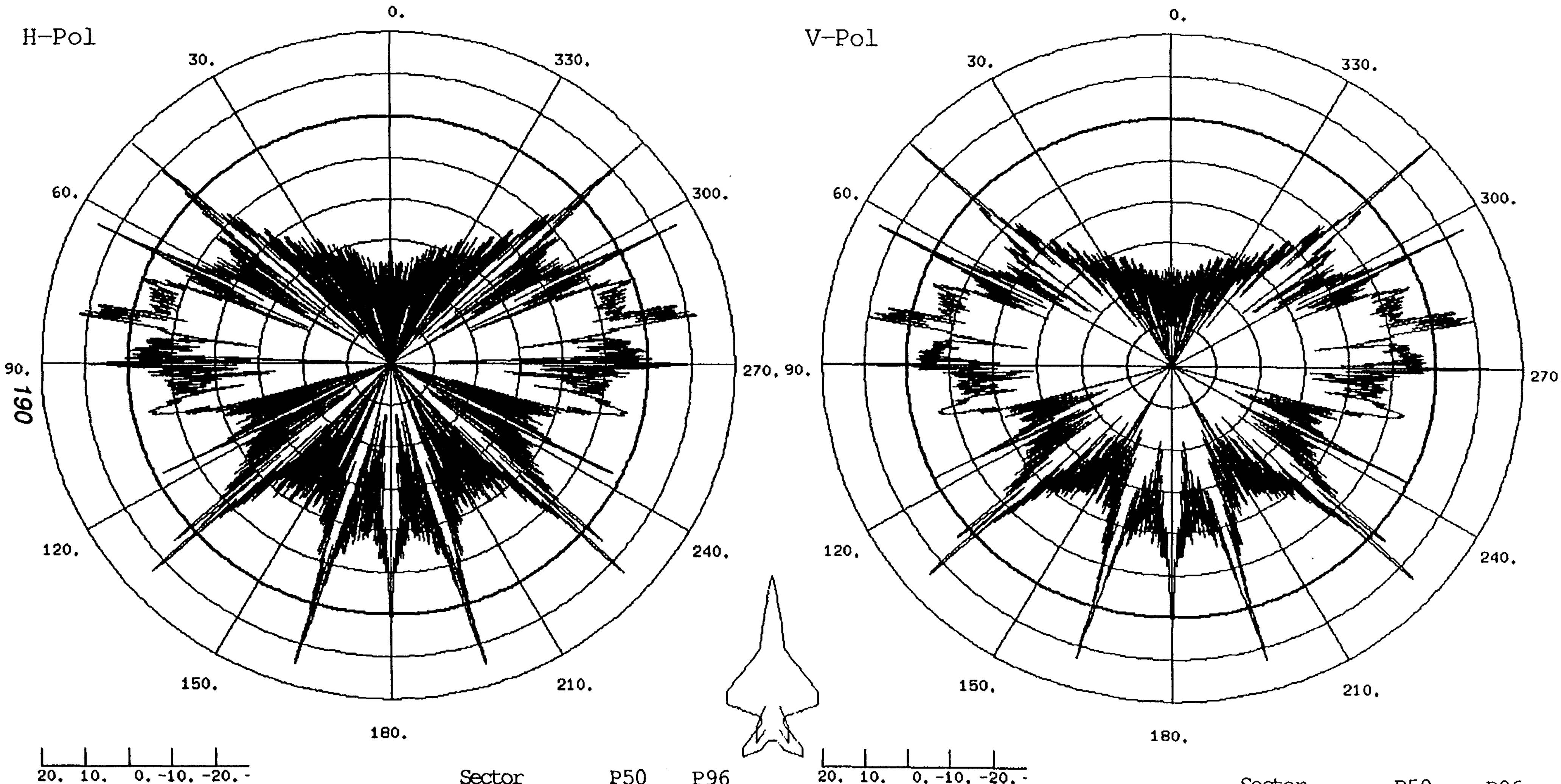

Sector		P50	P96
-30.0	30.0	-41.0	-34.1
60.0	120.0	-11.7	4.0
150.0	210.0	-11.7	4.0
240.0	300.0	-24.0	-1.3

Sector		P50	P96
-30.0	30.0	-40.7	-36.2
60.0	120.0	-13.3	1.8
150.0	210.0	-13.3	1.8
240.0	300.0	-24.0	-1.7

Figure C-15

BaseLine Configuation

Vertical Tails Removed

16.0 Ghz 0.0 Degrees elevation

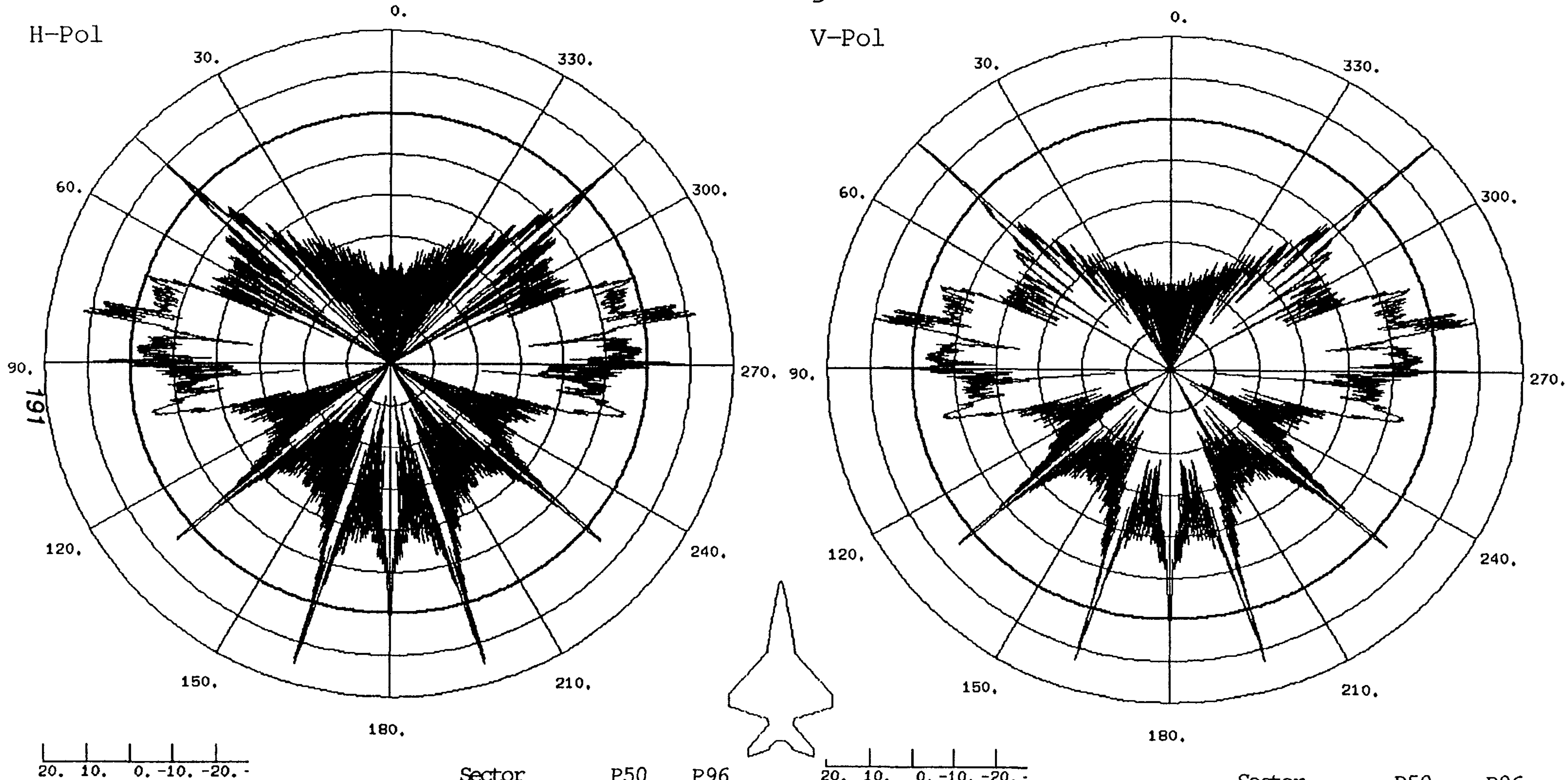

Sector		P50	P96
-30.0	30.0	-42.9	-34.4
60.0	120.0	-13.5	3.5
150.0	210.0	-13.5	3.5
240.0	300.0	-23.4	-1.5

Sector		P50	P96
-30.0	30.0	-42.9	-35.7
60.0	120.0	-15.5	1.4
150.0	210.0	-15.5	1.4
240.0	300.0	-24.5	-1.8

Figure C-16

BaseLine Configuation

Vertical Tails Removed & Aft Wings @ +20 Dihedral

16.0 Ghz 0.0 Degrees elevation

H-Pol

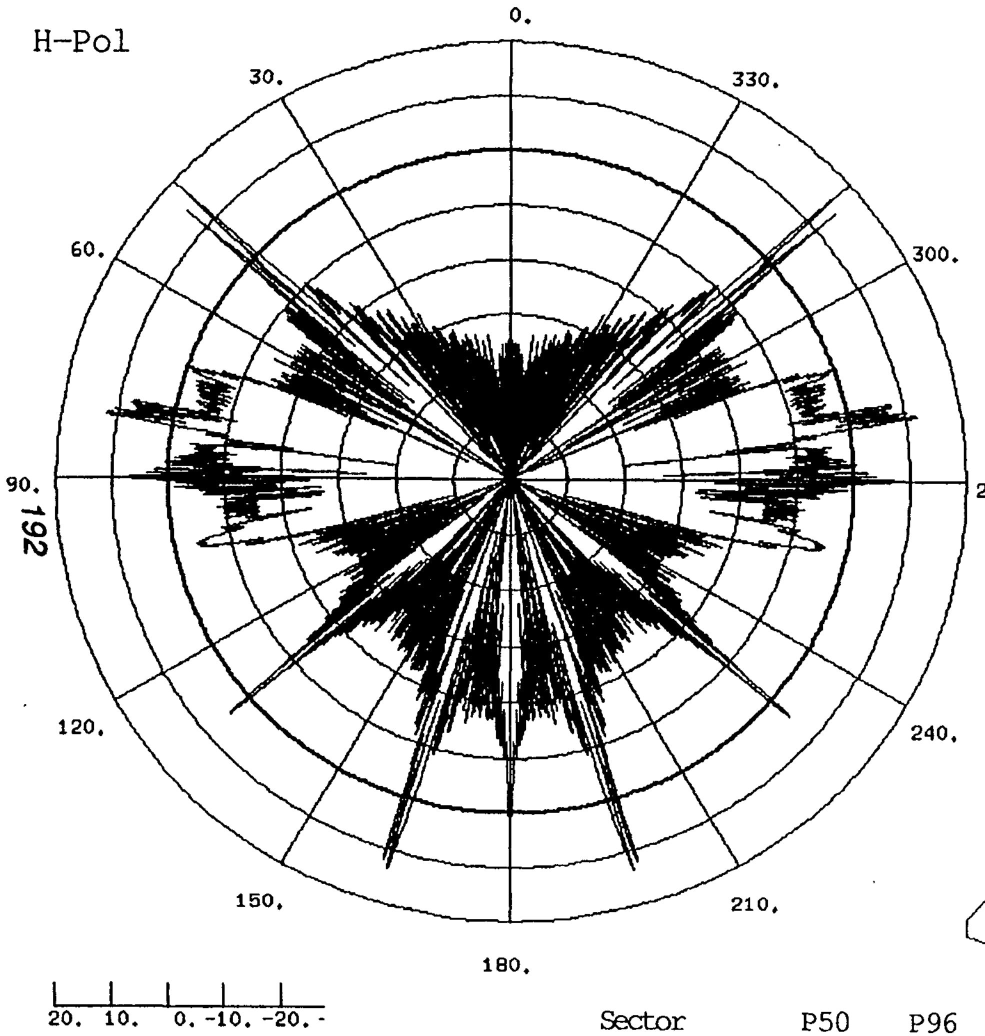

Sector		P50	P96
-30.0	30.0	-41.6	-34.2
60.0	120.0	-13.2	3.9
150.0	210.0	-13.2	3.9
240.0	300.0	-24.7	-1.5

V-Pol

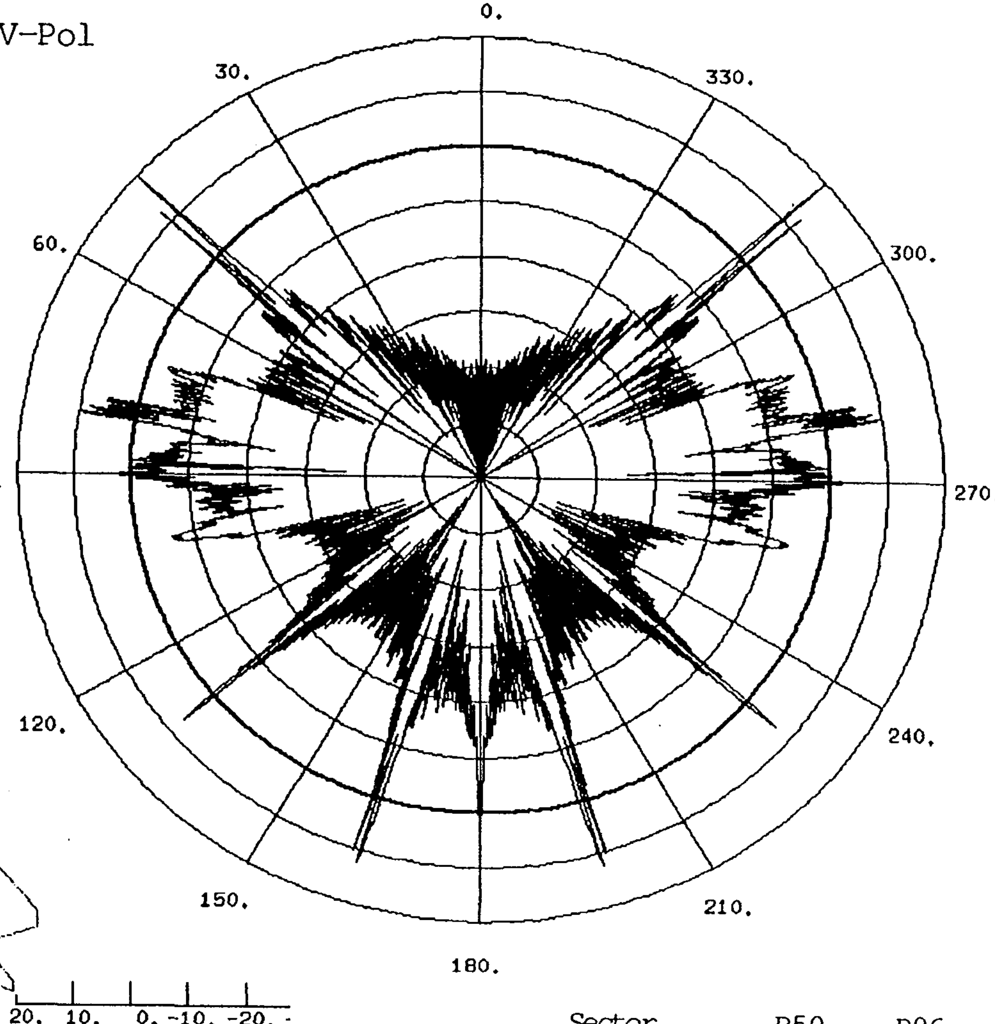

Sector		P50	P96
-30.0	30.0	-42.3	-35.0
60.0	120.0	-14.2	1.6
150.0	210.0	-14.2	1.6
240.0	300.0	-25.3	-1.8

Figure C-17

APPENDIX D

Summary of Analysis of Variable Dihedral Horizontal Tail Concept

This appendix contains a summary of the information used to integrate the variable dihedral horizontal tail. Included in the integration effort are the weight, structures and actuation sizing trades. The following figures are included:

Figure D-1	Weight Buildup and Concept Comparison
Figure D-2	Aft Configuration Features Comparison
Figure D-3	Body Boom Weight - Fixed Spindle (baseline)
Figure D-4	Body Boom Arrangement for Fixed Spindle
Figure D-5	Horizontal Stabilizer Spindle Weight Comparison
Figure D-6	Horizontal Stabilizer Spindle Sizing
Figure D-7	Horizontal Stabilizer Spindle Loads Comparison
Figure D-8	Horizontal Stabilizer Spindle Sizing Comparison
Figure D-9	Fixed Spindle Mid Boom
Figure D-10	Body Boom Arrangement for Variable Dihedral
Figure D-11	Body Boom Arr. for Var. Dihedral - Concept 2
Figure D-12	Rotary Hinge Torque Tube Arrangement
Figure D-13	Curtiss-Wright Power Hinge Sizing Chart
Figure D-14	Activation Cycles vs. Design Hinge Moment

WEIGHT BUILD-UPS - Comparisons

ITEM DESCRIPTION	Base Vertical Fin Fixed Spindle WEIGHT	-lb/vehicle	Variable Dihedral Concept 1 WEIGHT	-lb/vehicle	Variable Dihedral Concept 2 WEIGHT	-lb/vehicle
• **VERTICAL FIN STRUCTURE**	**398.0**		**0.0**		**0.0**	
• Vertical Fin Structure With LO Treatment		398.0		0.0		0.0
• **HORIZONTAL STABILIZER STRUCTURE**	**684.0**		**724.0**		**724.0**	
• Stabilizer Structure With LO Treatment Less Spindle		384.0		384.0		384.0
• Stabilizer Spindle		300.0		340.0		340.0
• **BODY STRUCTURE**	**750.0**		**768.7**		**735.2**	
• Fin - to - Body Attachment		150.0		0.0		0.0
• Body - Stabilizer Booms		600.0		768.7		735.2
• **FLIGHT CONTROL ACTUATION**	**201.0**		**1,368.3**		**676.8**	
• Rudder Actuation		51.0		0.0		0.0
• Stabilizer Actuation		150.0		150.0		150.0
• Variable Dihedral Rotary Actuation		0.0		1,218.3		526.8
• **HYDRAULICS**	**70.0**		**54.0**		**39.0**	
• Rudder Hydraulics		46.0		0.0		0.0
• Stabilizer Hydraulics		24.0		24.0		24.0
• Variable Dihedral Hydraulics		0.0		30.0		15.0
TOTAL WEIGHT	**2,103.0**		**2,915.0**		**2,175.0**	
ΔWEIGHT FROM BASE	**0.0**		**812.0**		**72.0**	

Figure D-1 Weight Buildup and Concept Comparison

AFT CONFIGURATION FEATURES

- VERTICAL FIN / RUDDER
- FIXED SPINDLE;
  ALL MOVING STABILIZER

- NO VERTICAL FIN
- VARIABLE DIHEDRAL;
  ALL MOVING STABILIZER

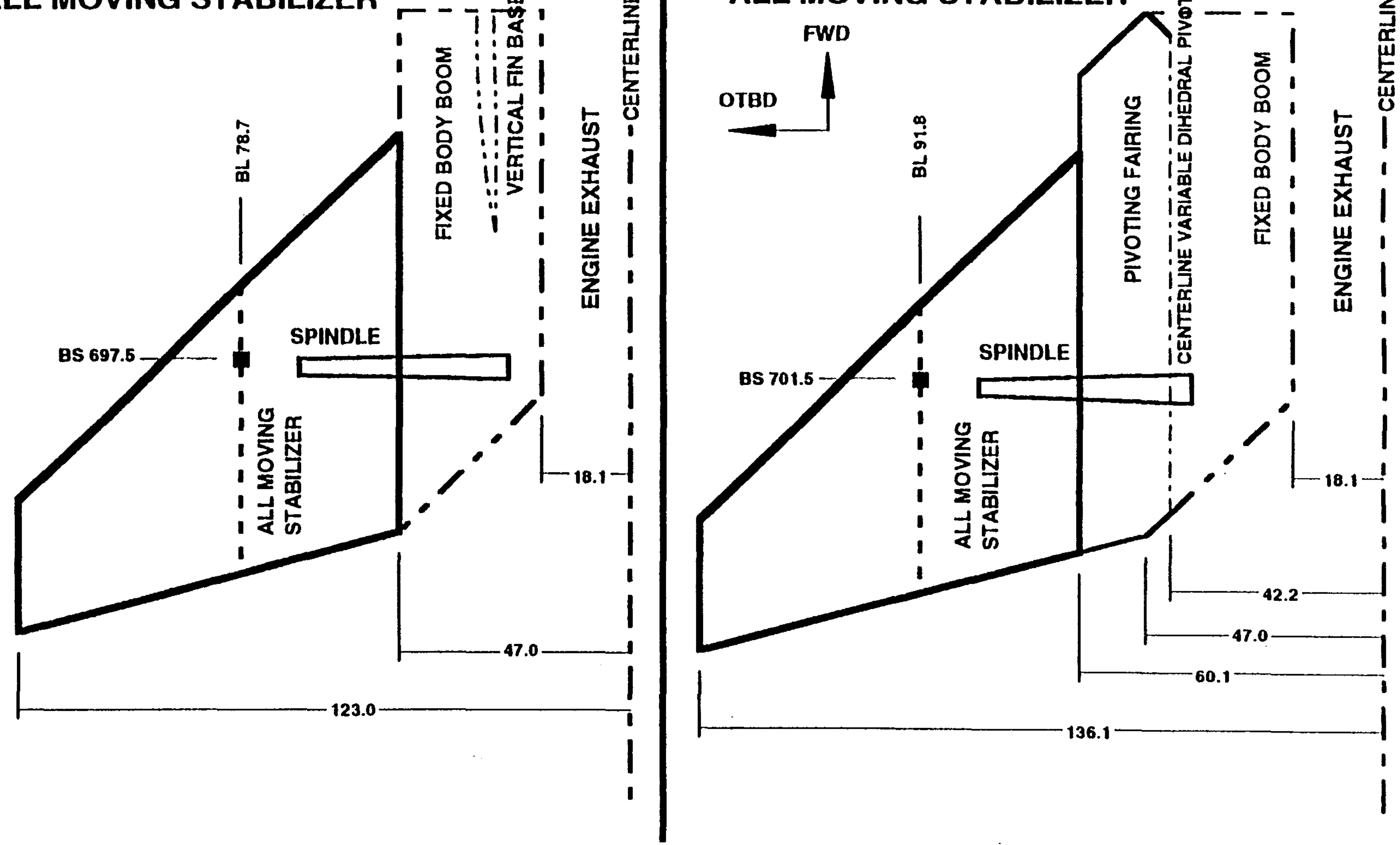

Figure D-2 Aft Configuration Features Comparison

BODY BOOM WEIGHT - Fixed Spindle

ITEM DESCRIPTION	WEIGHT -lb/vehicle	COMMENTS
COVERS	**404.4**	
• UPPER COVER	86.0	• Ti 6-4 Skins; tskins = 0.080 in to 0.125 in
• LOWER COVER	86.0	• Ti 6-4 Skins; tskins = 0.080 in to 0.125 in
• INBD WEB	55.7	• Ti 6-4 Skins; tskins = 0.080"
• INBD CHORDS	85.3	• Ti 6-4 Angle; Axx = 1.250 in2
• OTBD CHANNEL	54.6	• Ti 6-4 Channel; Axx = 1.600 in2
• FASTENING	36.8	• Allowance
FRAMES	**105.0**	
• STA 618	15.0	• YF-22 Ratio
• STA 644	15.0	• YF-22 Ratio
• STA 669	15.0	• YF-22 Ratio
• STA 694	30.0	• YF-22 Ratio
• STA 704	30.0	• YF-22 Ratio
ATTACHMENTS	**35.0**	
• OTBD SPINDLE BEARING INST.	15.0	• YF-22 Ratio
• INBD SPINDLE BEARING INST.	12.0	• YF-22 Ratio
• STABILIZER ACTUATOR ATTACHMENT	8.0	• YF-22 Ratio
MISCELLANEOUS	**20.6**	• Allowance
TOTAL BODY BOOM WEIGHT	**565.0**	

Figure D-3 Body Boom Weight - Fixed Spindle (baseline)

Body Boom Arrangement For Fixed Spindle

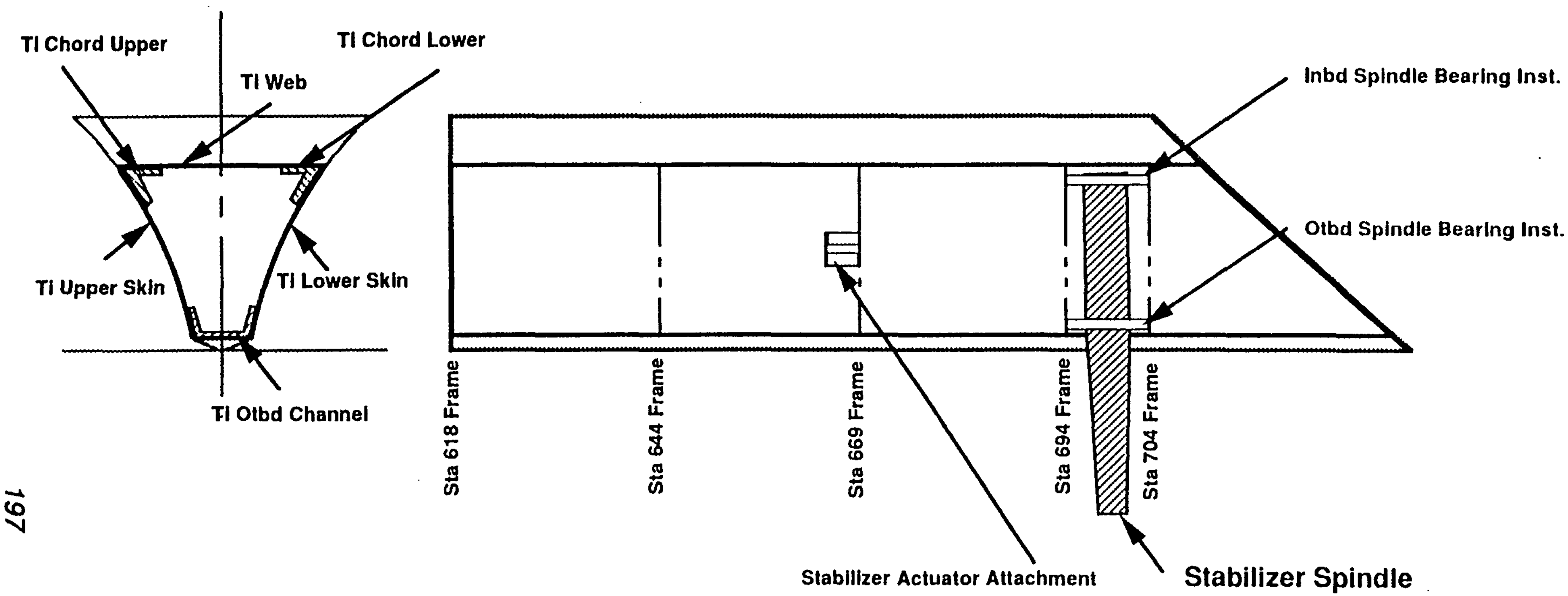

Item Description	Material
• Covers & Webs	Ti 6-4 Plate
• Chords	Ti 6-4 Plate Or Extrusions
• Frames	Ti 6-4 Plate
• Fittings	Ti 6-4 Extrusions
• Bearings	Steel
• Stabilizer Spindle	Steel

Figure D-4 Body Boom Arrangement for Fixed Spindle

HORIZONTAL STABILIZER SPINDLE WEIGHT COMPARISON

FIXED vs VARIABLE DIHEDRAL SPINDLE

FIXED SPINDLE:

STA -in	ΔI -in	DIAo -in	DIAI -in	twall -in	Axx -in2	WT/IN -lb/in	WT -lb/side
24.9	5.0	5.32	4.96	0.178	2.873	0.827	4.5
29.9	14.1	5.32	4.90	0.207	3.322	0.958	40.5
44.0	3.0	5.32	2.68	1.318	16.554	4.784	13.7
47.0	20.0	5.15	2.68	1.233	15.157	4.380	55.3
67.0	0.0	3.50	2.68	0.410	3.980	1.150	

MATERIAL:
- HI-STRENGTH STEEL
- Ftu = 240,000psi
- Fcy = -240,000psi
- Density = .289 lb/in3

BASIC SPINDLE	114.0	lb/side
SPINDLE ACTUATOR LUGS	12.0	
SPINDLE TO BODY ATTACHMENT	14.0	
MISC.	10.0	
TOTAL PER SIDE	**150.0**	**lb/side**
TOTAL PER AIRCRAFT	**300.0**	**lb/aircraft**

VARIABLE DIHEDRAL:

STA -in	ΔI -in	DIAo -in	DIAI -in	twall -in	Axx -in2	WT/IN -lb/in	WT -lb/side
38.0	4.1	6.50	6.07	0.217	4.283	1.238	7.0
42.1	4.1	6.50	5.73	0.386	7.414	2.141	13.4
46.2	13.9	6.50	4.75	0.876	15.477	4.473	61.4
60.1	20.0	5.15	2.68	1.233	15.157	4.380	55.3
80.1	0.0	3.50	2.68	0.410	3.980	1.150	

MATERIAL:
- HI-STRENGTH STEEL
- Ftu = 240,000psi
- Fcy = -240,000psi
- Density = .289 lb/in3

BASIC SPINDLE	137.1	lb/side
SPINDLE ACTUATOR LUGS	12.0	
SPINDLE TO TORQUE BOX ATTACHMENT	10.0	
MISC.	10.9	
TOTAL PER SIDE	**170.0**	**lb/side**
TOTAL PER AIRCRAFT	**340.0**	**lb/aircraft**

Figure D-5 Horizontal Stabilizer Spindle Weight Comparison

HORIZONTAL STABILIZER SPINDLE SIZING

Fixed & Variable Dihedral Spindles

REQUIREMENTS:

ITEM DESCRIPTION	LIMIT	ULTIMATE	COMMENTS
• HINGE MOMENT @ Side of Boom	1,971,200. in lb	2,956,800. in lb	• Per J. DAWDY(8/15/95) & W. PRICE(8/30/95)
• SHEAR LOAD @ Side of Boom	74,105. lb	111,158. lb	• From HM @ SOB & Geometry
• TORSION @ Side of Boom	181,199. in lb	271,798. in lb	• Per J. DAWDY(8/15/95) + 5% MAC Load Offset

GEOMETRY & MATERIAL:

ITEM DESCRIPTION	Fixed Sp'd	VD Sp'd	COMMENTS
• SPINDLE DIAouter @ Attach Bearings	5.32 in	6.50 in	• Estimate
• SPINDLE DIAouter @ Side of Boom	5.15 in	5.15 in	• Exceeds Drawing t/c @ SOB by $\Delta t = 0.65''$
• HI-STRENGTH STEEL i.e., ARAMET 100, etc.			
• TENSION ULTIMATE - Ftu	240,000. psi		
• COMPRESSION YIELD - Fcy	-240,000. psi		
• SHEAR ULTIMATE - Fsu	180,000. psi		
• DENSITY	0.289 lb/in3		

Figure D-6 Horizontal Stabilizer Spindle Sizing

HORIZONTAL STABILIZER SPINDLE LOADS COMPARISON

FIXED (FIX SPD) vs VARIABLE DIHEDRAL (VD SPD) SPINDLES

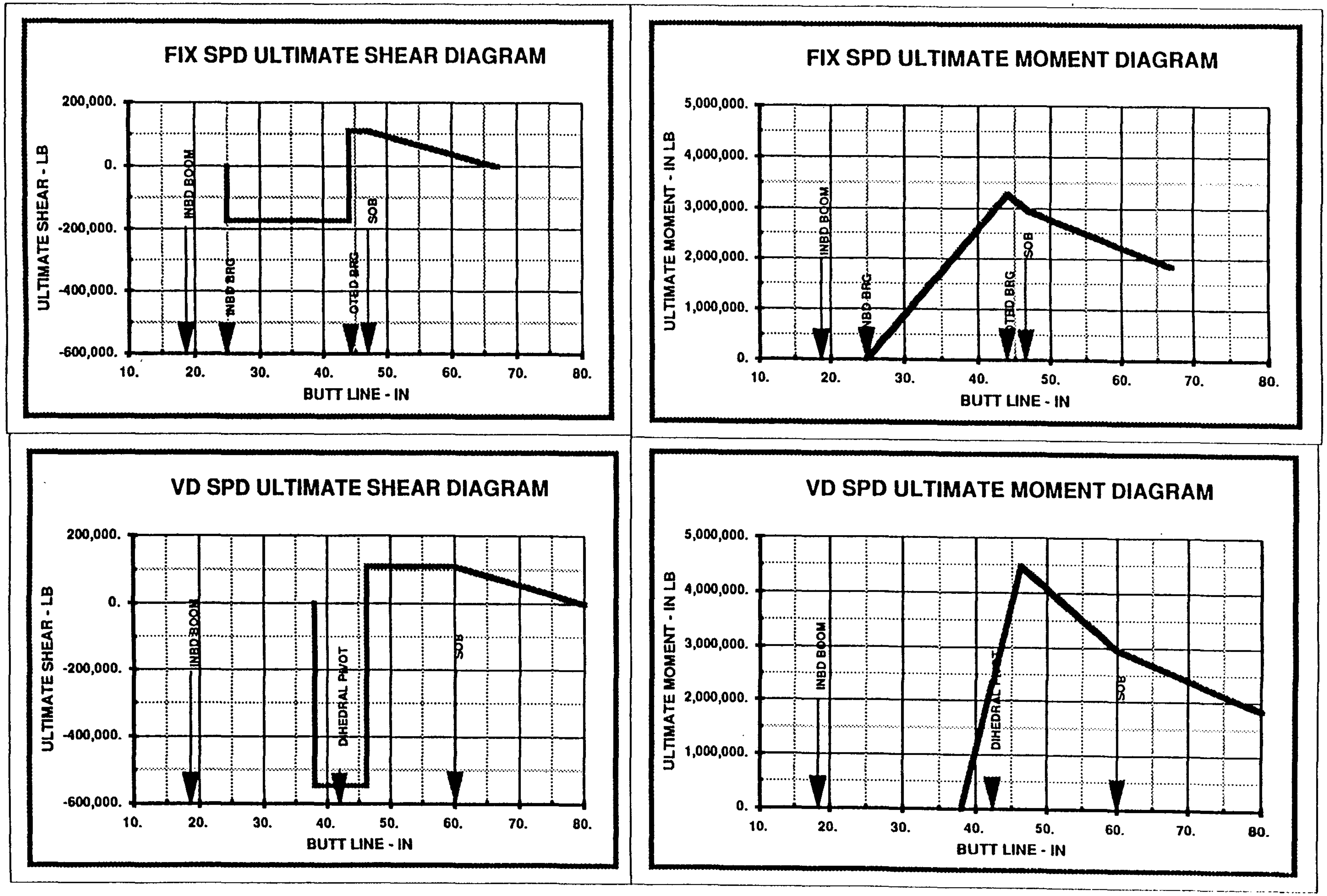

Figure D-7 Horizontal Stabilizer Spindle Loads Comparison

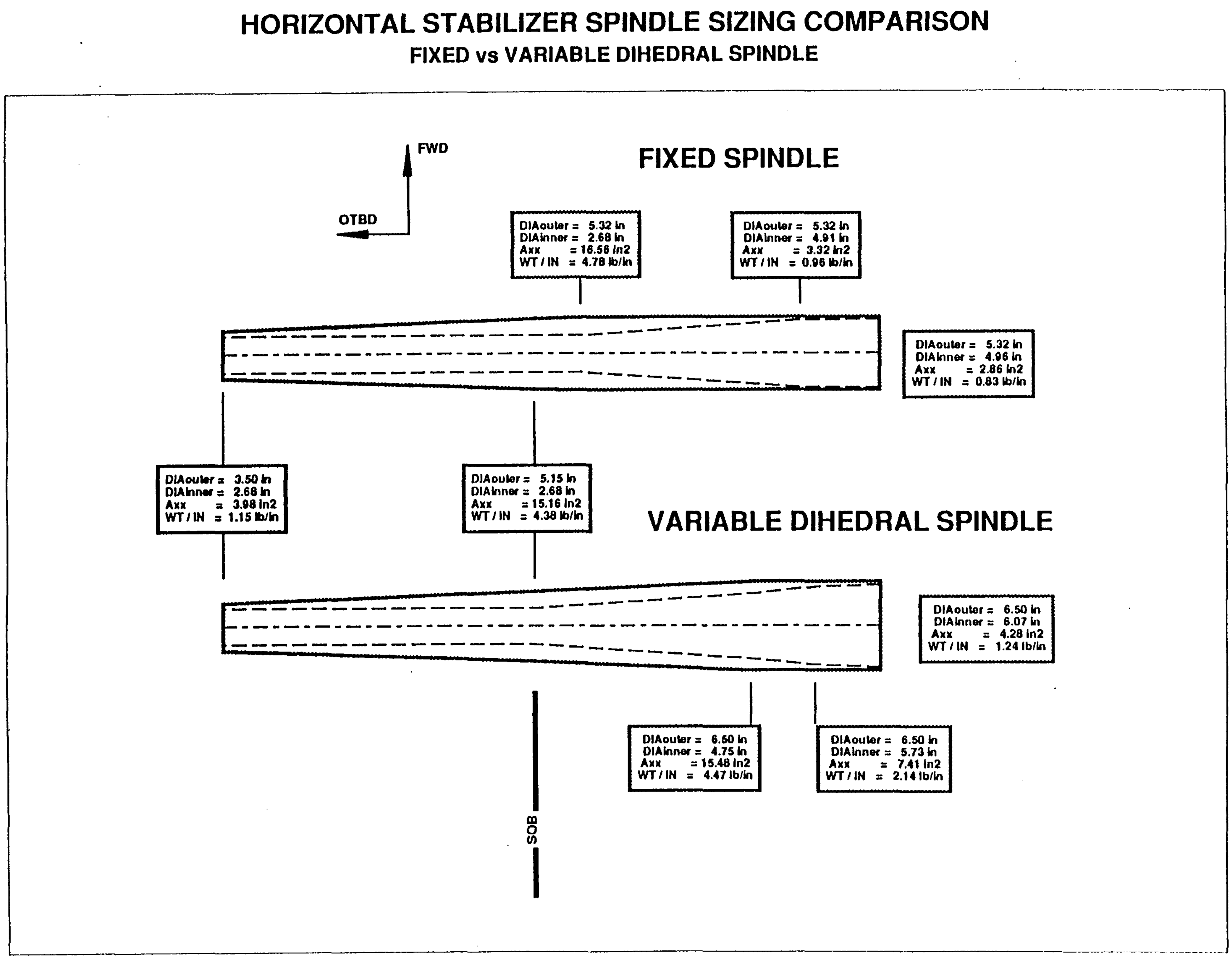

Figure D-8 Horizontal Stabilizer Spindle Sizing Comparison

FIXED SPINDLE MID BOOM

GEOMETRY (INPUTS):

OUTER DIAMETER =	5.316 in
and	
INNER DIAMETER =	0.000 in
or	
WALL THICKNESS =	0.207 in

APPLIED LOADS (INPUTS):

BENDING MOMENT - M =	860,425. in lb
AXIAL LOAD - Paxial =	4,000. lb
SHEAR LOAD - V =	172,085. lb
TORSION - T =	272,000. in lb

APPLIED STRESSES (CALCULATED):

{(M x c) ÷ Ixx} + {Paxial ÷ Axx} =	212,273. psi
{V ÷ (Axx)} + { T ÷ (2 x Rave^2 x PI x twall)} =	84,031. psi

SECTION PROPERTIES (CALCULATED):

Axx =	3.315 in2
lb / Running in =	0.958 lb / in
Ixx = Iyy =	10.836 in4
Ipolar =	21.671 in4
Px = Py =	1.808 in
Ppolar =	2.557 in
d/t =	25.74
Douter =	5.316 in
Dinner =	4.903 in
twall =	0.207 in
c÷Ixx =	0.245 in-3

MARGIN OF SAFETY =	0%

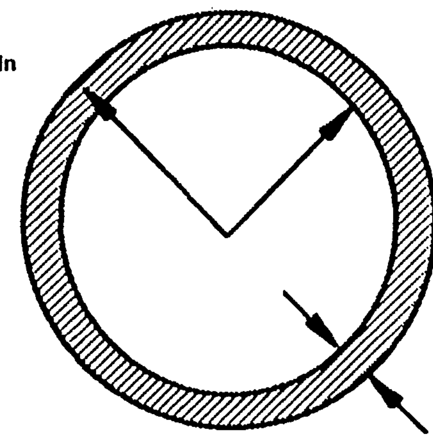

MATERIAL PROPERTIES (INPUTS):

TENSION ULTIMATE - Ftu =	240,000. psi
COMPRESSION YIELD - Fcy =	-240,000. psi
SHEAR ULTIMATE - Fsu =	180,000. psi
DENSITY =	0.289 lb / in-3
MATERIAL -	STEEL

OPTIMIZE

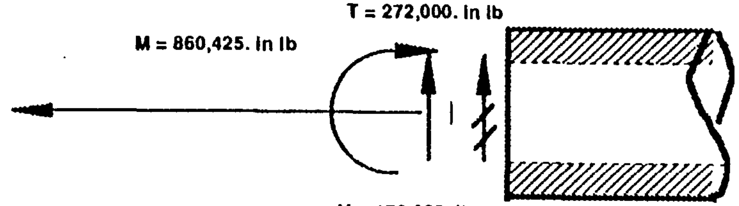

Figure D-9 Fixed Spindle Mid Boom

Body Boom Arrangement For Variable Dihedral

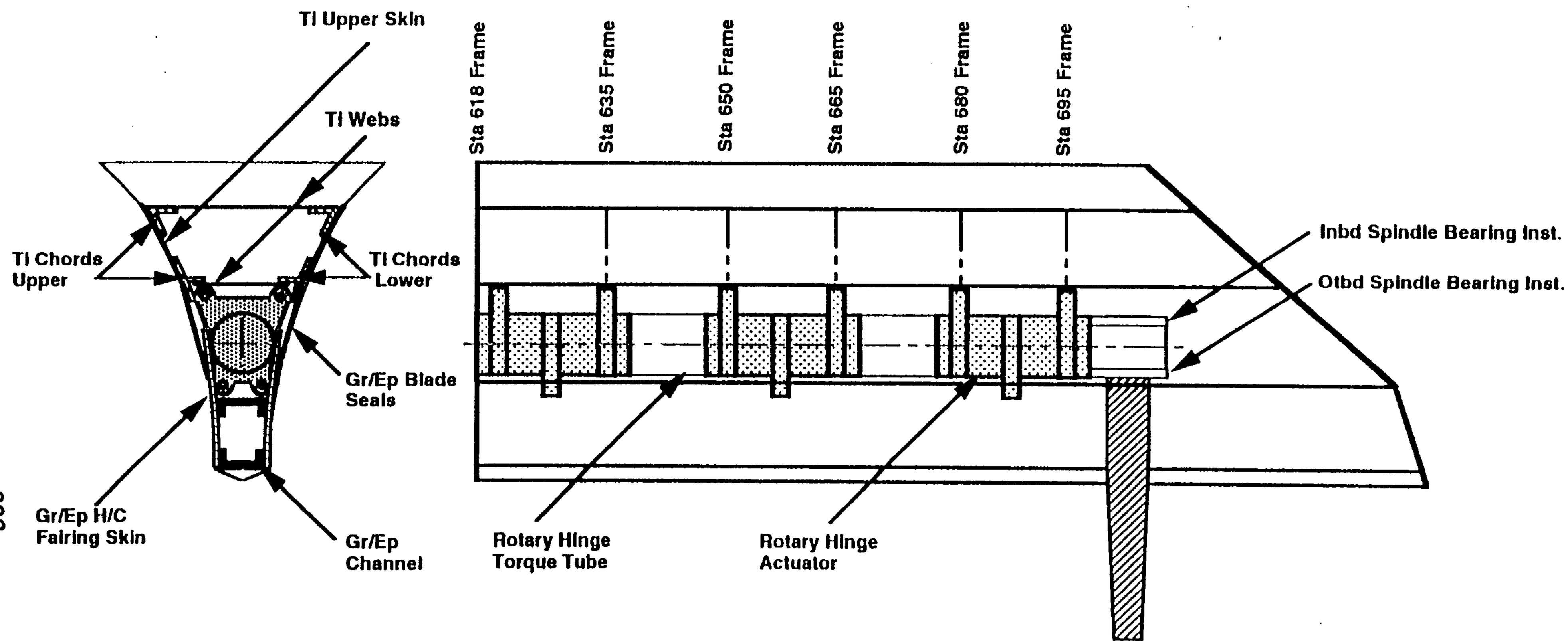

Item Description	Material
• Covers & Webs	Ti 6-4 Plate
• Chords	Ti 6-4 Plate Or Extrusions
• Frames	Ti 6-4 Plate
• Fittings	Ti 6-4 Extrusions
• Bearings	Steel
• Stabilizer Spindle	Steel
• Blade Seals	Gr/Ep Laminate
• Moveable Fairing Skin	H/C With Gr/Ep Faces; Nomex Core
• Fairing Channels	Gr/Ep Laminate
• Rotary Hinge Actuators	Steel
• Rotary Hinge Torque Tube	Steel

Figure D-10 Body Boom Arrangement for Variable Dihedral

Body Boom Arrangement For Variable Dihedral - Concept 2

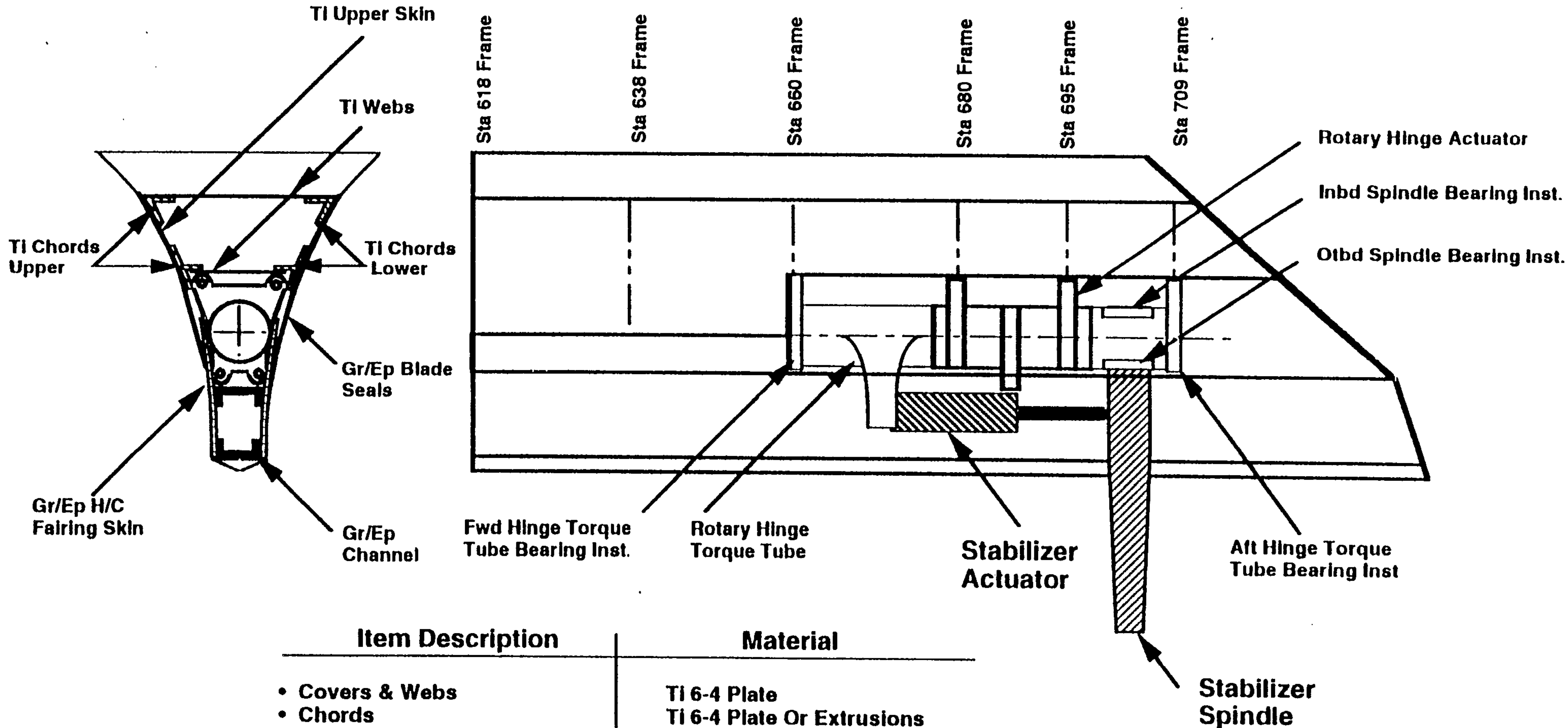

Item Description	Material
• Covers & Webs	Ti 6-4 Plate
• Chords	Ti 6-4 Plate Or Extrusions
• Frames	Ti 6-4 Plate
• Fittings	Ti 6-4 Extrusions
• Bearings	Steel
• Stabilizer Spindle	Steel
• Blade Seals	Gr/Ep Laminate
• Moveable Fairing Skin	H/C With Gr/Ep Faces; Nomex Core
• Fairing Channels	Gr/Ep Laminate
• Rotary Hinge Actuators	Steel
• Rotary Hinge Torque Tube	Steel

Figure D-11 Body Boom Arr. for Var. Dihedral - Concept 2

Rotary Hinge Torque Tube Arrangement

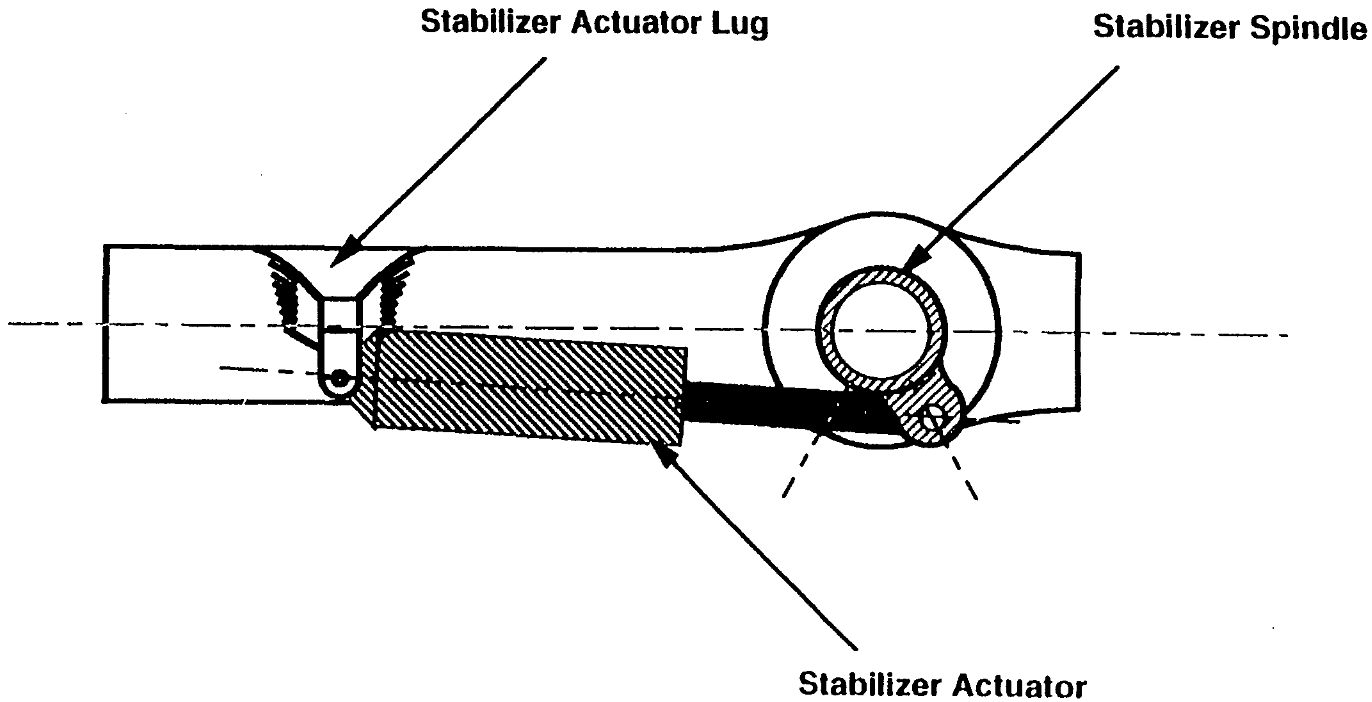

Figure D-12 Rotary Hinge Torque Tube Arrangement

DATA PER CURTISS-WRIGHT POWER HINGE DESIGNERS' HDBK

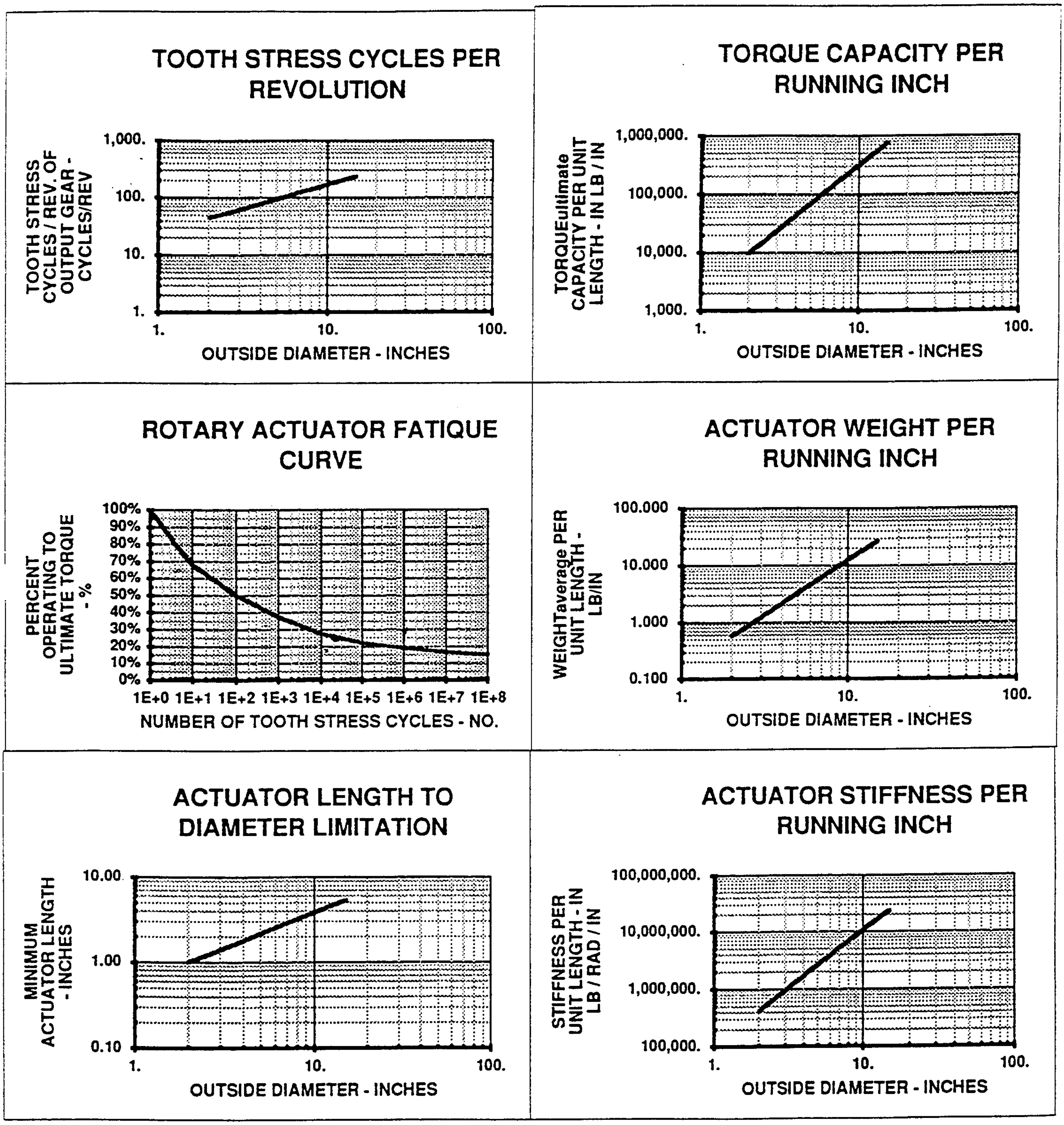

Figure D-13 Curtiss-Wright Power Hinge sizing Chart

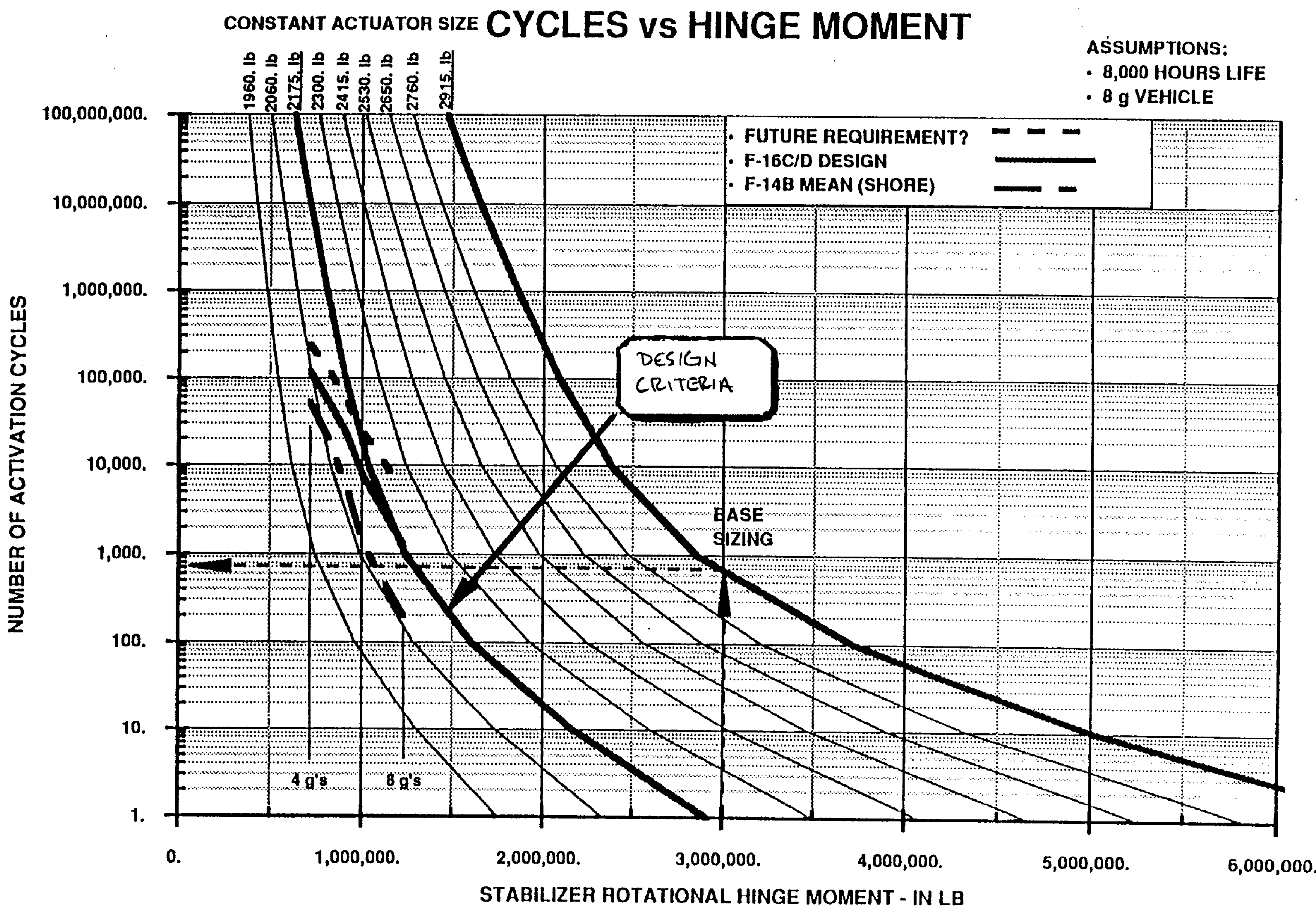

Figure D-14 Activation Cycles vs. Design Hinge Moment

APPENDIX E

Boeing Model-24F and Wind Tunnel Model 1798
Geometry Characteristics

This appendix contains the geometry characteristics of the Boeing Model-24F vehicle and of the associated Wind Tunnel Model 1798 in the following figures:

Figure E-1	Boeing Model-24F Full Scale Geometry
Figure E-2	3-Viewing Drawing - Model 1798
Figure E-3	Wing Planform Geometry - Model 1798
Figure E-4	Horizontal Tail Geometry - Model 1798
Figure E-5	Vertical Tail Geometry - Model 1798

CHARACTERISTICS	WING	HOR. TAIL (OUTBD BL47)	VER. TAIL (TRUE EACH)
AREA - REF, FT2	465	63.55	37.79
ASPECT RATIO - REF	2.20	2.52	1.06
TAPER RATIO - REF	.13	.34	.64
SPAN - TRUE, FT	31.95	6.33	6.32
ROOT CHORD - REF, IN.	308.5	90.06	87.42
TIP CHORD - REF, IN.	40.7	30.37	56.08
MAC - THEOR REF, IN.	208.85	65.15	72.91
DIHEDRAL, DEG	-9	0	62
SWEEP - LE/TE, DEG	47.5/-17.0	47.5/17.0	42.78/27.13
1/4 MAC - REF FUS STA	454.11	697.48	635.00
T/C - ROOT/TIP, %	4.5/3, $T/C^2=K$	5/3	5/3
TAIL VOL COEFF - $\bar{C}/4$- $\bar{C}/4$		.159	.077

Figure E-1 Boeing Model-24F Full Scale Geometry

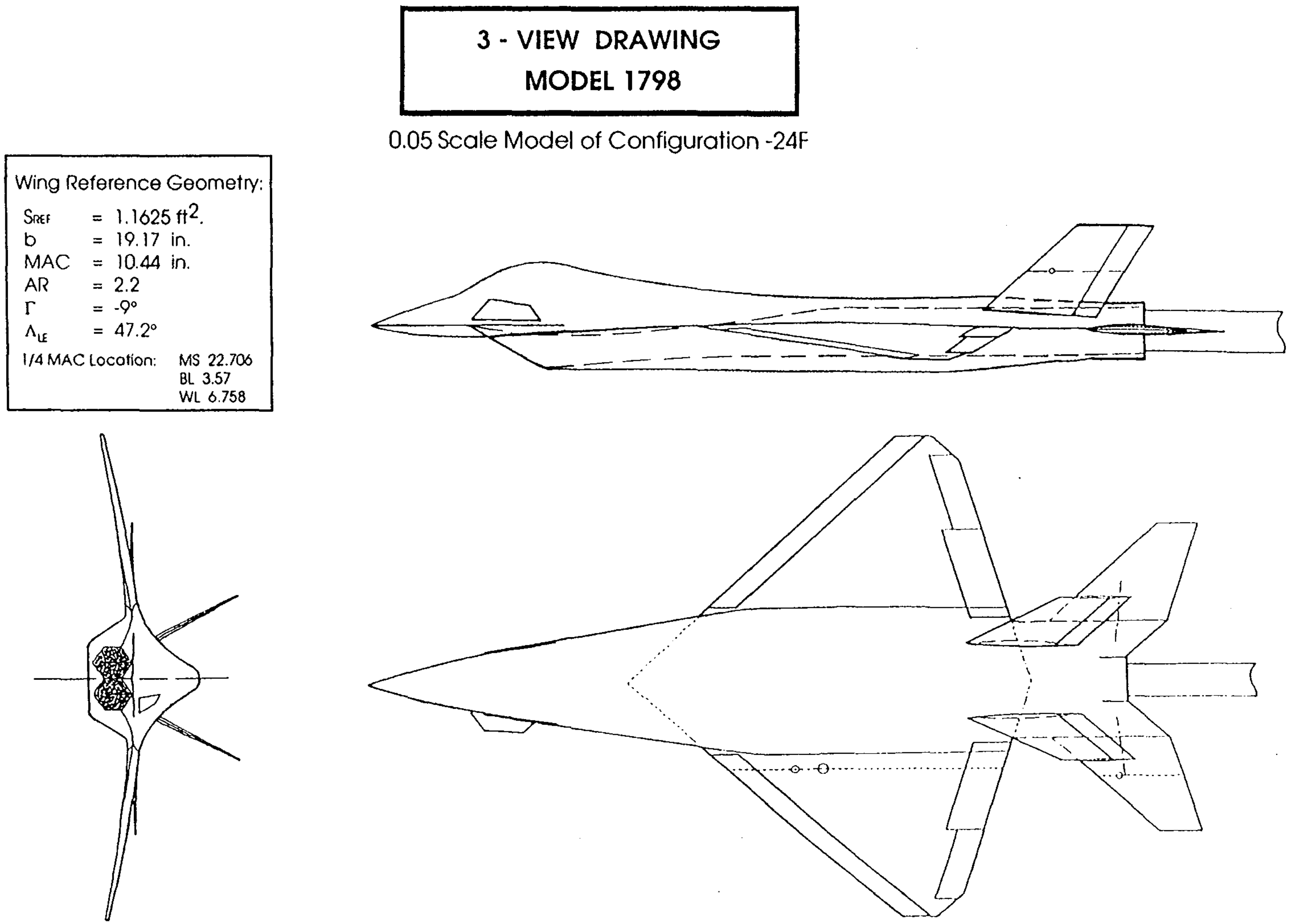

Figure E-2 3-View Drawing - Model 1798

WING PLANFORM GEOMETRY
W1 AND W1.1
MODEL 1798

0.05 Scale Model of Configuration -24F

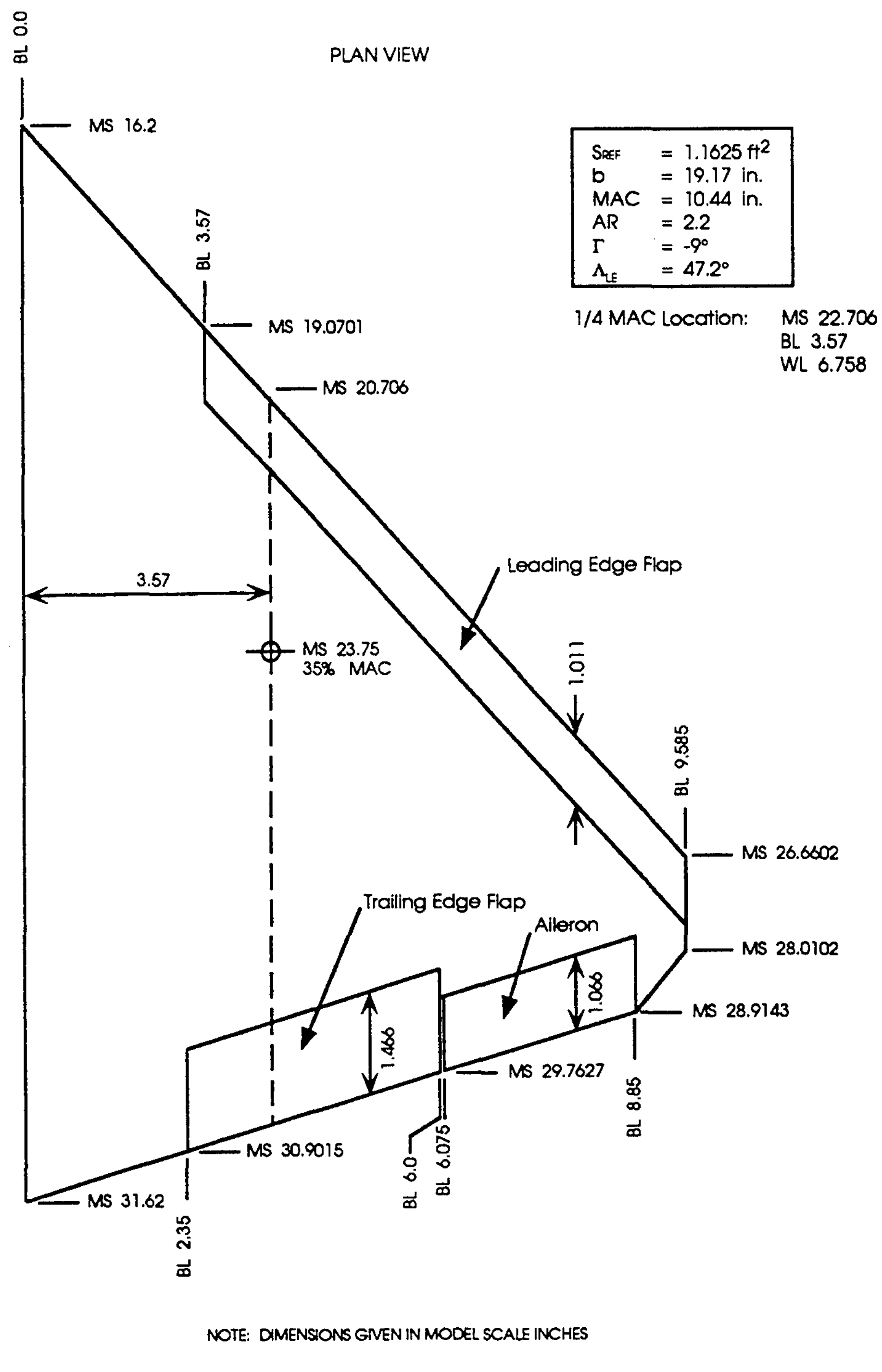

Figure E-3 Wing Planform Geometry - Model 1798

HORIZONTAL TAIL GEOMETRY
H1
MODEL 1798

0.05 Scale Model of Configuration -24F

TRUE VIEW

- Pivot Location MS 34.935
  BL 2.35
  WL 6.942

S_{REF}	= 0.0844 ft.^{2} each
b_{True}	= 3.916 in. each
AR	= 2.52
MAC	= 3.357 in.
Γ	= 0°
1/4 MAC Location	MS 34.874 BL 3.984 WL 6.942

Both horizontal tails pivot around an axis swept 6° from the pivot point.

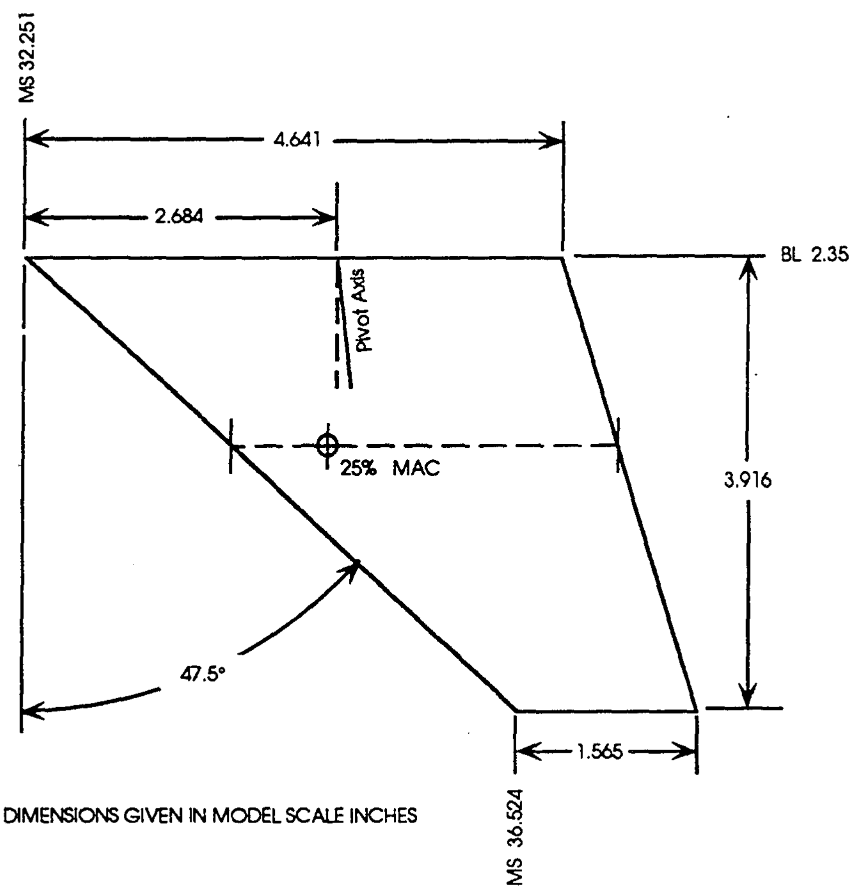

NOTE: DIMENSIONS GIVEN IN MODEL SCALE INCHES

Figure E-4 Horizontal Tail Geometry - Model 1798

VERTICAL TAIL GEOMETRY
V1
MODEL 1798

0.05 Scale Model of Configuration -24F

TRUE VIEW

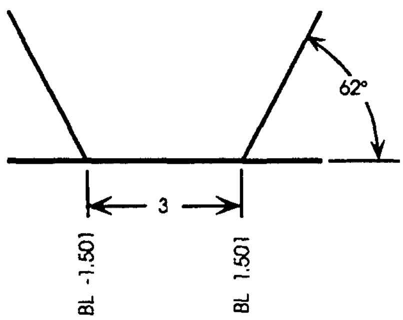

S_{REF} = 0.0912 ft.^{2} each
b_{True} = 3.8485 in.
AR = 1.1275
MAC = 3.694
Γ = 62°
1/4 MAC Location MS 31.75
BL 2.336
WL 9.278

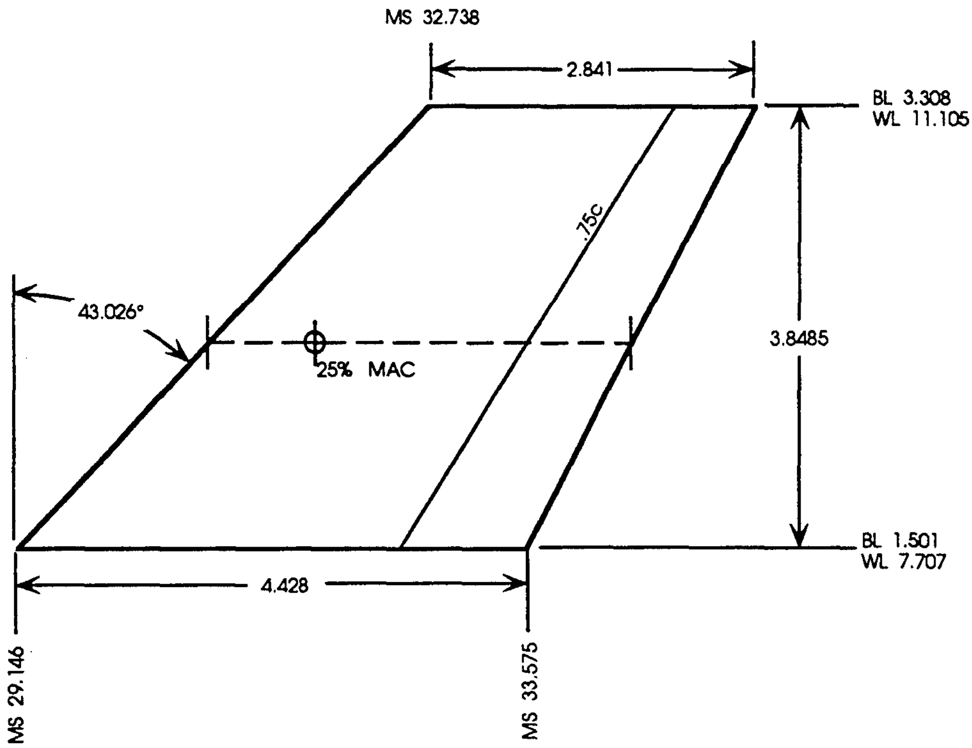

NOTE: DIMENSIONS GIVEN IN MODEL SCALE INCHES

Figure E-5 Vertical Tail Geometry - Model 1798

DEPARTMENT OF THE AIR FORCE
AIR FORCE RESEARCH LABORATORY
WRIGHT-PATTERSON AIR FORCE BASE OHIO 45433

9-14-99

MEMORANDUM FOR: Defense Technical Information Center/OMI
8725 John J. Kingman Rd, Suite 0944
Ft Belvoir, VA 22060-6218

FROM: Det 1 AFRL/WST
Bldg 640 Rm 60
2331 12th Street
Wright-Patterson AFB OH 45433-7950

SUBJECT: Notice of Changes in Technical Report(s) (See below)

Please change subject report(s) as follows:

The following have all been approved for public release; distribution is unlimited:

AFWAL-TR-83-3072, AD B955 265
WRDC-TR-90-3081, AD B166 585
WL-TR-96-3043, AD B212 813 OK ST-A
WL-TR-96-3094, AD B212 361 ~~STP~~
WL-TR-97-3059, AD B232 172 ~~ok~~

B212361

JOSEPH A. BURKE, Team Leader
STINFO and Technical Editing
Technical Information Division